Exponential asymptotics for discrete Painlevé equations

Steven Luu

A thesis submitted in fulfillment of
the requirements for the degree of
Doctor of Philosophy

School of Mathematics and Statistics
University of Sydney

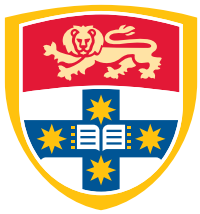

THE UNIVERSITY OF
SYDNEY

May 2018

CONTENTS

Abstract

Classical asymptotic power series methods are used for determining limiting behaviour for solutions of equations under some limit. This is particularly useful when dealing with transcendental solutions such as those of the Painlevé equations. However, asymptotic power series methods are unable to capture terms which are exponentially small. The behaviour of such terms varies across the complex plane and hence classical asymptotic power series expansions are only uniformly valid within sectors of the complex plane where these terms are exponentially small. In order to obtain improved asymptotic expansions which are valid within an extended sector we require methods which allow us to study behaviour that are exponentially small.

The aim of this thesis is to study Stokes phenomena, which arise from exponentially small terms present in solutions of both additive and multiplicative difference equations. Specifically, we undertake an asymptotic study of the second discrete Painlevé equation as the independent variable approaches infinity, and also consider the asymptotic behaviour of solutions of a q-Airy equation and the first q-Painlevé equation in the limits $|q| \to 1$ and $n \to \infty$. By investigating Stokes phenomena, we are able to obtain uniform asymptotic expansions of solutions of the second discrete Painlevé, the q-Airy and the first q-Painlevé equations.

We first show how exponential asymptotic methods can be applied to describe Stokes phenomena present in the solutions of additive difference equations by considering the second discrete Painlevé equation ($\mathrm{dP_{II}}$). We obtain two types of asymptotic series expansions which describe vanishing and non-vanishing type behaviour of $\mathrm{dP_{II}}$. In particular, we show that both types of solution behaviour can be expressed as asymptotic expansions, which are given as the sum of an optimally-truncated asymptotic series and an exponentially subdominant correction term. We determine the Stokes structure and investigate Stokes behaviour present in these solutions. We then use this information to show that the asymptotic expansions contain one free parameter hidden beyond-all-orders and determine the regions in which these asymptotic descriptions are valid. Furthermore, we deduce special asymptotic solutions which are valid in extended regions and draw parallels between the asymptotic solutions we find to the tronquée and tri-tronquée solutions of the second Painlevé equation.

Next we extend these methods to study Stokes phenomena present in the asymptotic solutions of q-difference equations in the limits $|q| \to 1$ and $n \to \infty$. In Chapter 4 we first consider a q-analogue of the Airy equation. By appropriately rescaling the problem, we apply the WKB method to show that the asymptotic behaviour of the q-Airy equation is expressible as a linear

combination of two exponential contributions. By comparing the relative dominance between these two contributions we are able to determine the Stokes structure and deduce the Stokes behaviour present within the asymptotic solution of the q-Airy equation.

In the second part of Chapter 4 we apply these techniques to also determine Stokes behaviour in the asymptotic solutions of the first q-Painlevé equation in the limits $|q| \to 1$ and $n \to \infty$. As in the case of $\mathrm{dP_{II}}$, we also obtain two classes of solution behaviour, which we call type A and type B asymptotic solutions. Using exponential asymptotics, we show that both solution classes may be described as a sum of an optimally-truncated asymptotic power series containing exponentially subdominant correction terms. In our asymptotic analysis of both the q-Airy and first q-Painlevé equations, we find that the Stokes and anti-Stokes curves are described by curves referred to as q-spirals. As a consequence, the Stokes structure for solutions of q-difference equations separate the complex plane into sectorial regions bounded by arcs of spirals rather than traditional rays.

Statement of Originality

This thesis was supervised by Prof. Nalini Joshi in collaboration with Dr. Christopher Lustri. Chapters 3 and 4 are based on collaborative research between Nalini Joshi, Christopher Lustri and myself. The results in Chapter 3 of this thesis were reported in the paper 'Stokes phenomena in Discrete Painlevé II' *Proc. R. Soc. A*, 473, 2017 [**84**]. Chapter 4 also contains new results on the q-Airy and q-Painlevé I equations which have not yet been published.

To the best of my knowledge, the contents of this thesis are of original work made by myself. The use of existing works have been acknowledged wherever necessary.

Acknowledgements

I would like to thank my supervisor, Nalini Joshi, for her on-going guidance and consistent motivation throughout the duration of the doctorate program. I am especially grateful for her support which provided me the means to attend various national and international conferences. Even though you have been very busy throughout these past few years, you have always made time for us to meet whenever I was in need. This project would not have been as successful as it was without your guidance and constant support.

I would also like to extend my gratitude to Christopher Lustri who I have also been working closely with since my honours year. I am very grateful for the tremendous amount of time and effort you have spent in guiding me, even when you were no longer working at the University of Sydney. The moments leading up to the thesis submission was one hell of a roller-coaster ride. Without your guidance and motivation I would have not been able to complete the doctorate as successfully as I did. It has been an honour to be your first PhD student.

I also extend my gratitude to my examiners who all gave very detailed and positive reviews for my thesis. It was very gratifying to know that my thesis was considered very highly by a few of the world's leading experts in the field of asymptotics!

I would also like to thank my fellow peers who have also gone through the PhD roller-coaster ride, especially those who I have known since undergrad. The program would not have been as enjoyable and bearable without the support and company everyone has offered.

And finally, I would like to thank my family for supporting me pursue my academic interests. It is now finally time to get out to the real world!

CHAPTER 1

Introduction

In this thesis, we are interested with the behaviour of solutions of difference equations under some limit. Asymptotic analysis allows us to determine the behaviour of solutions of a given equation as some limit is approached. These methods are useful as they provide approximations expressible in terms of elementary or previously known functions. This is particularly useful when the general expressions of the solutions are transcendental, which means that the solutions are not expressible in terms of elementary or previously known functions.

The difference equations we study in this thesis are equations known as the *discrete Painlevé equations*, which are the discrete analogues of the classical Painlevé equations. The reason we investigate the discrete Painlevé equations is because they appear in various fields of study, such as orthogonal polynomial theory, to discrete models of physical phenomena and in mathematical physics. Although the discrete Painlevé equations commonly arise in the study of physical systems, they are of particular interest as they are known to be integrable.

Using the discrete analogues of the Painlevé equations as a model, we will develop methods in order to obtain asymptotic descriptions of solutions of difference equations and uncover Stokes behaviour present in these solutions. In this chapter we introduce both the Painlevé equations and their discrete analogues and provide an overview of their history as well as their importance.

1.1. Painlevé Equations

In the 1900s, Painlevé [**125**, **126**], Gambier [**61**] and Fuchs [**60**] investigated a problem posed by Picard [**132**]. This problem was concerned with second order differential equations of the form

$$y'' = R(y, y', t), \tag{1.1}$$

where R is rational function of $y = y(t)$ and $y' = dy/dt$ and is analytic with respect to t. The goal was to classify differential equations of the form (1.1) under the condition that poles were the only movable singularities of the solutions of (1.1). That is, the location of the poles only depend on the initial conditions of (1.1). This particular property was later dubbed the *Painlevé property*.

Painlevé, Gambier and Fuchs produced a list of fifty equations which have the Painlevé property, of which forty four of these equations could be reduced to equations solvable in terms of either elliptic or previously known special functions such as the Airy or Bessel functions. The remaining six irreducible nonlinear equations were named as the Painlevé equations. The six Painlevé

equations are given by

$$
\begin{aligned}
\mathrm{P_I}: \quad & y'' = 6y^2 + t, \\
\mathrm{P_{II}}: \quad & y'' = 2y^3 + ty + \alpha, \\
\mathrm{P_{III}}: \quad & y'' = t(y')^2 - yy' + \delta t + \beta y + \alpha y^3 + \gamma t y^4, \\
\mathrm{P_{IV}}: \quad & y'' = \frac{1}{2}(y')^2 + \beta + 2(t^2 - \alpha)y^2 + 4ty^3 + \frac{3}{2}y^4, \\
\mathrm{P_V}: \quad & y'' = \left(\frac{1}{2y} + \frac{1}{y-1}\right)(y')^2 - \frac{1}{t}y' + \frac{(y-1)^2}{t^2}\left(\alpha y + \frac{\beta}{y}\right) + \gamma\frac{y}{t} + \delta\frac{y(y+1)}{y-1}, \\
\mathrm{P_{VI}}: \quad & y'' = \frac{1}{2}\left(\frac{1}{y} + \frac{1}{y-1} + \frac{1}{y-t}\right)(y')^2 - \left(\frac{1}{t} + \frac{1}{t-1} + \frac{1}{y-t}\right)y' \\
& \quad + \frac{y(y-1)(y-t)}{t^2(t-1)^2}\left(\alpha + \beta\frac{t}{y^2} + \gamma\frac{t-1}{(y-1)^2} + \delta\frac{t(t-1)}{(y-t)^2}\right),
\end{aligned}
$$

where $\alpha, \beta, \gamma, \delta$ are complex-valued parameters and the prime denotes derivatives with respect to t. Since the general solutions of the Painlevé equations are not expressible in terms of previously known functions they form new transcendental functions and are therefore referred to as the *Painlevé transcendents*.

Although the Painlevé equations were first considered purely as mathematical objects, they also appear in various studies of physical systems. The second Painlevé equation is related to the Korteweg-de Vries (KdV) equation, which models shallow water waves [**35**, **55**, **66**]. Claeys and Grava [**35**] developed a uniform asymptotic expansion for the KdV equation involving the solutions of the second Painlevé equation. In mathematical physics, the Painlevé equations also appear as solutions of the nonlinear Schrödinger equation [**22**, **99**].

The Painlevé equations also arise in the study of orthogonal polynomials [**16**, **20**, **50**, **54**, **97**]. When certain weights are chosen, the Painlevé equations can be obtained from the recurrence relations established by orthogonal polynomials. Interestingly, the Painlevé equations have also appeared in recent developments in quantum field theories and in the applications of random matrices [**39**, **51**, **59**, **130**, **144**, **145**, **150**, **151**, **151**].

As the Painlevé transcendents often appear in various nonlinear models they are often regarded as defining new nonlinear special functions [**36**, **75**]. In this respect, the Painlevé equations are regarded as being the nonlinear analogues of the classical linear special functions.

Interest towards the Painlevé equations is not only due to their appearance in physical applications, but also due to the fact that they are integrable. Integrable systems are those which allow global descriptions of solutions and are therefore suitable candidates as governing equations of models. The authors of [**135**] refer to the Painlevé equations as being on the borderline between trivial integrability and non-integrability.

1.2. Discrete Painlevé equations from the continuous Painlevé equations

Generic solutions of the Painlevé equations are known to be transcendental and hence their solutions are not expressible in terms of previously known functions. However, for certain choices of the parameter values appearing in the Painlevé equations it is possible to find exact solutions, which are expressible in terms of previously known special or rational functions. These are known as the *special solutions* of the Painlevé equations.

In this section, we discuss some special solutions of the Painlevé equations and show how difference equations can be obtained from these solutions. In particular, the difference equations obtained in this way can be identified as discrete analogues of the Painlevé as they tend to the continuous Painlevé equations under some limit.

As the first Painlevé equation does not have any parameters it does not have any special solutions. We therefore consider the second Painlevé equation. The second Painlevé equation is given by

$$y'' = 2y^3 + ty + \alpha, \tag{1.2}$$

where $y = y(t)$. It is easy to check that $y(t) = 0$ and $y(t) = t^{-1}$ are solutions of (1.2) with parameter values $\alpha = 0$ and $\alpha = 1$, respectively. As such, we let $y = y(t;\alpha)$ denote a solution of (1.2) with parameter value α.

The solutions $y(t;0)$ and $y(t;1)$ are known as the *rational solutions* of (1.2) and can be related by a transformation known as a *Bäcklund transformation*. Bäcklund transformations are expressions which relate differential equations and their solutions. In particular, Bäcklund transformations which relate two distinct solutions of the same equation are known as *auto-Bäcklund transformations*.

It can be shown that equation (1.2) admits the Bäcklund transformations

$$y(t;\alpha+1) = -y(t;\alpha) - \frac{\alpha + 1/2}{y'(t;\alpha) + y(t;\alpha)^2 + t/2}, \tag{1.3}$$

for $\alpha \neq -1/2$, and

$$y(t;\alpha-1) = -y(t;\alpha) + \frac{\alpha - 1/2}{y'(t;\alpha) - y(t;\alpha)^2 - t/2}, \tag{1.4}$$

for $\alpha \neq 1/2$ [**56**, **63**, **142**]. Hence, the Bäcklund transformation (1.3) relates the solution $y(t;\alpha+1)$ to $y(t;\alpha)$ provided that $\alpha \neq -1/2$, while (1.4) relates $y(t;\alpha-1)$ to $y(t;\alpha)$ provided that $\alpha \neq 1/2$.

The Bäcklund transformations (1.3) and (1.4) can be used to generate a list of rational solutions of (1.2). In this example, the substitution of $y(t;0) = 0$ into (1.3) can produce, after repeated iterations of (1.3), a set of rational solutions for positive integer values of α. The first few rational

solutions of (1.2) generated from (1.3) are given below

$$\begin{aligned} y(t;0) &= 0, \\ y(t;1) &= -\frac{1}{t}, \\ y(t;2) &= -\frac{2(-2+t^3)}{t(4+t^3)}, \\ y(t;3) &= -\frac{3t^2(160+8t^3+t^6)}{-320+24t^6+t^9}. \end{aligned}$$

A similar set of rational solutions of (1.2) for negative integer values of α can be generated from (1.4).

It is also possible to obtain difference equations from these transformations. By using equations (1.3) and (1.4) to eliminate $y'(t;\alpha)$ we can obtain the difference equation

$$\frac{\alpha+1/2}{y_{\alpha+1}+y_\alpha} + \frac{\alpha-1/2}{y_\alpha+y_{\alpha-1}} + 2y_\alpha^2 + t = 0, \tag{1.5}$$

where $y_\alpha = y(t;\alpha)$. Equation (1.5) therefore describes the evolution of y_α as α varies discretely for fixed t. If we let α be parametrized by $n+c$ where c is an arbitrary constant and let $y_n := y(t;\alpha)$, then (1.5) may be rewritten as

$$\frac{\eta_n}{y_{n+1}+y_n} + \frac{\eta_{n-1}}{y_n+y_{n-1}} + 2y_n^2 + t = 0, \tag{1.6}$$

where $\eta_n = n + c + 1/2$. It can be shown that under the limit

$$y_n = \rho(1+\epsilon^2 u(x)), \quad \eta_n = \rho^3(4+\epsilon^4 x), \quad t = -6\rho^2, \tag{1.7}$$

with $\rho^3\epsilon^5 = 1$, equation (1.6) produces, to leading order,

$$u'' = 6u^2 + x,$$

in the limit $\epsilon \to 0$ [**56**, **63**]. The limit (1.7) is known as the *continuum limit*. Hence, we find that the difference equation (1.6) tends to the first Painlevé equation under the continuum limit (1.7). We note that (1.6) first appeared in the work of Jimbo and Miwa [**77**] in 1981, however the continuum limit was not derived at the time.

Difference equations can also be obtained from the Bäcklund transformations of the other remaining Painlevé equations [**56**, **63**, **149**]. For example, under certain cases of parameters, the

Bäcklund transformations of the third Painlevé equation can be used to obtain the following difference equations

$$w_{n+1} + w_{n-1} = \frac{2z}{w_n^2} - \frac{4\eta_n}{w_n}, \tag{1.8}$$

$$\frac{\eta_{n+1}}{w_{n+1}w_n - 1} + \frac{\eta_n}{w_n w_{n-1} - 1} = \kappa\left(w_n + \frac{1}{w_n}\right) - (\eta_n + \mu), \tag{1.9}$$

$$\frac{\eta_{n+1}}{w_{n+1} + w_n} + \frac{\eta_{n-1}}{w_n + w_{n-1}} = -\kappa\left(1 + \frac{1}{w_n^2}\right) + \frac{\eta_n}{w_n}. \tag{1.10}$$

It was shown in [**56**] that (1.8) also produces the first Painlevé equation under some continuum limit, while (1.9) and (1.10) produce the second and third Painlevé equations, respectively under some continuum limit.

Although the difference equations (1.6), (1.8), (1.9) and (1.10) all arise from Bäcklund transformations of certain Painlevé equations, it is interesting to note that each of these difference equations produce, to leading order, a particular Painlevé equation under some continuum limit. These particular difference equations fall under a certain class of difference equations known as the *discrete Painlevé equations*.

1.3. Discrete Painlevé Equations

In the previous section, we encountered difference equations which tend to the classical Painlevé equations under some continuum limit. In this thesis, we will consider discrete Painlevé equations, which tend to one of the six Painlevé equations under some continuum limit and are named after the Painlevé equation they produce under this limit. For example, equations (1.8), (1.9) and (1.10) are known as discrete versions of Painlevé I, II and III, respectively.

Surprisingly, the first known appearance of a discrete Painlevé equation predates the discovery of their continuous counterparts. In 1885, Laguerre [**97**] was the first to work on integrable, discrete nonautonomous systems in his work on orthogonal polynomials. From the recurrence relations established by orthogonal polynomials, Laguerre was able to obtain the difference equation

$$x_{n+1} + x_n + x_{n-1} = \frac{n + \rho\Delta_n}{x_n}, \tag{1.11}$$

where $\Delta_n = (1-(-1)^n)/2$ and $\rho > -1$. In 1939, Shohat's [**146**] work on orthogonal polynomials also led him to discover the difference equation

$$x_{n+1} + x_n + x_{n-1} = \frac{z_n}{x_n} + 1, \tag{1.12}$$

where $z_n = \alpha n + \beta$ and n is an integer. However, no connection between equations (1.11) and (1.12) to the Painlevé equations was made at the time.

In 1990, Brézin and Kazakov [**28**] computed the continuum limit of (1.12) in their work on a field theoretic model of two-dimensional gravity. In particular, this limit showed that (1.12) tended

to the first Painlevé equation and hence (1.12) was then recognized as a discrete analogue of the first Painlevé equation.

In the same year, Periwal and Shevitz's [**131**] work on a unitary matrix model of two-dimensional string theory led them to the difference equation

$$\alpha_{n+1} + \alpha_{n-1} = \frac{-2(n+1)\alpha_n}{\lambda(1-\alpha_n^2)}, \tag{1.13}$$

where $\lambda \neq 0$ and α_n is related to the eigenvalues of a unitary matrix. They showed that the continuum limit of (1.13) produces the second Painlevé equation (with parameter value zero) and is therefore a discrete analogue of the second Painlevé equation.

These discoveries sparked a great deal of attention towards discrete analogues of the Painlevé equations, and ultimately led to the subsequent discovery of further discrete Painlevé equations. While discrete Painlevé equations were first identified in theoretical physics models, and arise from reductions of partial difference equations [**112**] there was no systematic method of constructing discrete integrable mappings at the time.

In 1991, Grammaticos, Ramani and Papageorgiou [**64**] developed the idea of *singularity confinement* with the goal of systematically deriving integrable mappings. This idea proved to be fruitful as it subsequently led to the discovery of many new examples of discrete Painlevé equations. The idea of this new approach was to directly apply an integrability detector to some functional form and select the integrable cases.

As the Painlevé equations are integrable, this new method should produce integrable mappings which could possibly be recognized as a discrete Painlevé equation. In a sense, singularity confinement is based on the study of all possible singularities of a given mapping and how it propagates upon repeated iteration [**63**, **64**]. If the singularity propagates indefinitely it is considered to be an essential singularity, otherwise it is said to be *confined*. In this sense, singularity confinement is considered to be a discrete manifestation of the Painlevé property and is therefore a possible candidate for the discrete Painlevé property [**63**, **136**, **138**]. An example is provided in Appendix A in order to illustrate the concept of singularity confinement.

The authors in [**64**] apply the singularity confinement criterion to a family of integrable mappings known as the QRT mappings [**134**]. Doing so, they were able to obtain the difference equations

$$x_{n+1} + x_n + x_{n-1} = \frac{z_n + \gamma(-1)^n}{x_n} + \delta, \tag{1.14}$$

$$x_{n+1} + x_{n-1} = \frac{z_n x_n + \gamma}{1 - x_n^2}, \tag{1.15}$$

where $z_n = \alpha n + \beta$ and $\alpha, \beta, \gamma, \delta$ are constants. Equations (1.14) and (1.15) are known as discrete Painlevé I and II, respectively. Hence, we see that the difference equations given by (1.11)

and (1.12) are particular cases of (1.14), while the difference equation (1.13) found in [**131**] is a particular case of (1.15).

Unlike their continuous counterparts, which can be written as six distinct canonical forms, there exist different versions of each discrete Painlevé equation. For example, the difference equations (1.6) and (1.14) are both discrete versions of the first Painlevé equation. To distinguish the various versions, prefixes are attached to their naming. For example, equation (1.6) is known as alternate discrete Painlevé I while (1.14) is simply referred to as discrete Painlevé I.

Sakai [**141**] produced a classification for discrete Painlevé equations motivated by the work of Okamoto [**116**], based on the resolutions of nine singularities on a complex projective space of dimension two. In particular, the continuous Painlevé equations appear as degenerate cases of this construction.

Although the discrete Painlevé equations can be characterized by rational surfaces, a list of the *standard* discrete Painlevé equations which arise from the singularity confinement criterion is listed in [**63**] and is given by

$$\text{dP}_\text{I}: \quad x_{n+1}+x_{n-1}=\frac{z_n}{x_n}-x_n+1,$$

$$q\text{-P}_\text{I}: \quad x_{n+1}x_{n-1}=\frac{1}{x_n}-\frac{1}{q_n x_n^2}, \tag{1.16}$$

$$\text{dP}_\text{II}: \quad x_{n+1}+x_{n-1}=\frac{z_n x_n+a}{1-x_n^2}, \tag{1.17}$$

$$q\text{-P}_\text{III}: \quad x_{n+1}x_{n-1}=\frac{(x_n-aq_n)(x_n-bq_n)}{(1-cx_n)(1-x_n/c)},$$

$$\text{dP}_\text{IV}: \quad (x_{n+1}+x_n)(x_n+x_{n-1})=\frac{(x_n^2-a^2)(x_n^2-b^2)}{(x_n-z_n)^2-c^2},$$

$$q\text{-P}_\text{V}: \quad (x_{n+1}x_n-1)(x_nx_{n-1}-1)=\frac{(x_n-a)(x_n-1/a)(x_n-b)(x_n-1/b)}{(1-cx_nq_n)(1-x_nq_n/c)},$$

$$\begin{aligned}\text{dP}_\text{V}: \quad & \frac{(x_{n+1}+x_n-z_{n+1}-z_n)(x_n+x_{n-1}-z_n-z_{n-1})}{(x_{n+1}+x_n)(x_n+x_{n-1})}\\ &=\frac{(x_n-z_n-a)(x_n-z_n+a)(x_n-z_n-b)(x_n-z_n+b)}{(x_n-c)(x_n+c)(x_n-d)(x_n+d)},\end{aligned}$$

$$\begin{aligned}q\text{-P}_\text{VI}: \quad & \frac{(x_{n+1}x_n-q_{n+1}q_n)(x_nx_{n-1}-q_nq_{n-1})}{(x_{n+1}x_n-1)(x_nx_{n-1}-1)},\\ &=\frac{(x_n-aq_n)(x_n-q_n/a)(x_n-bq_n)(x_n-q_n/b)}{(x_n-c)(x_n-1/c)(x_n-d)(x_n-1/d)},\end{aligned}$$

where $z_n=\alpha n+\beta$, $q_n=q_0\lambda^n$ and a,b,c,d are constants. We note that this is not a complete list of the discrete Painlevé equations as there are many versions of discrete Painlevé I-VI. The authoritative list can be found in [**141**], and in the review paper [**89**].

1.3.1. Types of difference equations.

The above list includes two different types of difference equations. The first case includes equations like (1.17) in which the independent variable takes the form $z_n = \alpha n + \beta$, which therefore evolves as an arithmetic progression. The second case includes equations like (1.16) in which the independent variable is of the form $q_n = q_0 \lambda^n$, which instead evolves as a geometrical progression.

Difference equations in which the independent variable evolves additively or multiplicatively are known as *additive difference equations* or *multiplicative difference equations*, respectively. Chapter 3 is concerned with additive difference equations, in which the second discrete Painlevé equation, (1.17), is the main equation of interest and Chapter 4 is concerned with multiplicative difference equations, in which we consider the q-Airy and the first q-Painlevé equations. For the remainder of this thesis, additive difference equations will be simply referred to as difference equations while multiplicative difference equations are referred to as q-difference equations.

1.3.2. Applications of discrete Painlevé equations.

New examples of discrete Painlevé equations obtained by the singularity confinement approach became the subject of further study as they are also found in the study of physical systems like their continuous counterparts. As we have mentioned earlier, discrete Painlevé equations have appeared in mathematical physics such as in discrete models describing two-dimensional quantum gravity [**28**, **57**, **59**, **130**, **131**].

The basis of these models have origins in orthogonal polynomial theory, in which discrete Painlevé equations have been found to commonly appear [**93**, **97**, **104**, **105**, **146**, **152**, **153**]. Discrete Painlevé equations have also been shown to appear as similarity reductions of integrable lattice equations such as the differential-difference analogues of the KdV and modified KdV equations [**111**, **112**].

Like their continuous counterparts, the general solutions of the discrete Painlevé equations are also transcendental. However, for specific choices of parameter values, special solutions of the discrete Painlevé equations may also be found. As in the case of the continuous Painlevé equations, these special solutions are also expressible in terms of rational functions and discrete analogues of special functions [**67**, **87**, **88**, **90**, **91**, **137**].

1.4. Some asymptotic results of the Painlevé equations

As both continuous and discrete Painlevé equations arise in the study of physical systems, the properties of these solutions are important for such applications. Although the general solutions to the Painlevé equations are transcendental, information regarding the behaviour of their solutions under some limit can be obtained using asymptotic analysis.

The first major asymptotic study of Painlevé equations was investigated by Boutroux [**23**] in 1913. In this study, all the possible local asymptotic behaviours of the first and second Painlevé

equation were found as the independent variable approached infinity. Boutroux discovered that the general asymptotic behaviour of the first and second Painlevé equations are described by elliptic functions. However, Boutroux also showed that there also exist less general asymptotic behaviour, which are asymptotically free of poles in certain sectors of the complex plane. These particular asymptotic solutions are known as the *tronquée* and *tri-tronquée* solutions [**23**].

Few asymptotic results are known for their discrete counterparts despite their appearance in various areas of potential application. The authors in [**79**, **83**] both find divergent asymptotic series expansions for solutions of the first discrete Painlevé equation as the independent variable approaches infinity. In particular, it was shown that these series expansions contain exponentially small terms. By investigating the behaviour of these exponentially small terms, both studies are able to determine regions in which the asymptotic series expansions found are uniformally valid.

Joshi and Takei [**86**] extended the exact WKB analysis to the alternate discrete Painlevé I equation, (1.6). In particular, they were able to calculate explicit connection formula, which describe Stokes behaviour in the transseries solutions of the alternative discrete Painlevé I equation.

Xu and Zhao [**157**] also consider the asymptotic study of the discrete Painlevé V equation using the Riemann-Hilbert approach. By using the nonlinear steepest descent method developed by Deift and Zhou [**45**], the authors in [**157**] find that the asymptotic behaviour of the solutions of discrete Painlevé V can be represented in terms of solutions of the fifth Painlevé equation.

In the case of the q-Painlevé equations, not much is known concerning the asymptotic behaviour of their solutions. Joshi [**80**] identified unstable solutions of the first q-Painlevé equation, dubbed quicksilver solutions. These quicksilver solutions are described by divergent asymptotic series expansion as the independent variable approaches infinity and were shown to be asymptotic to true solutions of the first q-Painlevé equation in a certain domain of the complex plane. Asymptotic analysis of the same equation was also considered by Joshi and Lobb [**82**] in the context of algebraic geometry. To the best of our knowledge, there have been no known studies on Stokes behaviour for the solutions of the q-Painlevé equations.

We also mention the work of Mano [**106**] and Joshi and Roffelson [**85**] who consider the asymptotic behaviour of variants of the sixth q-Painlevé equation from an isomonodromic deformation point of view. They achieve global results, which they define as solving the *connection problem*. In these studies, the connection problem aims to relate the asymptotic behaviour of solutions at the origin and infinity. However, the asymptotic expansions obtained in these studies are convergent whereas this thesis is primarily concerned with divergent asymptotic series expansions.

1.5. Thesis Outline

In Chapter 2 we present an overview to the ideas and asymptotic methods used in order to investigate the exponentially small behaviour present in the problems we study. The methods which allow us to study exponentially small behaviour are known as exponential asymptotics. In particular, we discuss the importance of *optimal truncation* and *late-order terms* in the development

of asymptotic power series expansions. Once the key ideas are established we demonstrate how to capture Stokes behaviour present in the solutions of the hyper-Airy equation. This chapter is mainly a review of previous work and techniques of modern asymptotics, except for Section 2.5, which contains a new example.

Chapters 3 and 4 explore how we can develop asymptotic series expansions of solutions of the discrete Painlevé equations as some limit is approached. In Chapter 3, we demonstrate how the exponential asymptotic methods based on the works of [**33**], [**92**] and [**121**] can be applied to additive difference equations. In particular, we study the behaviour of solutions of the second discrete Painlevé equation and consider the Stokes behaviour present in these solutions. We then find new asymptotic solutions, which share features with the (tri)-tronquée solutions of the second Painlevé equations.

We then extend these methods for q-difference equations in Chapter 4. We show applications to both linear and nonlinear q-difference equations through examples of the q-Airy and the first q-Painlevé equations. Both examples are challenging, however, the analysis for the q-Airy equation is much less difficult than that for the first q-Painlevé equation. The reason why the q-Airy is less difficult is because, after rescaling the problem, the leading order behaviour of the q-Airy equation may be described by two linearly independent exponential terms.

For the first q-Painlevé equation, the hidden exponentially small behaviour must first be determined by studying the divergent asymptotic series for which its solutions are asymptotic. The interesting features we find in this chapter are that the (anti-) Stokes curves are described by curves known as q-spirals. As a result, we find that these solutions are valid in sectorial-like regions bounded by arcs of spirals.

We then conclude the thesis in Chapter 5 with a summary of the thesis results and provide some potential suggestions for future research.

CHAPTER 2

Exponential Asymptotics

In order to understand the solution behaviour of the discrete Painlevé equations in some limit, we must explore behaviour that is exponentially small. Such behaviour is beyond the reach of classical asymptotic power series methods as they decay to zero faster than any positive power of ϵ in the limit $\epsilon \to 0$. Exponential asymptotics refers to a set of mathematical tools, which allow us to study behaviour that occurs on an exponentially small scale in the limit as some parameter becomes small. That is, for behaviour which is proportional to $\epsilon^{\gamma} \exp(-\alpha/\epsilon^{\beta})$ for $0 < \epsilon \ll 1$ where α, β are positive constants and constant γ.

The reason we are interested in exponentially small terms is because such terms are important in the development of uniform asymptotic expansions of functions. In the Poincaré sense (which we introduce in Section 2.1) a power series expansion can accurately approximate a given function up to algebraic error in some limit within a certain sector in the complex plane. However, using exponential asymptotics it is possible to obtain an error which is exponentially small in the limit and therefore obtaining, what Olver terms [**122**], an 'exponentially-improved' approximation.

The calculation of the exponentially small terms hidden within asymptotic expansions can be used to show that the original expansion is valid within an extended sector. The determination of exponentially small terms have been used to construct uniform asymptotic expansions of special functions such as the gamma function [**129**, **155**], generalized exponential functions [**78**, **122**], Riccati equations [**119**, **120**] and functions with integral representations [**8**, **123**, **128**, **156**].

Exponentially-improved asymptotic series expansions have also been developed for linear difference equations. Olver [**124**] constructed exponentially-improved asymptotic expansions for solutions of a particular class of second order linear difference equations in terms of inverse factorial series with applications to Legendre functions. This was then generalized by Olde Daalhuis [**118**] to a larger class of second order linear difference equations with applications to hypergeometric functions.

Exponential asymptotic methods have also been developed for nonlinear problems [**32**, **33**, **38**, **41**, **42**, **92**]. Costin and Kruskal [**41**] utilized exponential asymptotic methods to show under certain conditions, that there is a one-to-one correspondence between true solutions and formal power series solutions of a class of ordinary differential equations. Some examples of uniform asymptotic expansions for solutions of nonlinear equations include the Riccati type equations [**119**, **120**], Burgers equation [**31**] and the Painlevé equations [**39**, **40**, **79**, **86**, **120**].

Joshi and Lustri [**83**] applied exponential asymptotic methods to describe solutions of the first discrete Painlevé equation. They were able to determine regions in the complex plane in which solutions of the discrete Painlevé equation had the prescribed asymptotic behaviour by investigating Stokes behaviour exhibited by these solutions. By applying such methods, the asymptotic solutions found in [**83**] were also shown to share features with the tronquée and tri-tronquée solutions of the first Painlevé equation [**23**]. The methods applied in [**83**] were also extended to the asymptotic study of the second discrete Painlevé equation in [**84**].

Not only are exponentially small terms important in the construction of uniform asymptotic expansions, there exist a plethora of problems in which the main physics occur on an exponentially small scale. For example, exponential asymptotic methods can be used to determine existence conditions for solutions of physical models such as crystal growth models [**96**] and fluid dynamics models [**65**, **100–103**, **148**].

These methods have also played a key role in recent developments of quantum field theories. In particular, non-perturbative effects play an important role within these theories [**5**, **34**, **51**]. These effects are precisely those which can not be described using classical asymptotic power series, which are also known as perturbation series.

In this thesis we are primarily interested in the asymptotic study of solutions of difference equations as some limit is approached. More specifically, we are interested in difference equations known as the discrete Painlevé equations described in Chapter 1. We aim to find solutions of the discrete Painlevé equations which are described by divergent asymptotic power series and therefore display Stokes behaviour. As Stokes phenomenon requires exponentially small terms to be investigated, exponential asymptotic methods are required.

Although asymptotic power series methods can be used to accurately approximate functions, they are unable to capture terms which are exponentially small. Consequently, this can lead to misinterpretations, which we discuss in Section 2.1, in describing the function of interest. In this chapter, we discuss the limitations of classical asymptotic power series methods and describe the development of exponential asymptotic techniques, including super- and hyper-asymptotics.

In Section 2.1 we introduce Poincaré's definition of asymptotic power series and discuss how exponentially small terms are invisible to asymptotic power series methods. The failure to describe such terms gives rise to ambiguities regarding the function's asymptotic representation and its behaviour. Although the Poincaré definition can provide accurate approximations of a function under some limit, they cease to be accurate if the number of correction terms kept increases. We will find that asymptotic series are often divergent and hence the error of these approximations can increase without bound as the number of correction terms increases.

Section 2.2 introduces the idea of a superasymptotic approximation. Superasymptotic approximations are obtained by truncating an asymptotic series such that the error is minimized. In this sense, superasymptotic approximations are also known as *optimally-truncated series*. Heuristics

are introduced, which are useful for optimally truncating an asymptotic series. Darboux's theorem is also introduced, which shows that the late-order terms of an asymptotic power series behave asymptotically like a *factorial-over-power*. Following the ideas of Dingle [**48**] and Berry [**11**] it can be shown, by using Borel summation methods, that the error of a superasymptotic approximation is typically exponentially small, providing the pivotal first step in investigating exponentially small behaviour.

In Section 2.3 we introduce the idea of hyperasymptotics. These ideas allow us to study the error of superasymptotic approximations and therefore explicitly determine the exponentially small behaviour hidden within these expansions. As this involves the analysis of exponentially small terms, hyperasymptotics is also synonymous with the term exponential asymptotics. Hyperasymptotics were developed by Berry and Howls [**13**] in 1990 by extending the ideas of Dingle [**48**] and Écalle [**52**].

After providing the relevant background, we discuss Stokes phenomena in Section 2.4. Exponential asymptotic methods are necessary to describe Stokes phenomena as it involves the sudden appearance or disappearance of exponentially small terms as special curves in the complex plane are crossed. In Section 2.5 we investigate the asymptotic behaviour of solutions of the hyper-Airy equation. This new example illustrates Stokes behaviour displayed in asymptotic series solutions and demonstrates the exponential asymptotic methods utilized in this thesis.

2.1. Classical asymptotic power series

In this section we discuss the restrictions of Poincaré's definition of asymptotic power series. Before we introduce Poincaré's definition we define some notation used in this chapter. We say that a function $f(z;\epsilon)$ is *of order* $g(z;\epsilon)$ as $\epsilon \to \epsilon_0$ if there exists a $c > 0$ such that

$$|f(z;\epsilon)| \leq c|g(z;\epsilon)|, \tag{2.1}$$

for all ϵ sufficiently close to ϵ_0. We denote this using Landau's big O notation [**7**, **98**], by

$$f(z;\epsilon) = \mathcal{O}(g(z;\epsilon)), \tag{2.2}$$

as $\epsilon \to \epsilon_0$. Similarly, we say that $f(z;\epsilon)$ is *of order less than* $g(z;\epsilon)$ if, for every $c > 0$, (2.1) holds. We denote this using Landau's little o notation by

$$f(z;\epsilon) = o(g(z;\epsilon)), \tag{2.3}$$

as $\epsilon \to \epsilon_0$. Poincaré [**133**] gave the following definition of an asymptotic series.

Definition 2.4 (Poincaré [**24**, **48**])**.** *A function, $f(z;\epsilon)$, is asymptotic to a power series*

$$F(z;\epsilon) = \sum_{n=0}^{\infty} \epsilon^n f_n,$$

in some sector defined by $\mathcal{S} = \{z \in \mathbb{C} \mid \alpha < arg(z) < \beta\}$, if for each fixed N and sufficiently small ϵ, we have

$$\left| f(z;\epsilon) - \sum_{n=0}^{N-1} \epsilon^n f_n(z) \right| = \mathcal{O}(\epsilon^N), \tag{2.5}$$

as $\epsilon \to 0$, for all $z \in \mathcal{S}$. We denote this by

$$f(z;\epsilon) \sim \sum_{n=0}^{\infty} \epsilon^n f_n, \tag{2.6}$$

as $\epsilon \to 0$ and say that $F(z;\epsilon)$ is the asymptotic expansion of $f(z;\epsilon)$ in $\mathcal{S}$.

Some examples of asymptotic expansions are given below.

$$-e^{-z/\epsilon} \int_{-z/\epsilon}^{\infty} \frac{e^{-t}}{t} dt \sim \sum_{n=0}^{\infty} \epsilon^{n+1} \frac{\Gamma(n+1)}{(-z)^{n+1}}, \quad \text{for } \mathrm{Re}(z) < 0, \tag{2.7}$$

$$\sin(\epsilon z) \sim \sum_{n=0}^{\infty} \frac{(-1)^n (\epsilon z)^{2n+1}}{(2n+1)!}, \quad \text{for } z \in \mathbb{C}, \tag{2.8}$$

$$\sin(\epsilon z) + \frac{z e^{-z/\epsilon}}{1+\epsilon} \sim \sum_{n=0}^{\infty} \frac{(-1)^n (\epsilon z)^{2n+1}}{(2n+1)!}, \quad \text{for } \mathrm{Re}(z) > 0, \tag{2.9}$$

as $\epsilon \to 0$ (with $\epsilon > 0$). The ratio test can be used in these examples to show that the asymptotic power series given by (2.8) and (2.9) are convergent while the series in (2.7) is divergent. This is not surprising as the condition in Definition 2.4 involve partial sums, and is therefore not limited to convergent series expansions. In this thesis we are primarily interested in asymptotic power series which are divergent.

Let us consider the following functions

$$f_1(z) = \sin(\epsilon z),$$
$$f_2(z) = \sin(\epsilon z) + \frac{z e^{-z/\epsilon}}{1+\epsilon}.$$

In (2.8) and (2.9), we find that the functions $f_1(z)$ and $f_2(z)$ are described by the same asymptotic power series expansions in the limit $\epsilon \to 0$. However, the functions f_1 and f_2 differ by a term which is exponentially small in the limit $\epsilon \to 0$ (provided that $\mathrm{Re}(z) > 0$). Consequently, the functions f_1 and f_2 cannot be distinguished by their asymptotic series expansions.

The problem is that asymptotic power series described in Definition 2.4 are limited to approximating functions up to algebraic powers of ϵ. Therefore functions which are exponentially small in the limit $\epsilon \to 0$ are unable to be captured by classical asymptotic power series as they decay to zero faster than any power of ϵ. That is,

$$\exp(-\alpha/\epsilon^{\beta}) = o(\epsilon^n),$$

as $\epsilon \to 0$ for all integers n and $\alpha, \beta > 0$. Consequently, functions which are exponentially small in the limit $\epsilon \to 0$ can only be represented by the trivial power series

$$\exp(-\alpha/\epsilon^{\beta}) \sim 0 + 0 \cdot \epsilon + 0 \cdot \epsilon^2 + \cdots, \tag{2.10}$$

as $\epsilon \to 0$. The asymptotic power series (2.10) completely 'misses' these exponentially small terms and hence such terms are said to be hidden *beyond-all-orders* in powers of ϵ. Consequently, the

definition of asymptoticity due to Poincaré is unique up to the addition of functions which are exponentially small.

Misinterpretations of asymptotic series described in Poincaré's definition arise due to its failure to capture exponentially small terms. In the example of (2.9) we may expand the second term as a geometric series to obtain the expansion

$$f_2(z) = \sin(\epsilon z) + \frac{ze^{-z/\epsilon}}{1+\epsilon} \sim \sum_{n=0}^{\infty} \frac{(-1)^n(\epsilon z)^{2n+1}}{(2n+1)!} + ze^{-z/\epsilon}\sum_{n=0}^{\infty}(-\epsilon)^n, \tag{2.11}$$

as $\epsilon \to 0$ which is valid in the region $-\pi < \text{Arg}(z) \leq \pi$. The asymptotic power series representation of $f_2(z)$ can therefore be represented as the sum of two uniquely determined series expansions, in which the second series is multiplied by an exponentially small prefactor in a sector containing the positive real axis. In general, the *complete asymptotic expansion* of a function can be written as a sum of multiple series expansions such as

$$f(z) \sim \sum_{r=0}^{\infty} \epsilon^r f_r(z) + A(z;\epsilon)\sum_{r=0}^{\infty} \epsilon^r a_r(z) + B(z;\epsilon)\sum_{r=0}^{\infty} \epsilon^r b_r(z) + \cdots, \tag{2.12}$$

as $\epsilon \to 0$, and where $A(z;\epsilon)$ and $B(z;\epsilon)$ are functions which are exponentially small as $\epsilon \to 0$. In this case, the component sums which constitute a complete asymptotic expansion in (2.12) are referred to as *component asymptotic series*.

Under Poincaré's definition, the asymptotic series expansion of $f_2(z)$ is only described by the first component asymptotic series in (2.11) and is therefore only a valid approximation of $f_2(z)$ in the right half z-plane. In the left half z-plane, the exponential contribution switches in dominance to become exponentially large. This change in dominance is not described by the series expansion in Poincaré's definition. Hence, the series expansion in Poincaré's definition fails to represent the function outside the prescribed sector as it fails to capture the behaviour of the exponentially small terms. Consequently, misinterpretations of the functions asymptotic behaviour arise as the Poincaré's definition permits the neglect of exponentially small terms.

Dingle [**48**] proposes an extended definition of asymptotic power series, which is free of the ambiguities which arise from the neglect of exponentially small terms. Dingle defines a complete asymptotic expansion of a function $f(z)$ as an expansion containing asymptotic power series, which formally and exactly obeys all the relations satisfied by $f(z)$ in some limit, say $\epsilon \to 0$, throughout a certain sector in the complex plane [**48**]. Examples of these relations include

- The functional form of $f(z)$ as $\epsilon \to 0$, such as boundary conditions on $f(z)$ and its derivatives in the limit.
- The differential, difference or integral equation satisfied by $f(z)$.
- The relations involving parameters present in the problem.

Consequently, this extended definition allows asymptotic series to be uniquely defined up to exponentially small terms. Some examples demonstrating the utility of Dingle's extended definition of asymptotic series can be found in [**48**].

2.1.1. Truncation of asymptotic series expansions.

Asymptotic series are typically divergent, and hence we can no longer expect their error (which can be defined by (2.13)) to stay small as more terms in the series are kept. However, their error can be minimized. Definition 2.4 is a statement regarding the error of an asymptotic series as $\epsilon \to 0$ for fixed N. We instead consider equation (2.5) as $N \to \infty$ for fixed $0 < \epsilon \ll 1$. This can therefore be interpreted as investigating the behaviour of the error of an asymptotic power series when the number of correction terms kept increases for a given ϵ. Let us denote the truncation error of (2.6) by

$$R_N = f(z) - \sum_{n=0}^{N-1} \epsilon^n f_n \tag{2.13}$$

where $N \geq 1$. For convergent series, the truncation error in (2.13) decreases to zero, however, this is not true for asymptotic series expansions as they are typically divergent. In order to illustrate this, let us consider the exponential integral [**2**] which is defined by

$$\mathrm{Ei}(z;\epsilon) = -\int_{-z/\epsilon}^{\infty} \frac{e^{-t}}{t} dt. \tag{2.14}$$

Equation (2.14) has the following (Poincaré) asymptotic behaviour [**1**]

$$e^{z/\epsilon}\mathrm{Ei}(-z;\epsilon) \sim \sum_{r=0}^{\infty} \epsilon^{r+1} \frac{\Gamma(r+1)}{(-z)^{r+1}} =: F(z;\epsilon), \tag{2.15}$$

as $\epsilon \to 0$ which is valid over the phase range $-\pi < \mathrm{Arg}(z) < -\pi/2$ and $\pi/2 < \mathrm{Arg}(z) < \pi$. Let

$$F^{[N]}(z;\epsilon) := \sum_{r=0}^{N-1} \epsilon^{r+1} \frac{\Gamma(r+1)}{(-z)^{r+1}}, \tag{2.16}$$

$$R_N(z) := e^{z/\epsilon}\mathrm{Ei}(-z;\epsilon) - F^{[N]}(z;\epsilon), \tag{2.17}$$

denote the truncated asymptotic power series and truncation error of the asymptotic series (2.15), respectively.

By truncating the asymptotic expansion $F(z;\epsilon)$ in (2.15) at the N^{th} term and plotting the truncation error, we observe in Figure 2.1 that the error decreases until some minimum is attained at some N. The inclusion of additional terms causes the error to increase, causing the approximation to become worse. This occurs because there is a turning point at which $\Gamma(N+1) \approx \epsilon^{N+1}$ as $N \to \infty$ for fixed $\epsilon > 0$. Hence, the term $\Gamma(N+1)$ begins to grow faster than ϵ^{N+1} decays as $N \to \infty$.

The growth of the truncation error can be understood by considering the possible balance between algebraic powers of ϵ and terms that are exponentially small. The term ϵ^k decays more slowly than $\exp(-\alpha/\epsilon^\beta)$ as $\epsilon \to 0$ for any positive constants α, β and k. However, for fixed $\epsilon > 0$, it is possible to find a value of k such that these two terms are comparable in size. We can show

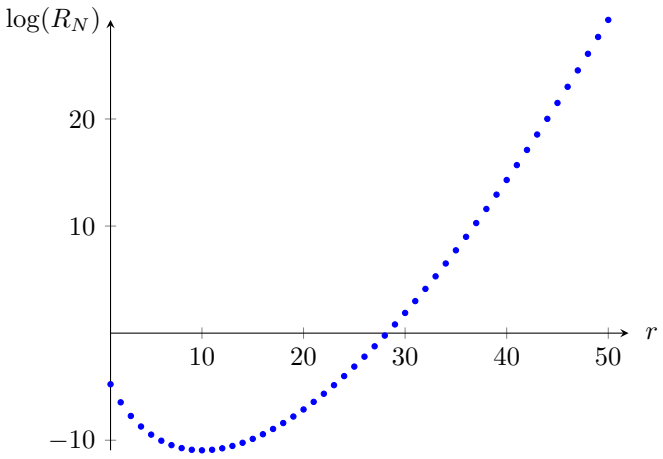

FIGURE 2.1. This figure shows the plot of $\log(R_N)$ appearing in (2.17) of the exponential integral for $z = 1$ and $\epsilon = 0.1$. For this fixed value of ϵ, the value to R_N decreases and attains a minimal value, which occurs at approximately $N \approx 10$. Additional correction terms cause the value of R_N to increase as N increases. The growth of R_N occurs after this minimum is because the term $\Gamma(N+1)$ grows faster than ϵ^N decays as $N \to \infty$.

this by considering the equation

$$\epsilon^k = \exp\left(-\frac{\alpha}{\epsilon^\beta}\right), \tag{2.18}$$

and calculating the value of k required for this to hold true. Solving for k in (2.18) shows that

$$k = -\frac{\alpha}{\log(\epsilon)\epsilon^\beta}, \tag{2.19}$$

which is large and positive as $\epsilon \to 0$. This suggests that it is possible to truncate an asymptotic series such that the error is comparable to an exponentially small term. Inclusion of higher order terms will fail to capture the exponentially small error and hence the asymptotic series representation appearing in Poincaré's definition does not converge to the function in question.

The asymptotic series we study in this thesis are those which are divergent for all values of $\epsilon > 0$. As we have seen in Figure 2.1, the truncation error of a divergent asymptotic power series grow without bound as the number of correction terms increase. Although these errors grow without bound, Figure 2.1 also demonstrates that we may truncate an asymptotic series such that the error is minimized.

2.2. Superasymptotics

In this section we discuss how asymptotic power series can be truncated such that the error is exponentially small, providing a key step towards the investigation of exponentially small terms. We also discuss Darboux's theorem, which was used by Dingle [**48**] to demonstrate that the late coefficient terms of an asymptotic power series behave generically as a *factorial-over-power* form.

This generic form for the late coefficients are related to the singularities of the function being approximated. This generic feature of asymptotic power series will prove to be important when we consider nonlinear equations later in this thesis.

In the previous section, we saw that an asymptotic series may be truncated such that the error is minimized. This observation introduces the idea of an *optimally-truncated* series. We say that an asymptotic series is optimally-truncated if we truncate the series such that the approximation error is minimized. We denote an optimally-truncated series of $f(z)$ in (2.6) by

$$f(z) = \sum_{r=0}^{N_{\text{opt}}-1} \epsilon^r f_r(z) + R_N(z), \tag{2.20}$$

where N_{opt} is the optimal truncation point and R_N is the optimally-truncated error. In the literature, R_N is also known as the *divergent tail* of an asymptotic series. Berry and Howls [**13**] gave the name *superasymptotics* to replace the term optimally-truncated asymptotic series. Minimizing the error of an asymptotic series by optimal truncation has been rigorously proven for a broad class of problems which can be formulated in terms of a Borel transform with well-separated singularities in the Borel plane (which we will encounter in Section 2.2.2) [**46**, **70**, **118**].

In order to optimally truncate an asymptotic power series, the behaviour of f_r in (2.6) must be known. A very useful heuristic which can be used to optimally truncate an asymptotic series is given by Boyd [**24**]. The heuristic states that for a fixed value of ϵ, the minimum error of an asymptotic series is usually obtained by truncating the series at its least term and discarding all higher order terms. Although this is a heuristic rule, it is very useful in practice and has been rigorously justified for some classes of asymptotic series [**41**, **42**, **117**].

It is typical that the optimally-truncated error is exponentially small in the limit $\epsilon \to 0$ [**13**, **24**, **25**]. In fact, we will show in Section 2.2.2 that the optimally-truncated error of a *factorially divergent* asymptotic series, such as (2.15), is indeed exponentially small. These are asymptotic power series whose coefficients behave as factorials.

Let us first calculate the optimal truncation point of (2.15). Using the heuristic given by Boyd [**24**], the optimal truncation point occurs when the term

$$\epsilon^N f_N = \frac{\epsilon^N \Gamma(N)}{(-z)^N}, \tag{2.21}$$

is minimal with respect to N and fixed ϵ. One possible method to calculate the optimal truncation point is to treat N as a continuous variable and minimize (2.21) using elementary calculus. We find that the first derivative of the coefficients in (2.21) is equal to

$$\frac{d}{dN}\left|\frac{\epsilon^N \Gamma(N)}{(-z)^N}\right| = -\left|\frac{\epsilon^N \Gamma(N)}{(-z)^N}\left(\log\left(-\frac{z}{\epsilon}\right) - \psi(N)\right)\right|, \tag{2.22}$$

where $\psi(z)$ is the digamma function [**2**], which is defined by

$$\psi(z) = \frac{\Gamma'(z)}{\Gamma(z)}.$$

Equation (2.22) is equal to zero when

$$\log\left(\frac{|z|}{\epsilon}\right) = \psi(N). \tag{2.23}$$

Now the equation $\psi(z) = \log(\alpha)$ for $\alpha \gg 1$ can be approximately solved by $z \sim \alpha - 1/2 + \mathcal{O}(\alpha^{-1})$ [**24**] and hence the approximate solution to (2.23) is

$$N_{\text{opt}} \sim \frac{|z|}{\epsilon}, \tag{2.24}$$

as $\epsilon \to 0$. We notice that $N_{\text{opt}} \to \infty$ as $\epsilon \to 0$ for fixed z and hence the limit $N_{\text{opt}} \to \infty$ is equivalent to the limit $\epsilon \to 0$ for fixed z. An equivalent method to calculate the optimal truncation point is to consider when the ratio of any two consecutive terms in an asymptotic series is close to unity. This amounts to finding the point N such that

$$\left|\frac{\epsilon^{n+1} f_{n+1}}{\epsilon^n f_n}\right| \approx 1, \tag{2.25}$$

as $N \to \infty$. Using equation (2.25) to find the optimal truncation point of (2.15) shows that

$$\left|\frac{\epsilon(N+1)}{-z}\right| \approx 1, \tag{2.26}$$

which implies that

$$N_{\text{opt}} \sim \frac{|z|}{\epsilon}, \tag{2.27}$$

as $\epsilon \to 0$ in agreement with (2.24). In general, any truncation point of a series expansion is necessarily required to be integer-valued. In particular, we take the integer value closest to the optimal truncation point, (2.27), for any fixed $\epsilon > 0$.

As the optimal truncation point has been determined we can directly compute the size of the optimally-truncated error of (2.15). From Definition 2.4 the optimally-truncated error is of order $\mathcal{O}(\epsilon^{N+1})$. Hence, by substituting the value of N_{opt} given by (2.24) into the expression for the optimally-truncated error we find that

$$\begin{aligned} |R_N| &= \left| f(z) - \sum_{r=0}^{N_{\text{opt}}-1} \epsilon^r f_r(z) \right|, \\ &\sim \left| \frac{\epsilon^{N_{\text{opt}}+1}\Gamma(N_{\text{opt}}+1)}{(-z)^{N_{\text{opt}}+1}} \right|, \\ &= \left| \frac{\epsilon^{N_{\text{opt}}+1}\Gamma(N_{\text{opt}}+1)}{z^{N_{\text{opt}}+1}} \right|, \end{aligned} \tag{2.28}$$

as $\epsilon \to 0$. By using Stirlings' formula for the leading order behaviour of the Gamma function [**1**, **2**]

$$\Gamma(an+b) \sim \sqrt{2\pi} e^{-an} (an)^{an+b-1/2} \left(1 + \mathcal{O}\left(\frac{1}{n}\right)\right), \tag{2.29}$$

as $n \to \infty$ and substituting this into (2.28) we find that

$$|R_N| \sim \sqrt{\frac{2\pi\epsilon}{|z|}} e^{-|z|/\epsilon}, \tag{2.30}$$

as $\epsilon \to 0$. We therefore find that the optimally-truncated error of (2.15) is indeed exponentially small.

In the example of the exponential integral, the exact form of the coefficients in (2.15) allowed us to determine N_{opt}. However, determining the exact form of the coefficients of an asymptotic series is often difficult to compute for most problems. As we will see in Section 2.2.1, the asymptotic behaviour of the coefficients contains all the necessary information required to compute N_{opt}.

The observation is that the optimal truncation point of an asymptotic series is typically large in the limit $\epsilon \to 0$. Therefore, for the purposes of optimal truncation, it is enough to determine the asymptotic behaviour of the coefficients as the summation index is large. These coefficients are known as the *late-order terms*. This is remarkably fortunate as it is much easier to determine the asymptotic behaviour of the coefficients instead of the exact form. As Berry states in [**10**, **12**], we therefore study the 'asymptotics of the asymptotics'. That is, finding the asymptotic behaviour of the coefficients of the asymptotic series.

Dingle's [**48**] investigations on asymptotic series revealed many deep and profound insights to the subject. Using a theorem of Darboux [**43**, **44**], Dingle was able to show that the asymptotic behaviour of the late-order terms of an asymptotic series are related to the singularities of the function they represent. Optimal truncation of an asymptotic series is then possible once the asymptotic behaviour of the late-order terms are determined.

2.2.1. Darboux's Theorem.

Dingle [**48**] noted the connection between a divergent asymptotic series and the function to which it is asymptotic by applying a theorem by Darboux [**43**, **44**]. This particular theorem demonstrates that the coefficients of a Maclaurin expansion of a function ϕ are determined by its singularities.

Using this theorem of Darboux, Dingle [**48**] was able to show that the late terms of an asymptotic series are generically described by a *factorial-over-power* form. These asymptotic series expansions are therefore factorially divergent. Once the behaviour of the late-order terms are obtained we will use Borel summation methods in order to show that the optimally-truncated error of this class of asymptotic power series is exponentially small. The theorem of Darboux which Dingle used is given below.

Theorem 2.31 (Theorem of Darboux)**.**
Suppose that a function $\phi(s)$ is singular at the set of points $\{s_i\}$, which all lie on the same Riemann sheet as the origin, and has a Maclaurin expansion of the form

$$\phi(s) = \sum_{r=0}^{\infty} a_r s^r, \tag{2.32}$$

with radius of convergence $R = min\,|s_i|$. Under these assumptions, the coefficients of the Maclaurin expansion (2.32) *have the following asymptotic behaviour*

$$a_r \sim \sum_i \binom{r+p_i-1}{r} \frac{1}{s_i^{r+p_i}} \sum_{k=0}^{\infty} \frac{(r+p_i-k-1)!(p_i-1)!}{(r+p_i-1)!(p_i-k-1)!} \frac{s_i^k \phi_i^{(k)}(s_i)}{k!}, \tag{2.33}$$

as $r \to \infty$, and where p_i are constants.

This particular theorem of Darboux [**43**, **44**] therefore provides a connection between the behaviour of the late terms of an asymptotic series and the singularities of the function they represent. The connection between the late-order terms and asymptotic series also reveals how a series expansion of a function diverges. Boyd [**24**, **25**] provides a list of heuristics, which although are not theorems, but are useful indicators of divergence for asymptotic series. One heuristic which is in close connection to Darboux's theorem states that a power series in ϵ will never converge to a function containing terms which is exponentially small in ϵ. In this case, the exponentially small terms contain (essential) singularities.

In order to show how Theorem 2.31 can be used to determine an asymptotic expansion for the late-order terms we reproduce and comment on Dingle's demonstration in [**48**]. We consider a function $\phi(s)$ which can be expanded as a Taylor series about the origin

$$\phi(s) = \sum_{r=0}^{\infty} a_r s^r, \tag{2.34}$$

which converges within a circle centered at the origin with radius R. Suppose that $\phi(s)$ is singular at the points $s = s_i$ with modulus $|s_i| \geq R$. In the neighbourhood of these singular points, the

function $\phi(s)$ can be written as

$$\phi(s) = \frac{\phi_i(s)}{(s_i - s)^{p_i}}, \tag{2.35}$$

where p_i is either a positive integer for poles or fractional for branch points and $\phi_i(s)$ can be expanded as a Taylor series about s_i. That is,

$$\phi_i(s) = \sum_{k=0}^{\infty} \frac{\phi_i^{(k)}(s_i)}{k!}(s_i - s)^k, \tag{2.36}$$

where $\phi^{(k)}$ denotes the k^{th} derivative of ϕ with respect to s. The goal is to rewrite (2.35) in terms of a series expansion about $s = 0$. By expanding $\phi(s)$ as a power series centered at the origin outside the circle of convergence we will find that the coefficients in (2.34) can be expressed as a factorial-over-power form.

Using binomial series we find that

$$(s_i - s)^{-p_i} = \frac{1}{s_i^{p_i}} \sum_{r=0}^{\infty} \binom{r + p_i - 1}{r} \left(\frac{s}{s_i}\right)^r. \tag{2.37}$$

Using (2.37) in (2.35) we find that $\phi(s)$ can be rewritten as

$$\begin{aligned} \phi(s) &= \frac{1}{(s_i - s)^{p_i}} \sum_{k=0}^{\infty} \frac{\phi_i^{(k)}(s_i)}{k!}(s_i - s)^k, \\ &= \sum_{r=0}^{\infty} \binom{r + p_i - 1}{r} \frac{s^r}{s_i^{r+p_i}} \left(\phi_i(s_i) - \frac{p_i - 1}{r + p_i - 1} s_i \phi_i'(s_i) + \cdots\right), \end{aligned} \tag{2.38}$$

for which (2.38) is a series expansion centered at the origin. The expression in (2.38) can then be used to show that

$$\phi(s) = \sum_{r=0}^{\infty} \binom{r + p_i - 1}{r} \frac{s^r}{s_i^{r+p_i}} \sum_{k=0}^{\infty} \frac{(r + p_i - k - 1)!(p_i - 1)!}{(r + p_i - 1)!(p_i - k - 1)!} \frac{s_i^k \phi_i^{(k)}(s_i)}{k!}, \tag{2.39}$$

$$\sim \sum_{r=0}^{\infty} \binom{r + p_i - 1}{r} \frac{s^r}{s_i^{r+p_i}} \left(\phi_i(s_i) + \mathcal{O}\left(\frac{1}{r}\right)\right) = \sum_{r=0}^{\infty} \frac{(r + p_i - 1)!}{r!(p_i - 1)!} \frac{s^r}{s_i^{r+p_i}} \phi_i(s_i). \tag{2.40}$$

Equation (2.39) shows that $\phi(s)$ can be re-expanded as a power series centered at the origin outside its radius of convergence. Of course, the price we pay to do this is that the resulting series expansion is divergent. More importantly, for large r, the term s_i^r in the denominator of (2.39) shows that the dominant contributions come from the singularities with smallest $|s_i|$. That is, the singularities closest to the origin of expansion.

Although the function $\phi(s)$ may be singular at more than one point, Dingle [**48**] shows that the late-order terms behaviour of the series expansion of $\phi(s)$ can be obtained in two ways. The first is to expand $\phi(s)$ about the singularity closest to the origin of expansion, to which the late terms expression is given by the sum in (2.33) for this chosen singularity. Alternatively, the behaviour

of a_r can be obtained by expanding $\phi(s)$ about every singularity, keeping only the first few terms of (2.33) and adding the contribution of each singularity. While both methods reach the same conclusion, Dingle shows that the latter option is more convenient to determine the asymptotic form of the late-order terms [**48**].

From Darboux's theorem we learn that the contribution to a_r, in (2.34), from the singularity, s_i, is given by

$$a_r \sim \frac{(r+p_i-1)!}{r!(p_i-1)!}\frac{\phi_i(s_i)}{s_i^{r+p_i}}, \tag{2.41}$$

as $r \to \infty$, which has the general form of

$$\frac{(r+\text{constant})!}{(\text{variable})^r}. \tag{2.42}$$

Dingle [**48**] was also able to extend this fact to asymptotic series and therefore the behaviour of the late-order terms are also predominantly governed by the singularities of the represented function. In our notation this means that the coefficients of the asymptotic power series in (2.6) are determined by the singularities of $f(z;\epsilon)$ closest to the origin. Generalizations of the factorial-over-power formulae described by (2.42) have also been studied in detail by Berry and Howls for the asymptotic expansion of integrals with coalescing saddles [**15**]. For a class of nonlinear problems, Chapman et al. [**32**] applied the following factorial-over-power ansatz

$$f_r(z) \sim \frac{F(z)\Gamma(r+\gamma)}{\chi(z)^{r+\gamma}}, \tag{2.43}$$

as $r \to \infty$ and where γ is a constant. This ansatz can be regarded as a generalization of (2.42), which was deduced from Darboux's theorem. According to Darboux's theorem, the function $\chi(z)$ appearing in (2.43) must encode the singularities of the function the asymptotic series represents and is therefore known as the *singulant*.

We now consider the class of asymptotic series which are factorially divergent. Factorially divergent series are asymptotic power series of the form (2.6) whose coefficients are asymptotically described by (2.43).

2.2.2. Optimally-truncated error via Borel summation.

In this section we will obtain explicit error bounds for the optimally-truncated error of an asymptotic power series using Borel summation methods. In particular, it will be shown that the optimally-truncated error of an asymptotic power series is exponentially small in the asymptotic limit.

By utilizing the integral representation of the Gamma function, Borel [**21**] observed that the sum of a divergent series could be defined as

$$\sum_{r=0}^{\infty} \epsilon^r f_r := \int_0^{\infty} e^{-t} \sum_{r=0}^{\infty} \frac{f_r}{\Gamma(r+1)} (\epsilon t)^r dt, \tag{2.44}$$

provided that the summation on the right hand side of (2.44) converges over some range of ϵt. Outside the radius of convergence, the sum under the integral of (2.44) can be analytically extended due to the multiplicative exponential factor in the integrand. Although the summation diverges, the exponential factor is exponentially small everywhere outside the radius of convergence, ensuring the convergence of the integral in (2.44). Hence, whenever this is possible, a *sum* may be assigned to an asymptotic power series and is interpreted to be the function which is asymptotic to the power series expansion. This is known as Borel's *resummation* procedure.

By Darboux's theorem, Dingle found that the coefficients terms, f_r, of (2.6) are generically proportional to a factorial of the form $\Gamma(r+\gamma)$ for sufficiently large r. In this case, we must exclude the early terms in (2.6) and introduce a modified version of Borel's resummation procedure [**37**,**48**].

Definition 2.45. *We define the Borel transform of a power series*

$$F(z;\epsilon) = \sum_{r=0}^{\infty} \epsilon^r f_r(z),$$

by

$$\mathcal{B}[F](z;t) := \sum_{r=0}^{\infty} t^r \frac{f_r(z)}{\Gamma(r+\gamma)}. \tag{2.46}$$

The Borel sum of $F(z;\epsilon)$ is defined to be

$$\mathcal{S}[F](z;\epsilon) := \int_0^{\infty} e^{-t} t^{\gamma-1} \mathcal{B}(z;\epsilon t) dt. \tag{2.47}$$

The Borel transform and Borel sum defined in Definition 2.45 are, by construction, formal inverses of each other and together constitute what is referred to as Borel's resummation method. Both Dingle [**48**] and Écalle [**52**] applied Borel summation methods in order to *resum* asymptotic series providing a sum to these series.

Recalling that the late-order terms behave as factorials, we therefore apply Borel's resummation method to the divergent tail (2.13) where the late-order terms have behaviour described by (2.43). Dingle [**48**] was the first to apply this procedure in order to show that the optimally-truncated error of a factorially divergent asymptotic series is indeed exponentially small after noting the generic behaviour of the coefficients implied by Darboux's theorem. As before we reproduce and comment upon the ideas of Dingle. The Borel transform of (2.13) is given by

$$\mathcal{B}[R_N] = \frac{F}{\chi^{\gamma}} \sum_{r=N}^{\infty} \left(\frac{t}{\chi}\right)^r, \tag{2.48}$$

where F and χ are functions of z. The Borel sum of R_N is then given by

$$\mathcal{S}[R_N] = \frac{F}{\chi^\gamma}\int_0^\infty e^{-t}t^{\gamma-1}\sum_{r=N}^{\infty}\left(\frac{\epsilon t}{\chi}\right)^r dt, \tag{2.49}$$

$$= \frac{F\epsilon^N}{\chi^{N+\gamma}}\int_0^\infty e^{-t}t^{N+\gamma-1}\frac{1}{1-\epsilon t/\chi}dt,. \tag{2.50}$$

The Borel summation procedure highlights a subtlety associated with asymptotic power series. The replacement of the series in (2.49) by its geometric sum is only valid in regions where $t < |\chi|/\epsilon$ for fixed small ϵ, but the range of integration is infinite. Hence, the asymptotic series for R_N is expected to diverge. A similar observation was noted by Boyd [**25**] in the Fourier integral representation of the solution in question. Nonetheless, outside the radius of convergence, the integrand is exponentially small and hence the integral is well defined.

We aim to find an upper bound of R_N in equation (2.50). We first note that

$$\frac{t^{N+\gamma-1}}{\epsilon t/\chi - 1} \leq \frac{t^{N+\gamma-1}}{\epsilon t/\chi},$$

for all $t \geq 0$ and fixed ϵ. Applying this upper bound to (2.50) we find that

$$\mathcal{S}[R_N] \leq -\frac{F\epsilon^{N-1}}{\chi^{N+\gamma-1}}\int_0^\infty e^{-t}t^{N+\gamma-2}dt,$$

$$= -\frac{F\epsilon^{N-1}}{\chi^{N+\gamma-1}}\Gamma(N+\gamma-1) = E(N), \tag{2.51}$$

where we have used the integral representation of the Gamma function [**2**] in order to obtain (2.51). In order to optimally truncate (2.13) we need to find the value of N such that the error bound, $E(N)$, in (2.51) is minimal. The optimal truncation point, N_{opt}, can be found by differentiating $|E(N)|$ with respect to N for fixed ϵ and finding the value of N for which the derivative is zero. The derivative of $|E(N)|$ is zero when

$$\psi(N_{\text{opt}}+\gamma-1) = \log\left(\frac{|\chi|}{\epsilon}\right), \tag{2.52}$$

where ψ is the digamma function. Following Boyd [**24**], (2.52) can be solve approximately to give

$$N_{\text{opt}} \sim \frac{|\chi|}{\epsilon}, \tag{2.53}$$

as $\epsilon \to 0$. The explicit upper bound to the optimally-truncated error can be obtained by substituting (2.53) into (2.51). Noting that the argument of the Gamma function is large, we apply Stirling's formula, which is given by (2.29), in order to show that

$$|R_N(z;\epsilon)| \leq \sqrt{\frac{2\pi}{|\chi|}}\frac{|F|}{\epsilon^{\gamma-1/2}}e^{-|\chi|/\epsilon}. \tag{2.54}$$

Hence, the optimally-truncated error of a factorially divergent asymptotic series is exponentially small in the limit $\epsilon \to 0$. We also note that this is in agreement with the calculated optimally-truncated error for the exponential integral given by (2.30) where $\chi = -z$, $F(z) = 1$ and $\gamma = 0$. Consequently, in regions where R_N is exponentially small, we say that R_N is exponentially *subdominant* relative to the leading order behaviour of (2.6).

Alternatively, the asymptotic behaviour for the optimally-truncated error may also be obtained from Definition 2.4. From Definition 2.4, the behaviour of the error is described by

$$|R_N| \sim \left|\epsilon^N f_N\right|, \tag{2.55}$$

as $\epsilon \to 0$. Replacing f_N and N by the late-order terms expression (2.43) and the optimal truncation point (2.53) in equation (2.55) we also obtain (2.54). Although these two methods come to the same conclusion, Borel summation highlights the subtle cause of divergence of an asymptotic power series and also produces explicit bounds on the error.

As the error of superasymptotic approximations are exponentially small, any behaviour which is of order $\mathcal{O}(\exp(-\alpha/\epsilon^\beta))$ is therefore contained within this error. Hence, optimal truncation of an asymptotic series therefore provides the essential step which will enable us to compute the exponentially small contributions hidden within these series. In the next section will explore how mathematical techniques known as *hyperasymptotics* or *exponential asymptotics* can be used in order to study terms hidden beyond-all-orders.

2.3. Hyperasymptotics

In Section 2.2 we showed how truncating an asymptotic series at its least term produces an error which is exponentially small in the limit $\epsilon \to 0$. However, the exponentially small terms we are interested in are not explicitly visible at the level of superasymptotics. Further analysis is still required to explicitly determine the form and behaviour of such terms.

In this section we discuss the development and demonstrate the ideas of exponential asymptotic methods, which allow behaviour occurring on an exponentially small scale to be explicitly investigated. In general, these methods form a systematic study of exponentially small behaviour. As the optimally-truncated error of factorially divergent asymptotic series are known to be exponentially small in the limit $\epsilon \to 0$, these methods can be applied to investigate this error.

One first notable step towards the investigation of exponentially small terms hidden within asymptotic power series was investigated by Dingle. By resumming the truncated error of an asymptotic power series using Borel summation, Dingle was able to express (2.50) as

$$R_N(z) = \epsilon^N f_N(z) \Lambda_{n+\gamma},$$

where

$$\Lambda_{N+\gamma} = \frac{1}{\Gamma(N+\gamma)} \int_0^\infty e^{-t} t^{N+\gamma-1} \frac{1}{1-\epsilon t/\chi} dt. \tag{2.56}$$

The expression appearing in (2.56) is one of four expressions known as Dingle's *basic terminants* [**48**]. Using his theory of terminants, Dingle showed that functions represented by factorially

divergent asymptotic power series expansions can be expressed as

'first N terms of asymptotic expansion + N^{th} term $\times$ terminant'.

Inspired by Dingle's ideas, Berry applied Borel's summation method to the optimally-truncated error of an asymptotic series [**10**, **11**] in order to study the apparent discontinuous change in the asymptotic representation of the Airy function in the complex plane. This apparent change in the asymptotic expansion of a function is generally known as the Stokes phenomenon, which we discuss further in Section 2.4.

The innovative ideas of Berry led to the subsequent development of *hyperasymptotic* methods. In 1990, Berry and Howls [**13**] were the first to develop a technique which improved upon superasymptotic expansions of Schrödinger type differential equations. The idea was to replace the coefficients appearing in the error of the superasymptotic approximation not by the leading order asymptotic behaviour of the late terms, but by its complete asymptotic expansion.

Darboux's theorem tells us the complete asymptotic expansion of the late-order terms with leading order behaviour (2.43) can be expressed by a series expansion of the form

$$f_r(z) \sim \frac{F(z)}{\chi(z)^{r+\gamma}} \sum_{k=0}^{\infty} a_k(z)\Gamma(r+\gamma-k), \tag{2.57}$$

as $r \to \infty$ where $a_0(z) = 1$. We note that the first term of (2.57) produces (2.43) to leading order. By using the complete expansion for the late-order terms, the optimally-truncated error in (2.20) can be rewritten as

$$\begin{aligned} R_N &\sim \sum_{r=N_{\text{opt}}}^{\infty} \epsilon^r f_r(z), \\ &\sim \sum_{r=N_{\text{opt}}}^{\infty} \frac{\epsilon^r F(z)}{\chi(z)^{r+\gamma}} \sum_{k=0}^{\infty} a_k(z)\Gamma(r+\gamma-k), \\ &= \frac{F(z)}{\chi(z)^{\gamma}} \sum_{r=0}^{\infty} a_r(z) \sum_{k=N_{\text{opt}}}^{\infty} \left(\frac{\epsilon}{\chi(z)}\right)^k \Gamma(k+\gamma-r), \end{aligned} \tag{2.58}$$

as $\epsilon \to 0$. Borel's resummation procedure can then be applied to the 'k-sum' appearing in equation (2.58) in order to obtain the asymptotic expansion

$$R_N = \frac{F\epsilon^{N_{\text{opt}}}}{\chi^{N_{\text{opt}}+\gamma}} \sum_{r=0}^{\infty} a_r(z) \int_0^{\infty} e^{-t} t^{N+\gamma-r-1} \frac{1}{1-\epsilon t/\chi} dt, \tag{2.59}$$

where N_{opt} is given by (2.53) as $\epsilon \to 0$. In this way an asymptotic series expansion for the optimally-truncated error is obtained. The integral expression appearing in (2.59) is precisely the expression of Dingle's terminant with $N = N_{\text{opt}}$.

The integrand in (2.59) has a singularity at $t = \chi/\epsilon$. In particular, this singularity lies of the path of integration if $\chi/\epsilon \in \mathbb{R}^+$. Since we consider $\epsilon > 0$ in this thesis, the path of integration of

(2.59) contains a singularity if $\mathrm{Re}(\chi) > 0$ and $\mathrm{Im}(\chi) = 0$. We will see in Section 2.4, that the pole structure of R_N coincides with the characterization for Stokes curves and gives rise to the Stokes phenomenon. In fact, the contribution due to the Stokes phenomenon is given by the residue of (2.59) at the singularity, which is proportional to $F(z)\exp(-\chi(z)/\epsilon)\epsilon^{-\gamma}$. This is detailed in Appendix C.

The resulting series expansion of the optimally-truncated error is also divergent and therefore the procedure of optimal truncation and resummation can also be applied to this series expansion. Repeated iterations of this procedure produces a sequence of finite series expansions, which Berry and Howls name as *hyperseries*. These hyperseries were found to involve terms of the original asymptotic series expansion and are multiplied by a multiple integral expression known as *hyperterminants*. These hyperterminants are the hyperasymptotic generalizations of Dingle's basic terminants. This method of systematically reducing the exponentially small error produces an asymptotic series expansion, which attains accuracy greater than the superasymptotic error. The resulting approximation obtained from this method is known as a *hyperasymptotic* approximation.

Subsequent papers based on the original paper by Berry and Howls [**13**] extended the method of hyperasymptotics to problems with established asymptotic results and demonstrated the applicability of the hyperasymptotic method. In [**14**], Berry and Howls considered integrals of the form

$$\int_\gamma g(z)\exp(-kf(z))dz, \tag{2.60}$$

where $|k|$ is a large parameter, f, g are analytic functions and γ is a contour passing through a saddle point of $f(z)$. Berry and Howls apply the hyperasymptotic method in order to find approximations which include exponentially small contributions due to other saddle points of $f(z)$ not present on the steepest descent contour. This study refined the method of steepest descents to include exponentially small error.

Howls [**70**] extended these results to integrals of the form (2.60) with finite endpoints, and obtained results analogous to [**14**]. As the Borel transform method falls under the class of integrals considered in [**14**, **70**], these investigations effectively established the applicability of the hyperasymptotic method for all systems that possess a Borel transform representation, regardless of their original formulation.

Following the works of both [**14**, **70**], the hyperasymptotic method was then shown to be applicable for multidimensional variants of (2.60) in [**71**] and [**46**].

2.3.1. Applications of Hyperasymptotics.

Hyperasymptotic or exponential asymptotic methods allow us to explicitly study the optimally-truncated error and also determine its asymptotic series expansion. One particular application of exponential asymptotic methods is to study behaviour known as Stokes phenomenon. Stokes phenomenon or Stokes behaviour describes the sudden appearance or disappearance of an exponentially small term within an asymptotic expansion as we cross a ray in the complex plane. The first

hyperasymptotic method developed to understand Stokes phenomenon was by Berry [**10**, **11**] who showed the change due to Stokes phenomenon in the Airy equation is continuous by investigating (2.56) in the neighbourhood of Stokes curves. This was the first demonstration of the *Stokes smoothing* technique.

Berry's ideas in [**10**,**11**] brought new insights on the role of Stokes curves, subsequently leading to the development of new methods to describe and calculate Stokes phenomenon. One particular method developed by Olde Daalhuis et al. [**121**] utilizes the method of matched asymptotic expansions in order to describe Stokes phenomenon for a certain class of linear ordinary differential equations. Without the need of Borel summation methods, the matched asymptotic expansions approach by Olde Daalhuis et al. [**121**] also shows that the variation across Stokes curves is described by the error function in agreement with Berry [**10**].

The idea is to expand the solution of the differential equation as an asymptotic power series in ϵ after which the solution is then expressed as the difference between the optimally-truncated asymptotic power series and a remainder term. In this way, the exponentially small behaviour present in the problem is isolated away from the terms which dominate it. Matched asymptotic expansions can then be used to investigate the variation of the remainder term in the neighbourhood of Stokes curves. The method presented in [**121**] is of interest when the solutions to differential equations are not expressible in terms of integral expressions.

Chapman et al. [**32**] extended the methodology presented in [**121**] to nonlinear differential equations. Chapman et al. exploit the generic factorial-over-power behaviour of the late-order terms, allowing optimal truncation methods to be applied to nonlinear problems. As the problem investigated in [**121**] is linear, the factorial-over-power ansatz is not necessary as the exact form for the coefficient terms may be determined.

Exponential asymptotic methods based on the methodology developed by Chapman et al. [**32**] were also extended for partial differential equations [**33**] and differential-difference equations [**92**].

2.4. Stokes Phenomenon

A function, $f(z)$, in some sector of the complex plane can be approximated by an asymptotic power series say

$$f(z) \sim \sum_{r=0}^{\infty} \epsilon^r f_r(z), \tag{2.61}$$

as $\epsilon \to 0$. However, the function $f(z)$ can have different asymptotic series expansions in different sectors of the complex plane since any arbitrary multiple of an asymptotic power series prefactored by an exponentially small term can be added to the asymptotic representation and such a term may not be small in all directions. Hence, when different sectors are crossed, the asymptotic expansion may appear to change discontinuously.

This discontinuous change in the asymptotic representation is due to the appearance or disappearance of exponentially small terms. This behaviour is known generally as Stokes phenomenon or Stokes behaviour. The appearance or disappearance of exponentially small terms in the asymptotic expansion is also referred to as *Stokes switching*. The curves separating two adjacent sectors in which Stokes switching occurs are known as *Stokes curves*. An example of Stokes curves for the hyper-Airy equation, which we will consider in Section 2.5, is illustrated in Figure 2.2.

In Figure 2.2 the non-shaded region denotes regions in which $Y(z) \sim Y_1(z)$ as $\epsilon \to 0$ where $Y(z)$ is a solution of the hyper-Airy equation (2.68) and where $Y_1(z)$ is given by equation (2.71). As the Stokes curve separating the non-shaded and light blue shaded regions is crossed, the asymptotic expansion of $Y(z)$ is now described by $Y(z) \sim Y_1(z) + 2\pi Y_3(z)$ as $\epsilon \to 0$. The asymptotic expansion contains a term proportional to $Y_3(z)$, which is exponentially small in this region. Continuing into the green-shaded region, another exponentially small term, $Y_2(z)$, suddenly appears, and the behaviour is now described by $Y(z) \sim Y_1(z) + 2\pi Y_3(z) + 2i\pi Y_2(z)$ as $\epsilon \to 0$. This Stokes switching behaviour will be explicitly calculated in Section 2.5.5. Similarly, Stokes behaviour is also present in the lower half plane of Figure 2.2. In Figure 2.2, the subdominant exponential, $Y_4(z)$, is switched on in the dark-blue shaded region while the subdominant exponential, $Y_1(z)$, is switched on in the pink-shaded region.

Stokes curves may be characterized in the following way. Consider the function $f(z)$ in (2.61). Then by optimal truncation methods the asymptotic expansion of $f(z)$ may be described by

$$f(z) = \sum_{r=0}^{N_{\text{opt}}-1} \epsilon^r f_r(z) + R_N(z). \tag{2.62}$$

Since the optimally-truncated error is exponentially small in ϵ we can express the remainder term in (2.62) as

$$f(z) = e^{-\chi_0(z)/\epsilon} \sum_{r=0}^{N_{\text{opt}}-1} \epsilon^r f_r(z) + \sum_i e^{-\chi_i(z)/\epsilon} \phi_i(z), \tag{2.63}$$

where $\phi_i(z)$ are formal power series in ϵ and we assume that $\text{Re}(\chi_j) > \text{Re}(\chi_i) > 0$ for $j > i$. In the expression given by (2.63), we have multiplied the optimally-truncated series by the unit prefactor, which we write as $\exp(-\chi_0/\epsilon)$ where $\chi_0(z) = 0$. We say that the exponential contribution due to χ_i, the term $\exp(-\chi_i/\epsilon)$, is exponentially subdominant compared to the leading order behaviour f_0 in regions where $\text{Re}(\chi_i) > 0$.

Olde Daalhuis et al. [**121**] describes Stokes phenomenon as the change in the remainder of an optimally-truncated asymptotic series in regions where it is comparable in size to subdominant contributions. In this way, the Stokes curves of (2.63) may be characterized by the condition

$$\text{Im}(\chi_i - \chi_j) = 0, \tag{2.64}$$

for $i \neq j$. If we are only interested in the leading order behaviour of subdominant exponentials appearing in (2.63), e.g. the case when $j = 1$, then the Stokes curves are given by

$$\text{Im}(\chi_0 - \chi_1) = \text{Im}(-\chi_1) = 0,$$

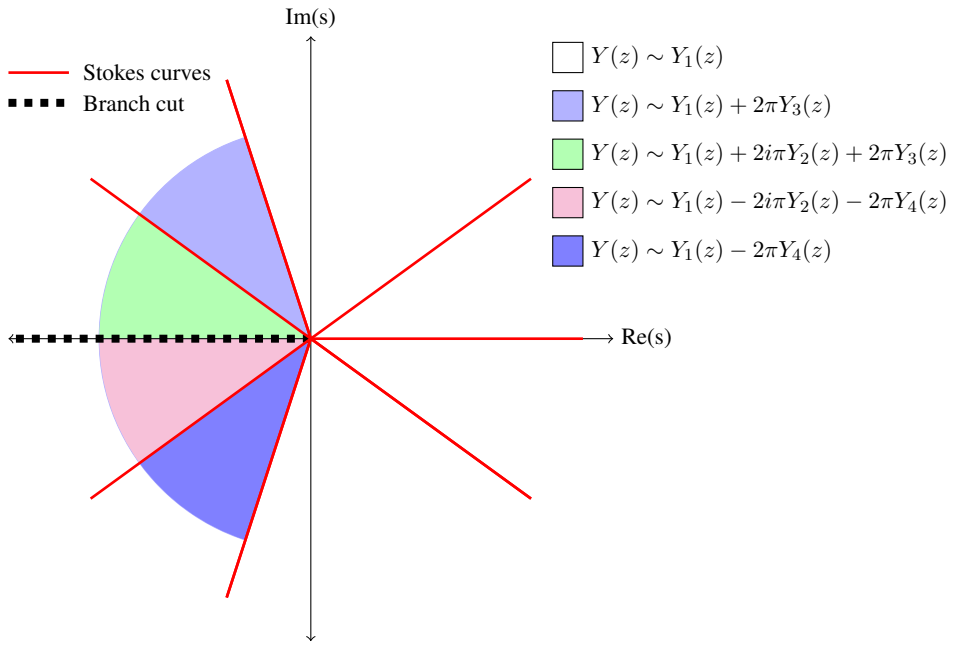

FIGURE 2.2. This figure illustrates Stokes behaviour present in the asymptotic solutions of the hyper-Airy equation as $\epsilon \to 0$. As Stokes curves (red curves) are crossed a subdominant exponential is switched on due to Stokes switching. In the non-shaded regions the asymptotic solution is described, to leading order, by the term $Y_1(z)$, which is given in (2.71). In each colour shaded region, the asymptotic behaviour of the hyper-Airy equation is described by different asymptotic series expansions. Each of these expansions differ by a term proportional to Y_j for $j = 2, 3, 4$, which is exponentially subdominant compared to Y_1.

since $\chi_0 = 0$. Hence, a Stokes curve of the leading order subdominant exponential is given by

$$\text{Im}\,(\chi_1) = 0. \tag{2.65}$$

Another curve which plays an important role in Stokes phenomenon are curves known as *anti-Stokes curves*. These are the curves across which exponential contributions exchange dominance. That is, a subdominant exponential becomes dominant and vice versa as anti-Stokes curves are crossed. As an example, when anti-Stokes curves are crossed the subdominant exponential, $e^{-\chi_1/\epsilon}$, now dominates the term f_0 in (2.63). Since f_0 is no longer the dominant behaviour for $f(z)$, anti-Stokes curves mark the boundaries of regions in which $f(z) \sim f_0(z)$ as $\epsilon \to 0$. Anti-Stokes curves may be characterized by the condition

$$\text{Re}(\chi_i - \chi_j) = 0, \tag{2.66}$$

for $i \neq j$. Similarly, if we are only interested in the leading order behaviour of subdominant exponentials appearing in (2.63), e.g. the case when $j = 1$, then the anti-Stokes curves are given

by

$$\text{Re}(\chi_0 - \chi_1) = \text{Re}(-\chi_1) = 0.$$

Hence, an anti-Stokes curve of the leading order subdominant exponential is given by

$$\text{Re}\,(\chi_1) = 0. \tag{2.67}$$

Historically, the first account of the Stokes phenomena was encountered by Stokes [**147**] in his study of the Airy function. At the time, the change in the asymptotic series expansion of the Airy function appeared to be discontinuous, presenting a paradox as the Airy function is entire, meaning it is analytic and finite at all points in the complex plane. By using exponential asymptotic methods Berry [**10**, **11**] was able to resolve this paradox, showing that variation across Stokes curves could be approximated by the continuous error function.

In the next section we demonstrate Stokes behaviour for the hyper-Airy equation. In particular, we demonstrate the exponential asymptotic method developed by Olde Daalhuis [**121**] in order to calculate such behaviour. Using this methodology, we will find asymptotic expansions of the form (2.6) whose late-order terms are given by a factorial-over-power form (2.43).

2.5. Example: the hyper-Airy equation

We now apply the ideas discussed in Sections 2.2 and 2.3 in order to study Stokes behaviour in the solutions of the hyper-Airy equation. The hyper-Airy equation is a fourth order generalization of the Airy equation [**8**]. It is given by

$$y'''' = xy, \tag{2.68}$$

where $y = y(x)$ and the prime denotes differentiation with respect to x. For the purpose of this thesis, we introduce a small parameter, ϵ, such that the limit $|x| \to \infty$ is equivalent to the limit $\epsilon \to 0$. This can be done by rescaling the variables of (2.68).

2.5.1. Rescaling the hyper-Airy equation.

We introduce ϵ by applying the rescalings

$$y(x) = \epsilon^{3/10} Y(z), \quad x = \frac{z}{\epsilon^{4/5}}. \tag{2.69}$$

We note the there is no need to introduce ϵ in this example since z scales with ϵ. This is done for pedagogical reasons as the problems considered in this thesis are formulated such that the asymptotic limit of interest is $\epsilon \to 0$. Under this choice of scalings, (2.68) can be rewritten as

$$\epsilon^4 Y'''' = zY, \tag{2.70}$$

where the prime now denotes derivatives with respect to z. We wish to study the behaviour of solutions to (2.70) as $\epsilon \to 0$, i.e. the far field behaviour of (2.68). It can be shown by the well-known WKB method [**8**, **29**, **76**, **94**, **154**] that solutions of (2.70) have the asymptotic behaviours

$$Y_j(z) \sim \frac{C_j}{z^{3/8}} \exp\left(\frac{4\omega_j z^{5/4}}{5\epsilon}\right), \tag{2.71}$$

as $\epsilon \to 0$, where C_j are arbitrary constants, $\omega_1 = -\omega_2 = -1$ and $\omega_3 = -\omega_4 = -i$. These four behaviours describe four linearly independent solutions of the hyper-Airy equation. For this demonstration, we will study solutions of (2.70) with behaviour

$$Y(z) \sim Y_1(z) = \frac{1}{z^{3/8}} \exp\left(-\frac{4z^{5/4}}{5\epsilon}\right), \tag{2.72}$$

as $\epsilon \to 0$ in some sector S_c', say, containing the positive real z axis. We may now calculate the asymptotic power series expansion as the leading order behaviours of the hyper-Airy equation have been determined.

2.5.2. Asymptotic series expansion.

In order to construct an asymptotic series expansion for $Y(z)$, we scale out the leading order behaviour by writing

$$Y(z) \sim \frac{1}{z^{3/8}} \exp\left(-\frac{4z^{5/4}}{5\epsilon}\right) g(z), \tag{2.73}$$

where $g \sim 1 + \mathcal{O}(\epsilon)$ as $\epsilon \to 0$ in S_c'. Substituting (2.73) into (2.70) we obtain the equation

$$\begin{aligned} -4z^{3/4}\epsilon g^{(1)} &+ \epsilon^2\left(6z^{1/2}g^{(2)} - \frac{3}{2z^{1/2}}g^{(1)} + \frac{45}{32z^{11/4}}g\right), \\ &+ \epsilon^3\left(-4z^{1/4}g^{(3)} + \frac{3}{z^{3/4}}g^{(2)} - \frac{69}{16z^{7/4}}g^{(1)} + \frac{225}{64z^{11/4}}g\right), \\ &+ \epsilon^4\left(g^{(4)} - \frac{3}{2z}g^{(3)} + \frac{99}{32z^2}g^{(2)} - \frac{627}{128z^3}g^{(1)} + \frac{16929}{4096z^4}g\right) = 0, \end{aligned} \tag{2.74}$$

where the superscripts '(j)' denote the j-th derivative with respect to z. We expand $g(z)$ as an asymptotic power series in ϵ by writing

$$g(z) = \sum_{r=0}^{\infty} \epsilon^r g_r(z). \tag{2.75}$$

By substituting (2.75) into (2.74) and equating powers of ϵ we find that the first few terms are given by

$$g_0 = 1, \quad g_1 = -\frac{9}{32z^{5/4}}, \quad g_2 = \frac{441}{2048z^{5/2}}, \quad g_3 = -\frac{30303}{327680z^{15/4}}. \tag{2.76}$$

We observe from (2.76) that the coefficients $g_1(z), g_2(z)$ and $g_3(z)$ are singular at $z = 0$. In general, the coefficients of (2.75) satisfy the following recurrence relation

$$\begin{aligned} 4z^{3/4}g_{r-1}^{(1)} &= 6z^{1/2}g_{r-2}^{(2)} - \frac{3}{2z^{1/2}}g_{r-2}^{(1)} + \frac{45}{32z^{11/4}}g_{r-2}, \\ &- 4z^{1/4}g_{r-3}^{(3)} + \frac{3}{z^{3/4}}g_{r-3}^{(2)} - \frac{69}{16z^{7/4}}g_{r-3}^{(1)} + \frac{225}{64z^{11/4}}g_{r-3}, \\ &+ g_{r-4}^{(4)} - \frac{3}{2z}g_{r-4}^{(3)} + \frac{99}{32z^2}g_{r-4}^{(2)} - \frac{627}{128z^3}g_{r-4}^{(1)} + \frac{16929}{4096z^4}g_{r-4}, \end{aligned} \tag{2.77}$$

for integers $r \geq 4$. By recursively solving (2.77) we may uniquely determine the coefficients $g_r(z)$ with appropriate boundary conditions, and hence obtain an asymptotic power series expansion for the solutions of the hyper-Airy equation. This is not practical since the calculation of later terms become increasingly laborious. Instead we apply the factorial-over-power ansatz used by Chapman et al. [**32**] to determine the asymptotic behaviour of the late-order terms in the limit $r \to \infty$.

2.5.3. Late-order terms analysis.

The first few coefficients in (2.76) reveal that they contain a singularity at $z = 0$. From (2.77) we observe that the calculation of successive coefficients involve repeated differentiation of the previous terms. Consequently, the *strength* of the singularity, that is, the order of the singularity, increases for each derivative taken. Hence, the asymptotic behaviour of the late-order terms will be a factorial-over-power form described in (2.43).

We therefore assume that the coefficient, g_r, is described by the factorial-over-power ansatz,

$$g_r \sim \frac{G\Gamma(r+\gamma)}{\chi^{r+\gamma}}, \tag{2.78}$$

as $r \to \infty$, where G and χ are functions of z. The first two derivatives of (2.78) are calculated below

$$\begin{aligned}
g_r' &\sim \frac{(-\chi')G\Gamma(r+\gamma+1)}{\chi^{r+\gamma+1}} + \frac{G'\Gamma(r+\gamma)}{\chi^{r+\gamma}}, \\
g_r'' &\sim \frac{(-\chi')^2 G\Gamma(r+\gamma+2)}{\chi^{r+\gamma+2}} + \left(2(-\chi')G' + (-\chi'')G\right)\frac{\Gamma(r+\gamma+1)}{\chi^{r+\gamma+1}} + \frac{G''\Gamma(r+\gamma)}{\chi^{r+\gamma}}.
\end{aligned}$$

In general, it can be shown using induction that the j^{th} derivative of (2.78) is given by

$$\begin{aligned}
\frac{d^j}{dz^j}\left(\frac{G\Gamma(r+\gamma)}{\chi^{r+\gamma}}\right) &\sim \frac{(-\chi')^j G\Gamma(r+\gamma+j)}{\chi^{r+\gamma+j}} + \binom{j}{1}\frac{(-\chi')^{j-1}G'\Gamma(r+\gamma+j-1)}{\chi^{r+\gamma+j-1}}, \\
&\quad + \binom{j}{2}\frac{(-\chi')^{j-2}(-\chi'')G\Gamma(r+\gamma+j-1)}{\chi^{r+\gamma+j-1}} + \mathcal{O}(\Gamma(r+\gamma+j-2)), \\
&= (-\chi')^j g_{r+j}, \\
&\quad + \left(\binom{j}{1}(-\chi')^{j-1}\frac{G'}{G} + \binom{j}{2}(-\chi')^{j-2}(-\chi'')\right) g_{r+j-1} + \mathcal{O}(g_{r+j-2}),
\end{aligned} \tag{2.79}$$

as $r \to \infty$ and where we have used the notation $\mathcal{O}(g_r)$ to be equivalent to $\mathcal{O}(\Gamma(r+\gamma)\chi^{-r-\gamma})$ as $r \to \infty$. Applying (2.78) into (2.77) we obtain

$$\begin{aligned}
&6z^{1/2}\left((\chi')^2 g_r + (-2\chi'\frac{G'}{G} - \chi'')g_{r-1}\right) + \frac{3}{2z^{1/2}}\chi' g_{r-1},\\
&-4z^{1/4}\left(-(\chi')^3 g_r + (3(\chi')^2\frac{G'}{G} + 3\chi'\chi'')g_{r-1}\right) + \frac{3}{z^{3/4}}(\chi')^2 g_{r-1},\\
&(\chi')^4 g_r + \left(-4(\chi')^3\frac{G'}{G} - 6(\chi')^2\chi''\right)g_{r-1} + \frac{3}{2z}(\chi')^3 g_{r-1} + \cdots,\\
&\sim 4z^{3/4}\left(-\chi' g_r + \frac{G'}{G}g_{r-1}\right),
\end{aligned} \tag{2.80}$$

where the neglected terms are of order $\mathcal{O}(g_{r-2})$ as $r \to \infty$. By matching orders of $\mathcal{O}(g_r)$ as $r \to \infty$, we will obtain equations which allow us to determine the singulant and prefactor of the late-order terms, (2.78).

2.5.3.1. *Calculating the singulant, χ.*

Matching terms of order $\mathcal{O}(g_r)$ in (2.80) we find the leading order equation is given by

$$-4z^{3/4}(-\chi') + 6z^{1/2}(-\chi')^2 - 4z^{1/4}(-\chi')^3 + (-\chi')^4 = 0, \quad \chi(0) = 0, \tag{2.81}$$

where the last condition arises because $\chi(z)$ must vanish at the singularities of $g_r(z)$. Since (2.81) is a quartic polynomial in χ' we may solve for χ' in order to find

$$\chi' = -2z^{1/4}, \quad \chi' = -(1+i)z^{1/4}, \quad \chi' = -(1-i)z^{1/4} \quad \chi' = 0,$$

which are all subject to the condition $\chi(0) = 0$. From these equations, it can be shown that

$$\chi_1 = -\frac{8z^{5/4}}{5}, \quad \chi_2 = -\frac{4}{5}(1+i)z^{5/4}, \quad \chi_3 = -\frac{4}{5}(1-i)z^{5/4}. \tag{2.82}$$

We note that although equation (2.81) admits the solution $\chi = 0$, we reject this solution since (2.43) would be undefined.

2.5.3.2. *Calculating the prefactor, G.*

As the singulant χ has been determined in Section 2.5.3.1 we are now able to determine the form of the prefactor, G. Matching terms of $\mathcal{O}(g_{r-1})$ in (2.80) gives the equation

$$\begin{aligned}
4z^{3/4}\frac{G'}{G} &= -4(\chi')^3\frac{G'}{G} - 6(\chi')^2\chi'' + \frac{3}{2z}(\chi')^3 + \frac{3}{z^{3/4}}(\chi')^2,\\
&\quad + 6z^{1/2}\left(-2\chi'\frac{G'}{G} - \chi''\right) + \frac{3}{2z^{1/2}}\chi' - 4z^{1/4}\left(3(\chi')^2\frac{G'}{G} + 3\chi'\chi''\right),
\end{aligned} \tag{2.83}$$

which can be simplified to give

$$\frac{G'}{G} = \frac{3(4z\chi'' - \chi')}{8z(\chi' + z^{1/4})}. \tag{2.84}$$

As the singulant expressions were calculated in Section 2.5.3.1, we may then solve (2.84). As each of the singulants are proportional to $z^{5/4}$ we find that

$$4z\chi'' - \chi' = 0,$$

for each singulant. Therefore, the solution of (2.84) for each choice of χ_i is

$$G_1 = \Lambda_1, \quad G_2 = \Lambda_2, \quad G_3 = \Lambda_3, \tag{2.85}$$

where Λ_i are constants. Hence we find that the leading order behaviour of the late-order terms is given by

$$g_r(z) \sim \frac{\Lambda_1\Gamma(r+\gamma_1)}{(-8z^{5/4}/5)^{r+\gamma_1}} + \frac{\Lambda_2\Gamma(r+\gamma_2)}{(-4(1+i)z^{5/4}/5)^{r+\gamma_2}} + \frac{\Lambda_3\Gamma(r+\gamma_3)}{(-4(1-i)z^{5/4}/5)^{r+\gamma_3}}, \tag{2.86}$$

as $r \to \infty$. The expression of the late-order terms (2.86) is therefore composed of three terms. We note that in the limit $r \to \infty$ and for real z, the late-order terms expression are dominated by the contributions which come from χ_2 and χ_3 since $|\chi_2| = |\chi_3| < |\chi_1|$. Consequently, we may write

$$g_r(z) \sim \frac{\Lambda_2\Gamma(r+\gamma_2)}{(-4(1+i)z^{5/4}/5)^{r+\gamma_2}} + \frac{\Lambda_3\Gamma(r+\gamma_3)}{(-4(1-i)z^{5/4}/5)^{r+\gamma_3}}, \tag{2.87}$$

as $r \to \infty$. In Section 2.5.5 we will discover that exponentially small contributions hidden within (2.75) are proportional to $\exp(-\chi/\epsilon)$. Therefore the exponential contributions associated with χ_2 and χ_3 are subdominant whereas the exponential contribution associated with χ_1 is sub-subdominant in regions where $\mathrm{Re}(z) > 0$.

In order to completely determine the form of the late-order terms we must also determine the values of γ_j and Λ_j. This can be done by matching the late-order expression given in (2.86) to the leading order behaviour in the neighbourhood of the singularity.

2.5.3.3. *Calculating the value of γ_i.*

To determine the correct values of γ_i in (2.86) we recall that g_1 has a pole at $z = 0$ of strength $5/4$. Since the dominant behaviour of (2.77) is given by the dominant balance

$$4z^{3/4}g'_{r-1} \sim 6z^{1/2}g''_{r-2}, \tag{2.88}$$

as $r \to \infty$, it follows that the set of singular points of g_r will be the same as that of g_1 for all r. Furthermore, we deduce from (2.88) that if g_{r-1} has a singularity at s_0 with strength ν then g_r will be singular at s_0 with strength $\nu + 5/4$.

Hence, since we know that g_1 is singular at $z = 0$ with strength $5/4$, this implies that g_r will be singular at $z = 0$ with strength $5r/4$. For consistency in the singular behaviour of the late-order terms expression, (2.86), we require that $5(r+\gamma_j)/4 = 5r/4$ for $j = 1, 2, 3$ and therefore

$$\gamma_j = 0,$$

for $j = 1, 2, 3$.

2.5.3.4. *Calculating the value of* Λ.

The value of Λ_2 and Λ_3 in (2.87) can be numerically determined as follows. We first multiply (2.87) by i and rearrange the expression to obtain

$$i2^{r/2}\frac{g_r(z)}{\Gamma(r)}\left(-\frac{4z^{5/4}}{5}\right)^r \sim i\Lambda_2 e^{-i\pi r/4} + i\Lambda_3 e^{i\pi r/4}, \tag{2.89}$$

as $r \to \infty$. By appropriately adding (or subtracting) successive terms in (2.89) we can obtain formulas for the constants Λ_j, in the limit $r \to \infty$. Doing this, we obtain

$$2i\Lambda_2 = \lim_{r\to\infty}\left(-\frac{4\sqrt{2}z^{5/4}}{5e^{-i\pi/4}}\right)^r\left[\frac{ig_r(z)}{\Gamma(r)} - \left(-\frac{4\sqrt{2}z^{5/4}}{5}\right)^2\frac{g_{r+2}(z)}{\Gamma(r+2)}\right], \tag{2.90}$$

$$2i\Lambda_3 = \lim_{r\to\infty}\left(-\frac{4\sqrt{2}z^{5/4}}{5e^{i\pi/4}}\right)^r\left[\frac{ig_r(z)}{\Gamma(r)} + \left(-\frac{4\sqrt{2}z^{5/4}}{5}\right)^2\frac{g_{r+2}(z)}{\Gamma(r+2)}\right]. \tag{2.91}$$

By using the recurrence relation (2.77) in order to compute a sufficiently large number of terms, g_r, we can then use equations (2.90) and (2.91) to numerically determine the values of Λ_2 and Λ_3. We computed the first 1000 g_r terms to find that

$$\Lambda_2 \approx 0.1125 + 0.1125i, \tag{2.92}$$

$$\Lambda_3 \approx 0.1125 - 0.1125i. \tag{2.93}$$

We note that the results from (2.90) and (2.91) are possible because the singularities of χ_2 and χ_3 are equidistant to the origin. In this example, the singularities are all located at the origin, $z = 0$. If this is not the case, the methods outlined by Olde Daalhuis [**117**] can be applied to determine the values of Λ_i.

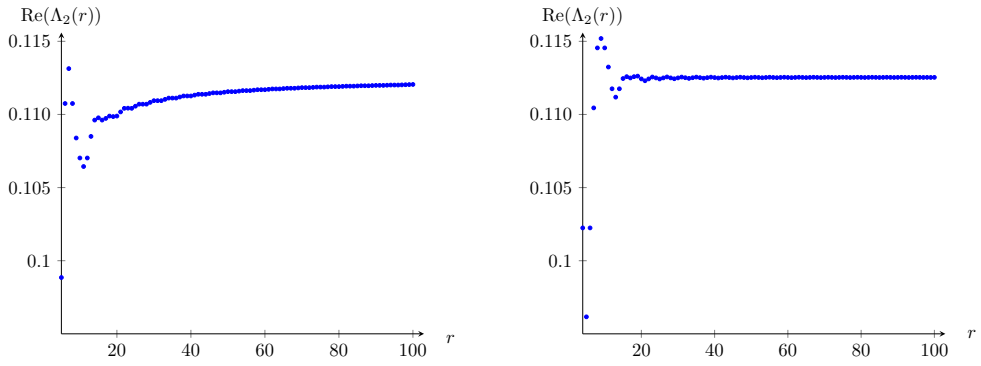

(A) Real part of Λ_2. (B) Imaginary part of Λ_2.

FIGURE 2.3. This figure illustrates the approximation for Λ_2 in (2.87). We see that as r increases, the approximation for Λ_2 tends to the limiting value calculated to be approximately $0.1125 + 0.1125i$.

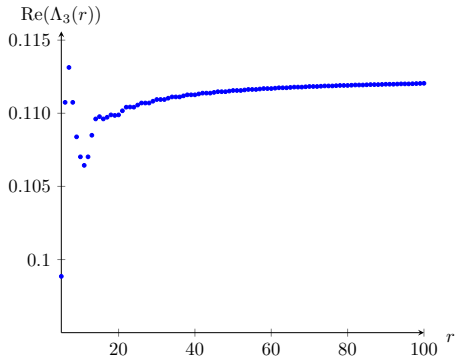

(A) Real part of Λ_3.

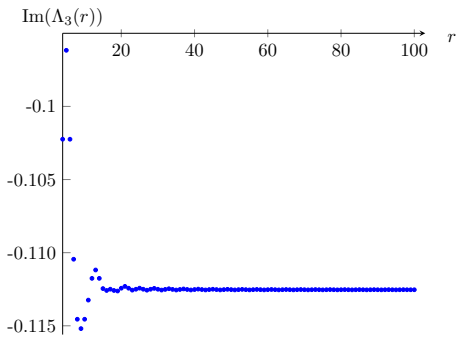

(B) Imaginary part of Λ_3.

FIGURE 2.4. This figure illustrates the approximation for Λ_3 in (2.87). We see that as r increases, the approximation for Λ_3 tends to the limiting value calculated to be approximately $0.1125 - 0.1125i$.

2.5.4. Optimal truncation.

Since the asymptotic behaviour of the late-order terms is composed of three terms, the series (2.75) can be separated into three component asymptotic series, that is,

$$g(s) \sim \sum_{r=0}^{\infty} \frac{\epsilon^r \Lambda_1 \Gamma(r)}{(-8z^{5/4}/5)^r} + \sum_{r=0}^{\infty} \frac{\epsilon^r \Lambda_2 \Gamma(r)}{(-4(1+i)z^{5/4}/5)^r} + \sum_{r=0}^{\infty} \frac{\epsilon^r \Lambda_3 \Gamma(r)}{(-4(1-i)z^{5/4}/5)^r}, \tag{2.94}$$

as $\epsilon \to 0$. Let us denote in (2.94) the first component series by $G_1(z)$, the second component series by $G_2(z)$ and the third component series by $G_3(z)$. In order to optimally truncate (2.94) we truncate one of the three component asymptotic series, G_j. The subsequent analysis will be performed for general χ and F with the particular choice made afterwards. Using the heuristic (2.25) we find that optimal truncation point of the component series G_j is given by

$$N_{\text{opt},j} \sim \frac{|\chi_j|}{\epsilon},$$

as $\epsilon \to 0$. To ensure that the optimal truncation point is integer valued we set

$$N_{\text{opt},j} = \frac{|\chi_j|}{\epsilon} + \kappa_j, \tag{2.95}$$

where $\kappa_j \in [0, 1)$. Then, the optimal truncation of the asymptotic power series (2.75) is given by

$$g(z) = \sum_{r=0}^{N_{\text{opt}}-1} \epsilon^r g_r(z) + R_N(z), \tag{2.96}$$

where R_N is the optimally-truncated error.

2.5.5. Analysis of the remainder using exponential asymptotics.

In order to study the exponentially small contributions present in (2.96) we investigate R_N. Substituting (2.96) into (2.74) and using equation (2.77) to cancel terms we find that

$$\begin{aligned}
&-4z^{3/4}\epsilon R_N^{(1)} + \epsilon^2\left(6z^{1/2}R_N^{(2)} - \frac{3}{2z^{1/2}}R_N^{(1)} + \frac{45}{32z^{11/4}}R_N\right),\\
&+\epsilon^3\left(-4z^{1/4}R_N^{(3)} + \frac{3}{z^{3/4}}R_N^{(2)} - \frac{69}{16z^{7/4}}R_N^{(1)} + \frac{225}{64z^{11/4}}R_N\right),\\
&+\epsilon^4\left(R_N^{(4)} - \frac{3}{2z}R_N^{(3)} + \frac{99}{32z^2}R_N^{(2)} - \frac{627}{128z^3}R_N^{(1)} + \frac{16929}{4096z^4}R_N\right) \sim -4z^{3/4}\epsilon^{N+1}g_N' + \cdots,
\end{aligned} \tag{2.97}$$

as $\epsilon \to 0$. We have seen in Section 2.2 that the optimally-truncated error is proportional to the first neglected term, that is, $R_N = \mathcal{O}(\epsilon^N g_N)$. Hence we may neglect higher order correction terms in ϵ, which are of order $\mathcal{O}(\epsilon^{N+2}g_{N+2})$ as $\epsilon \to 0$. We first consider the term on the right-hand side of equation (2.97). By replacing g_N by its asymptotic behaviour (2.86), we find that the inhomogeneous term in (2.97) can be written as

$$\begin{aligned}
-4z^{3/4}\epsilon^{N+1}g_N' &\sim -4z^{3/4}\epsilon^{N+1}\frac{d}{dz}\frac{\Lambda\Gamma(N)}{\chi^N},\\
&= -4z^{3/4}\epsilon^{N+1}\left(\frac{(-\chi')\Lambda\Gamma(N+1)}{\chi^{N+1}}\right),\\
&= 4z^{3/4}\epsilon^{N+1}\frac{\chi'\Lambda\Gamma(N+1)}{\chi^{N+1}},\\
&= 4z^{3/4}\epsilon^{N+1}\chi' g_{N+1},
\end{aligned} \tag{2.98}$$

as $\epsilon \to 0$. By using Stirlings formula, which is given by (2.29), and substituting the optimal truncation point (2.95) into (2.98) we find that inhomogeneous term is asymptotically given by

$$\begin{aligned}
-4z^{3/4}\epsilon^{N+1}g_N' &\sim 4z^{3/4}\epsilon^{|\chi|/\epsilon+\kappa+1}\frac{\chi'\Lambda\Gamma\left(\frac{|\chi|}{\epsilon}+\kappa+1\right)}{\chi^{|\chi|/\epsilon+\kappa+1}},\\
&\sim 4z^{3/4}\epsilon^{|\chi|/\epsilon+\kappa+1}\frac{\chi'\Lambda}{\chi^{|\chi|/\epsilon+\kappa+1}}\sqrt{2\pi}e^{-|\chi|/\epsilon}\left(\frac{|\chi|}{\epsilon}\right)^{|\chi|+\kappa+1/2},\\
&= 4z^{3/4}\epsilon^{1/2}\frac{\chi'\Lambda}{\chi^{|\chi|/\epsilon+\kappa+1}}\sqrt{2\pi}e^{-|\chi|/\epsilon}\,|\chi|^{|\chi|+\kappa+1/2},
\end{aligned} \tag{2.99}$$

as $\epsilon \to 0$. From (2.99) we find that the inhomogeneous term of (2.97) is exponentially small everywhere except in the neighbourhood of the Stokes curve. Hence, away from Stokes curves, equation (2.97) can be approximated by its homogeneous version in the limit $\epsilon \to 0$. We therefore seek a solution to the homogeneous version of (2.97). We apply the WKB ansatz

$$R_N(z) = a(z)e^{b(z)/\epsilon}, \tag{2.100}$$

for the homogeneous solution of equation (2.97). We call $a(z)$ and $b(z)$ the *WKB amplitude factor* and *WKB phase factor* of (2.100), respectively. The first few derivatives of the WKB ansatz are calculated below

$$R_N' = \frac{b'}{\epsilon}R_N + \frac{a'}{a}R_N,$$
$$R_N'' = \left(\frac{b'}{\epsilon}\right)^2 R_N + 2\left(\frac{b'}{\epsilon}\right)\frac{a'}{a}R_N + \left(\frac{b''}{\epsilon}\right)R_N + \frac{a''}{a}R_N,$$

etc. In general, it can be shown using mathematical induction that the j^{th} derivative of the WKB ansatz (2.100) is given by

$$\frac{d^j}{dz^j}(ae^{b/\epsilon}) \sim \left(\frac{b'}{\epsilon}\right)^j R_N + \left(\binom{j}{1}\left(\frac{b'}{\epsilon}\right)^{j-1}\frac{a'}{a} + \binom{j}{2}\left(\frac{b'}{\epsilon}\right)^{j-2}\left(\frac{b''}{\epsilon}\right)\right)R_N + \mathcal{O}\left(\frac{R_N}{\epsilon^{j-2}}\right), \tag{2.101}$$

as $\epsilon \to 0$. Substituting the ansatz (2.100) into the homogeneous version of (2.97) gives

$$\begin{aligned} 0 = &-4z^{3/4}\epsilon\left(\frac{b'}{\epsilon}+\frac{a'}{a}\right)R_N + 6z^{1/2}\epsilon^2\left(\left(\frac{b'}{\epsilon}\right)^2 + 2\frac{b'}{\epsilon}\frac{a'}{a} + \frac{b''}{\epsilon}\right)R_N - \frac{3\epsilon^2}{2z^{1/2}}\frac{b'}{\epsilon}R_N, \\ &- 4z^{1/4}\epsilon^3\left(\left(\frac{b'}{\epsilon}\right)^3 + 3\left(\frac{b'}{\epsilon}\right)^2\frac{a'}{a} + 3\frac{b'}{\epsilon}\frac{b''}{\epsilon}\right)R_N + \frac{3\epsilon^3}{z^{3/4}}\left(\frac{b'}{\epsilon}\right)^2 R_N, \\ &+ \epsilon^4\left(\left(\frac{b'}{\epsilon}\right)^4 + 4\left(\frac{b'}{\epsilon}\right)^3\frac{a'}{a} + 6\left(\frac{b'}{\epsilon}\right)^2\frac{b''}{\epsilon}\right)R_N - \frac{3\epsilon^4}{2z}\left(\frac{b'}{\epsilon}\right)^3 + \mathcal{O}(\epsilon^2 R_N), \end{aligned} \tag{2.102}$$

as $\epsilon \to 0$. By matching terms of $\mathcal{O}(R_N)$ as $\epsilon \to 0$ in equation (2.102) we find that the leading order equation is given by

$$\mathcal{O}(R_N): \quad -4z^{3/4}b' + 6z^{1/2}(b')^2 - 4z^{1/2}(b')^3 + (b')^4 = 0. \tag{2.103}$$

Continuing to the next order, we match terms of $\mathcal{O}(\epsilon R_N)$ to find that

$$\begin{aligned} 4z^{3/4}\frac{a'}{a} = &\, 4(b')^3\frac{a'}{a} + 6(b')^2 b'' - \frac{3}{2z}(b')^3, \\ &+ 6z^{1/2}\left(2b'\frac{a'}{a} + b''\right) - \frac{3}{2z^{1/2}}b' - 4z^{1/4}\left(3(b')^2\frac{a'}{a} + 3b'b''\right) + \frac{3}{z^{3/4}}(b')^2. \end{aligned} \tag{2.104}$$

By comparing equation (2.103) to the singulant equation (2.81) we find that they coincide provided that WKB phase factor, $b(z)$, is equal to $-\chi(z)$. Similarly, comparison between equations (2.104) and (2.83) show that $G(s)$ and $a(s)$ satisfy the same first order differential equation and hence the WKB amplitude factor, $a(s)$, is a constant. The homogeneous solutions of (2.97) are therefore given by

$$R_{N,\text{hom}}(s) \sim C_j e^{-\chi_j(s)/\epsilon}, \tag{2.105}$$

as $\epsilon \to 0$ for $j = 1, 2, 3$ and where C_j is an arbitrary constant. Hence, by truncating the j^{th} component series in (2.94) optimally, we obtain an error which is exponentially small in the limit $\epsilon \to 0$ in regions where $\text{Re}(\chi_j) > 0$ for $j = 1, 2, 3$.

2.5.5.1. *Stokes smoothing.*

In the following analysis we will investigate Stokes behaviour associated with the subdominant exponentials. In Section 2.5.3 we found that $|\chi_1| > |\chi_2| = |\chi_3|$. Consequently, we learn from (2.105) that the exponential contributions associated with χ_1 is exponentially smaller than the exponential contributions associated with χ_2 and χ_3. Hence, the exponential contribution associated with χ_2 and χ_3 are subdominant while the exponential contribution associated with χ_1 is sub-subdominant. Consequently, there will be a component asymptotic series multiplied by the sub-subdominant exponential contained within (2.96). This will also display Stokes behaviour induced by the leading order term g_0.

Away from the Stokes curves, R_N is described asymptotically by $R_{N,\text{hom}}$ in the limit $\epsilon \to 0$. However in the neighbourhood of Stokes curves, R_N exhibits Stokes phenomena and is therefore no longer described by $R_{N,\text{hom}}$. In order to capture the Stokes behaviour of R_N we write

$$R_N = \mathcal{S}_j \Lambda_j R_{N,\text{hom}}, \tag{2.106}$$

where we include Λ_j for algebraic convenience. The function $\mathcal{S}_j = \mathcal{S}_j(z)$ has variations taking place only in the neighbourhood of Stokes curves and therefore constant otherwise. The function $\mathcal{S}$ is referred as the *Stokes multiplier*. Substitution of (2.106) into equation (2.97) gives

$$\begin{aligned}\epsilon\Bigg(&-4z^{3/4}\frac{\mathcal{S}'}{\mathcal{S}} - 4(\chi')^3\frac{\mathcal{S}'}{\mathcal{S}} - 6(\chi')^2\chi'' + \frac{3}{2z}(\chi')^3 - 6z^{1/2}\left(2\chi'\frac{\mathcal{S}'}{\mathcal{S}} + \chi''\right), \\ &+ \frac{3}{2z^{1/2}}\chi' - 4z^{1/4}\left(3(\chi')^2\frac{\mathcal{S}'}{\mathcal{S}} + 3\chi'\chi''\right) + \frac{3}{z^{3/4}}(\chi')^2\Bigg)R_N \sim 4z^{3/4}\epsilon^{N+1}\chi' g_{N+1} + \cdots,\end{aligned} \tag{2.107}$$

as $\epsilon \to \infty$. Simplification of (2.107) gives

$$\begin{aligned}\mathcal{S}_j' &\sim -\frac{z^{3/4}}{(z^{1/4}+\chi_j')^3}\frac{\chi_j'\epsilon^N g_{N+1}}{\Lambda_j}e^{\chi_j/\epsilon}, \\ &\sim -\frac{z^{3/4}}{(z^{1/4}+\chi_j')^3}\frac{\chi_j'\epsilon^N\Gamma(N+1)}{\chi_j^{N+1}}e^{\chi_j/\epsilon},\end{aligned} \tag{2.108}$$

as $\epsilon \to 0$. Since the singulants are explicitly given in equation (2.82) we find that the term

$$\frac{z^{3/4}}{(z^{1/4}+\chi_j')^3} = \begin{cases} -1 & =: K_1, \quad \text{for } j = 1, \\ -i & =: K_2, \quad \text{for } j = 2, \\ i & =: K_3, \quad \text{for } j = 3, \end{cases}$$

and hence we may replace this term by the constant K_j for the particular choice of χ_j. We first make a change of variable to write $\mathcal{S}$ as a function of χ instead of s. Under this change of variables, equation (2.108) becomes

$$\frac{d\mathcal{S}_j}{d\chi_j} \sim -\frac{K_j\epsilon^N\Gamma(N+1)}{\chi_j^{N+1}}e^{\chi_j/\epsilon}, \tag{2.109}$$

as $\epsilon \to \infty$. Noting the form of the optimal truncation point, (2.95), we then make the change of variables $\chi_j = re^{i\theta}$ and restrict ourselves to curves with fixed r. The fast variations in the remainder term of (2.96) is captured as the phase of z varies. Consequently, in order to capture the Stokes behaviour we investigate variations with respect to θ. This transformation gives

$$\frac{d}{d\chi} = \frac{1}{ire^{i\theta}}\frac{d}{d\theta}$$

and hence equation (2.109) can be rewritten as

$$\frac{d\mathcal{S}_j}{d\theta} \sim -ire^{i\theta}K_j\frac{\epsilon^{r/\epsilon+\kappa_j}}{(re^{i\theta})^{r/\epsilon+\kappa_j+1}}\Gamma\left(\frac{r}{\epsilon}+\kappa_j+1\right)\exp\left(\frac{re^{i\theta}}{\epsilon}\right), \tag{2.110}$$

as $\epsilon \to 0$ where we have replaced N_{opt} by (2.95). Applying Stirling's formula (2.29) to (2.110) we obtain after simplification

$$\frac{d\mathcal{S}_j}{d\theta} \sim -\frac{iK_j}{\sqrt{\epsilon}}\sqrt{2\pi r}\exp\left(\frac{r}{\epsilon}(e^{i\theta}-1-i\theta)+i\theta\kappa_j\right), \tag{2.111}$$

as $\epsilon \to 0$. We see from equation (2.111) that the variation of $\mathcal{S}_j$ is exponentially small almost everywhere except when

$$e^{i\theta} - 1 - i\theta = 0,$$

which occurs when $\theta = 0$. In view of the transformation $\chi = re^{i\theta}$, this value of θ occurs when χ is purely real and positive. We note that this coincides with the characterization of Stokes curve given by condition (2.64). Hence, we find that the variation of $\mathcal{S}$ indeed occurs in the neighbourhood of the Stokes curves.

To investigate the variation in the neighbourhood of $\theta = 0$, we rescale the problem by setting $\theta = \sqrt{\epsilon}\phi$. By applying this choice of rescaling in θ we find that the variation in the neighbourhood of $\theta = 0$ is given by the equation

$$\frac{d\mathcal{S}_j}{d\phi} \sim -iK_j\sqrt{2\pi r}e^{-r\phi^2/2}, \tag{2.112}$$

as $\epsilon \to 0$. By integrating equation (2.112) we find that

$$\begin{aligned}\mathcal{S}_j &\sim -iK_j\sqrt{2\pi}\left(\int_{-\infty}^{\phi\sqrt{r}} e^{-x^2/2}dx + D_j\right),\\ &= -iK_j\pi\left(\text{erf}\left(\theta\sqrt{\frac{r}{2\epsilon}}\right)+\hat{D}_j\right),\end{aligned} \tag{2.113}$$

as $\epsilon \to 0$ and $\hat{D}_j = \sqrt{2/\pi}D_j$ where D_j is an arbitrary constant. The variation of $\mathcal{S}_j$, to leading order, is described by the error function [**1**] and is therefore indeed continuous. Furthermore, we find that Stokes switching occurs over an interval of size $\mathcal{O}(\sqrt{\epsilon})$ centered at Stokes curve described by $\theta = 0$. From equation (2.113) we find that the Stokes multiplier also contain a free parameter in the form of $\hat{D}_j$.

Away from the Stokes curve ($\theta = 0$) we find that the change in $\mathcal{S}$ is given by

$$\begin{aligned}\Delta\mathcal{S} &:= \mathcal{S}^+ - \mathcal{S}^-, \\ &= -iK_j\sqrt{2\pi}\int_{-\infty}^{\infty} e^{-x^2/2}dx, \\ &= -2i\pi K_j, \end{aligned} \tag{2.114}$$

and therefore

$$\begin{aligned}\Delta R_N &:= R_N^+ - R_N^-, \\ &= -2i\pi K_j e^{-\chi_j/\epsilon}, \end{aligned} \tag{2.115}$$

where R_N^+ and R_N^- denote R_N in regions where $\mathrm{Im}(\chi) > 0$ and $\mathrm{Im}(\chi) < 0$, respectively. We will use the notation $\Delta\mathcal{S}$ to denote the jump in Stokes multipliers across Stokes curves throughout this thesis. Hence, the asymptotic power series expansion of the solution of (2.74) containing exponentially small corrections is given by

$$g(z) \sim \sum_{r=0}^{N_{\text{opt}}-1} \epsilon^r g_r - \sum_{j=1}^{3} iK_j\sqrt{2\pi}\left(\text{erf}\left(\theta\sqrt{\frac{r}{2\epsilon}}\right) + \hat{D}_j\right)\Lambda_j e^{-\chi_j/\epsilon}, \tag{2.116}$$

as $\epsilon \to 0$ and N_{opt} the optimal truncation point. Therefore, we find an asymptotic solution to (2.70) which is described by

$$\begin{aligned}Y(z) &\sim \frac{1}{z^{3/8}}\exp\left(\frac{-4z^{5/4}}{5\epsilon}\right)\left(\sum_{r=0}^{N_{\text{opt}}-1}\epsilon^r g_r - \sum_{j=1}^{3} iK_j\sqrt{2\pi}\left(\text{erf}\left(\theta\sqrt{\frac{r}{2\epsilon}}\right) + D_j\right)\Lambda_j e^{-\chi_j/\epsilon}\right), \\ &= Y_1(z)\sum_{r=0}^{N_{\text{opt}}-1}\epsilon^r g_r - \sum_{j=1}^{3} iK_j\sqrt{2\pi}\left(\text{erf}\left(\theta\sqrt{\frac{r}{2\epsilon}}\right) + D_j\right)\Lambda_j Y_{j+1}(z), \end{aligned} \tag{2.117}$$

as $\epsilon \to 0$ and where $Y_j(z)$ is given by (2.71).

2.5.6. Stokes structure.

With the results for χ given by (2.82), we can investigate the switching behaviour of the exponentially small contributions. From Figures 2.5a and 2.6a we see that $\mathrm{Re}(\chi_2)$ and $\mathrm{Re}(\chi_3)$ are both negative along the positive real z axis. The exponential contributions associated with χ_2 and χ_3 are therefore exponentially large there. In this case, the asymptotic expansion (2.117) no longer describes a solution to (2.70) which is asymptotic to $Y_1(z)$ as $\epsilon \to 0$ in $\mathcal{S}_c'$. In order for the asymptotic series expansion (2.117) to describe a solution asymptotic to $Y_1(z)$ we require the values of $\mathcal{S}_j$ to be equal to zero on the positive real axis. As $\mathrm{Im}(\chi_j) < 0$ along the positive real axis, this is equivalent to the condition $\mathcal{S}_j \to 0$ as $\theta \to -\infty$, which gives $D_j = 1$ for $j = 2, 3$.

Similarly, Figure 2.7a shows that $\mathrm{Re}(\chi_1) < 0$ in the neighbourhood of the real positive z axis and therefore the exponential contribution due to χ_1 must also be absent in these regions. Consequently, the value of $\mathcal{S}_1$ is also required to be zero and therefore $D_1 = 1$. Figures 2.5b

and 2.6b illustrate the Stokes switching behaviour of the subdominant exponentials associated with χ_2 and χ_3. In Figure 2.5b we see that the contribution $\exp(-\chi_2/\epsilon)$ is switched on as the upper Stokes curve is crossed, switching on the subdominant contribution $-2i\pi K_2 \exp(-\chi_2/\epsilon)$ in the asymptotic expression (2.116). Similarly, in Figure 2.6b the exponential contribution due to χ_3 is switched on across the lower Stokes curve, and therefore the asymptotic series expansion contains the subdominant contribution $-2i\pi K_3 \exp(-\chi_3/\epsilon)$ as a result of Stokes phenomenon. In Figures 2.5b and 2.5b the blue shaded regions denote regions in which there are exponentiall small terms present in the asymptotic solution (2.117).

Since the general solution of (2.70) is composed of a linear combination of solutions described by (2.71), the remaining sub-subdominant exponential is also present in the asymptotic expansion (2.116). The sub-subdominant exponential is the exponential contribution associated with χ_1. Therefore, the composite behaviour must include Stokes switching behaviour of $\exp(-\chi_1/\epsilon)$. Figure 2.7b illustrates the Stokes switching behaviour of the sub-subdominant exponential contribution due to χ_1, while Figure 2.8 illustrates the composite behaviour of (2.117). In this figure, the regions shaded in blue represent regions in which the exponentially subdominant contributions, Y_2, Y_3 and Y_4 are present in the asymptotic expansion (2.117).

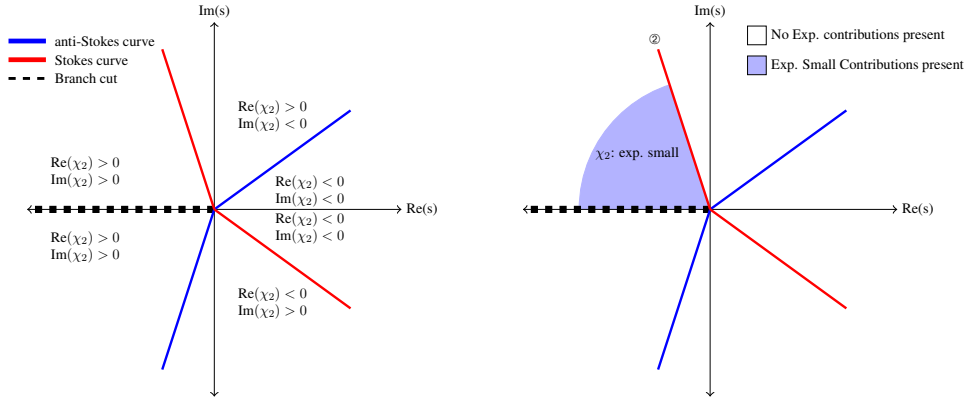

(A) Stokes and anti-Stokes curves for χ_2.

(B) Exponential terms due to χ_2.

FIGURE 2.5. This figure illustrates the Stokes structure and the Stokes switching behaviour of the exponential contributions due to χ_2, which is given by (2.71), in the complex z-plane. The Stokes and anti-Stokes curves are denoted by the red and blue curves, respectively while the branch cut is denoted by the dashed curve. The regions shaded in blue denote those which contain the exponentially small term associated with χ_2. The exponential contribution associated with χ_2 is switched across the Stokes curves denoted by ②. This convention will be followed in subsequent figures.

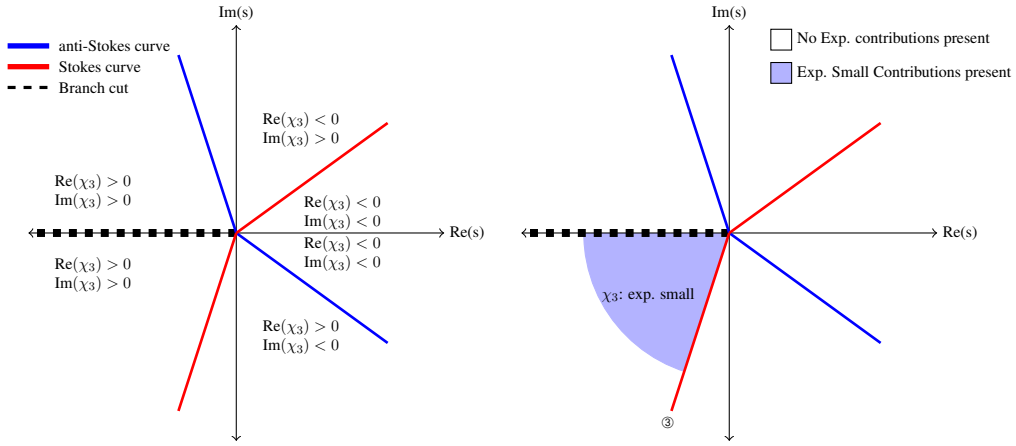

(A) Stokes and anti-Stokes curves for χ_3. (B) Exponential terms due to χ_3.

FIGURE 2.6. This figure illustrates the Stokes structure and the Stokes switching behaviour of exponential contributions due to χ_3, which is given by (2.71), in the complex z-plane. The red curves denote the Stokes curves, blue curves denote anti-Stokes curves and the dashed curve represent a branch cut. The regions shaded in blue denote those which contain the exponentially small term associated with χ_3.

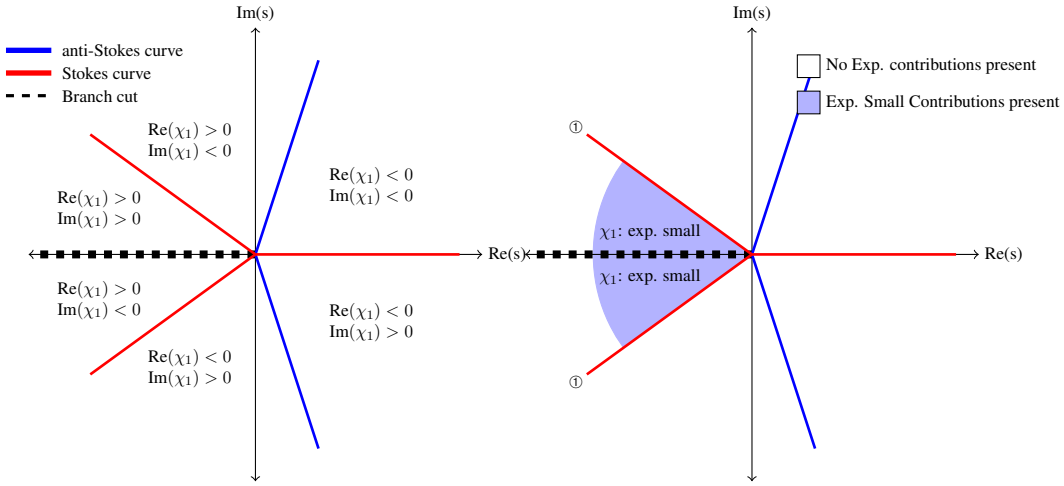

(A) Stokes and anti-Stokes curves for χ_1. (B) Exponential terms due to χ_1.

FIGURE 2.7. This figure illustrates the Stokes structure and the Stokes switching behaviour of exponential contributions due to χ_1, which is given by (2.71), in the complex z-plane. The red curves denote the Stokes curves, blue curves denote anti-Stokes curves and the dashed curve represent a branch cut. The regions shaded in blue denote those which contain the exponentially small term associated with χ_1.

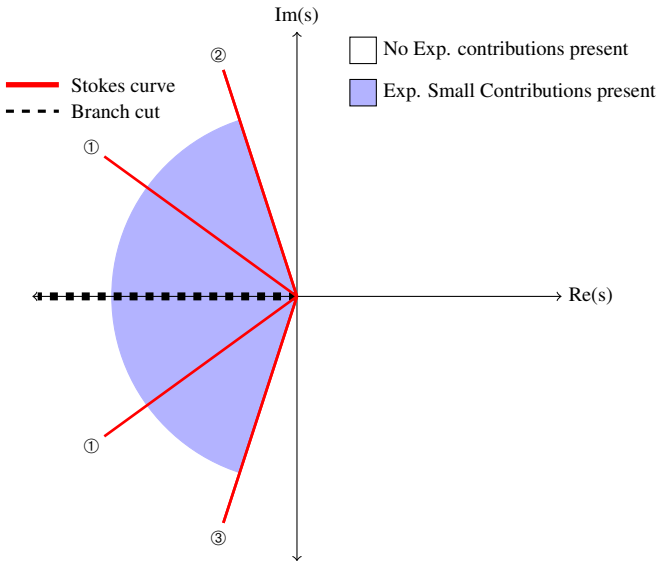

FIGURE 2.8. This figure illustrates the composite behaviour of the asymptotic solution given by (2.117) as $\epsilon \to 0$. This picture is a combination of Figures 2.7b, 2.5b and 2.6b where only the active Stokes curves are illustrated. The blue shaded regions denote regions which contain exponentially small terms present in the asymptotic expansion (2.117).

We have therefore constructed an asymptotic power series expansion describing the behaviour of solutions of the hyper-Airy equation (2.70) in the limit $\epsilon \to 0$ which contains exponentially subdominant correction terms. This is given by (2.117). By considering Stokes behaviour present in these solutions, we are able to obtain a uniform asymptotic expansion for (2.70) which is valid everywhere in the complex z-plane except along the negative real axis.

2.6. Further Ideas

Stokes phenomena are generally well understood in the case of second-order linear differential equations [**26**,**73**,**127**]. For nonlinear differential equations, and also higher-order linear differential equations, extra complications may occur in addition to the typical Stokes behaviour found in the linear case. These effects include behaviour known as higher-order Stokes phenomenon, which was originally studied by Howls, Langman and Olde Daalhuis [**72**] and second-generation Stokes phenomena [**33**].

Higher-order Stokes phenomenon is the behaviour in which Stokes lines themselves can switch on or off as *higher-order Stokes curves* are crossed [**31**, **33**, **72**, **73**]. The vanishing of usual Stokes curves was also discovered by Aoki, et al. in [**6**]. This behaviour may occur whenever the asymptotic series expansion of a solution is composed of at least three component asymptotic series each multiplied by a distinct exponential prefactor with argument say, χ_i/ϵ where $i = 0, 1, 2$ [**73**]. In this case, it is possible to find a region in which there is an ordering in $\mathrm{Re}(\chi_i/\epsilon)$. This allows

the possibility of Stokes behaviour interactions between the subdominant and sub-subdominant exponentials. Hence, in order to capture higher-order Stokes phenomena, the behaviour of sub-subdominant exponentials must be considered.

Higher-order Stokes phenomenon is also observable in the factorial-over-power ansatz for the late-order terms. Such behaviour arises when the prefactor term of the late-order terms ansatz also displays Stokes behaviour; this was found to be the case in [**33**]. Higher-order Stokes curves are given by the condition

$$\operatorname{Im}\left(\frac{\chi_i-\chi_j}{\chi_j-\chi_k}\right)=0, \tag{2.118}$$

where $i\neq j\neq k$ [**33**, **73**]. Furthermore, they often emerge from and terminate at the intersection points of usual Stokes curves known as *Stokes-crossing points*.

Second-generation Stokes phenomenon occurs when the subdominant exponential contribution in the asymptotic expansion is responsible for the Stokes switching of further terms beyond all orders, that is, sub-subdominant exponential terms [**33**]. This phenomenon occurs when the subdominant exponential contribution of an optimally-truncated asymptotic series is also described by a divergent asymptotic series expansion. For example, (2.63) may have the series expansion

$$f(z)=e^{-\chi_0(z)/\epsilon}\sum_{r=0}^{N_{\text{opt}}-1}\epsilon^r f_r(z)+\sum_i e^{-\chi_i(z)/\epsilon}\sum_{r=0}^{\infty}\epsilon^r h_r(z), \tag{2.119}$$

as $\epsilon\to 0$. The asymptotic series expansion of the subdominant exponential in (2.119) can also be optimally-truncated by writing

$$f(z)=e^{-\chi_0(z)/\epsilon}\sum_{r=0}^{N_{\text{opt}}-1}\epsilon^r f_r(z)+\sum_i e^{-\chi_i(z)/\epsilon}\left(\sum_{r=0}^{N_{\text{opt},i}-1}\epsilon^r h_r(z)+R_{N,i}(z)\right), \tag{2.120}$$

as $\epsilon\to 0$. The Stokes switching behaviour of the sub-subdominant remainder terms, $R_{\text{N},i}$, may then be studied using exponential asymptotic methods. In this way, it is possible that the asymptotic series solution exhibits a complicated hierarchy of Stokes switching behaviour. The first known account of this behaviour appeared in [**9**] in the study of n^{th} order linear differential equations. At the time of their investigations the second-generation Stokes curves were known as 'new Stokes curves'.

We will find in Chapter 3 that the leading order subdominant contribution present in the asymptotic solutions of the second discrete Painlevé equation are not affected by higher-order and second-generation Stokes behaviour. However, there is one particular case of the first q-discrete Painlevé equation which may possibly display higher-order Stokes phenomena. This is described in Chapter 4, although we do not consider this in detail as it lies outside the scope of this thesis.

CHAPTER 3

Additive difference equations

In this chapter we study the asymptotic behaviour of solutions satisfying a nonlinear additive difference equation in the limit as the independent variable approaches infinity. More specifically, we consider the second discrete Painlevé equation. We will find that the asymptotic behaviour of solutions of the second discrete Painlevé equation can be described by asymptotic power series. These asymptotic power series will be shown to be factorially divergent and hence contain exponentially small terms and display Stokes behaviour. The results found for the second discrete Painlevé equation are new and have been published in [**84**].

In Section 3.1 we introduce and motivate the study of additive difference equations. Solutions of difference equations are defined over a discrete domain with a fixed step size. By introducing a small parameter, ϵ, difference equations can be rescaled such that the step sizes are defined by the small parameter. This choice of rescaling allows the solutions of difference equations to be expanded as a power series in ϵ where the difference equation may be treated as a differential equation of infinite order.

In Section 3.2 we consider the second discrete Painlevé equation ($\mathrm{dP_{II}}$) and investigate its solution behaviour as the independent variable, n, is large. We will discover in Section 3.3 that $\mathrm{dP_{II}}$ has two types of asymptotic behaviour in the limit $n \to \infty$, which we refer to as vanishing and non-vanishing type behaviours. Vanishing type behaviour is first investigated in Section 3.4 while non-vanishing type behaviour is considered in Section 3.5. We show that these behaviours can be described using classical asymptotic power series methods. However, these series expansions will be shown to be divergent and hence exponential asymptotic methods are required in order to determine the exponentially small terms hidden within these asymptotic expansions. In particular, we will find that these asymptotic solutions share similar features with the tronquée and tri-tronquée solutions of the second Painlevé equation.

3.1. Introduction

In this chapter we will study the solutions of additive difference equations as the independent variable approaches infinity. More specifically, we will study solutions of the discrete Painlevé equations. We will find that the power series expansions of these solutions are divergent and hence exponential asymptotic methods are required in order to understand the behaviour of the exponentially small terms present within these expansions.

Difference equations are ubiquitous in the study of physical systems. They can be found in areas such as in theoretical physics applications where discrete models are used to develop quantum field theories [**59**, **131**, **144**]. Difference equations are also used in engineering and mathematical finance applications where large discrete data sets are involved.

Although various physical phenomena are often modelled by differential equations, in practice, the solutions are often generated numerically for some given set of data. In this way, the numerical evaluation of their solutions ultimately reduces to the computation of discrete sets of data. As the data sets involved are discrete, the governing equations or models must also be discretized. A common procedure used to discretize a given differential equation is by *finite difference methods*.

The finite difference method obtains an approximation of some given function say $y(x)$, by the functions values at a finite set of the independent variable, x. The variable, x, can be discretized by setting $x_n = x_0 + nh$ where x_0 is some arbitrary starting point, $n \in \mathbb{Z}$ and h is a prescribed step size.

In principle, the variable, x, and the step size, h, may be complex-valued. In this case, the domain for which the dependent variable is defined on can be thought of as a lattice defined implicitly in two dimensional real space or equivalently, a one dimensional complex space. For clarity, we will treat the variables and step sizes as real-valued quantities.

The forward evolution of the variable x_n is therefore described by the map $n \mapsto n + 1$. In this way, the value of the solution at the next time step, x_{n+1}, can be defined by

$$y(x_{n+1}) = y(x_n + h).$$

Provided that the step size, h, is small, we may Taylor expand $y(x_n + h)$ about x_n to give

$$y(x_{n+1}) = y(x_n + h) = y(x_n) + hy'(x_n) + \mathcal{O}(h^2),$$

as $h \to 0$; this approximation is known as a *forward difference*. Under this discretization, a differential equation of the form

$$y'(x) = f(x, y(x)), \qquad y(x_0) = y_0, \tag{3.1}$$

can be approximated by

$$\frac{y(x_n + h) - y(x_n)}{h} + \mathcal{O}(h) = f(x_n, y(x_n)),$$

which can then be rewritten as

$$y_{n+1} = y_n + hf(x_n, y_n) + \mathcal{O}(h^2), \tag{3.2}$$

where $y_n = y(x_n)$ and $y_{n+1} = y(x_{n+1}) = y(x_n + h)$. In fact, the method of obtaining equation (3.2) with terms of order $\mathcal{O}(h^2)$ neglected is known as the forward Euler method.

The finite difference method can also be used to discretize partial differential equations. As an example, let us consider the wave equation

$$u_{xx} - c^2 u_{yy} = 0, \tag{3.3}$$

where $u = u(x, y)$ and c a nonzero constant. In the same way, the independent variables are discretized by setting $x = x_0 + nh$ and $y = y_0 + mk$ where x_0, y_0 are arbitrary constants, $n, m \in \mathbb{Z}$ and h and k are the prescribed step sizes of the variables x and y, respectively. The second order partial derivatives can then be approximated by

$$u_{xx} = \frac{u_{n+1,m} - 2u_{n,m} + u_{n-1,m}}{h^2} + \mathcal{O}(h^3), \tag{3.4}$$

$$u_{yy} = \frac{u_{n,m+1} - 2u_{n,m} + u_{n,m-1}}{k^2} + \mathcal{O}(k^3). \tag{3.5}$$

Noting the forms of (3.4), these difference approximations are referred to as *central differences*. Using the central differences (3.4) and (3.5), the wave equation (3.3) can be rewritten as the second order partial difference equation

$$\frac{u_{n+1,m} - 2u_{n,m} + u_{n-1,m}}{h^2} - c^2 \frac{u_{n,m+1} - 2u_{n,m} + u_{n,m-1}}{k^2} = 0. \tag{3.6}$$

Under this discretization, the (x, y)-domain becomes a two-dimensional lattice with spacings h and k. In general, this approach can be used in order to discretize n^{th} order (partial) differential equations to produce n^{th} order (partial) difference equations. Figures 3.1a and 3.1b illustrate the domain on which the solutions of difference equations are defined. In Figure 3.1a, the solution $u(x)$ is defined over the set of points defined by $x = x_0 + nh$, which lies along the continuous x-axis. Whereas in Figure 3.1b the solution $u(x, y)$ is defined over a two-dimensional lattice generated by $(x_0 + nh, y_0 + nk)$. We note that the step sizes h and k in Figure 3.1b are not necessarily equal.

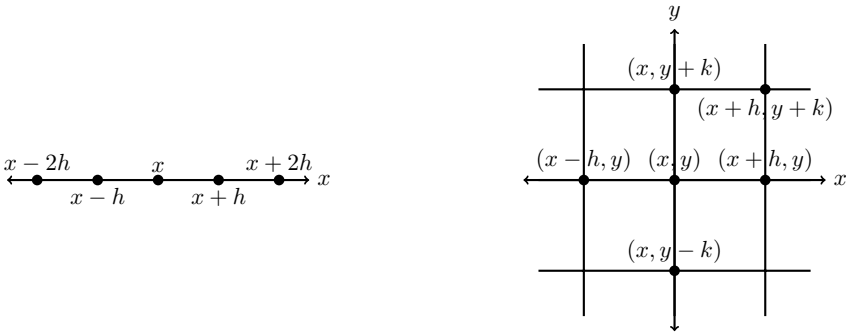

(A) Discrete domain for $u(x)$ with step size defined by h.

(B) Discrete domain for $u(x, y)$ with step sizes h and k.

FIGURE 3.1. The solutions of difference equations are defined over a discrete set of points.

Difference equations constructed in this way limit to the original differential equation as the step sizes approach zero; this is known as the continuum limit. For example, the difference equation (3.2) tends to the differential equation (3.1) in the limit $h \to 0$ while the (3.6) tends to (3.3) in the limit $h \to 0$ and $k \to 0$.

3.2. Discrete Painlevé II

In this chapter we seek to develop a methodology in order to study the asymptotic behaviour of solutions of nonlinear difference equations, in particular, the discrete Painlevé equations.

As an asymptotic study on the first discrete Painlevé equation has been investigated by Joshi and Lustri [**83**], we consider the second discrete Painlevé equation

$$x_{n+1} + x_{n-1} = \frac{(\alpha n + \beta)x_n + \gamma}{1 - x_n^2}, \tag{3.7}$$

in the asymptotic limit $n \to \infty$. This equation is of interest in mathematical physics [**58**, **104**, **105**, **130**, **146**, **153**] and also appears as a reduction of the discrete modified Korteweg-de Vries (mKdV) equation [**111**, **112**].

Another version of (3.7) exists for which the γ term changes with n [**63**]. This version can be obtained by applying the singularity confinement criterion on the McMillan map

$$x_{n+1} + x_{n-1} = \frac{a_n x_n + b_n}{1 - x_n^2}.$$

The authors of [**63**] show that the singularity confinement criterion gives $b_n = \gamma + \delta(-1)^n$ and $a_n = \alpha n + \beta$. The odd-even dependence can be removed by choosing $\delta = 0$, producing (3.7).

Equation (3.7) tends to the second continuous Painlevé equation ($\mathrm{P_{II}}$) in the continuum limit $x_n = \epsilon w$, $z_n = \alpha n + \beta = 2 + \epsilon^2 t$ and $\gamma = \epsilon^3 \mu$ as $\epsilon \to 0$,

$$\mathrm{P_{II}}: \qquad \frac{d^2 w}{dt^2} = 2w^3 + tw + \mu. \tag{3.8}$$

Using exponential asymptotic techniques we will find solutions to (3.7), which are asymptotically free of poles within certain regions of the complex plane. We begin the analysis by finding the formal series solutions containing exponentially small terms, then study Stokes behaviour present within these asymptotic solutions. Finally, we use these results to determine the regions in which these series expressions describe the dominant asymptotic behaviour. Furthermore, we will find that these asymptotic solutions share features with the tronquée and tri-tronquée solutions of the second continuous Painlevé equation ($\mathrm{P_{II}}$) [**23**].

Exponential asymptotic techniques for differential-difference equations were developed by King and Chapman [**92**] in order to study a nonlinear model of atomic lattices based on the work of [**32**, **121**]. Joshi and Lustri [**83**] applied the Stokes smoothing technique described in [**92**] to the first discrete Painlevé equation and obtained asymptotic approximations containing exponentially small contributions. Motivated by their work, we extend this to $\mathrm{dP_{II}}$ in order to study asymptotic solutions with similar features.

3.3. Scalings of discrete Painlevé II

As we are interested in studying the behaviour of solutions of (3.7) in the limit $n \to \infty$, we introduce the small parameter ϵ by setting $s = \epsilon n$ and let $X(s) = x_n$. Applying this choice of scalings to (3.7) gives

$$(X(s+\epsilon) + X(s-\epsilon))(1 - X(s)^2) = \left(\frac{\alpha s}{\epsilon} + \beta\right) X(s) + \gamma, \tag{3.9}$$

where we now consider the limit $\epsilon \to 0$. If we assume that $X(s) \sim X_0$ as $\epsilon \to 0$ then we obtain the following asymptotic equation

$$2X_0(1 - X_0^2) \sim \left(\frac{\alpha s}{\epsilon} + \beta\right) X_0 + \gamma, \tag{3.10}$$

as $\epsilon \to 0$. From equation (3.10) we may deduce the possible dominant balances. If we assume that $X_0 \ll 1$, we obtain the balance

$$X_0 \sim -\frac{\gamma\epsilon}{\alpha s},$$

as $\epsilon \to 0$. If we instead look for solutions which are large as $\epsilon \to 0$, that is, $X_0 \gg 1$, then the dominant balance we find from (3.10) is given by

$$-2X_0^3 \sim \frac{\alpha s}{\epsilon} X_0,$$

as $\epsilon \to 0$, and therefore find solutions that have behaviour

$$X_0 \sim \pm\sqrt{-\frac{\alpha s}{2\epsilon}},$$

as $\epsilon \to 0$. Hence, we will study solutions of (3.9) which have behaviours given by $X(s) = \mathcal{O}(\epsilon)$ and $X(s) = \mathcal{O}(\epsilon^{-1/2})$ as $\epsilon \to 0$. We call the solutions which scale like $\mathcal{O}(\epsilon)$ or $\mathcal{O}(\epsilon^{-1/2})$ vanishing and non-vanishing type solutions, respectively.

The parameters appearing in (3.9) can also be rescaled. Following Kruskal's principle of maximal balance [**95**] the parameter scalings are chosen to retain many terms as possible in the leading order expression. Kruskal's principle ensures that a wide range of solutions are represented by the rescaled expression and that other scalings can be obtained by considering various limiting behaviours of the solution. Applying Kruskal's principle of maximal balance in (3.10) for the vanishing type behaviour informs us to rescale the parameters according to

$$s = \epsilon n; \quad x_n = \epsilon f(s), \quad \alpha = \epsilon\hat{\alpha}, \quad \beta = \hat{\beta}, \quad \gamma = \epsilon\hat{\gamma}. \tag{3.11}$$

Similarly, for non-vanishing type behaviour, the scalings we choose are

$$s = \epsilon n; \quad x_n = \frac{1}{\sqrt{\epsilon}} g(s), \quad \alpha = \hat{\alpha}, \quad \beta = \frac{\hat{\beta}}{\epsilon}, \quad \gamma = \frac{\hat{\gamma}}{\epsilon^{3/2}}. \tag{3.12}$$

In the next section we first consider vanishing type asymptotics of (3.7). We begin the analysis by finding formal asymptotic power series expansions containing exponentially small terms in some sector containing the positive real axis. We will find that the asymptotic power series diverges factorially and hence exponentially small terms are present within the asymptotic expansion. As

these solutions contain exponentially small terms, we apply exponential asymptotic methods in order to study Stokes behaviour present within these asymptotic solutions. Using these results we determine the regions in the complex plane in which these series expression describe solutions with the prescribed asymptotic behaviour.

The same analysis will then be applied to non-vanishing type solutions of (3.7) in Section 3.5. Although the analysis is near identical, these solutions will be shown to display more complicated behaviour than the solutions which vanish in the limit $\epsilon \to 0$. However, by carefully considering the behaviour of the exponentially small terms present within the asymptotic series expansion of non-vanishing type solutions, we also determine the regions in which these series expansion are valid.

3.4. Vanishing asymptotics of discrete Painlevé II

In this section, we investigate the vanishing type asymptotic behaviour of discrete Painlevé II. We therefore study equation (3.7) under the scalings (3.11). We will determine the asymptotic series expansion and use exponential asymptotic methods in order to describe the Stokes behaviour present in these solutions.

3.4.1. Asymptotic series expansions.

In order to study the asymptotic behaviour of solutions to (3.7) which vanish in the limit $n \to \infty$ we introduce the small parameter, ϵ, by applying the scalings given by (3.11). We drop the hat notation in the subsequent analysis for simplicity. Applying the scalings (3.11) into (3.7) gives us the rescaled equation

$$\big(f(s+\epsilon)+f(s-\epsilon)\big)\big(1-\epsilon^2 f(s)^2\big)=(\alpha s+\beta)f(s)+\gamma, \tag{3.13}$$

where we consider the limit $\epsilon \to 0$. We assume that $f(s)$ is an analytic function of s so that we may expand the solutions as a Taylor series in powers of ϵ in (3.13) to give

$$\sum_{j=0}^{\infty}\frac{2\epsilon^{2j}f^{(2j)}(s)}{(2j)!}\left(1-\epsilon^2 f(s)^2\right)=(\alpha s+\beta)f(s)+\gamma, \tag{3.14}$$

where the superscript '(j)' denotes the j^{th} derivative with respective to s. Under this choice of scalings the difference equation becomes an infinite order differential equation. We now expand the solution, $f(s)$, as an asymptotic power series in ϵ by writing

$$f(s)\sim\sum_{r=0}^{\infty}\epsilon^r f_r(s) \tag{3.15}$$

as $\epsilon \to 0$. This allows us to rewrite equation (3.14) as

$$\sum_{j=0}^{\infty}\frac{2\epsilon^{2j}}{(2j)!}\sum_{k=0}^{\infty}\epsilon^k f_k^{(2j)}\left(1-\epsilon^2\sum_{l=0}^{\infty}\epsilon^l f_l\sum_{m=0}^{\infty}\epsilon^m f_m\right)=(\alpha s+\beta)\sum_{j=0}^{\infty}\epsilon^j f_j+\gamma. \tag{3.16}$$

Matching orders of ϵ in equation (3.16) as $\epsilon \to 0$, we obtain the equations

$$\begin{aligned}
\mathcal{O}(\epsilon^0): &\qquad 2f_0 = (\alpha s + \beta) f_0 + \gamma, \\
\mathcal{O}(\epsilon^1): &\qquad 2f_1 = (\alpha s + \beta) f_1, \\
\mathcal{O}(\epsilon^2): &\qquad 2f_2 = (\alpha s + \beta) f_2 + 2f_0^3 - f_0''.
\end{aligned}$$

Solving these equations gives

$$f_0 = -\frac{\gamma}{\alpha s + \beta - 2}, \qquad f_1 = 0, \qquad f_2 = -\frac{2\gamma(\alpha - \gamma)(\alpha + \gamma)}{(\alpha s + \beta - 2)^4}. \tag{3.17}$$

We see from equation (3.17) that the leading order solution is singular when

$$\alpha s + \beta - 2 = 0,$$

which occurs at the point $s = (2 - \beta)/\alpha$. Hence f_0 has a simple pole located at $s = (2 - \beta)/\alpha$, which is also a pole of strength four for f_2. In general, we find

$$\mathcal{O}(\epsilon^r): \qquad \sum_{j=0}^{\lfloor r/2 \rfloor} \frac{2f_{r-2j}^{(2j)}}{(2j)!} - \sum_{m=0}^{r-2} f_m \sum_{l=0}^{r-m-2} f_l \sum_{j=0}^{\lfloor (r-m-l-2)/2 \rfloor} \frac{2f_{r-m-l-2j-2}^{(2j)}}{(2j)!} = (\alpha s + \beta) f_r, \tag{3.18}$$

for $r \geq 2$. Rearranging equation (3.18) to obtain an expression for f_r gives

$$(\alpha s + \beta - 2) f_r = \sum_{j=1}^{\lfloor r/2 \rfloor} \frac{2f_{r-2j}^{(2j)}}{(2j)!} - \sum_{m=0}^{r-2} f_m \sum_{l=0}^{r-m-2} f_l \sum_{j=0}^{\lfloor (r-m-l-2)/2 \rfloor} \frac{2f_{r-m-l-2j-2}^{(2j)}}{(2j)!}. \tag{3.19}$$

From the recurrence relation in (3.19) we can show that the terms f_{2n+1} are identically zero as a consequence of the fact that $f_1 = 0$. Consequently, the asymptotic power series (3.15) only contains even powers of ϵ.

Proposition 1. *All the odd coefficients of the asymptotic series* (3.15) *are zero. That is,* $f_{2n+1} = 0$ *for all* $n \geq 0$.

Proof. We first apply $r \mapsto 2r + 1$ to (3.19) so that we are only dealing with the odd coefficients. The case $n = 1$ is easy to show; a direct calculation can easily show that $f_3 = 0$. We then assume that $f_{2m+1} = 0$ is true for $m = 0, 1, 2, ..., K$ where K is arbitrary and show that it is also true for $m = K + 1$. This is easy to see, because the first sum in (3.19) has subscript $f_{2r-2j+1}$ which is always odd, so there will be no contributions from this term. The remaining triple sum involves the subscripts $f_{2r-m-l-2j-1} f_l f_m$. We will also show that this term produces no contributions.

The first subscript can be written has $f_{2(n-j)-m-l-1}$ and this is always odd provided that $m+l$ is even. In this case, $m + l$ can be a combination of either (odd+odd) or (even+even) but for either combination, the resulting term will always be zero, since there will always be at least one odd subscript. In order to obtain a nonzero contribution, we require the first subscript to be even, which means that $m + l$ must be odd. In this case, $m + l$ must be (odd+even), which ensures that one subscript is odd, and therefore the whole term is zero. Thus, our proposition is proved. □

From the recurrence relation (3.19) we observe that the calculation of f_r requires two differentiations of f_{r-2}. Hence, if f_0 has an algebraic singularity of strength k then f_2 will have the same

singularity but with strength $k+2$. The late-order terms will therefore have factorial-over-power behaviour and hence can be described by (2.43). Consequently, the asymptotic series (3.15) is therefore factorially divergent and will exhibit Stokes behaviour.

We have determined the leading order asymptotic solution to (3.13) and the recurrence equation for the coefficients of (3.15). Furthermore, we discovered that the coefficients terms in (3.15) are singular and the late-order terms are described by a factorial-over-power form due to repeated differentiation, which causes the asymptotic series to be divergent. Optimal truncation methods are required in order to capture and study the exponentially small terms present within these asymptotic series expansions.

In the subsequent analysis we will optimally truncate the asymptotic series, which requires the form of the coefficients to be known. In the next section, we will determine the general behaviour of f_r as $r \to \infty$, enabling us to optimally truncate (3.15) and investigate Stokes behaviour present in these asymptotic solutions.

3.4.2. Late-order terms analysis.

In this section, we completely determine the leading order behaviour of the late-order terms, enabling us to optimally truncate (3.15). As discussed in Section 2.2.1, the behaviour of the late-order terms are related to the singularities of the function we are approximating. We find from (3.18) that the calculation of the coefficients involve repeated differentiations of previous terms which are singular. Consequently, the behaviour of the late-order terms will take a factorial-over-power form described by (2.43). We therefore apply the ansatz

$$f_r \sim \frac{F(s)\Gamma(r+k)}{\chi(s)^{r+k}}, \tag{3.20}$$

as $r \to \infty$, where $\chi(s)$ is the singulant, $F(s)$ is the prefactor and k is a constant. Recalling that the singulant vanishes at the singularities of the leading order solution we deduce that the singulant is subject to the condition

$$\chi\left(\frac{2-\beta}{\alpha}\right) = 0.$$

We apply (3.20) to equation (3.18) and match orders of r as $r \to \infty$. The leading order equation as $r \to \infty$ is given by

$$\mathcal{O}(f_r): \qquad \sum_{j=0}^{\lfloor r/2 \rfloor} \frac{2(-\chi')^{2j}}{(2j)!} \frac{F\,\Gamma(r+k)}{\chi^{r+k}} = (\alpha s+\beta)\frac{F\,\Gamma(r+k)}{\chi^{r+k}}. \tag{3.21}$$

From the recurrence relation (3.19), the triple sum contains terms of size $\mathcal{O}(f_{r-2})$, and is therefore negligible when matching terms of size $\mathcal{O}(f_{r-1})$ as $r \to \infty$. Continuing to the next order as

$r \to \infty$, we obtain the equation

$$\mathcal{O}(f_{r-1}): \qquad \sum_{j=1}^{\lfloor r/2 \rfloor} \frac{2}{(2j)!} \left(\binom{2j}{1} (-\chi')^{2j-1} F' + \binom{2j}{2} (-\chi')^{2j-2} (-\chi'') F \right) = 0, \tag{3.22}$$

after simplification. Equations (3.21) and (3.22) can be solved to calculate χ and F, respectively.

3.4.2.1. *Calculating the singulant, χ.*

In order to determine the singulant, $\chi(s)$, we consider (3.21) which can be reduced to

$$\sum_{j=0}^{\lfloor r/2 \rfloor} \frac{2(-\chi')^{2j}}{(2j)!} = (\alpha s + \beta). \tag{3.23}$$

We replace the upper summation limit by infinity in (3.23) and in doing so we only introducing exponentially small error to the singulant as $r \to \infty$ [**92**], which may be neglected here (see Appendix B). Replacing the upper summation limit by infinity in equation (3.23) gives

$$\cosh(\chi') = \frac{\alpha s + \beta}{2}$$

which has solutions

$$\chi' = \pm \cosh^{-1}\left(\frac{\alpha s + \beta}{2} \right) + 2M\pi i, \tag{3.24}$$

where $M \in \mathbb{Z}$. Noting that there are two different equations for the singulant, we name them $\chi_1(s)$ and $\chi_2(s)$ with the choice of the positive and negative signs, respectively. In general, the behaviour of f_r will be the sum of expressions (3.20), with each value of M and sign of the singulant [**48**]. However, by Darboux's theorem, this sum will be dominated by the two terms associated with $M = 0$ as this is the value for which $|\chi|$ is smallest [**32, 43, 44, 48**]. Thus, we consider the $M = 0$ case in the subsequent analysis.

Recalling that the singulant must vanish at the singularity, $s_0 = (2 - \beta)/\alpha$, and therefore $\chi(s_0) = 0$. In order to solve for χ, we apply a change of variables to equation (3.24) by setting $u = (\alpha s + \beta)/2$, which gives

$$\chi(s) = \pm \frac{2}{\alpha} \int_{u(s_0)}^{u} \cosh^{-1}(u) du, \tag{3.25}$$

where $u(s_0) = 1$. From the list of integrals for the inverse hyperbolic functions provided in Section 4.4 of [**1**], we can evaluate (3.25) to obtain

$$\chi_1 = \frac{2}{\alpha} \left(\left(\frac{\alpha s + \beta}{2} \right) \cosh^{-1}\left(\frac{\alpha s + \beta}{2} \right) - \sqrt{\left(\frac{\alpha s + \beta}{2} \right)^2 - 1} \right), \tag{3.26}$$

$$\chi_2 = -\chi_1. \tag{3.27}$$

3.4.2.2. *Calculating the prefactor, F.*

In order to find the prefactor associated with each singulant we solve equation (3.22). As before, we extend the upper summation limits to infinity in equation (3.22), obtaining

$$-2F'\sinh(\chi') - \chi''\cosh(\chi')F = 0. \tag{3.28}$$

This equation is independent of the choice of χ_i due to the even and odd properties of cosh and sinh functions, respectively. Equation (3.28) can be solved explicitly to obtain

$$F_i(s) = \frac{\Lambda_i}{\sqrt{\sinh(\chi'(s))}}, \tag{3.29}$$

where $i = 1, 2$, and Λ_i are arbitrary constants. We also note that the parameter, γ, does not appear in either the singulant or prefactor equations. As a consequence, γ will not play any role in the Stokes phenomena to leading order in ϵ.

Substituting (3.26), (3.27) and (3.29) into (3.20) we find that the late-order terms of (3.15) are given by

$$f_r(s) \sim \frac{\Lambda_1\Gamma(r+k)}{\sqrt{\sinh(\chi_1')}\chi_1^{r+k}} + \frac{\Lambda_2\Gamma(r+k)}{\sqrt{\sinh(\chi_1')}\chi_2^{r+k}}, \tag{3.30}$$

as $r \to \infty$. In order to completely determine the form of the late-order terms, we must also determine the values of k and Λ_i in (3.30). This can be done by matching the late-order expression given in (3.30) to the leading-order behaviour in the neighbourhood of the singularity. We therefore determine the behaviour of χ and F in the neighbourhood of the singularity.

3.4.2.3. *Calculating the value of k.*

In order to determine the value of k we first determine the behaviour of χ and F near the singularity. For $|\alpha| \neq 0$, the behaviour of the singulant near the singularity is given by

$$\begin{aligned} \chi_1 &\sim -\frac{2\sqrt{\alpha}}{3}(s-s_0)^{3/2}, \\ \chi_2 &\sim \frac{2\sqrt{\alpha}}{3}(s-s_0)^{3/2}, \end{aligned} \tag{3.31}$$

as $s \to s_0$. By substituting the expressions (3.31) into equation (3.28) we find that

$$-\sqrt{\alpha(s-s_0)}F_i' \sim \frac{\sqrt{\alpha}}{4\sqrt{s-s_0}}F_i, \tag{3.32}$$

as $s \to s_0$ and $i = 1, 2$. Solving equation (3.32), we find that the local behaviour of the prefactor about the singularity is given by

$$F_i \sim \frac{\Lambda_i}{(s-s_0)^{1/4}} \tag{3.33}$$

where $i = 1, 2$. Hence, by substituting (3.31) and (3.33) into (3.30) we find that local behaviour of the late-order terms near the singularity is given by

$$f_r \sim \frac{\Lambda_1 \Gamma(r+k)}{(s-s_0)^{1/4}\big(-\frac{2}{3}\sqrt{\alpha}(s-s_0)^{3/2}\big)^{r+k}} + \frac{\Lambda_2 \Gamma(r+k)}{(s-s_0)^{1/4}\big(\frac{2}{3}\sqrt{\alpha}(s-s_0)^{3/2}\big)^{r+k}}, \tag{3.34}$$

as $s \to s_0$.

From the discussion after equation (3.19), we know that if the singularity of f_0 is of strength one, then the strength of the singularity of f_r is equal to $3r/2 + 1$. From (3.34) we find that the strength of the singularity is equal to $3(r+k)/2 + 1/4$. Hence, for consistency in the singular behaviour of the late-order terms expression (3.34), we require that

$$\frac{3(r+k)}{2} + \frac{1}{4} = \frac{3r}{2} + 1,$$

and therefore $k = 1/2$.

3.4.2.4. *Calculating the value of* Λ.

Although the values of Λ_i appearing in (3.30) is not required in the subsequent analysis they may be determined numerically for completeness. We first rewrite the expression in equation (3.30) as

$$\frac{f_r(s)\sqrt{\sinh(\chi_1')}\chi_1^{r+1/2}}{\Gamma(r+1/2)} \sim \Lambda_1 + (-1)^{r+1/2}\Lambda_2, \tag{3.35}$$

as $r \to \infty$. Since the singularities of both χ_1 and χ_2 are located at $s = (2-\beta)/\alpha$, and are therefore equidistant to the origin, we may follow the methodology demonstrated in Section 2.5.3.4 in order to calculate Λ_i. By appropriately adding (or subtracting) successive terms of (3.35), we can obtain formulas for the constants, Λ_i, in the limit $r \to \infty$. Doing this, we obtain

$$2\Lambda_1 = \lim_{r\to\infty}\left[\frac{f_{2r}\sqrt{\sinh(\chi_1')}\chi_1^{2r+1/2}}{\Gamma(2r+1/2)} + \frac{f_{2r-1}\sqrt{\sinh(\chi_1')}\chi_1^{2r-1/2}}{\Gamma(2r-1/2)}\right], \tag{3.36}$$

$$-2i\Lambda_2 = \lim_{r\to\infty}\left[\frac{f_{2r}\sqrt{\sinh(\chi_1')}\chi_1^{2r+1/2}}{\Gamma(2r+1/2)} - \frac{f_{2r-1}\sqrt{\sinh(\chi_1')}\chi_1^{2r-1/2}}{\Gamma(2r-1/2)}\right]. \tag{3.37}$$

In Section 3.4.1, we showed that all the odd terms of the asymptotic series vanish. Thus, we observe that the second terms of the expressions (3.36)-(3.37) is equal to zero. As a consequence, we find that $\Lambda_1 = -i\Lambda_2$. In principle, the value of Λ_i may be computed using equations (3.36)-(3.37). In order for the limits (3.36)-(3.37) to converge, a sufficiently large number of the terms f_r are required to be computed. Indeed f_r may be computed using (3.19); however, this approach is an inefficient way of calculating Λ_i as it requires repeatedly differentiating terms like (3.26).

An alternative and more efficient method of calculating Λ_i is to match the expansion (3.15) with the inner expansion in the vicinity of the singularity, s_0. This method therefore involves

taking the inner limit of (3.34). From (3.34), we write

$$f_r \sim \frac{a_r}{(s-s_0)^{3r/2+1}}, \tag{3.38}$$

as $s \to s_0$. Substituting this form for f_r into (3.19), gives

$$\alpha a_r = \left(\frac{3r}{2}-2\right)\left(\frac{3r}{2}-1\right) a_{r-2} - 2\sum_{l=0}^{r-2}\sum_{k=0}^{r-l-2} a_{r-l-k-2}a_k a_l, \tag{3.39}$$

for $r \geq 2$, where $a_0 = -\gamma/\alpha$ and $a_1 = 0$. Following this method, we numerically compute the value of Λ_i, using the Mathematica 10 package, with parameter values $\alpha = -2, \beta = 1$ and $\gamma = 1$. Using the difference equation (3.39) we may compute the coefficients a_r of the inner expansion of f_r, which is given by (3.38). For sufficiently large values of f_r computed, we then use the formulas (3.36)-(3.37) to find that

$$\Lambda_1 \approx 0.0757 - 0.0757\, i,$$
$$\Lambda_2 \approx 0.0757 + 0.0757\, i.$$

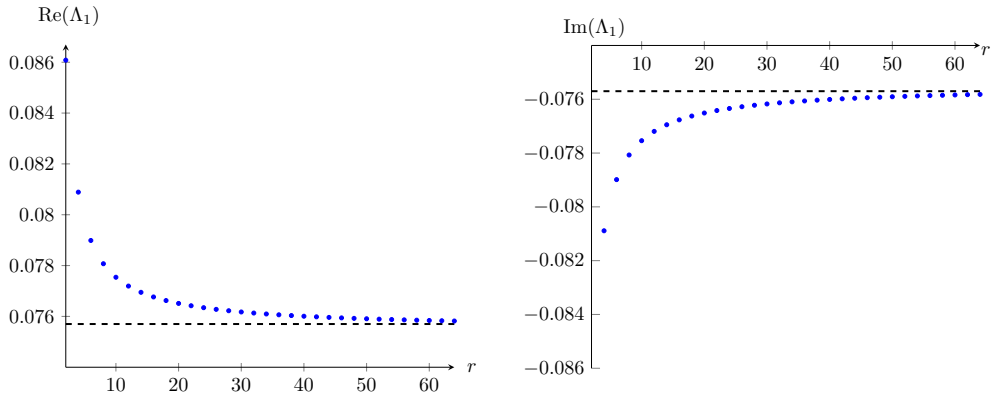

(A) Real part of Λ_1. (B) Imaginary part of Λ_1.

FIGURE 3.2. This figure illustrates the approximation for Λ_1 defined by (3.36) with $\alpha = -2, \beta = 1$ and $\gamma = 1$. We see that as r increases, the approximation for Λ_1 tends to the limiting value described by the black, dashed curve. The approximation for Λ_2 defined by (3.37) may be obtained from this information since $\Lambda_1 = -i\,\Lambda_2$.

The approximate values for Λ_1 and Λ_2 are illustrated in Figures 3.2a and 3.2b. Therefore, the explicit form of the late order terms is given by

$$f_r(z) \sim \frac{\Lambda_1 \Gamma(r+1/2)}{\sqrt{\sinh(\chi_1')}\chi_1^{r+1/2}} + \frac{\Lambda_2(-1)^{r+1/2}\Gamma(r+1/2)}{\sqrt{\sinh(\chi_1')}\chi_1^{r+1/2}}, \tag{3.40}$$

as $r \to \infty$. Recalling that the odd coefficients identically vanish, (3.40) can be further simplified to give

$$f_{2r}(s) \sim \frac{2\Lambda_1 \Gamma(2r+1/2)}{\sqrt{\sinh(\chi_1')}\chi_1^{2r+1/2}}, \tag{3.41}$$

as $r \to \infty$, where χ_1 is given in equation (3.26) and the values to Λ_1 can be calculated from equation (3.36).

3.4.3. Vanishing behaviour remainder analysis.

In the previous section we successfully calculated the behaviour of the late-order terms in the asymptotic series expansion. From this calculation we noted that the late-order terms behave as factorials and hence the asymptotic series we deal with are indeed divergent. As such, we expect exponentially small contributions to be present within these asymptotic series and therefore expect the Stokes phenomena to occur.

In order to determine the behaviour of the exponentially small contributions in the neighbourhood of the Stokes curve we need to optimally truncate (3.15). We truncate the asymptotic series by writing

$$f(s) = \sum_{r=0}^{N-1} \epsilon^r f_r(s) + R_N(s), \tag{3.42}$$

where N is the optimal truncation point and R_N is the optimally-truncated error. We choose N such that the series are truncated after their smallest terms. As discussed in Section 2.2, optimal truncation can be achieved by truncating the asymptotic series at the least term [**24**]. By using the behaviour of the late-order terms provided in (3.41) and using equation (2.25) we find that

$$\left| \frac{\epsilon^{2N+2} f_{2N+2}}{\epsilon^{2N} f_{2N}} \right| \sim 1 \Longrightarrow N \sim \frac{|\chi_1|}{2\epsilon},$$

as $\epsilon \to 0$. As this quantity may not necessarily be integer valued, we therefore choose $\omega \in [0,1)$ such that

$$N = \frac{|\chi_1|}{2\epsilon} + \omega \tag{3.43}$$

is integer valued.

We substitute the optimally-truncated series (3.42) into the governing equation (3.14), and use the recurrence relation (3.18) to eliminate terms. Doing so, we obtain the equation

$$\begin{aligned}\sum_{j=1}^{\infty} \frac{2\epsilon^{2j} R_N^{(2j)}}{(2j)!} - \epsilon^2 \sum_{r=0}^{N-1} \epsilon^{2r} \sum_{j=0}^{\infty} \frac{2\epsilon^{2j} f_{2r}^{(2j)}}{(2j)!} \left(2R_N \sum_{k=0}^{N-1} \epsilon^{2k} f_{2k} + R_N^2 \right) \\ - \epsilon^2 \sum_{j=0}^{\infty} \frac{2\epsilon^{2j} R_N^{(2j)}}{(2j)!} \left(\left(\sum_{r=0}^{N-1} \epsilon^{2r} f_{2r} \right)^2 - 2R_N \sum_{r=0}^{N-1} \epsilon^{2r} f_{2r} + R_N^2 \right) \\ - 2\epsilon^{2N} f_{2N} + \ldots \sim (\alpha s + \beta - 2) R_N,\end{aligned} \tag{3.44}$$

where the omitted terms are smaller than those which have been retained in the limit $\epsilon \to 0$.

Away from the Stokes curve, the inhomogeneous terms of equation (3.44) are negligible, and we apply a WKB analysis to the homogeneous version of (3.44). We therefore apply the ansatz $R_N = a(s)e^{b(s)/\epsilon}$ to the homogeneous version of (3.44) and match orders of ϵ as $\epsilon \to 0$. The leading order equation as $\epsilon \to 0$ can be shown to be

$$\sum_{j=0}^{\infty} \frac{2\epsilon^{2j}}{(2j)!}\left(\frac{b'(s)}{\epsilon}\right)^{2j} a(s)e^{b(s)/\epsilon} = \big(\alpha s + \beta\big)a(s)e^{b(s)/\epsilon}.$$

Comparing this to equation (3.21), we see that they coincide provided that $b(s) = -\chi(s)$. Continuing to the next order in ϵ we find that $a(s)$ satisfies the equation

$$\mathcal{O}(\epsilon): \qquad \sum_{j=1}^{\infty} \frac{2}{(2j)!}\left(\binom{2j}{1}(b')^{2j-1}\frac{a'}{a} + \binom{2j}{2}(b')^{2j-2}b''\right) = 0,$$

which is precisely equation (3.28) with $a(s) = F(s)$. Hence, away from the Stokes curve, the optimally-truncated error takes the form $R_N(s) \sim F(s)e^{-\chi/\epsilon}$ as $\epsilon \to 0$.

3.4.3.1. *Stokes smoothing.*

As the exponentially small error term will experience Stokes switching, we therefore set

$$R_N(s) = \mathcal{S}(s)F(s)e^{-\chi(s)/\epsilon},$$

where $\mathcal{S}(s)$ is the Stokes multiplier that switches rapidly in the neighbourhood of the Stokes curve. We apply this form to equation (3.44) and after some cancellation we find that

$$2\epsilon\mathcal{S}'Fe^{-\chi/\epsilon}\sum_{j=1}^{\infty}\frac{(2j)(-\chi')^{2j-1}}{(2j)!} \sim 2\epsilon^{2N}f_{2N}$$

as $N \to \infty$. Rearranging this equation and applying the form of f_N as given by (3.20) we find that

$$\frac{d\mathcal{S}}{ds} \sim -2\epsilon^{2N-1}e^{\chi/\epsilon}\frac{\Gamma(2N+1/2)}{\sinh(\chi')\chi^{2N+1/2}}. \tag{3.45}$$

As in the example of the hyper-Airy equation as demonstrated in Chapter 2, we will make the change of variables in order to write $\mathcal{S}$ as a function of χ instead of s. Under this change of variables equation (3.45) becomes

$$\frac{d\mathcal{S}}{d\chi} \sim -2\epsilon^{2N-1}e^{\chi/\epsilon}\frac{\Gamma(2N+1/2)}{\chi'\sinh(\chi')\chi^{2N+1/2}}. \tag{3.46}$$

Then, by noting the form of N, we rewrite χ in terms of polar coordinates by setting $\chi = \rho e^{i\theta}$, where we then investigate variations with respect to the fast variable θ. The change of variables given by $\chi = \rho e^{i\theta}$ gives

$$\frac{d}{d\chi} = \frac{1}{i\rho e^{i\theta}}\frac{d}{d\theta}. \tag{3.47}$$

Under this transformation the optimal truncation point can be rewritten as $N = \rho/2\epsilon + \omega$, and equation (3.45) becomes

$$\frac{d\mathcal{S}}{d\theta} \sim -2i\rho e^{i\theta}\epsilon^{\rho/\epsilon+2\omega-1}\frac{\Gamma(\rho/\epsilon+2\omega+1/2)}{\chi'\sinh(\chi')(\rho e^{i\theta})^{\rho/\epsilon+2\omega+1/2}}\exp\left(\frac{\rho e^{i\theta}}{\epsilon}\right). \tag{3.48}$$

Under this change of variables, the expression $\chi'\sinh(\chi')$ is a function depending on $s(\theta)$ and fixed parameter ρ, which we will denote by $H(s(\theta);\rho)$. We apply Stirling's formula [**2**] to (3.48) and after simplification we obtain

$$\frac{d\mathcal{S}}{d\theta} \sim -\frac{2i\sqrt{2\pi\rho}}{\epsilon H(s(\theta);\rho)}\exp\left(\frac{\rho}{\epsilon}(e^{i\theta}-1-i\theta)-i\theta(2\omega-1/2)\right). \tag{3.49}$$

The right hand side is exponentially small except in the neighbourhood of $\theta = 0$, which is exactly where the Stokes curve lies (where χ is purely real and positive). In order to study the Stokes phenomena we now rescale about the neighbourhood of the Stokes curve in order to study the variation in $\mathcal{S}$. Applying the scaling $\theta = \sqrt{\epsilon}\hat{\theta}$ to (3.49) gives us

$$\frac{1}{\sqrt{\epsilon}}\frac{d\mathcal{S}}{d\hat{\theta}} \sim -\frac{2i\sqrt{2\pi|\chi|}}{\epsilon H(|\chi|)}\exp\left(-\frac{|\chi|\hat{\theta}^2}{2}\right), \tag{3.50}$$

as $\epsilon \to 0$. We note that to leading order in ϵ, $H(s(\theta);\rho)$ will only depend on $\rho = |\chi|$ near the Stokes curve. Integrating (3.50) we find that

$$\begin{aligned}\mathcal{S} \sim &-\frac{2i\sqrt{2\pi|\chi|}}{\sqrt{\epsilon}H(|\chi|)}\left(\frac{1}{\sqrt{|\chi|}}\int_{-\infty}^{\hat{\theta}\sqrt{|\chi|}} e^{-s^2/2}ds + C\right),\\ =&-\frac{2i\pi}{\sqrt{\epsilon}H(|\chi|)}\left(\text{erf}\left(\sqrt{\frac{|\chi|}{2\epsilon}}\theta\right)+C\right),\end{aligned} \tag{3.51}$$

where C is an arbitrary constant. Thus, as Stokes curves are crossed, the Stokes multiplier changes in value by

$$\Delta\mathcal{S} \sim -\frac{4i\pi}{\sqrt{\epsilon}H(|\chi|)}, \tag{3.52}$$

and hence the exponential contribution, R_N, which experiences Stokes switching, changes by

$$\Delta R_N \sim -\frac{4i\pi}{\sqrt{\epsilon}H(|\chi|)}F(s)e^{-\chi/\epsilon},$$

as Stokes curves are crossed. We note that the error function smoothing for the Stokes multiplier may also be obtained following the work of Berry [**11**]. This requires computing the Borel sum of the divergent tail of (3.15) and is outlined in Appendix C.

Consequently, the optimally-truncated asymptotic series (3.42) can be rewritten explicitly as

$$f(s) \sim \sum_{r=0}^{N-1}\epsilon^r f_r(s) + \mathcal{S}_1F_1e^{-\chi_1/\epsilon} + \mathcal{S}_2F_2e^{-\chi_2/\epsilon}, \tag{3.53}$$

as $\epsilon \to 0$ where $\mathcal{S}_i$ varies in value by (3.52) as Stokes curves are crossed, the leading orders are given in (3.17), and the late-order behaviour is given in (3.20). This expression is therefore an accurate asymptotic approximation up to exponentially small terms in regions where the dominant asymptotic behaviour is described by the power series (3.15). We note that (3.53) contains one parameter of freedom; either $\mathcal{S}_1$ or $\mathcal{S}_2$ is free. This will be further explained in Section 3.4.5.

We have successfully determined a family of asymptotic solutions to (3.13), which contain exponentially small error. These exponentially small terms exhibit Stokes switching and therefore the expression (3.53) describes the asymptotic behaviour in certain regions of the complex plane. The regions of validity for (3.53) will be determined in the next section.

3.4.4. Asymptotic expansions in terms of the original variables.

In this section we will express the asymptotic solution (3.53) in terms of the original variables, n, by reversing the scaling transformations described by (3.11). Reversing the scalings described by (3.11), we find from (3.26) that

$$\chi_1(n) = \frac{2\epsilon}{\alpha}\left(\left(\frac{\alpha n+\beta}{2}\right)\cosh^{-1}\left(\frac{\alpha n+\beta}{2}\right) - \sqrt{\left(\frac{\alpha n+\beta}{2}\right)^2 - 1}\right). \tag{3.54}$$

Comparing the expressions given by (3.26) and (3.54) shows that the expression for the singulant in terms of n is equal to expression given by (3.26) with $s \mapsto n$, multiplied by ϵ. Hence, the prefactor, $F(s)$, is given by

$$F_i(n) = \frac{\Lambda_i}{\sqrt{\sinh(\epsilon\chi_1'(n))}} \sim \frac{\Lambda_i}{\sqrt{\epsilon\chi_1'(n)}}, \tag{3.55}$$

as $\epsilon \to 0$. Substituting (3.54) and (3.55) into (3.41) shows that the expression for the late-order terms in terms of n is given by

$$f_{2r}(n) \sim \frac{2\Lambda_1\Gamma(2r+1/2)}{\chi_1'(n)\chi_1(n)^{2r+1/2}\epsilon^{2r+1/2}}, \tag{3.56}$$

as $\epsilon \to 0$. Similarly the expression of the Stokes multiplier, (3.51), in terms of n is given by

$$\mathcal{S}(n) \sim -\frac{2i\pi}{\sqrt{\epsilon}H(|\chi|)}\left(\text{erf}\left(\sqrt{\frac{|\chi|}{2}}\theta\right) + C\right), \tag{3.57}$$

and hence the expression for the Stokes multiplier in terms of n is identical to (3.51) with $s \mapsto n$. We define the following functions of n

$$\Psi(n) = \frac{2}{\alpha}\left(\left(\frac{\alpha n+\beta}{2}\right)\cosh^{-1}\left(\frac{\alpha n+\beta}{2}\right) - \sqrt{\left(\frac{\alpha n+\beta}{2}\right)^2 - 1}\right), \tag{3.58}$$

$$\hat{\mathcal{S}}(n) = -\frac{2i\pi}{H(|\chi|)}\left(\text{erf}\left(\sqrt{\frac{|\chi|}{2}}\theta\right) + C\right), \tag{3.59}$$

Hence, the expression of (3.53) in terms of n is given by

$$x_n \sim \sum_{r=0}^{N-1} \frac{2\Lambda_1 \Gamma(2r+1/2)}{\Psi'(n)\Psi(n)^{2r+1/2}} + \hat{\mathcal{S}}_1(n)\frac{\Lambda_1 e^{-\Psi(n)}}{\sqrt{\Psi'(n)}} + \hat{\mathcal{S}}_2(n)\frac{\Lambda_2 e^{\Psi(n)}}{\sqrt{\Psi'(n)}}, \tag{3.60}$$

as $|n| \to \infty$. In the next section we will determine the Stokes structure in the complex s-plane by considering where the behaviours of the exponential terms, $e^{-\chi_1(s)/\epsilon}$ and $e^{-\chi_2(s)/\epsilon}$ in (3.53). In the complex n-plane, the Stokes structure may be obtained by considering the behaviours of the exponential terms , $e^{\pm\Psi(n)}$ in (3.60). Since we showed that the expressions for the singulants, are identical when written in terms of either s or n, we deduce that the Stokes structure in both the complex s- and complex n-planes will be identical.

3.4.5. Stokes structure.

With the results for χ_1 and χ_2 given by (3.26) and (3.27), we can investigate the switching behaviour of the exponentially small contributions. As demonstrated in Section 3.4.3.1, we found that the exponential contributions present in the series expansion (3.15) are proportional to $\exp(-\chi/\epsilon)$. These terms are exponentially small when $\mathrm{Re}(\chi) > 0$ and exponentially large when $\mathrm{Re}(\chi) < 0$. In order to investigate how these terms behave we consider the solution's Stokes structure. We recall that Stokes curves follow curves where $\mathrm{Im}(\chi) = 0$ while anti-Stokes curves follow curves where $\mathrm{Re}(\chi) = 0$. Additionally, we recall that exponentially small terms may only switch across Stokes curves where $\mathrm{Re}(\chi) > 0$.

In order to illustrate the Stokes structure for the vanishing asymptotic solutions of (3.13) we choose a representative set of parameters. In particular, we demonstrate this for the case where $\alpha = -1$ and $\beta = -1$. In the general case where $\alpha, \beta \in \mathbb{C}$, we find that complex α rotates the Stokes structure, while complex β translates it. These effects are illustrated in Figures (3.6a) and (3.6b).

In Figure 3.3a we see that there are three Stokes curves and two anti-Stokes curves emanating from the singularity in the complex s-plane. The Stokes curve located on the positive real axis switches the exponential contributions associated with χ_2, while the remaining two Stokes curves switches the exponential associated with χ_1. Additionally, there is a branch cut located along the negative real axis extending to the singularity, $s_0 = 1$. Using this knowledge, we can determine the switching behaviour as the Stokes curves are crossed.

Since there are six critical curves (Stokes, anti-Stokes curves and a branch cut) in total, we see in Figure 3.3a, that the Stokes structure naturally separates the complex s-plane into separate regions. We have the freedom to choose within which region we wish to have an asymptotic solution described by the power series (3.15). The most natural region to choose is one containing the positive real axis.

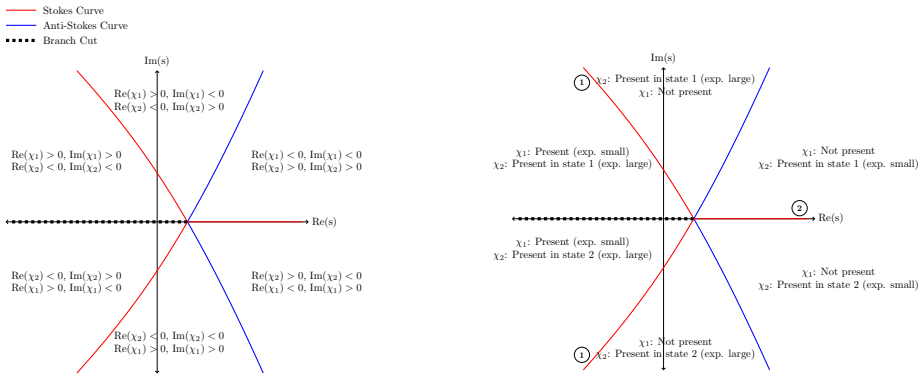

(A) Singulant behaviour. (B) Exponential behaviour.

FIGURE 3.3. These figures depict the Stokes structure of the series solution (3.15) of $\mathrm{dP_{II}}$ for parameter values $\alpha = 1$ and $\beta = 1$. Figure 3.3a illustrates the behaviour of the singulants as Stokes and anti-Stokes curves (denoted by red and blue curves, respectively) are crossed. Figure 3.3b illustrates the regions of the complex s-plane in which the exponential contributions associated with χ_1 and χ_2 are present. The exponential contribution associated with χ_1 is switched across the Stokes curves denoted by ①, which the contribution associated with χ_2 is switched when crossing the Stokes curve denoted by ②. This convention will be followed in subsequent figures.

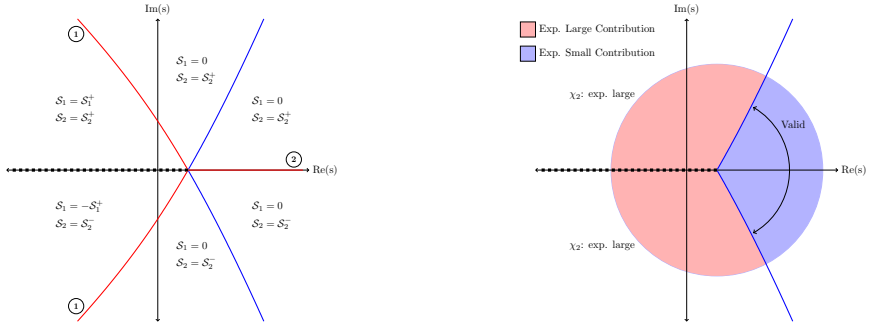

(A) Stokes multipliers. (B) Regions of validity.

FIGURE 3.4. These figures depict the Stokes structure of the series solution (3.15) of $\mathrm{dP_{II}}$ for parameter values $\alpha = 1$ and $\beta = 1$. Figure 3.4a shows the switching behaviour of the Stokes multiplier, $\mathcal{S}_i$, as Stokes curves are crossed. Figure 3.4b illustrates the regions of validity for the general asymptotic solution (3.53) with $\mathcal{S}_1 = 0$ and a free parameter, $\mathcal{S}_2$. The red shaded regions depict where exponentially-large terms are present, whereas the blue shaded regions indicate the presence of exponentially small terms present. The dominant asymptotic behaviour is described by the power series (3.15) in the region bounded by the anti-Stokes curves containing the positive real axis. Elsewhere, it will be exponentially dominated and the asymptotic behaviour will no longer be described by the power series expression.

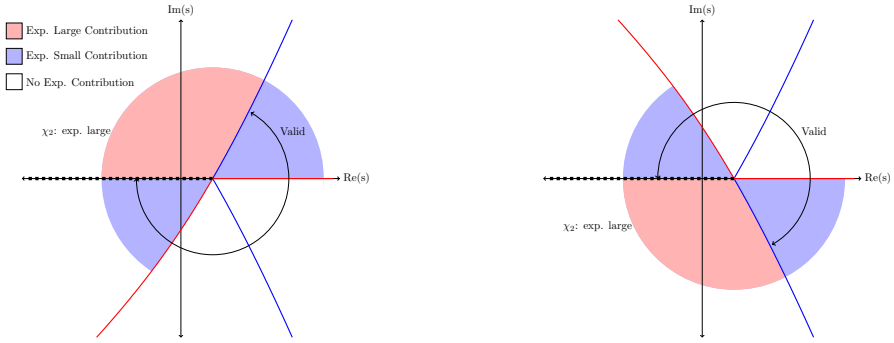

(A) First special asymptotic solution. (B) Second special asymptotic solution.

FIGURE 3.5. This figure illustrates special asymptotic solutions given in (3.53), for $\alpha = 1$ and $\beta = 1$. Figure 3.5a demonstrates that if we demand that the exponential contribution due to χ_2 be not present in the region below the real positive axis ($\mathcal{S}_2^- = 0$) then the range of validity can be extended. This is also equivalent to specifying that the dominant asymptotic behaviour is described by the power series (3.15) about the lower anti-Stokes curve. Figure 3.5b demonstrates the extended region of validity if the exponential contributions due to χ_2 is not present in the region above the real positive axis ($\mathcal{S}_2^+ = 0$). This is also equivalent to specifying that the asymptotic behaviour is described by the power series expression (3.15) about the upper anti-Stokes curve. Unshaded regions indicate regions in which there are no exponential contributions.

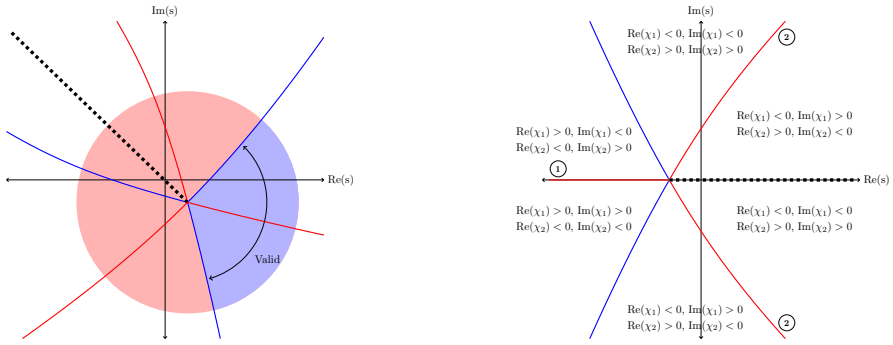

(A) Stokes structure with complex parameters $\alpha = e^{i\pi/4}$ and $\beta = 1$. (B) Stokes structure with parameters $\alpha = -1$ and $\beta = 1$.

FIGURE 3.6. These figures depict the Stokes structure for complex parameters. Figure 3.6a illustrates the Stokes structure for parameters $\alpha = e^{i\pi/4}$ and $\beta = 1$ with the region of validity for a general asymptotic solution. We see that the Stokes structure has been rotated clockwise by $\pi/4$ as a result of α being complex. We also note that the branch cut has been chosen arbitrarily. Figure 3.6b illustrates the Stokes structure for $\alpha = -1$ and $\beta = 1$. The structure is a rotation by π, as expected.

We now determine in which of these regions the dominant asymptotic behaviour may be described by the power series (3.15), referred to as regions of validity. From Figure 3.3 we deduce that the remainder term associated with χ_1 must not be present in the neighbourhood of this Stokes curve as it would exponentially dominate the leading order solution of (3.53). In order for the power series solution (3.15) to describe the dominant asymptotic behaviour we require the remainder term associated with χ_1 be absent on the positive real axis, and therefore $\mathcal{S}_1 = 0$.

However, we see that the remainder term associated with χ_2 is exponentially small since $\mathrm{Re}(\chi_2) > 0$, and therefore that the series component of (3.53) contains the dominant asymptotic behaviour. Hence, the value of $\mathcal{S}_2$ about the real axis may be freely specified, and will therefore contain a free parameter.

Since the remainder term associated with χ_2 will exhibit Stokes switching, the value of $\mathcal{S}_2$ will vary as it crosses a Stokes curve; say, from state one to state two. We denote this by writing $\mathcal{S}_2^-$ and $\mathcal{S}_2^+$. Consequently, we conclude that the exponentially small contributions associated with χ_1 is present in the regions bounded by the Stokes curves located in the upper and lower complex plane containing the branch cut. If we assume that $\mathcal{S}_2$ is nonzero on either side of the positive real axis, then the asymptotic series (3.53) is dominated by the power series expression in the region bounded by the anti-Stokes curves containing the positive real axis and contains exponentially small contributions; this is illustrated in Figure 3.4b.

We may repeat the process for the remaining five critical curves in order to obtain other types of asymptotic solutions with different ranges of validity. This results in the determination of two types of asymptotic solution classes. Type one solutions describe those in which the dominant asymptotic behaviour is described by the power series (3.15) within some region which contain a free parameter hidden beyond-all-orders. However, for special choices of the free parameter of type one solutions, we can obtain asymptotic solutions with an extended range of validity; these are referred to as type two solutions. Type two asymptotic solutions are illustrated in Figures 3.5a and 3.5b.

3.5. Non-vanishing asymptotics of discrete Painlevé II

We have completed the analysis for solutions with the behaviour $x_n \ll 1$ as $n \to \infty$ of equation (3.7). In addition to these solutions, there exist those which grow in the asymptotic limit, that is, $x_n \gg 1$ as $n \to \infty$. The analysis involved in the subsequent sections is nearly identical to Sections 3.4.1 and 3.4.3. Hence, we will omit the details and only provide the key results. The scaling for non-vanishing x_n behaviour, and the appropriate choice of parameter sizes, is given in equation (3.12). As before, we drop the hat notation for simplicity. Applying the non-vanishing type scalings (3.12) into (3.7) we obtain

$$(g(s+\epsilon) + g(s-\epsilon))(\epsilon - g(s)^2) = (\alpha s + \beta)g(s) + \gamma, \tag{3.61}$$

as $\epsilon \to 0$.

3.5.1. Asymptotic analysis of non-vanishing solutions.

We then expand $g(s)$ as an asymptotic power series in ϵ,

$$g(s) \sim \sum_{r=0}^{\infty} \epsilon^r g_r(s), \tag{3.62}$$

as $\epsilon \to 0$. Substituting (3.62) into (3.61) and by matching coefficients of ϵ we can show that the leading order solution satisfies

$$-2g_0^3 = (\alpha s + \beta)g_0 + \gamma. \tag{3.63}$$

As (3.63) is a cubic in g_0, there will be three possible leading order behaviours as $\epsilon \to 0$. The three solutions of (3.63) are

$$g_{0,1} = \frac{\Psi}{(2\sqrt{27})^{2/3}(\sqrt{\Phi} + 108\gamma)^{1/3}} - \frac{(\sqrt{\Phi} + 108\gamma)^{1/3}}{432^{1/3}}, \tag{3.64}$$

or

$$g_{0,2} = \frac{-(1 + i\sqrt{3})\Psi}{(2\sqrt{216})^{2/3}(\sqrt{\Phi} + 108\gamma)^{1/3}} + \frac{(1 - i\sqrt{3})(\sqrt{\Phi} + 108\gamma)^{1/3}}{(3456)^{1/3}}, \tag{3.65}$$

$$g_{0,3} = \frac{-(1 - i\sqrt{3})\Psi}{(2\sqrt{216})^{2/3}(\sqrt{\Phi} + 108\gamma)^{1/3}} + \frac{(1 + i\sqrt{3})(\sqrt{\Phi} + 108\gamma)^{1/3}}{(3456)^{1/3}}, \tag{3.66}$$

where $\Psi = 6(\alpha s + \beta)$ and $\Phi = 4\Psi^3 + 11664\gamma^2$. We also note that the leading order equation (3.63) is invariant under the mapping $g_0 \mapsto \omega^2 g_0$ with $\alpha s + \beta \mapsto \omega(\alpha s + \beta)$. In general, we have

$$\mathcal{O}(\epsilon^r): \qquad (\alpha s + \beta)g_r = \sum_{j=0}^{\lfloor (r-1)/2 \rfloor} \frac{2g_{r-2j-1}^{(2j)}}{(2j)!} - \sum_{m=0}^{r} g_m \sum_{l=0}^{r-m} g_l \sum_{j=0}^{\lfloor (r-m-l)/2 \rfloor} \frac{2g_{r-m-l-2j}^{(2j)}}{(2j)!}, \tag{3.67}$$

for $r \geq 1$. In order to determine the behaviour of the coefficients in (3.62) we study the singularities of the leading order behaviour.

3.5.2. Singularities of the leading order behaviour.

In this section we determine the singularities of the leading order behaviour and deduce the behaviour of the leading order term in the neighbourhood of these singularities. The singularities of g_0 occur when the discriminant of (3.63) is equal to zero. In fact, the discriminant of (3.63) is precisely given by Φ and hence the singularities of g_0 satisfy

$$\Phi = 4 \times 6^3(\alpha s + \beta)^3 + 11664\gamma^2 = 0, \tag{3.68}$$

which occurs at the points

$$s_{0,1} = \frac{-2\beta - (2\sqrt{27})^{2/3}\gamma^{2/3}}{2\alpha}, \tag{3.69}$$

$$s_{0,2} = \frac{-\beta}{\alpha} + \frac{3(1+i\sqrt{3})\gamma^{2/3}}{(16)^{1/3}\alpha}, \tag{3.70}$$

$$s_{0,3} = \frac{-\beta}{\alpha} + \frac{3(1-i\sqrt{3})\gamma^{2/3}}{(16)^{1/3}\alpha}. \tag{3.71}$$

However, it can be shown by Taylor expansion that the leading order behaviours, $g_{0,j}$, are only singular at two of these three points. Taylor expanding $g_{0,j}$ about the points $s_{0,j}$, shows that

$$g_{0,1} \sim -(2\gamma)^{1/3} + \frac{2^{2/3}\alpha}{9\gamma^{1/3}}(s - s_{0,1}) + \mathcal{O}((s-s_{0,1})^2), \quad \text{as } s \to s_{0,1}, \tag{3.72}$$

$$g_{0,1} \sim \frac{i(i+\sqrt{3})\gamma^{1/3}}{2^{5/3}} + A\sqrt{s - s_{0,2}} + \mathcal{O}(s - s_{0,2}), \quad \text{as } s \to s_{0,2}, \tag{3.73}$$

$$g_{0,1} \sim -\frac{i(-i+\sqrt{3})\gamma^{1/3}}{2^{5/3}} + \bar{A}\sqrt{s - s_{0,3}} + \mathcal{O}(s - s_{0,3}), \quad \text{as } s \to s_{0,3}, \tag{3.74}$$

where

$$A = -\frac{(3+i\sqrt{3})\sqrt{\alpha\gamma^{4/3}(-1+i\sqrt{3})}}{12\gamma^{2/3}}, \tag{3.75}$$

and $\bar{A}$ denotes the complex conjugate of A. Hence, the leading order behaviour described by $g_{0,1}$ is singular at the points $s_{0,2}$ and $s_{0,3}$. Similarly, it can be shown that

$$g_{0,2} \sim \frac{\gamma^{1/3}}{2^{2/3}} - \frac{i\sqrt{\alpha\gamma^{4/3}}}{\sqrt{6}\gamma^{2/3}}\sqrt{s - s_{0,1}} + \mathcal{O}(s - s_{0,1}), \quad \text{as } s \to s_{0,1}, \tag{3.76}$$

$$g_{0,2} \sim \frac{(1-i\sqrt{3})\gamma^{1/3}}{2^{2/3}} - \frac{i(-i+\sqrt{3})\alpha}{9\times 2^{1/3}\gamma^{1/3}}(s - s_{0,2}) + \mathcal{O}((s-s_{0,2})^2), \quad \text{as } s \to s_{0,2}, \tag{3.77}$$

$$g_{0,2} \sim -\frac{i(-i+\sqrt{3})\gamma^{1/3}}{2^{5/3}} + B\sqrt{s - s_{0,3}} + \mathcal{O}(s - s_{0,3}), \quad \text{as } s \to s_{0,3}, \tag{3.78}$$

$$g_{0,3} \sim \frac{\gamma^{1/3}}{2^{2/3}} + \frac{i\sqrt{\alpha\gamma^{4/3}}}{\sqrt{6}\gamma^{2/3}}\sqrt{s - s_{0,1}} + \mathcal{O}(s - s_{0,1}), \quad \text{as } s \to s_{0,1}, \tag{3.79}$$

$$g_{0,3} \sim \frac{i(i+\sqrt{3})\gamma^{1/3}}{2^{5/3}} + \bar{B}\sqrt{s - s_{0,2}} + \mathcal{O}(s - s_{0,2}), \quad \text{as } s \to s_{0,2}, \tag{3.80}$$

$$g_{0,3} \sim \frac{(1+i\sqrt{3})\gamma^{1/3}}{2^{2/3}} + \frac{i(i+\sqrt{3})\alpha}{9\times 2^{1/3}\gamma^{1/3}}(s - s_{0,3}) + \mathcal{O}((s-s_{0,3})^2), \quad \text{as } s \to s_{0,3}, \tag{3.81}$$

where

$$B = \frac{(3-i\sqrt{3})\sqrt{\alpha\gamma^{4/3}(-1-i\sqrt{3})}}{12\gamma^{2/3}}, \tag{3.82}$$

and $\bar{B}$ denotes the complex conjugate of B. We therefore find that $g_{0,2}$ is singular at $s_{0,1}$ and $s_{0,3}$ while $g_{0,3}$ is singular at $s_{0,1}$ and $s_{0,2}$. We note that singularities of $g_{0,j}$ may also arise at points where $\sqrt{\Phi}+108\gamma=0$; however it can be shown that these singularities are present on the sheets of (3.64)-(3.66) under the mapping $\sqrt{\Phi}\mapsto-\sqrt{\Phi}$, and are hence not present on the primary sheet containing the singularities $s_{0,j}$. Hence, by Darboux's theorem, these singularities will generate sub-subdominant exponential terms.

3.5.3. Late-order terms analysis.

As we have determined that the leading order behaviours given by (3.64) and (3.65) are singular in the complex s-plane we are now able to determine the behaviour of the coefficients in (3.62). From equation (3.67) we observe that the calculation of g_r requires two differentiations of g_{r-2}. Hence, if g_0 has a singularity of strength p then f_2 will have the same singularity but with strength $p+2$. As in the analysis of the vanishing type asymptotics found in Section 3.4.3, we find that the late-order terms for the non-vanishing type asymptotics also have factorial-over-power behaviour. The late-order terms ansatz for g_r is therefore

$$g_r(s)\sim\frac{G(s)\Gamma(r+\kappa)}{\eta(s)^{r+\kappa}}, \tag{3.83}$$

as $r\to\infty$. Applying (3.83) into (3.67) and matching orders of $\mathcal{O}(g_r)$ we obtain the following equations

$$\mathcal{O}(g_r):\quad \alpha s+\beta=-4g_0^2-2g_0^2\sum_{r=0}^{\lfloor r/2\rfloor}\frac{(-\eta')^{2j}}{(2j)!}, \tag{3.84}$$

$$\begin{aligned}\mathcal{O}(g_{r-1}):\quad 0=2\sum_{j=0}^{\lfloor (r-1)/2\rfloor}\frac{(-\eta')^{2j}}{(2j)!}-2g_0g_1\sum_{j=0}^{\lfloor (r-1)/2\rfloor}\frac{(\eta')^{2j}}{(2j)!}-8g_0g_1-2g_0g_1\sum_{j=0}^{\lfloor r/2\rfloor}\frac{(-\eta')^{2j}}{(2j)!},\\ -2g_0^2\sum_{j=0}^{\lfloor r/2\rfloor}\frac{1}{(2j)!}\left(\binom{2j}{1}(-\eta')^{2j-1}\frac{G'}{G}+\binom{2j}{2}(-\eta')^{2j-2}(-\eta'')\right),\end{aligned} \tag{3.85}$$

as $\to\infty$. We then replace the upper summation limits of (3.86) and (3.87) by infinity, and only introduce exponentially small error, to find that $\eta(s)$ and $G(s)$ solve the equations

$$\cosh(\eta')=\frac{-(\alpha s+\beta+4g_0^2)}{2g_0^2}, \tag{3.86}$$

and

$$2g_0^2\sinh(\eta')G'+g_0^2\eta''\cosh(\eta')G+(2-4g_0g_1)\cosh(\eta')G-8g_0g_1G=0, \tag{3.87}$$

respectively. Unlike f_0, g_0 has multiple singular points, and hence the Stokes and anti-Stokes curves of the non-vanishing solutions of (3.61) will be more complicated than those described in Section 3.4.5. This is illustrated in Figures 3.7a and 3.7b in Section 3.5.4.

3.5.3.1. *Calculating the singulant, η.*

In this section we are only interested in computing Stokes behaviour of the leading order subdominant exponentials present in (3.62). As these terms are proportional to $e^{-\eta/\epsilon}$, we therefore only calculate the singulant, η, in (3.83). By using the leading order equation (3.63), we can rewrite (3.86) as

$$\begin{aligned}\eta(s;j) &= \pm\int_{s_{0,j}}^{s}\left(\cosh^{-1}\left(\frac{\alpha s+\beta+4g_0(t)^2}{-2g_0(t)^2}\right)+2iM\pi\right)\,dt,\\ &= \pm\int_{s_{0,j}}^{s}\cosh^{-1}\left(\frac{\gamma-2g_0(t)^3}{2g_0(t)^3}\right)dt,\end{aligned}\tag{3.88}$$

where $s_{0,j}$ denotes the singularities of the leading order term, g_0, and where we have chosen the value $M=0$ following Section 3.4.2 as this is the value for which $|\eta|$ is smallest. The integral expression found in (3.88) denotes the singulant, which vanishes at the singularity $s_{0,j}$. As demonstrated in Section 3.4.5, we may use the solution to (3.88) to determine the Stokes structure of the asymptotic solution (3.62).

As there are three distinct leading order solutions for (3.62) we will proceed with the analysis for one particular chosen leading order behaviour. For the purpose of this demonstration we will consider (3.62) with leading order behaviour (3.64). The Stokes structure for the other leading order behaviours of (3.62) described by (3.65)-(3.66) may also be determined using the same methodology. Since the leading order equation (3.63) is invariant under the mapping $g_0\mapsto\omega^2 g_0$ with $\alpha s+\beta\mapsto\omega(\alpha s+\beta)$ and that the singulant expression only depends on g_0, the (anti-) Stokes curves associated with (3.65)-(3.66) may be obtained from the Stokes structure associated with (3.64) under this mapping.

The singularities of the chosen leading order term, (3.64), were shown to occur at $s_{0,2}$ and $s_{0,3}$ given by (3.70) and (3.71), respectively. We will therefore observe that the Stokes and anti-Stokes curves emerge from two singularities as opposed to one singularity when we compare the Stokes structure to that found in Section 3.4.5. Changing the variable of integration by setting $u=g_0(t)$ allows us to rewrite the integral (3.88) as

$$\begin{aligned}\eta(s;j) &= \pm\int_{g_0(s_{0,j})}^{g_0(s)}\cosh^{-1}\left(\frac{2u^3-\gamma}{-2u^3}\right)\left(\frac{\gamma-4u^3}{\alpha u^2}\right)du,\\ &= \pm\left(\frac{3\gamma}{\alpha g_0}\sqrt{1-\frac{4g_0^3}{\gamma}}-\frac{2g_0^3+\gamma}{\alpha g_0}\cosh^{-1}\left(\frac{\gamma}{2g_0^3}-1\right)\right),\end{aligned}\tag{3.89}$$

where $g_0=g_0(s)$ for $j=2,3$ and $4g_0^3(s_{0,j})=\gamma$. From (3.89) we observe that the expressions for $\eta(s;2)$ and $\eta(s;3)$ are the same; however, these expressions correspond to different branches of a multivalued function. The computation of $\eta(s;2)$ requires a Riemann sheet of the integrand in (3.89) to be chosen which contains the singularity $s_{0,2}$. Similarly, computing $\eta(s;3)$ requires a sheet of the integrand in (3.89) to be chosen which contains the singularity $s_{0,3}$. In particular, for

each of the two singularities, $s_{0,j}$, there are two corresponding singulants, which differ only by a change of sign. We denote the singulants by

$$\eta_1 = \eta(s;2), \quad \eta_2 = -\eta_1, \quad \eta_3 = \eta(s;3), \quad \eta_4 = -\eta_3. \tag{3.90}$$

We therefore have two exponential contributions present in the asymptotic expansion (3.62). The asymptotic series expansions containing the exponentially small contributions is therefore given by

$$g(s) \sim \sum_{r=0}^{N_1-1} \epsilon^r g_r(s) + \mathcal{S}_1 e^{-\eta_1/\epsilon} + \mathcal{S}_2 e^{-\eta_2/\epsilon} + \mathcal{S}_3 e^{-\eta_3/\epsilon} + \mathcal{S}_4 e^{-\eta_4/\epsilon}, \tag{3.91}$$

where N_1 is the optimal truncation point of (3.62) and $\mathcal{S}_i$ are the Stokes multipliers of the exponential contributions associated with η_i.

3.5.4. Stokes structure.

Once the singulant, η, is determined we may determine the Stokes structure of the asymptotic solution as the exponentially small contributions are proportional to $\exp(-\eta/\epsilon)$. As discussed in Section 3.4.5, the exponentially small contributions present are generally proportional to $\exp(-\eta/\epsilon)$, and we may therefore obtain the Stokes structure to (3.62) by studying η. In this section, we will describe the Stokes structure and determine the regions of validity of (3.62) with leading order behaviour (3.64) with parameter values $\alpha = 2, \beta = -1$ and $\gamma = 2$.

The Stokes and anti-Stokes curves emanating from the singularities, $s_{0,j}$, may then be determined by the conditions

$$\text{Im}(\eta_i(s)) = 0,$$

and

$$\text{Re}(\eta_i(s)) = 0,$$

respectively. The Stokes structure of the asymptotic solution with leading order term given by (3.64) is illustrated in Figures 3.7a and 3.7b. In Figure 3.7a we see that there are three Stokes, two anti-Stokes curves and a branch cut emanating from the upper singularity. The two Stokes curves located on either side of the branch cut of the upper singularity switches the exponential contribution associated with η_1, while the remaining Stokes curve emanating from the upper singularity switches the exponential associated with η_2.

We now determine regions in the complex plane in which the asymptotic behaviour may be described by the power series expansion (3.62) with leading order term (3.64). From Figure 3.7a we deduce that the remainder term associated with η_2 must not be present in the neighbourhood of the Stokes curve immediately to the right of the branch cut as it would exponentially dominate the leading order term (3.64). In order for the power series expansion (3.62) to describe the dominant asymptotic behaviour we require the remainder term associated with η_2 to be absent in this region, and hence $\mathcal{S}_2 = 0$.

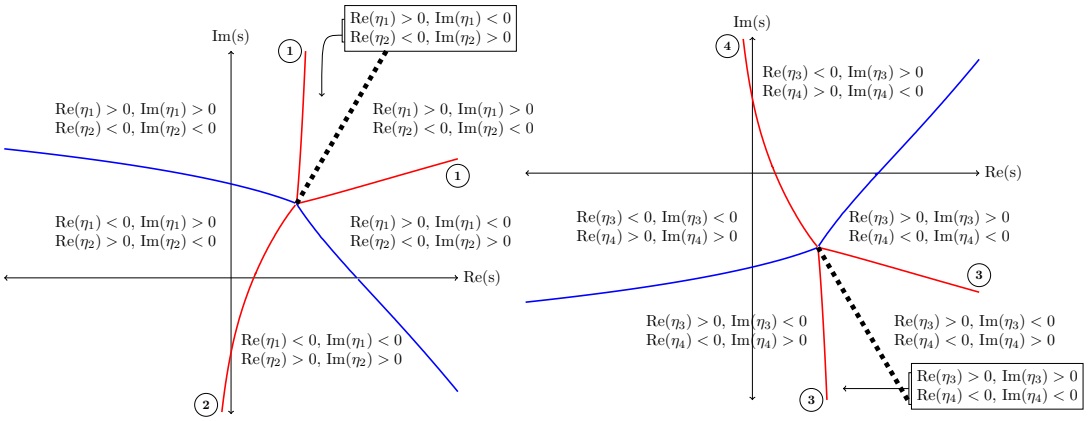

(A) Stokes structure emerging from upper singularity.

(B) Stokes structure emerging from lower singularity.

FIGURE 3.7. This figure illustrates the Stokes structure for non-vanishing asymptotic solutions of $\mathrm{dP_{II}}$ described by (3.91). In this case, the Stokes and anti-Stokes curves emerge from two singularities rather than one. We also note the Stokes structure in the upper half plane is symmetric to the Stokes structure in the lower half plane.

However, we see that the remainder term associated with η_1 is exponentially small in this region since $\mathrm{Re}(\eta_1) > 0$. Hence, the value of $\mathcal{S}_1$ in this region may be freely specified and will therefore contain a free parameter. The remainder term associated with η_2 will therefore exhibit Stokes switching behaviour as it crossed a Stokes curve, say, from state one to state two. Consequently, we conclude that the exponentially small contribution associated with η_2 is present in the region bounded by the branch cut of the upper singularity and the lower anti-Stokes curve. If we assume that $\mathcal{S}_1$ is nonzero on either side of the lower Stokes curve emerging from the upper singularity then the asymptotic power series (3.62) is dominated by the term g_0 (3.64) in the region bounded by the branch cut of the upper singularity and the lower anti-Stokes curve. This is illustrated in Figure 3.8a.

We obtain asymptotic solutions which exhibit similar features to those described in Section 3.4.5. Type one solutions are those in which the dominant asymptotic behaviour described by the asymptotic power series (3.62) within some region which contain a free parameter hidden beyond-all-orders. These asymptotic solutions have regions of validity within two adjacent regions of the complex s-plane. However, for special choices of the within type one solutions, the range of validity can be extended by two additional adjacent regions in the complex s-plane; type two solutions. Type two solutions are the special solutions of (3.7) which contain no free parameters and are therefore uniquely defined. The ranges of validity for type two solutions is illustrated in Figure 3.8b.

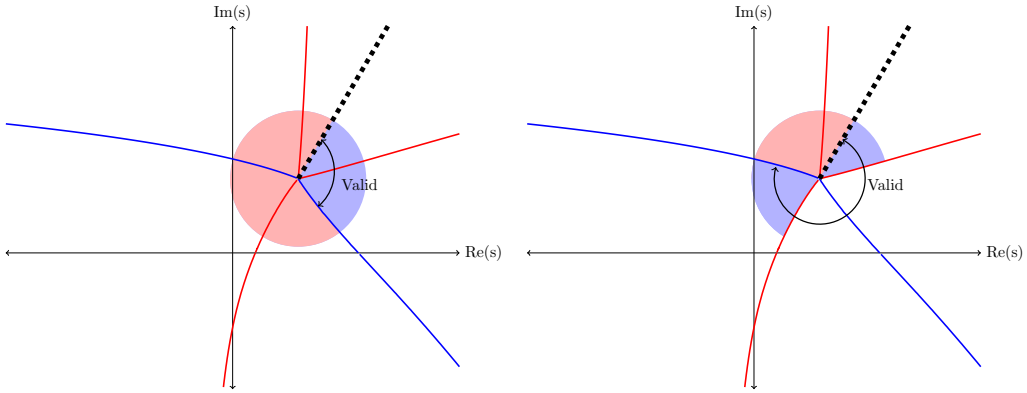

(A) General asymptotic solution. (B) Special asymptotic solution.

FIGURE 3.8. This figure illustrates the asymptotic solutions described by the power series (3.62) about the Stokes curve extending to the real positive direction. The blue shaded regions show the presence of exponentially small contributions, while the contributions are exponentially large in the red shaded regions. Unshaded regions illustrate no exponential contributions and therefore the asymptotic behaviour is described by the leading order solution (3.64). Figures 3.8a illustrate the regions of validity of a general asymptotic solution about the upper singularity. This asymptotic solution contain one free parameter hidden beyond-all-orders. The regions of validity to these asymptotic solutions may be extended as shown in figure 3.8b. This is possible if we demand that the exponential term be absent in the appropriate region. Due to the symmetry of the Stokes structure, the region of validity to the contribution due to the lower singularity is symmetric with respect to the real axis.

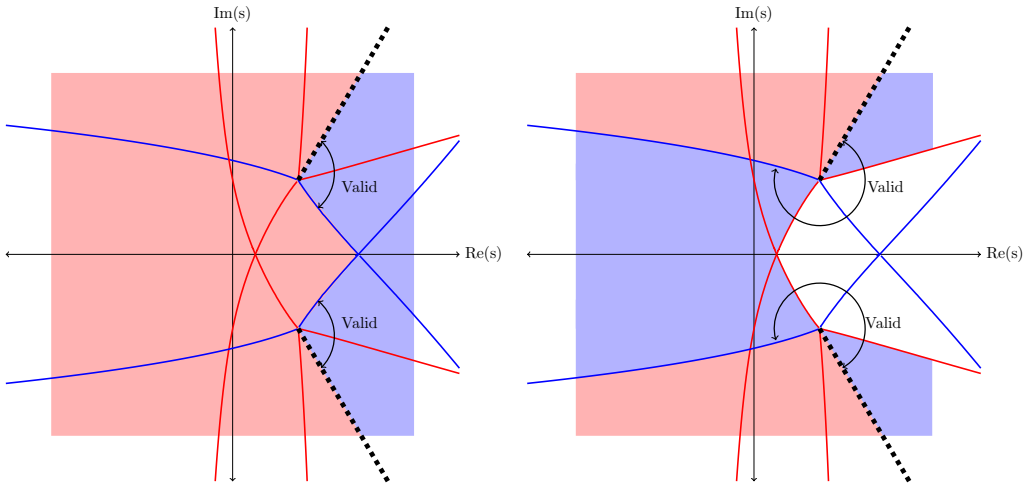

(A) Composite general asymptotic solution. (B) Composite special asymptotic solution.

FIGURE 3.9. This figure illustrates the regions of validity of the composite general and special asymptotic solutions of dP_{II} described by (3.62). Here the shading has the meaning described in Figure 3.4b. Due to the symmetry of the Stokes structure illustrated in Figures 3.8a and 3.8b, the composite behaviour for the general and special asymptotic solutions can be obtained. No interaction effects occur at the intersection between Stokes curves on the real axis, as $\mathrm{Re}(\eta)$ takes the same value for both contributions at this point, and therefore both contributions are the same size as $\epsilon \to 0$.

The analysis for the behaviours of the exponential contributions associated with η_3 and η_4 emanating from the lower singularity can be similarly repeated. In particular, we may deduce from Figure 3.7 that $\mathcal{S}_3$ may be free specified while we must take $\mathcal{S}_4 = 0$. Moreover, the symmetry between the singularities depicted in Figures 3.7 and 3.9 suggest that the Stokes multipliers $\mathcal{S}_1$ and $\mathcal{S}_3$ are complex conjugates of each other. Consequently, the non-vanishing asymptotic solution (3.91) contains one free parameter hidden beyond all orders.

As the asymptotic solution is singular at both the upper and lower singularities, the general asymptotic expression involves the combinations of the exponential contributions due to both the lower and upper singularities. The composite behaviour of type one and type two solutions is illustrated in Figures 3.9a and 3.9b.

Similarly in Section 3.4.5, we have the freedom to choose any of the other Stokes or anti-Stokes curve about which the dominant asymptotic behaviour is described by the power series (3.62). As a result, other asymptotic solutions can be obtained by rotating a known asymptotic solution through two adjacent regions. Thus, we have determined the regions of validity for the asymptotic solutions of $\mathrm{dP_{II}}$ which grow in the limit $\epsilon \to 0$ and qualitatively determined the Stokes behaviour present within these solutions.

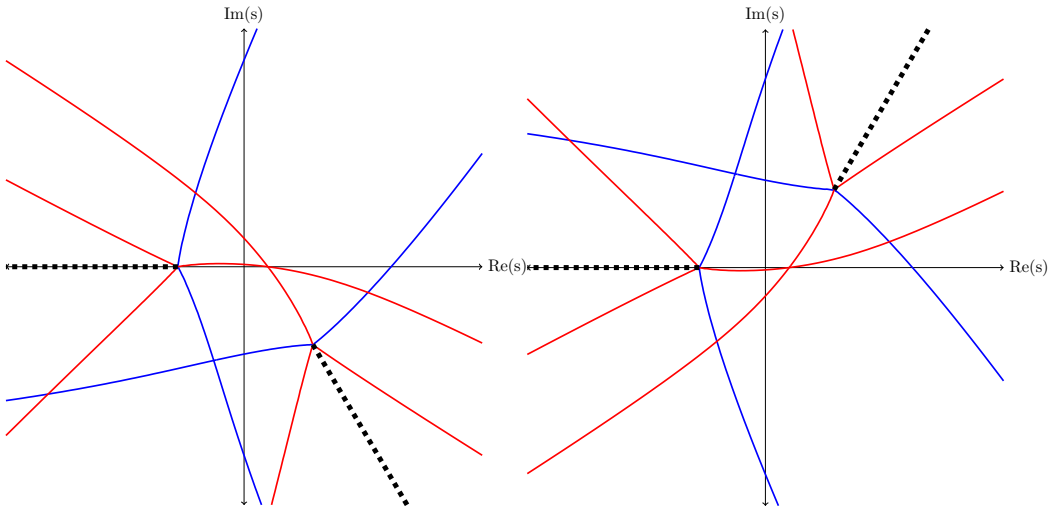

(A) Stokes structure of $g_{0,2}$. (B) Stokes structure of $g_{0,3}$.

FIGURE 3.10. Figures 3.10a and 3.10b illustrates the Stokes structure of (3.91) with leading order behaviour given by (3.65) or (3.66), respectively. These Stokes structure are related to the Stokes structure illustrated in figure 3.9 under the mapping $\alpha s + \beta \mapsto \omega(\alpha s + \beta)$, where $\omega^3 = 1$.

We have demonstrated the Stokes structure for the non-vanishing asymptotic solution (3.62) with leading order behaviour (3.64). Recall that the leading order equation (3.63) is invariant under

the mapping $g_0 \mapsto \omega^2 g_0$ with $\alpha s + \beta \mapsto \omega(\alpha s + \beta)$. Since the singulant expression, (3.89), only depends on g_0, the Stokes structure for the remaining two non-vanishing asymptotic solutions may be obtained by applying the mapping $g_0 \mapsto \omega^2 g_0$ and $\alpha s + \beta \mapsto \omega(\alpha s + \beta)$ to (3.89). The Stokes structure of (3.91) with leading order behaviour given by (3.65) or (3.66) are illustrated in Figures 3.10a and 3.10b, respectively.

3.6. Numerical computation for discrete Painlevé II

In this section we give a numerical example of (3.7) for the choice of $\alpha = 3/4, \beta = -1$ and $\gamma = 2$. Given two initial conditions, x_0 and x_1, a sequence of solutions may be obtained by repeatedly iterating (3.7). In general, only a certain choice of initial conditions will give a solution of (3.7) which tends to the asymptotic behaviour of interest. We follow the numerical method demonstrated by [**83**], originally based on the works of [**81**] to find appropriate initial conditions which tend to the non-vanishing solution, (3.91), of (3.7).

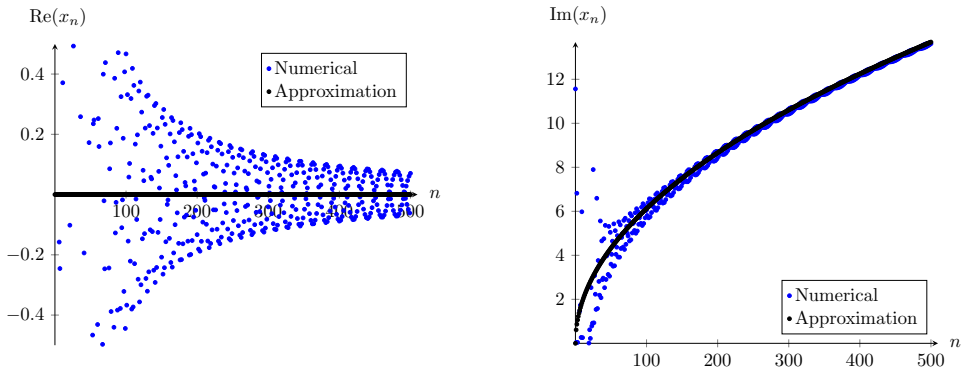

(A) Numerical values of Re(x_n). (B) Numerical values of Im(x_n)

FIGURE 3.11. This figure illustrates the behaviour of the solutions to (3.7) with $\alpha = 3/4, \beta = -1$ and $\gamma = 2$. The boundary conditions are chosen such that $x_0 = 4.184860673 + 11.56360129i$ and $x_1 = 0.987362366 + 0.04392112i$. The values of x_n are represented as blue circles, and the nonvanishing asymptotic solution, $x_n \sim i\sqrt{\alpha n/2}$ as $n \to \infty$, is represented by the black cross marks. From Figures 3.11a and 3.11b we see that the behaviour of the difference equation tends to the asymptotic expression for large n.

Figure 3.11 illustrates a comparison between the numerical solution of (3.7) with $\alpha = 3/4, \beta = -1, \gamma = 2$ and the initial conditions $x_0 = 4.184860673 + 11.56360129i, x_1 = 0.987362366 + 0.04392112i$ and the leading order term of (3.91). Figure 3.11a and 3.11b show that real part of x_n converges slower compared to the imaginary part of x_n to the leading order asymptotic approximation for large n.

We remark that the ideas of [**81**, **83**] may also be used to find initial conditions for which the behaviour of (3.7) tends to the vanishing asymptotic solution (3.53). However, we had very limited

success using this approach due to the high sensitivity to numerical error. More sophisticated numerical methods are required to be developed in order to capture vanishing type solution behaviour, which is beyond the scope of this thesis.

3.7. Conclusions

In this chapter, we used exponential asymptotics methods to compute and investigate the asymptotic solutions to the second discrete Painlevé equation whose leading order behaviour can be described by rational expressions such as (3.17), (3.64), or (3.65). We then determined the Stokes structure and used this information to deduce the regions of validity to these asymptotic solutions. The asymptotic solutions obtained are given as the sum of a truncated asymptotic power series and an exponentially subdominant correction term given by (3.53).

In Sections 3.4.1 and 3.4.3, we considered asymptotic solutions which vanish as $n \to \infty$. Using exponential asymptotics, we determined the form of subdominant exponential contributions present in the asymptotic solutions, which are defined up to two free Stokes-switching parameters. From this behaviour, we deduced the associated Stokes structure, illustrated in Figure 3.3. By considering the Stokes phenomenon, we found that the dominant asymptotic behaviour is described by a power series (3.15) in a region of the complex plane centered around the positive real axis. Furthermore, we found that it is possible to select the Stokes parameters so that the exponential contribution is absent in the region where it would normally become large. Consequently, the regions of validity for these associated special asymptotic solutions are a significantly larger region of the complex plane, as shown in Figure 3.5a.

In Section 3.5, we considered the equivalent analysis for asymptotic solutions of the second discrete Painlevé equation which grow as $n \to \infty$, rather than vanishing. By applying exponential asymptotic methods, we again determined the Stokes structure present in these asymptotic solutions. We note that the structure of Stokes and anti-Stokes curves for this problem, illustrated in Figures 3.7a and 3.7b, is significantly more complicated than in the vanishing case. Despite this, careful analysis of the exponentially small asymptotic contributions in the problem is sufficient for us to determine the regions of validity for the asymptotic series. We again find that the asymptotic behaviour contains free Stokes switching parameters, and that these parameters may again be chosen such that the exponential contributions disappear in regions where they would otherwise become exponentially large. This causes the associated asymptotic series expression to have a larger region of validity, illustrated in Figure 3.9b, including the entire real axis.

We note that, when the scalings for the vanishing case, (3.11), and the non-vanishing case, (3.12), are undone, we find that the leading order solutions of $\mathrm{dP_{II}}$ are given by $x_n \sim -\gamma/\alpha n$ and $x_n \sim \pm i\sqrt{\alpha n/2}$ as $n \to \infty$, respectively. From this analysis, we determine two types of asymptotic behaviours; type one solutions contain a free parameter hidden beyond-all-orders and type two solutions are uniquely determined with an extended region of validity.

Features of these asymptotic solutions are shared with the classical tronquée and tri-tronquée solutions of $\mathrm{P_{II}}$, (3.8). The tronquée solutions contain free parameters hidden beyond-all-orders

while the tri-tronquée are uniquely defined, both of which are described by asymptotic power series in certain sectors in the complex plane separated by Stokes and anti-Stokes curves. In particular, the tronquée and tri-tronquée solutions of the second Painlevé equation are described by divergent power series with leading order behaviours $w \sim \sqrt{-t/2}$ or $w \sim -\mu/t$, respectively as $|t| \to \infty$. These similarities are shared with the asymptotic behaviours we found for $\mathrm{dP_{II}}$.

The asymptotic study considered in [**83**] used the same ideas to investigate asymptotic solutions for the first discrete Painlevé equation ($\mathrm{dP_I}$). The qualitative features of the asymptotic solutions obtained in this study are very similar to those in [**83**]. Using these ideas, both [**83**] and the current study were able to determine solutions which are asymptotically free of poles to nonlinear discrete equations. An important distinction between both the Stokes structure of classic (tri-)tronquée solutions of the Painlevé equations and the Stokes structure found in [**83**] is that the regions of validity for the asymptotic behaviours found in this study are bounded by curves rather than rays.

CHAPTER 4

Multiplicative difference equations

The main goal of this chapter is to investigate Stokes behaviour in solutions of q-difference equations. In Chapter 3 we showed how to describe such behaviour for solutions of additive difference equations by considering the second discrete Painlevé equation as the independent variable approaches infinity. This was possible by an appropriate choice of scalings for the variables involved in the problem. Following the ideas presented in Chapter 3, we show how to describe Stokes behaviour for q-difference equations.

In this chapter we will consider the asymptotic behaviour of solutions of q-difference equations in the limit $|q| \to 1$. In particular we study q-analogues of the Airy and first Painlevé equation, both of which are described by second order q-difference equations. In general, a k^{th} order q-difference equation is of the form

$$F(y(q^k x), y(q^{k-1}x), y(q^{k-2}x), \ldots, y(qx), y(x), x) = 0, \tag{4.1}$$

where x is the independent variable, a parameter $q \in \mathbb{C}$ such that $|q| \neq 0, 1$ and $y(x)$ is the dependent variable. In principle, for some fixed value of $x \in \mathbb{C}$, the value of $y(q^k x)$ may be computed if the values of $y(x)$ at the points $\{x, qx, q^2x, \ldots, q^{k-2}x, q^{k-1}x\}$ are known.

If the independent variable is parametrized by setting $x = x_0 q^n$ for some $x_0 \in \mathbb{C}$ and $n \in \mathbb{Z}$, then (4.1) may be rewritten as

$$F(y_{n+k}, y_{n+k-1}, y_{n+k-2}, \ldots, y_{n+2}, y_{n+1}, y_n, x_0 q^n) = 0, \tag{4.2}$$

where $y_n = y(x)$. This parametrization therefore transforms a k^{th} order q-difference equation into a k^{th} order additive difference equation. Multiplicative and additive difference equations are similar in the sense that a sequence of solutions to both types of equations (of k^{th} order) can be obtained recursively from the governing equation provided there are k initial values ,i.e., if the values of $y(0), y(1), \ldots, y(k-1)$ are known. However, there is one distinct difference which distinguishes these two types of equations.

The parametrization $x = x_0 q^n$ where $n \in \mathbb{Z}$, which we denote by $x_0 q^{\mathbb{Z}}$, describes a discrete set of points, which lie along the curve $x = x_0 q^s$ where $s \in \mathbb{R}$ and where the principal branch of q^s is taken. Since q is a complex-valued parameter such that $|q| \neq 0, 1$, the curve $x = x_0 q^s$ describes a curve known as a *q-spiral*. Hence, the solutions of q-difference equations are iterated along a q-spiral rather than a straight line as in the case of additive difference equations. Since the parameter q is responsible for this geometric evolution, multiplicative difference equations are also

known as *q-difference equations*. In particular, distinct choices of x_0 produce distinct q-spirals and hence an infinite number of distinct q-spirals are needed to cover the entire complex x-plane.

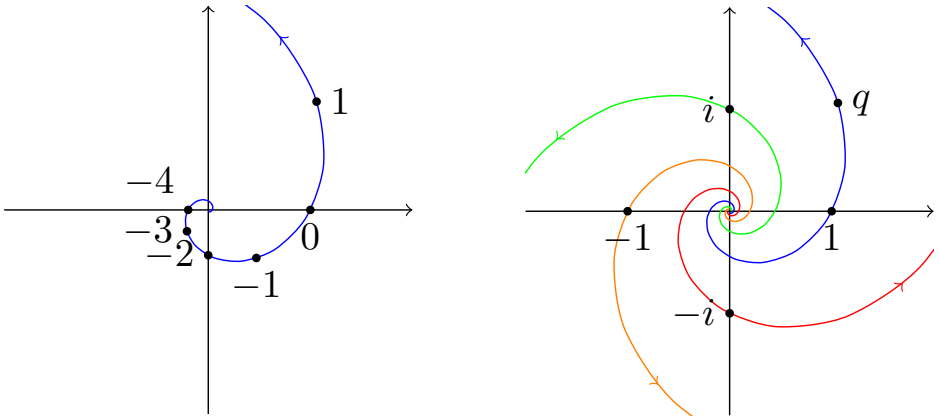

(A) Discrete domain of solutions of q-difference equations.

(B) Four continuous q-spirals.

FIGURE 4.1. This figure illustrates the discrete domain on which the solutions of q-difference equations are iterated over for the choice of $q = 1 + i$. This domain takes the form $x = x_0 q^n$ for some $x_0 \in \mathbb{C}$ and fixed $q \in \mathbb{C}$. In Figure 4.1a the dots with labels n denote the solution at the n^{th} time step. These discrete domains lie along curves known as q-spirals; four distinct q-spirals are illustrated in Figure 4.1b. In this figure, the blue, orange, green and red spirals correspond to q-spirals with the choices $x_0 = 1, -1, i, -i$, respectively. The arrows on each spiral denote the direction of the forward iteration. As $|q| > 1$, the forward iteration tends to ∞ while backward iteration tends to 0.

In the spirit of Chapter 3, we apply a specific choice of scalings in order to investigate Stokes behaviour present in solutions of q-difference equations. In Chapter 3 we demonstrated how to apply the exponential asymptotic methods developed by King and Chapman [**92**], based on the works Chapman et al. [**32**] and Olde Daalhuis [**121**], in order to study nonlinear additive difference equations. We found that by rescaling the independent variable of an additive difference equation we could transform a difference equation into another difference equation whose step size is small in the chosen limit.

As discussed earlier, q-difference equations can be rewritten as an additive difference equation by setting $x = x_0 q^n$. The method demonstrated in Chapter 3 will not work for q-difference equations as terms of the form q^n appear in the rescaled equations, which cannot be expanded as a power series in n as $n \to \infty$. We therefore extend the methods used in Chapter 3 for q-difference equations by choosing an appropriate choice of scalings for the parameter q.

The outline of this chapter is as follows. We first provide a brief survey of divergent series found within the context of q-difference equations and describe analogues of the factorial growth, Borel summation methods and behaviour known as q-Stokes phenomenon.

In Section 4.2 we discuss the choice of scalings, which we will apply in the analysis of the q-Airy and first q-Painlevé equation. The scalings we apply is given by $x = q^n$ where $n = s/\epsilon$ and $q = 1 + \epsilon$. Under this choice of scaling, the asymptotic analysis of q-difference equations are investigated in the complex s-plane. Hence, in order to interpret the results found in the complex s-plane in the complex x-plane, we must understand the mapping defined by this choice of scaling. In particular, we will discover in Section 4.2 that it is sufficient to analyse the rescaled problem in a semi-infinite domain of the complex s-plane rather than the whole complex s-plane.

In Section 4.3 of this chapter we consider a q-analogue of the Airy function, known as the q-Airy equation. By following the scaling approach used in Chapter 3 we will determine the asymptotic solutions of the q-Airy equation in the limit $|q| \to 1$ and $n \to \infty$, its associated Stokes structure and deduce Stokes behaviour present in these solutions. In particular, we will find that the solutions obtained from this approach share features with the asymptotic behaviour of the continuous Airy functions.

In Section 4.4, we follow Chapter 3 and extend the analysis to study solutions of the first q-Painlevé equation (q-$\mathrm{P_I}$). The solutions we find in this section are described by asymptotic power series containing exponentially small correction terms as $|q| \to 1$ and $n \to \infty$. In particular, we describe two solution behaviours of q-$\mathrm{P_I}$, which we call type A and type B solutions. For both types, we determine their associated Stokes structure and the Stokes behaviour present within these asymptotic solutions.

All results found for the q-Airy and first q-Painlevé equations in this chapter are entirely new, unless stated otherwise.

4.1. Introduction

In this chapter we extend the methodology presented in Chapter 3 to describe Stokes behaviour in solutions of q-difference equations. In this section we discuss the current situation regarding divergent series solutions of q-difference equations and propose an approach to extend the methods applied in Chapter 3 to study solutions described by divergent series.

As in the case of both differential and difference equations, solutions of q-difference equations may also be described by divergent asymptotic series expansions. In order to draw parallels between the form of divergent series found in q-difference and continuous equations we consider the following q-difference equation

$$xy(qx) - y(x) = -1, \tag{4.3}$$

where $x \in \mathbb{C}$ and $q \in \mathbb{C}$ such that $|q| \neq 0, 1$. It can be shown that (4.3) admits a solution which is asymptotic to the formal power series solution [**159**]

$$y(x) \sim \sum_{n=0}^{\infty} q^{n(n-1)/2} x^n, \tag{4.4}$$

as $|x| \to 0$. By the ratio test, we find that (4.4) is divergent for $|q| > 1$. For this reason, we restrict our attention to the case $|q| > 1$. The series expansion in (4.4) is considered to be a q-analogue of

the *Euler series* [**143**, **158**], which is given by the formal series

$$f(x) \sim \sum_{n=0}^{\infty} n!(-x)^{n+1}, \tag{4.5}$$

as $|x| \to 0$. We note that (4.5) is also divergent and is asymptotic to a solution of the differential equation

$$x^2 f'(x) + f(x) = -x. \tag{4.6}$$

By observation we see that the coefficients in (4.4) grow as $q^{n(n-1)/2}$ as $n \to \infty$. This turns out to be a generic feature of divergent formal series solutions of q-difference equations [**47**,**140**,**158**,**160**]. Examples of series expansions whose coefficients grow like $q^{\alpha n^2}$ where $\alpha > 0$ have appeared in the study of the q-analogues of the Bessel function [**161**], Airy function [**107**, **110**] and the first Painlevé equation [**80**, **113**, **114**]. The coefficients of divergent power series expansion of solutions to q-difference equations are generically proportional to

$$q^{\alpha n^2},$$

as $n \to \infty$ where $\alpha > 0$. As the formal series expansions of solutions of differential equations generically diverge as a factorial [**48**], the term $q^{n(n-1)/2}$ is considered to be a q-analogue of the factorial function [**140**, **158**, **160**]. This is also the reason why (4.4) is regarded as a q-analogue of the Euler series, (4.5).

In principle, optimal truncation methods can also be applied to study divergent asymptotic series expansions of solutions of q-difference equations. Applying the idea of optimal truncation discussed in Section 2.2, the series expansion given by (4.4) can be optimally-truncated by writing

$$y\,(x) = \sum_{n=0}^{N_{\text{opt}}-1} q^{n(n-1)/2} x^n + R_N(x), \tag{4.7}$$

where N_{opt} is the optimal truncation point. In order to find the value of N for which the coefficient in (4.4) is least, we use the heuristic given by (2.25) and find that

$$N_{\text{opt}} \sim -\frac{\log|x|}{\log|q|}, \tag{4.8}$$

as $|x| \to 0$, which shows that $N_{\text{opt}} \gg 1$ in the limit $|x| \to 0$. Furthermore, we can provide an estimate to the optimally-truncated error of (4.4). Since the optimally-truncated error of (4.4) is proportional to the first neglected term, we have

$$R_N = \mathcal{O}\big(q^{N(N-1)/2} x^N\big), \tag{4.9}$$

as $|x| \to 0$, and hence

$$R_N \sim q^{N(N-1)/2} x^N, \tag{4.10}$$

as $|x| \to 0$. Then, by substituting (4.8) into (4.10) we find that

$$R_N \sim \frac{\sqrt{x}}{q^{1/8}} \exp\left(\frac{1}{2}\left(\frac{\log|x|}{\log|q|}\right)^2 \log(q) - \frac{\log|x|}{\log|q|}\log(x)\right), \tag{4.11}$$

as $|x| \to 0$. If we let $x = |x|\, e^{i\theta}$ and $q = |q|e^{i\psi}$ then (4.11) can be rewritten as

$$R_N \sim \frac{\sqrt{x}}{q^{1/8}} \exp\left(-\frac{1}{2}\left(\frac{\log|x|}{\log|q|}\right)^2 + i\left(\frac{\psi}{2}\left(\frac{\log|x|}{\log|q|}\right)^2 - \theta\frac{\log|x|}{\log|q|}\right)\right), \tag{4.12}$$

as $|x| \to 0$. Hence, we find that the optimally-truncated error of the q-Euler series, (4.4), is exponentially small in the limit $|x| \to 0$ for $|q| > 1$. To possibly investigate Stokes behaviour present in (4.4), if any, we consider the optimally-truncated error, R_N. The substitution of (4.7) into (4.3) gives

$$xR_N(qx) - R_N(x) = -q^{N(N-1)/2}x^N. \tag{4.13}$$

In the case of differential and additive difference equations, the WKB method would be applied in order to determine the form of $R_N(x)$. However, there is no known analogue of the WKB method for q-difference equations, which is a development beyond the scope of this thesis.

4.1.1. q-Borel summation methods.

In the continuous theory, Borel summation methods are also used to describe Stokes behaviour by resumming divergent asymptotic series expansions. The q-analogues of these methods have also been developed for linear q-difference equations [**47**, **140**, **158**, **160**, **162**]. We first define some notation used in this chapter following the standard notation used in Sections 5.18, 17.2-17.4 of [**1**]. The *q-Pochhammer symbol* is defined by

$$(a;q)_n = \prod_{j=0}^{n-1}(1-aq^j), \tag{4.14}$$

$$(a;q)_0 = 1, \tag{4.15}$$

and

$$(a;q)_\infty = \lim_{n\to\infty}(a;q)_n. \tag{4.16}$$

Moreover, we denote

$$(a_1, a_2, \cdots, a_m; q)_n = (a_1;q)_n(a_2;q)_n \cdots (a_m;q)_n. \tag{4.17}$$

The *q-factorial* is defined by

$$[n]_q! = \frac{(q;q)_n}{(1-q)^n}, \tag{4.18}$$

and the *Jackson integral* [**62**] is defined by

$$F(x) = \int_0^x f(t)d_qt = (1-q)x\sum_{n=0}^{\infty} f(q^nx)q^n. \tag{4.19}$$

The function $e_q(x)$ [**47**, **62**] is defined to be

$$\begin{aligned} e_q(x) =& (-(1-p)x;p)_\infty, \\ =& \sum_{n=0}^{\infty}\frac{x^n}{[n]_q!}, \end{aligned} \tag{4.20}$$

where $p = q^{-1}$. From equation (4.14), we find that $e_q(x)$ is equal to zero at the points $x = -p^{-\mathbb{Z}}/(1-p)$. The *basic hypergeometric series* [**62**] are defined by

$$ {}_r\varphi_s(a_1,\cdots,a_r;b_1,\cdots,b_s;q,x) = \sum_{n=0}^{\infty} \frac{(a_1,\cdots,a_r;q)_n}{(b_1,\cdots,b_s;q)_n(q;q)_n} \left((-1)^n q^{n(n-1)/2}\right)^{1+s-r} x^n. \tag{4.21} $$

The *theta function of Jacobi* is defined by the following series

$$ \theta_q(x) = \sum_{n\in\mathbb{Z}} q^{n(n-1)/2} x^n. \tag{4.22} $$

The analogues of the Borel transform and Borel sum in the theory of linear q-difference equations are known as the q-Borel transform and q-Borel sum, respectively. Collectively, we refer to these techniques as q-Borel summation methods. Di Vizio and Zhang [**47**] define the q-Borel transform of a power series of the form

$$ \sum_{n=0}^{\infty} a_n x^{n+1}, \tag{4.23} $$

as

$$ \mathrm{B}_q : \quad \sum_{n=0}^{\infty} a_n x^{n+1} \mapsto \sum_{n=0}^{\infty} \frac{a_n}{q^{n(n-1)/2}} \zeta^n = \phi(\zeta). \tag{4.24} $$

The q-Borel sum of (4.23) in the direction of $\lambda \in \mathbb{C}\backslash\{0,\infty\}$ is defined by

$$ \mathcal{S}_q^{[\lambda]}\phi = \frac{q}{1-p} \int_{\lambda p^{\mathbb{Z}}} \frac{\phi(\frac{\zeta}{1-p})}{e_q(\frac{\zeta}{(1-p)x})} d_p\zeta, \quad x \notin (p-1)\lambda q^{\mathbb{Z}}, \tag{4.25} $$

where $p = q^{-1}$. In view of the Jackson integral, (4.19), the q-Borel sum given in (4.25) is a discrete summation of (4.23) along the q-spiral defined by $\lambda p^{\mathbb{Z}}$. This is defined everywhere in the complex plane except at the q-spiral defined by $(p-1)\lambda q^{\mathbb{Z}}$. On this particular q-spiral, the denominator of the integrand in (4.25) is equal to zero and hence describe the poles of (4.25). Furthermore, for each choice of λ, the q-Borel sum constructs a sum of (4.23) along each distinct direction of summation.

4.1.2. q-Stokes phenomenon.

This method of resumming divergent series for linear q-difference equations uncovers behaviour referred to as *q-Stokes phenomenon*. However, q-Stokes phenomenon is unlike the classical Stokes phenomenon for differential equations. This is because the q-Borel sum in (4.25) constructs a distinct meromorphic solution for each distinct choice of λ [**47**]. In particular, Di Vizio and Zhang show in [**47**] that the difference in sums along two distinct q-spirals is proportional to a product of q-Jacobi theta functions.

In the usual case, the Borel sum assigns a sum to a divergent series, which is interpreted as the function asymptotic to this series. The q-Borel sum also does this, however, the resulting sum is described by an asymptotic expansion which is valid in the whole complex plane except on the

q-spiral defined in (4.25). The asymptotic expansion does not vary in the complex plane and hence does not describe the usual Stokes behaviour; an example showing this explicitly will be given in Section 4.3. The notion of q-Stokes phenomenon and its differences to the classical Stokes phenomenon in differential equations are detailed in [**47**, **140**].

One particular application of q-Borel resummation is to develop connection formula for linear q-special functions. These q-special functions include q-analogues of the Airy, Bessel and hypergeometric functions. A connection formula is an expression which relates the solution behaviour of an equation under a given asymptotic limit to the solution behaviour as another limit is approached. Examples include formulae which relate the solution behaviour at infinity to its behaviour at the origin or those which relate the solution between two distinct approaches toward infinity.

Morita constructed a connection formula relating solutions of a q-analogue of the Airy equation at the origin and infinity [**107**, **110**]. Following the work of Morita [**108**], Ohyama was also able to construct connection formula for a certain class of basic hypergeometric series [**115**]. In both studies, asymptotic solutions for linear q-difference equations are obtained by applying q-Borel summation methods to formal series expansions. The resulting connection formula obtained after applying this method is referred to as the q-Stokes phenomenon in these research papers.

These descriptions of q-Stokes phenomenon are not quite what we are seeking to capture in this thesis. We are interested in describing solutions of q-difference equations, which contain exponentially small behaviour and exhibits Stokes switching. In order to capture this behaviour for q-difference equations, we apply an adaptation of the method demonstrated in Chapter 3.

4.1.3. Describing Stokes phenomena for q-difference equations.

In order to study Stokes behaviour in solutions of q-difference equations we will apply a certain choice of scalings to the problem of interest. Recall that q-difference equations can also be regarded as additive difference equations under the parametrization $x = x_0 q^n$. If we are interested in the behaviour of their solutions as the independent variable is large, we find that under this parametrization, the limit $|x| \to \infty$ is equivalent to $n \to \infty$ provided that $|q| > 1$.

Harris and Sibuya [**68**] prove the existence of true solutions for a class of nonlinear additive difference equations, which have asymptotic behaviour described by formal power series. In particular, these nonlinear difference equations are those for which the equation may be expanded as a power series in the independent variable, n. However, the parametrization $x = x_0 q^n$ applied to nonautonomous q-difference equations introduce terms of the form q^n. Terms of this form can not be expanded as an asymptotic power series in n as $n \to \infty$ and hence the results in [**68**] are not applicable in describing the asymptotic behaviour of solutions for q-difference equations.

In Chapter 3 we introduced a small parameter, ϵ, by rescaling the variables of the difference equation of interest. Under the choice of scaling, the original difference equation was rescaled into another difference equation in which the step sizes are defined by ϵ.

Hence, in hindsight this choice of rescaling can be considered as a continuum limit inspired approach as the step sizes of the rescaled problem approach zero in the limit $\epsilon \to 0$. We call this the *continuum limit-like* approach in order to distinguish from the continuum limit for discrete Painlevé equations, which yield the differential Painlevé equations.

In order to apply the continuum limit-like approach, we additionally rescale the parameter q such that $q \to 1$. The choice of scaling we apply is $q = 1 + \epsilon$ for the case $|q| > 1$. By applying this additional choice of rescaling, terms of the form q^n are then able to be expanded as a power series in ϵ.

4.2. Riemann sheets : Reverting the transformations

In order to study Stokes behaviour present in the solutions of q-difference equations we apply the scalings $s = \epsilon n$ and $q = 1 + \epsilon$ to the independent variable $x = x_0 q^n$. We note that since we allow s to be complex-valued, we may set $x_0 = 1$ without loss of generality. Under this choice of scaling, it is possible to expand the independent variable as a power series in ϵ. To leading order, the rescaling transformation is given by

$$\begin{aligned} x =& q^n, \\ =& (1+\epsilon)^{s/\epsilon}, \qquad (4.26) \\ \sim& e^s + \mathcal{O}(\epsilon), \qquad (4.27) \end{aligned}$$

as $\epsilon \to 0$. In this case, we find that the limit $\epsilon \to 0$ is equivalent to the double limit $|q| \to 1$ and $n \to \infty$ rather than being equivalent to the independent variable approaching infinity, as was the case in Chapter 3. We therefore study the solutions of q-difference equations in the limit $|q| \to 1$ and $n \to \infty$ rather than $|x| \to \infty$.

Furthermore, to leading order in ϵ, the transformation from the original variable x to the new variable s is described by the mapping

$$x \mapsto s : \quad x = e^s. \qquad (4.28)$$

Hence, for any given $s \in \mathbb{C}$ we can find all $x \in \mathbb{C}$ as the exponential is an entire function. However, problems arise when we want to determine s given any $x \in \mathbb{C}$ as logarithms are involved in the inverse transformation. In order for this transformation to be single-valued, a logarithmic type branch cut must be defined in the complex x-space. By taking an appropriate choice of branch cut, the results found in the complex s-plane may be mapped to the complex x-space by the transformation (4.28) and interpreted appropriately.

Since the function e^s is $2\pi i$-periodic in s, a semi-infinite domain in the complex s-plane is sufficient to cover the whole complex x-plane. We define the semi-infinite domain, $\mathcal{D}_{\text{base}}$, by

$$\mathcal{D}_{\text{base}} = \{s \in \mathbb{C} \mid \text{Im}\,(s) \in (a, b]\},$$

where $b - a = 2\pi$. We call $\mathcal{D}_{\text{base}}$ a *base domain*. The simplest base domain are those for which $a = -b$; these are referred to as *symmetric base domains*. The most natural symmetric base domain

is given by

$$\mathcal{D}_0 = \{s \in \mathbb{C} \mid \mathrm{Im}(s) \in (-\pi, \pi]\}\,, \tag{4.29}$$

which we call the *principal symmetric base domain* and we define the k^{th}*-adjacent domain* as

$$\mathcal{D}_k = \{s \in \mathbb{C} \mid \mathrm{Im}(s) \in (-\pi + 2k\pi, \pi + 2k\pi]\}\,, \tag{4.30}$$

for any $k \in \mathbb{Z}\backslash\{0\}$.

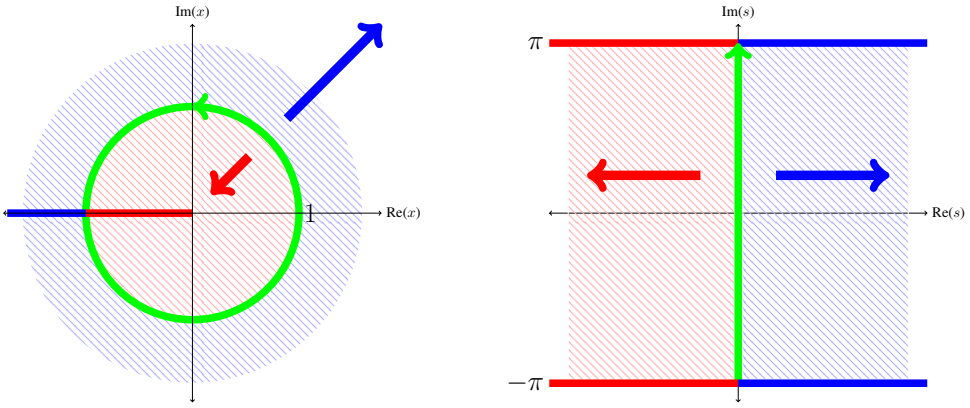

(A) Regions in the complex x-plane (B) Regions in the domain $\mathcal{D}_0$

FIGURE 4.2. This figure illustrates the correspondence between the complex-s and complex x-planes. In particular, Figure 4.2b illustrates the principal domain, $\mathcal{D}_0$, which covers the whole x-plane under the transformation (4.28) minus the branch cut of the logarithm. The upper and lower boundaries of $\mathcal{D}_0$ are defined by $\mathrm{Im}(s) = \pm\pi$. As the transformation is given by $x \sim e^s$ as $\epsilon \to 0$, the crossing of either the upper or lower boundaries of $\mathcal{D}_0$ into the adjacent domains described by $\mathcal{D}_k$ correspond to the logarithmic Riemann sheets in the complex x-plane.

For convenience, we simply refer $\mathcal{D}_0$ as the *principal domain*. In view of the mapping of (4.28), adjacent domains represent the various logarithmic Riemann sheets in the complex x-plane. When we consider the first q-Painlevé equation in Section 4.4, we will find that the leading order behaviour is $2\pi i$-periodic in s. In particular, the Stokes behaviour of the asymptotic solutions we find will be shown to only depend on the leading order behaviour. Consequently, the Stokes structure is also $2\pi i$-periodic and hence the Stokes structure in the adjacent domains, $\mathcal{D}_k$, may be obtained by translating the Stokes structure in $\mathcal{D}_0$ by an appropriate integer multiple of $2\pi i$. Hence, we restrict the subsequent analysis to the domain $\mathcal{D}_0$ as this corresponds to the principal Riemann sheet in the complex x-plane.

Figures 4.2a and 4.2b illustrate correspondences between particular regions and curves under the transformation (4.28). We see that the imaginary s axis is mapped to the unit circle in the complex x-plane. Additionally, the mapping (4.28) sends the left-half complex s-plane to the interior of the unit circle while the right-half complex-s plane is mapped its exterior.

Furthermore, curves with fixed values of $\mathrm{Re}(s)$ are mapped to closed circles in the complex x-plane, which when traversed anti-clockwise denote the values of increasing $\mathrm{Im}(s)$. Figure 4.2b represents the domain $\mathcal{D}_0$ in the complex s-plane. The upper and lower boundaries of $\mathcal{D}_0$ define a logarithmic branch cut along the negative real axis of the complex x-plane.

4.3. A q-analogue of the Airy equation

Before we consider nonlinear q-difference equations we first study a second order linear q-difference equation. As the Airy equation is a typical example of Stokes behaviour for second order linear differential equations we investigate the solutions of a q-analogue of the Airy function.

In the literature, there are two known q-analogues for the Airy equation. Their respective solutions are known as the *Ramanujan function* and the *q-Airy function*. The Ramanujan function, $\mathrm{A}_q(x)$, is defined by the series

$$\mathrm{A}_q(x) = \sum_{n=0}^{\infty} \frac{q^{n^2}}{(q;q)_n}(-x)^n = {}_0\varphi_1(-;0;q,-qx), \tag{4.31}$$

and satisfies the equation

$$xu(qx) - u(x) + u(x/q) = 0. \tag{4.32}$$

Another solution of (4.32) is given by

$$u(x) = \theta_q(x)\,{}_2\varphi_0(0,0;-;q,-x), \tag{4.33}$$

where we note that the basic hypergeometric series ${}_2\varphi_0(0,0;-;q,-x)$ is divergent. The Ramanujan function first appeared in the works of Ramanujan [**139**]. In particular, Ismail [**74**] calculated the result

$$\lim_{n\to\infty} \frac{q^{n^2}}{t^n} h_n(\sinh(\zeta_n)\,|q) = \mathrm{A}_q\left(\frac{1}{t^2}\right), \tag{4.34}$$

where $e^{\zeta_n} = tq^{-n/2}$ and $h_n(\cdot|q)$ are the q-Hermite polynomials. To understand why (4.31) is regarded as a q-analogue of the Airy function we consider the following result

$$\lim_{n\to\infty} \frac{e^{-x^2/2}}{3^{1/3}\pi^{-1/4}2^{2/n+1/4}\sqrt{n!}} H_n(x) = \mathrm{Ai}(t), \tag{4.35}$$

where $x = \sqrt{2n+1} - 2^{1/2}3^{1/3}n^{1/6}t$, $H_n(x)$ are the Hermite polynomials and $\mathrm{Ai}(x)$ is the continuous Airy function [**107**]. The result given by (4.35) describes the asymptotics around the smallest and largest zeros of the Hermite polynomials; this is known as the Plancherel-Rotach asymptotic formula for the Hermite polynomials. The result given in (4.34) is the q-analogue of (4.35) as it involves the product between some ratio depending on n and the q-Hermite polynomials. Due to this, the Ramanujan function is considered to be a q-analogue of the Airy function.

The other q-analogue of the Airy function is called the q-Airy function and is defined by the series

$$\mathrm{Ai}_q(x) = \sum_{k=0}^{\infty} \frac{(-1)^k q^{k(k-1)/2}}{(-q,q;q)_k}(-x)^k = {}_1\varphi_1(0;-q;q,-x), \tag{4.36}$$

which satisfies

$$u(qx) + \frac{x}{q}u(x) - u(x/q) = 0. \tag{4.37}$$

Another solution of (4.37) is given by

$$\exp(i\pi \log_q(x))\mathrm{Ai}_q(x). \tag{4.38}$$

It was shown in [**67**] that the q-Airy function is a special solution of the second q-Painlevé equation. Furthermore, the authors of [**67**] showed that under the continuum limit

$$q = e^{-\delta^3/2}, \quad x = -2ie^{-2\delta^2/2} = -2iq^{s/\delta}, \quad u(x) = e^{i\pi \log_q(t)/2}v(t), \tag{4.39}$$

the equation (4.37) yields

$$v''(s) = -sv(s),$$

as $\delta \to 0$. Following the naming convention of the discrete Painlevé equations, equation (4.37) is therefore known as the q-Airy equation.

The Ramanujan function and the q-Airy function are related to each other by the so called connection problem. By using the q-Borel summation method introduced by Zhang [**160**], Morita [**107**] was able to obtain a connection formula relating the solutions of (4.31) at infinity to solutions of (4.36) at the origin.

Morita [**109**, **110**] also applies the q-Borel summation method to resum the formal series given by (4.33). More specifically, Morita shows that

$$\begin{aligned}\theta_q(x){}_2\varphi_0(0,0;-;q,-x/q) =&(q;q)_\infty \frac{\theta_q(x)\theta_{q^2}(-\lambda^2/qx)}{\theta_q(-\lambda/q)\theta_q(\lambda/x)}){}_1\varphi_1(0;q;q^2,q^2/x),\\ &+\frac{\lambda(q;q)_\infty}{x(1-q)}\frac{\theta_q(x)\theta_{q^2}(-\lambda^2/x)}{\theta_q(-\lambda/q)\theta_q(\lambda/x)}){}_1\varphi_1(0;q^3;q^2,q^3/x),\end{aligned} \tag{4.40}$$

for any $x \in \mathbb{C}\backslash\{-\lambda q^{\mathbb{Z}}\}$ where $\lambda \in \mathbb{C}\backslash\{0,\infty\}$ [**110**]. This method of resummation allowed Morita to assign a sum to (4.33), which is expressible in terms of convergent series expansions at infinity [**109**,**110**]. Morita refers to this as the Stokes phenomenon for linear q-difference equations. However, the formula in (4.40) is valid everywhere in the complex x-plane except along the q-spiral defined by $-\lambda q^{\mathbb{Z}}$. Therefore the expression in (4.40) does not vary in different regions of the complex plane. Using q-Borel summation methods, both Morita [**108**] and Ohyama [**115**] resum divergent series expansion for certain classes of basic hypergeometric series in order to obtain connection formula similar to (4.40), which they refer as q-Stokes phenomenon.

The Stokes phenomenon described in [**108**, **110**, **115**] is therefore not the usual case of Stokes phenomenon we have described in Chapters 2 and 3 in the sense that the asymptotic series expansion of a function differs by an exponentially small term in different regions of the complex plane. In order to investigate solutions of q-difference equation which display Stokes behaviour, we extend the techniques presented in Chapter 3.

4.3.1. Asymptotic analysis of the q-Airy equation.

We demonstrate how to extend the scaling approach presented in Chapter 3 to linear q-difference equations by considering the q-Airy equation given by (4.37). In particular, we will determine the Stokes structure of the solutions of the q-Airy equation and qualitatively investigate Stokes behaviour present in these solutions.

First, we transform the q-difference equation (4.37) into an additive difference equation by setting $x = q^n$. Under this parametrization, equation (4.37) can be rewritten as

$$u_{n+1} + q^{n-1}u_n - u_{n-1} = 0, \tag{4.41}$$

where $u_n = u(q^n)$, $u_{n+1} = u(q^{n+1})$ and $u_{n-1} = u(q^{n-1})$. As we have discussed in Section 4.1, a straightforward application of the rescalings used in Chapter 3 is not helpful because of the q^n term. These terms cannot be expanded in powers of n as $n \to \infty$. In order to overcome this, we apply the continuum limit-like approach by also rescaling the parameter q in addition to n. The scalings we apply are

$$n = \frac{s}{\epsilon}, \qquad q = 1 + \epsilon, \tag{4.42}$$

where we now consider the limit $\epsilon \to 0$. The rescaled version of (4.41) is then given by

$$u(s+\epsilon) + (1+\epsilon)^{s/\epsilon - 1}u(s) - u(s-\epsilon) = 0, \tag{4.43}$$

as $\epsilon \to 0$. Under this choice of rescaling it is now possible to expand the nonautonomous term, q^n, in powers of ϵ. Furthermore, we assume that $u(s)$ is an analytic function in s in order to expand the solutions in equation (4.43) to give

$$2\sum_{j=0}^{\infty} \epsilon^{2j+1} \frac{u_j^{(2j+1)}(s)}{(2j+1)!} + (1+\epsilon)^{s/\epsilon - 1}u(s) = 0. \tag{4.44}$$

Attempting to expand the solution, $u(s)$, as an asymptotic power series in ϵ produces the trivial power series expansion where the coefficients are identically zero. This suggests that the solution is exponentially small. We therefore apply a WKB ansatz for $u(s)$ and seek a solution of (4.44) with the form

$$u(s) \sim a(s)e^{f(s)/\epsilon}, \tag{4.45}$$

as $\epsilon \to 0$. Making this substitution into (4.44) we obtain

$$2\sum_{j=0}^{\infty} \frac{(f')^{2j+1}}{(2j+1)!}u + 2\epsilon \sum_{j=0}^{\infty} \frac{1}{(2j+1)!}\left(\binom{2j+1}{1}(f')^{2j}\frac{a'}{a} + \binom{2j+1}{2}(f')^{2j-1}f''\right)u,$$
$$+ e^s u - \frac{s+2}{2}e^s \epsilon u + \mathcal{O}(\epsilon^2 u) = 0 \tag{4.46}$$

as $\epsilon \to 0$. We then proceed to match terms of $\mathcal{O}(\epsilon^j e^{f(s)/\epsilon})$ as $\epsilon \to 0$ for $j = 0, 1$. The leading order equation in (4.46) is given by

$$\mathcal{O}(e^{f/\epsilon}): \quad 2\sum_{j=0}^{\infty} \frac{(f')^{2j+1}}{(2j+1)!} + e^s = 0, \tag{4.47}$$

which can be simplified to give

$$2\sinh(f') + e^s = 0. \tag{4.48}$$

Matching at the next subsequent order, we obtain the equation

$$\mathcal{O}(\epsilon e^{f/\epsilon}): \quad 2\sum_{j=0}^{\infty} \frac{1}{(2j+1)!}\left(\binom{2j+1}{1}(f')^{2j}\frac{a'}{a} + \binom{2j+1}{2}(f')^{2j-1}f''\right) - \frac{(s+2)}{2}e^s = 0, \tag{4.49}$$

which simplifies and rearranged to give

$$2\cosh(f')\frac{a'}{a} + f''\sinh(f') - \frac{(s+2)}{2}e^s = 0. \tag{4.50}$$

Equation (4.48) and (4.50) can be solved to find $f(s)$ and $a(s)$, respectively. As in the analysis for the hyper-Airy equation in Chapter 2, the Stokes curves may be determined by condition (2.64), which only require the WKB phase factors to be known.

We will therefore compute the WKB phase factors in the next section, which will allow us to determine the Stokes structure of the q-Airy function. Once the Stokes structure has been determined in the complex-s plane we may reverse the transformation in order to obtain the corresponding Stokes structure in the complex x-plane. Before we move on to the analysis of the WKB phase factors (4.48), we first discuss invariant functions of q-difference equations known as q-periodic functions.

4.3.2. q-periodic functions.

In the theory of linear differential and difference equations, it is well known that the general solutions of n^{th} order linear differential or difference equations form a linear combination of n distinct linearly independent solutions. Such solutions are known as *fundamental solutions*. This is the theory of superposition in linear differential and difference equations [**4**, **53**].

There is an analogous theory for linear q-difference equations, which has been developed by Birkhoff [**17–19**], Carmichael [**30**] and Adams [**3**]. In was shown by Adams [**3**] that the n^{th} order system of first order q-difference equations of the form

$$Y(qx) = A(x)Y(x), \quad |q| \neq 1, \tag{4.51}$$

where $A(x)$ is analytic or has a pole at $x = \infty$ and $|A(x)| \neq 0$, always admit n linearly independent fundamental solutions. As in the case of linear differential and difference equations, the general solution of linear q-difference of the form (4.51) is a linear combination of the fundamental solutions. However, the constants appearing in this linear combination are not constants in the usual sense, but functions which are invariant under the shift $x \mapsto qx$.

In order to illustrate this, let $Y_i(x)$ denote a fundamental solution of (4.51). That is, $Y_i(x)$ is a solution of (4.51), and consider the following function

$$G(x) = \sum_{i=1}^{n} F_i(x) Y_i(x), \tag{4.52}$$

where $F_i(x)$ is an arbitrary function of x. Under the shift $x \mapsto qx$ the function (4.52) reads

$$\begin{aligned} G(qx) &= \sum_{i=1}^{n} F_i(qx) Y_i(qx), \\ &= \sum_{i=1}^{n} F_i(qx) A(x) Y_i(x), \end{aligned}$$

where we have used the fact that $Y_i(x)$ is a solution of (4.51). If (4.52) is to be a solution of (4.51) then it is required that

$$F_i(qx) = F_i(x),$$

for all i. Hence, 'constants' for q-difference equations are replaced by functions defined by

$$F(qx) = F(x). \tag{4.53}$$

Functions which satisfy (4.53) are known as *q-periodic functions*. Consequently, Birkhoff [**19**] defines any two functions which differ by a multiplicative q-periodic function to be linearly dependent.

In our analysis of q-difference equations, we rescale the variables in order to study Stokes behaviour in solutions of q-difference equations in the limit $|q| \to 1$. It is therefore natural to ask what these q-periodic functions correspond to under our choice of rescaling.

The first of these transformations is to parametrize the independent variable by setting $x = q^n$. This converts equation (4.53) into

$$\hat{F}(n+1) = \hat{F}(n), \tag{4.54}$$

where $\hat{F}(n) = F(x)$. We then introduce ϵ by setting $s = \epsilon n$. This transforms (4.54) into

$$\tilde{F}(s+\epsilon) = \tilde{F}(s), \tag{4.55}$$

where $\tilde{F}(s) = \hat{F}(n)$. We therefore discover that q-periodic functions correspond to functions with the property (4.55). That is, q-periodic functions correspond to functions which are invariant under the shift $s \mapsto s + \epsilon$. For example, the function given by

$$g(x) = \exp\left(2iM\pi \frac{\log(x)}{\log(q)}\right), \tag{4.56}$$

where $M \in \mathbb{Z}$ is a q-periodic function, as it satisfies (4.53). Then by setting $x = q^n$ with $s = \epsilon n$, the function (4.56) corresponds to the function

$$g(s) = \exp\left(\frac{2iM\pi s}{\epsilon}\right). \tag{4.57}$$

The notion of q-periodic functions will be important in the following analysis of the WKB phase factors of the q-Airy equation.

4.3.3. WKB phase factor analysis for q-Airy.

In this section we determine the WKB phase factors of the rescaled q-Airy equation by studying equation (4.48). We will find that there are infinitely many WKB phase factor terms for (4.45), which would suggest there are infinitely many WKB solutions. However, we show that all but two of these contributions are determined up to multiplication of a q-periodic function. In the sense of Birkhoff, the two distinct WKB solutions describe two linearly independent solutions of (4.43).

Solving for $f'(s)$ in (4.48) we obtain the equations

$$f_1'(s;M_1) = -\sinh^{-1}\left(\frac{e^s}{2}\right) + 2iM_1\pi,, \tag{4.58}$$

$$f_2'(s;M_2) = \sinh^{-1}\left(\frac{e^s}{2}\right) + i\pi + 2iM_2\pi,, \tag{4.59}$$

where $M_1, M_2 \in \mathbb{Z}$. We define, as in [**2**], the inverse sinh function by

$$\sinh^{-1}(z) = \log(z + \sqrt{z^2+1}).$$

Hence, the functions $f_j'(s;M_i)$ have branch points whenever

$$\left(\frac{e^s}{2}\right)^2 + 1 = 0.$$

The points at which this occurs is given by

$$s_{\text{BP}} = \log(2) \pm \frac{i\pi}{2} + i\pi K, \tag{4.60}$$

where $K \in \mathbb{Z}$. In $\mathcal{D}_0$, the relevant branch points are therefore

$$s_{\text{BP}} = \log(2) \pm \frac{i\pi}{2}. \tag{4.61}$$

From equations (4.58) and (4.59) it appears we have infinitely many phase factors as we obtain a particular phase factor for each choice $M \in \mathbb{Z}$. However, we will show that the phase factors $f_i(s;M_i)$ with nonzero values of M_i yield WKB solutions of the form (4.45) multiplied by q-periodic functions. Consequently, the phase factors, $f_i(s;0)$, describe the two linearly independent solutions of (4.43) in the sense of Birkhoff.

In order to show this, we integrate (4.58) in order to find that

$$\begin{aligned} f_1(s;M_1) &= -\int_{\hat{s}}^{s} \sinh^{-1}\left(\frac{e^t}{2}\right) dt + 2iM_1\pi s, \\ &= -\chi(s) + 2iM_1\pi s, \end{aligned}$$

where $\hat{s}$ is an arbitrary point and

$$\chi(s) = \int_{\hat{s}}^{s} \sinh^{-1}\left(\frac{e^t}{2}\right) dt.$$

Then under the WKB ansatz (4.45), a solution of (4.43) is therefore of the form

$$u_1(s; M_1) \sim a_1(s) e^{-\chi(s)/\epsilon} \exp\left(\frac{2iM_1\pi s}{\epsilon}\right),$$

as $\epsilon \to 0$.

The term $\exp(2iM_1\pi s/\epsilon)$ is precisely the function described by (4.57) and hence corresponds to a q-periodic function. Therefore, the WKB solutions with nonzero values of M_1 are equal to the WKB solution with $M_1 = 0$ multiplied by a q-periodic function. Consequently, the WKB solution $u_1(s; 0)$ describes a linearly independent solution of (4.43) in the sense of Birkhoff [**19**].

A similar argument shows that the WKB phase factor, $f_2(s; 0)$, describes the second linearly independent solution of (4.43). Therefore, we consider the cases where M_1 and M_2 are chosen to be zero in equations (4.58) and (4.59) as these describe the two linearly independent solutions of (4.43).

The solutions of equations (4.58) and (4.59) with M_1 and M_2 equal to zero gives

$$f_1(s) = -\int_{\hat{s}}^{s} \sinh^{-1}\left(\frac{e^t}{2}\right) dt, \tag{4.62}$$

$$f_2(s) = -f_1(s) + i\pi(s - \hat{s}), \tag{4.63}$$

where $\hat{s}$ is an arbitrary point. The two linearly independent solutions of (4.43) are then given by

$$u_1(s; 0) \sim C_1(s) a_1(s) e^{f_1(s)/\epsilon}, \tag{4.64}$$

$$u_2(s; 0) \sim C_2(s) a_2(s) e^{(-f_1(s) + i\pi(s-\hat{s}))/\epsilon}, \tag{4.65}$$

as $\epsilon \to 0$ where $C_1(s), C_2(s)$ are two arbitrary q-periodic functions and $a_1(s), a_2(s)$ are yet to be determined.

4.3.4. WKB amplitude factor analysis for q-Airy.

In this section we determine the WKB amplitude factors, $a(s)$. We therefore aim to solve equation (4.50) and hence completely determine the form of the leading order behaviour of (4.43). As there are two distinct solutions for $f(s)$, there are therefore two corresponding solutions for $a(s)$.

In fact, it can be shown that $a_1(s)$ and $a_2(s)$ are related to each other. In order to show this, we consider the equations involving the WKB phase factors. Equation (4.63) shows that

$$f_2'(s) = -f_1'(s) + i\pi.$$

Using this formula and hyperbolic identities, we find that

$$\begin{aligned}\cosh(f_2') &= -\cosh(f_1'),\\ \sinh(f_2') &= \sinh(f_1'),\\ f_2'' &= -f_1'.\end{aligned}$$

Using this information, equation (4.50) gives

$$2\cosh(f_1')\frac{a_1'}{a_1} + f_1''\sinh(f_1') - \frac{s+2}{2}e^s = 0, \tag{4.66}$$

$$-2\cosh(f_1')\frac{a_2'}{a_2} - f_1''\sinh(f_1') - \frac{s+2}{2}e^s = 0. \tag{4.67}$$

Then, by subtracting equations (4.66) and (4.67) from each other, the exponential term can be removed in order to obtain the equation

$$2\cosh(f_1')\left(\frac{a_1'}{a_1} + \frac{a_2'}{a_2}\right) + 2f_1''\sinh(f_1') = 0. \tag{4.68}$$

We may directly integrate (4.68) in order to find that

$$a_1(s)a_2(s) = \frac{\Lambda}{\cosh(f_1'(s))}, \tag{4.69}$$

where Λ is a constant of integration. Rearranging the expression in (4.69) shows that

$$a_2(s) = \frac{\Lambda}{a_1(s)\cosh(f_1'(s))}. \tag{4.70}$$

Once the explicit form of $a_1(s)$ is determined the explicit form of $a_2(s)$ can be calculated. As the amplitude factor satisfies a first order linear differential equation, (4.66) can be integrated to give

$$a_1(s) = \frac{\Lambda_1}{\sqrt{\cosh(f_1'(s))}}\exp\left(\int^s \frac{(t+2)e^t}{4\cosh(f_1'(t))}dt\right), \tag{4.71}$$

where Λ_1 is a constant of integration. Substituting (4.71) into (4.70) shows that

$$a_2(s) = \frac{\Lambda_2}{\sqrt{\cosh(f_1'(s))}}\exp\left(-\int^s \frac{(t+2)e^t}{4\cosh(f_1'(t))}dt\right), \tag{4.72}$$

where $\Lambda_2 = \Lambda/\Lambda_1$.

4.3.5. Complete asymptotic power series.

In the previous sections we determined the explicit form of the phase factors of the WKB ansatz, (4.45). We therefore find that the solutions of the rescaled q-Airy equation, (4.43), are

described by

$$u(s) \sim C_1(s)\frac{\Lambda_1}{\sqrt{\cosh(f_1'(s))}}\exp\left(\int^s \frac{(t+2)e^t}{4\cosh(f_1'(t))}dt\right)e^{f_1(s)/\epsilon} + C_2(s)\frac{\Lambda_2}{\sqrt{\cosh(f_1'(s))}}\exp\left(-\int^s \frac{(t+2)e^t}{4\cosh(f_1'(t))}dt\right)e^{(-f_1(s)+i\pi(s-\hat{s}))/\epsilon}, \tag{4.73}$$

as $\epsilon \to 0$ and where $C_1(s)$ and $C_2(s)$ are q-periodic functions. For convenience, we let

$$U_1(s) = \frac{\Lambda_1}{\sqrt{\cosh(f_1'(s))}}\exp\left(\int^s \frac{(t+2)e^t}{4\cosh(f_1'(t))}dt\right)e^{f_1(s)/\epsilon}, \tag{4.74}$$

$$U_2(s) = \frac{\Lambda_2}{\sqrt{\cosh(f_1'(s))}}\exp\left(-\int^s \frac{(t+2)e^t}{4\cosh(f_1'(t))}dt\right)e^{(-f_1(s)+i\pi(s-\hat{s}))/\epsilon}. \tag{4.75}$$

The asymptotic solution given by (4.73) is therefore a linear combination of the exponential contributions $U_1(s)$ and $U_2(s)$. This is similar to the result for the classical Airy function, in which its asymptotic solution is described, to leading order, by the expression

$$y(z) \sim D_1\frac{e^{-\zeta}}{z^{1/4}} + D_2\frac{e^{\zeta}}{z^{1/4}}, \tag{4.76}$$

as $|z| \to \infty$ where $\zeta = 2z^{3/2}/3$ and D_1, D_2 are constants.

In the analysis of the hyper-Airy equation, which we considered in Chapter 2, the general asymptotic series expansion was shown to be composed of a sum of component asymptotic power series in ϵ, each of which are multiplied by distinct exponential terms; this is due to the fact that the governing equation is linear. In particular, these exponential prefactors are precisely the leading order behaviours of the hyper-Airy equation obtained by the WKB method.

In general, the full asymptotic series expansion of (4.73) may be obtained by writing $u(s) = U_j(s)g_j(s)$ for $j = 1, 2$ where $g_j(s)$ is an asymptotic power series in ϵ. By scaling out the leading order behaviour, $U_j(s)$, the governing equation for $g_j(s)$ can be obtained, from which the asymptotic series expansion of $g_j(s)$ may be determined.

However, we do not require the full asymptotic series expansion to be known as we are only interested in computing the Stokes structure and using this to qualitatively deduce Stokes behaviour present in (4.73). We note that Dingle outlines a procedure on how to obtain the full asymptotic series expansion of the WKB method for a class of second order difference equations [**49**].

In principle, the complete asymptotic series expansion of (4.43) is of the form

$$u(s) \sim C_1(s)U_1(s)\sum_{r=0}^{\infty}\epsilon^r v_{1,r}(s) + C_2(s)U_2(s)\sum_{r=0}^{\infty}\epsilon^r v_{2,r}(s), \tag{4.77}$$

as $\epsilon \to 0$. We note that when the asymptotic solution, (4.77), is written in terms of the original variable x, the limit $\epsilon \to 0$ is equivalent to the limits $|q| \to 1$ and $n \to \infty$. From the form of (4.77),

we may deduce Stokes behaviour present within the asymptotic solutions of the q-Airy equation in the limits $|q| \to 1$ and $n \to \infty$.

4.3.6. Stokes structure of q-Airy.

In order to describe the Stokes geometry of the asymptotic solutions of the q-Airy equation, we must first determine the *turning points* of the WKB solutions given by (4.73). Turning points of the WKB approximation are points at which the approximation breaks down as the amplitude factors become singular at such points [**8**]. In particular, these points are also the points from which the Stokes and anti-Stokes curves emanate.

Following Joshi and Takei [**86**], the turning points, s_0, of the WKB solution, (4.45), may be defined by the condition

$$f_i'(s_0) = f_j'(s_0), \tag{4.78}$$

for $i \neq j$. Using (4.78), the turning points of (4.73) satisfy

$$\begin{aligned} f_1'(s_0) =& f_2'(s_0), \\ =& - f_1'(s_0) + i\pi. \end{aligned} \tag{4.79}$$

By using the expression for $f_1(s)$, which is given by (4.62), we find that the turning point, s_0, satisfies

$$-\sinh^{-1}\left(\frac{e^{s_0}}{2}\right) = \sinh^{-1}\left(\frac{e^{s_0}}{2}\right) + i\pi, \tag{4.80}$$

which can be solved to give

$$s_{0,m} = \log(2) - \frac{i\pi}{2} + 2im\pi, \tag{4.81}$$

where m is an integer. Hence, in the complex s-plane, there are infinitely many turning points of the WKB solution (4.45). However, in the domain $\mathcal{D}_0$, the point $s_0 := s_{0,0}$ is the only turning point. Furthermore, we note that equations (4.66) and (4.67) indeed become singular at the turning point, $s_{0,m}$, as the term $\cosh(f_1')$ vanishes at these points. We recall that the phase factors, $f_1(s)$ and $f_2(s)$ are integrated from an arbitrary point $\hat{s}$. As $\hat{s}$ is arbitrary, we may replace it by the turning point $s_{0,m}$. Hence, equations (4.62) and (4.63) show that $f_1(s_{0,m}) = 0 = f_2(s_{0,m})$.

We are now able to determine the Stokes geometry of the asymptotic solution (4.77). We may use conditions (2.64) and (2.66) given in Chapter 2 to determine the Stokes and anti-Stokes curves, respectively. These conditions tell us that the Stokes and anti-Stokes curves of (4.77) are given by

$$\mathrm{Im}\left(2f_1(s) - \int_{s_{0,m}}^{s} i\pi dt\right) = 0, \tag{4.82}$$

$$\mathrm{Re}\left(2f_1(s) - \int_{s_{0,m}}^{s} i\pi dt\right) = 0, \tag{4.83}$$

respectively and where f_1 is given by (4.62). Hence, the replacement of $\hat{s}$ by $s_{0,m}$ in equations (4.62) and (4.63) result in the Stokes and anti-Stokes curves to emerge from the turning point. Let us define the function

$$\eta(s; s_{0,m}) = 2f_1(s) - \int_{s_{0,m}}^{s} i\pi dt, \tag{4.84}$$

for the choice of m. In particular, the Stokes curves emanating from the turning point $s_{0,m}$ are obtained when the imaginary part of (4.84) is equal to zero. We will now show that we may restrict the analysis to the domain $\mathcal{D}_0$.

From equation (4.81), we see that $s_{0,m+1} = s_{0,m} + 2i\pi$, and hence these turning points are all vertical translations of each other by some integer multiple of $2i\pi$. Recall that the union of the domains $\mathcal{D}_k$ cover the entire complex s-plane. We will show that the Stokes structure emanating from the singularity $s_{0,m}$ is identical to those which emanate from the singularity $s_{0,m+1}$ under the shift $s \mapsto s + 2i\pi$. To show this, equation (4.84) tells us that

$$\eta(s + 2i\pi; s_{0,m+1}) = 2\int_{s_{0,m+1}}^{s+2i\pi} \sinh^{-1}\left(\frac{e^t}{2}\right) dt - \int_{s_{0,m+1}}^{s+2i\pi} i\pi dt. \tag{4.85}$$

Then under the change of variables, $t = x + 2i\pi$, the integral in (4.85) is equal to

$$\begin{aligned}\eta(s + 2i\pi; s_{0,m+1}) =& 2\int_{s_{0,m}}^{s} \sinh^{-1}\left(\frac{e^t}{2}\right) dt - \int_{s_{0,m}}^{s} i\pi dt, \\ =& \eta(s; s_{0,m}).\end{aligned} \tag{4.86}$$

Hence, the Stokes structure emanating from the singularities $s_{0,m}$ and $s_{0,m+1}$ are identical as the difference between these two singularities is precisely equal to $2i\pi$. Furthermore, the domains $\mathcal{D}_k$ contains the points under the condition $\mathrm{Im}(s) \in (-\pi + 2k\pi, pi + 2k\pi]$ and hence each adjacent domain are also vertical translations of each other by some integer multiple of $2\pi i$.

We may therefore restrict the subsequent analysis to the principal domain, $\mathcal{D}_0$, and hence consider the Stokes structure emanating from the singularity, s_0. Consequently, the Stokes structure emanating from the remaining singularities in the domains $\mathcal{D}_k$ may be obtained by vertical translations of the Stokes structure in $\mathcal{D}_0$ by integer multiples of $2i\pi$.

The Stokes structure of (4.77) in the complex s-plane is illustrated in Figure 4.3. In Figure 4.3 we find that there are two Stokes curves emanating from the turning point s_0, which is also a branch point. Furthermore, we also find three anti-Stokes curves emanating from the turning point.

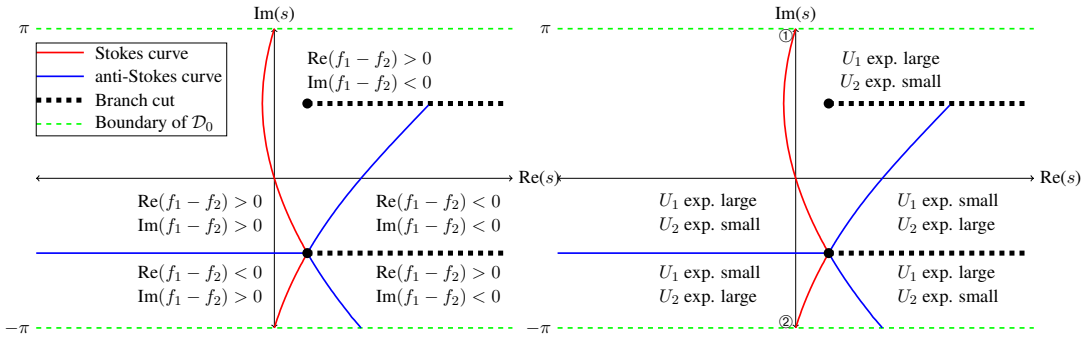

(A) Behaviour of the WKB phase factors, $f_i(s)$. (B) Behaviour of the exponentials, $U_i(s)$.

FIGURE 4.3. These figures illustrate the Stokes structure for the rescaled q-Airy equation in $\mathcal{D}_0$, with branch points given by (4.61). The upper and lower boundaries of $\mathcal{D}_0$ are denoted by the dashed green lines and occur at $\mathrm{Im}(s) = \pm\pi$. Figure 4.3a illustrates the behaviour of the phase factors, $f_i(s)$, as Stokes and anti-Stokes curves are crossed. Figure 4.3b illustrates the regions of $\mathcal{D}_0$ in which the exponential contributions associated with f_1 and f_2, which we denote by U_1 and U_2, respectively, are exponentially large or small. The exponential contributions associated with f_1 and f_2 are switched across the Stokes curves denoted by ① and ②, respectively.

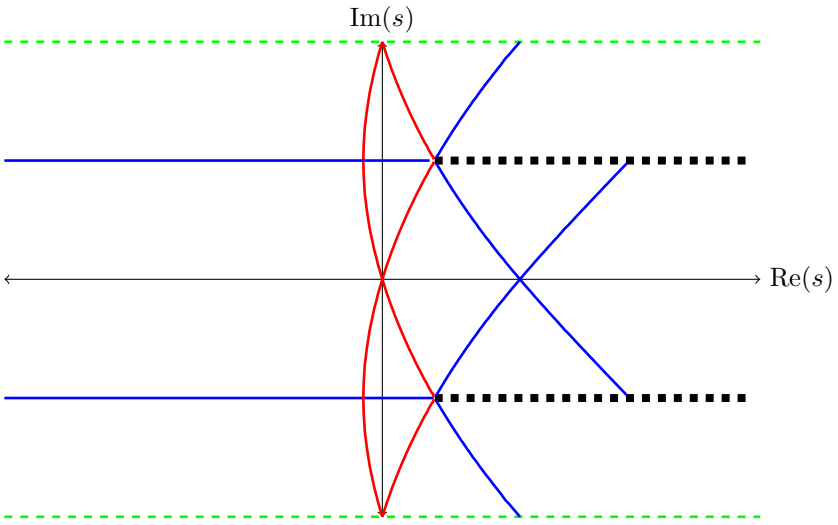

FIGURE 4.4. This figure illustrates the complete Stokes structure for the rescaled q-Airy equation in $\mathcal{D}_0$. There is also a turning point at the upper branch point since $f_1'(s;0) = f_2'(s;-1)$. Consequently, there is also a set of (anti-) Stokes curves emerging from the upper branch point and hence the Stokes structure is symmetric about the real s-axis.

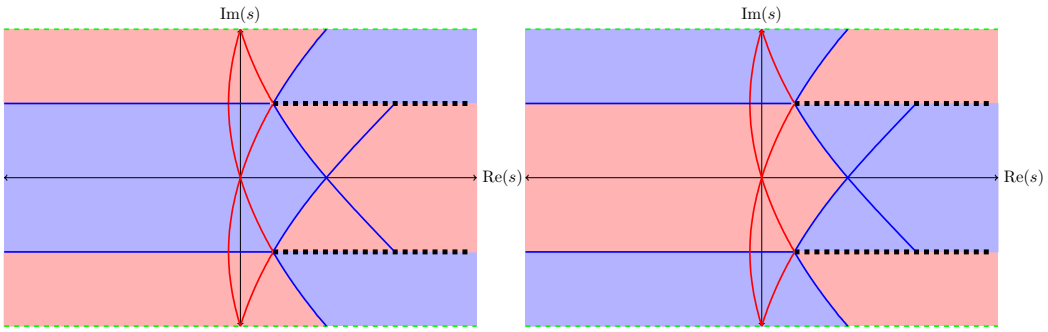

(A) Regions of validity for U_1. (B) Regions of validity for U_2.

FIGURE 4.5. This figure illustrates the regions of $\mathcal{D}_0$ in which the exponentials U_1 and U_2 describe the asymptotic behaviour of (4.43). In figure 4.5a, U_1 describes the asymptotic behaviour of (4.43) in the limit $\epsilon \to 0$ in the regions shaded in blue. However, U_1 does not describe the asymptotic behaviour in the regions shaded in red since the exponential contribution, U_2, is present and large in these regions.

We recall that Stokes switching occurs across Stokes curves where $\text{Re}(f_i - f_j) > 0$. When these conditions are met, the dominant exponential $U_i = e^{f_i/\epsilon}$ switches on the subdominant exponential, $U_j = e^{f_j/\epsilon}$. In Figure 4.3 we see that in the neighbourhood of the upper Stokes curve (red curve), U_2 is exponentially subdominant since $\text{Re}(f_1 - f_2) > 0$. Therefore the dominant behaviour U_1 switches on the subdominant exponential U_2 as the upper Stokes curve is crossed. Similarly, in the neighbourhood of the lower Stokes curve, we find that $\text{Re}(f_2 - f_1) > 0$. In this region, the exponential contribution, U_2, exponentially dominates the exponential contribution, U_1. Consequently, U_2 switches on U_1 as the lower Stokes curve is crossed.

The regions in $\mathcal{D}_0$ for which the asymptotic behaviour of (4.43) is described by either U_1 or U_2 is illustrated in Figure 4.5. As the asymptotic solution of (4.43) is described by (4.77), the exponential contribution, U_1, describes the asymptotic behaviour in regions where it is not dominated by U_2. From Figure 4.3b we find that U_1 is not dominated by U_2 in the region of $\mathcal{D}_0$ bounded by the upper anti-Stokes curve emanating from the lower branch point, the anti-Stokes curve emanating from the lower branch point which extends to negative infinity and the real s-axis. Another region of $\mathcal{D}_0$ where U_1 is not dominated by U_2 is bounded by the lower branch cut, the lower anti-Stokes curve emanating from the lower branch point and the boundary $\text{Im}(s) = -\pi$. Furthermore, since the Stokes structure is symmetric about the real s-axis, the regions of validity in the upper half of $\mathcal{D}_0$ are given by the vertical reflection of the previously described regions about the real s-axis and is illustrated in Figure 4.5a. Similarly, U_2 dominates U_1 in the complimentary regions as illustrated in Figure 4.5b.

As the Stokes structure and switching behaviour of the exponential contributions have been determined in the domain $\mathcal{D}_0$, we may finally determine the corresponding Stokes structure in the complex x-plane. In order to determine the corresponding Stokes structure in the x-plane we

reverse the scaling transformations (4.42). We recall that the choice of scalings were given by

$$x = q^n, \quad n = \frac{s}{\epsilon}, \quad q = 1 + \epsilon,$$

and therefore

$$s = \frac{\epsilon \log(x)}{\log(1+\epsilon)} \sim \log(x) + \mathcal{O}(\epsilon), \tag{4.87}$$

as $\epsilon \to 0$. As the inverse transformation (4.87) has an error of order $\mathcal{O}(\epsilon)$, the whole complex x-plane is not covered. We remark that for finite values of $0 < \epsilon \ll 1$, using the exact expression for the inverse transformations produces two logarithmic branch cuts rather than one. Under the leading order approximation of the inverse transformation, $\mathcal{D}_0$ covers the entire complex x-plane except for the negative real x-axis, which is a logarithmic branch cut. This branch cut is illustrated in Figure 4.6 as the dashed green curve.

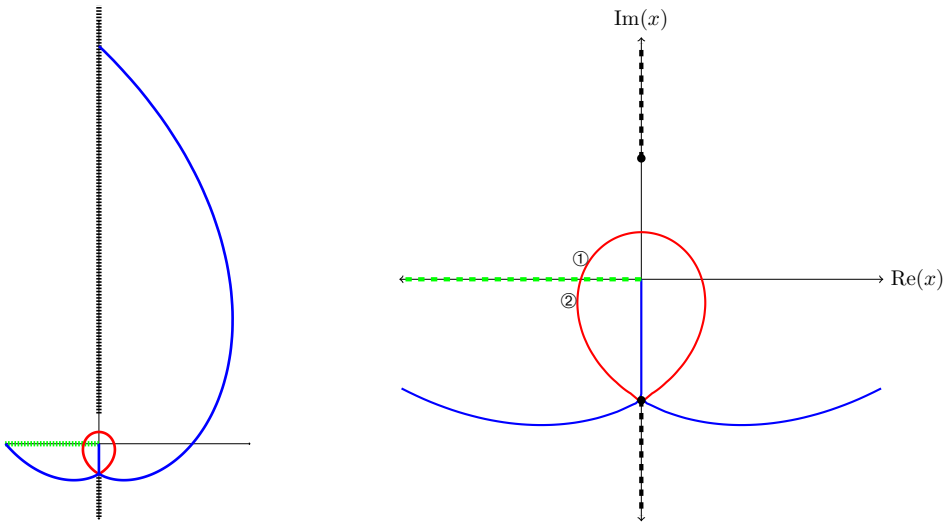

(A) Stokes structure of (4.77)

(B) Zoomed in version of Figure 4.6a

FIGURE 4.6. Stokes structure for the q-Airy equation in the complex x-plane. The Stokes and anti-Stokes curves are denoted by red and blue curves, respectively. The branch cuts of f_i are denoted by black curves which extend to infinity from the singularities, $s = \log(2) \pm i\pi/2$, and the dashed curves represent the logarithmic branch cut of the inverse transformation (4.87). In Figure 4.6a we see that one anti-Stokes curve spirals out from the turning point towards a logarithmic branch cut in the complex x-plane. The other anti-Stokes curve spirals towards the a branch cut of phase factor, f_i. In the complex x-plane, the Stokes and anti-Stokes curves are described by q-spirals, and therefore separate the complex plane into sectorial regions bounded by arcs of spirals.

Hence, by applying the inverse transformation given by (4.87) we may obtain the corresponding Stokes structure in the complex x-plane. Without loss of generality, we demonstrate the Stokes

structure of the q-Airy equation for $q = 1 + 0.2i$. By substituting $s = \epsilon \log_q(x)$ into the phase factors, $f_j(s)$, we use MATLAB to compute the Stokes structure in the complex x-plane. The Stokes structure of the asymptotic solution (4.77) in the limit $\epsilon \to 0$ is illustrated in Figure 4.6. In Figure 4.6, the Stokes curves are depicted in red while the anti-Stokes are depicted in blue. The branch cuts emanating from the branch points, $s = \log(2) \pm i\pi/2$, to infinity are denoted by the dashed curves.

In Figure 4.6 we find that the Stokes curves of (4.77) in the x-plane emanate from the turning point, s_0, and spiral towards the upper and lower logarithmic branch cuts of the inverse mapping. In fact, these Stokes curves continue onto the adjacent Riemann sheets of the inverse transformation. The branch cuts of the asymptotic solution (4.77) extend towards infinity in the x-plane as the branch cuts in the s-plane extend towards infinity as $\mathrm{Re}(s) \to \infty$.

Due to the inverse transformation (4.87), the Stokes and anti-Stokes curves are described by spiral-like curves in the complex x-plane. Consequently, the Stokes and anti-Stokes curves therefore separate the complex x-plane into sectorial regions bounded by arcs of spirals as illustrated in Figure 4.6.

4.4. The first q-Painlevé equation

In Section (4.3) we demonstrated that the Stokes geometry for linear q-difference equations may be computed using an extension of the scaling approach presented in Chapter 3. The extension required the parameter, q, to also be rescaled such that it approaches unity in the limit.

We now demonstrate how this method can be applied to study solutions of nonlinear q-difference equations in the limits $|q| \to 1$ and $n \to \infty$. In particular, we will also determine the Stokes switching behaviour of these solutions. As in Chapter 3, we consider the q-discrete analogues of the Painlevé equations. More specifically, we consider a q-analogue of the first Painlevé equation (q-P$_{\mathrm{I}}$). This is given by

$$\overline{w}\underline{w} = \frac{1}{w} - \frac{1}{xw^2}, \tag{4.88}$$

where $q \in \mathbb{C}$ such that $|q| \neq 0, 1$, $w = w(x)$, $\overline{w} = w(qx)$,$\underline{w} = w(x/q)$ and $x = x_0 q^n$. We wish to study the behaviour of solutions of (4.88) in the limits $|q| \to 1$ and $n \to \infty$.

One major asymptotic study of (4.88) was investigated by Joshi in [**80**] in which two types of solution behaviours of (4.88) were found. The solutions found in this study are each described by asymptotic series expansions in inverse powers of x, one of which is divergent. In the following section we give a brief summary of the results found by Joshi in [**80**].

4.4.1. Known results for q-Painlevé I.

This section is a summary of some results for the first q-Painlevé equation found by Joshi in [**80**]. We first define some notation used in this study. Let $w = w(x) = w(x_0 q^n) = w_n$, $w = w(qx) = w(x_0 q^{n+1}) = w_{n+1}$, $w = w(x/q) = w(x_0 q^{n-1}) = w_{n-1}$ and note that the limit

$|x| \to \infty$ is equivalent to $n \to \infty$ for $|q| > 1$. We first note that the first q-Painlevé equation, (4.88), is invariant under the symmetry

$$w \mapsto \omega w, \quad \text{with} \quad x \mapsto \frac{x}{\omega}, \tag{4.89}$$

where $\omega^3 = 1$. This will be a useful property in our analysis of (4.88) in Section 4.4.3. Joshi was able to find two types of asymptotic behaviours of (4.88) in the limit $|x| \to \infty$, which are called *nonzero asymptotic behaviour* and *vanishing asymptotic behaviour*.

Joshi showed that the nonzero asymptotic solutions of (4.88) are described by

$$w(x) = \sum_{r=0}^{\infty} \frac{a_r}{x^r}, \tag{4.90}$$

as $|x| \to \infty$ where

$$a_0^3 = 1, \tag{4.91}$$

$$a_1 = \frac{-1}{q + 1 + q^{-1}}, \tag{4.92}$$

$$a_r = \frac{-1}{q^n + 1 + q^{-n}} \left(\sum_{l=1}^{r-1} a_l a_{r-l} (q^{2l-r} + 1) + \sum_{m=1}^{r-1} \sum_{j=0}^{r-m} \sum_{l=0}^{r} a_j a_{r-m-j} a_l a_{m-l} q^{r-m-2j} \right), \tag{4.93}$$

for $r \geq 2$. From (4.91) we see there are three distinct choices for the leading order behaviour, a_0, and hence there are three distinct solutions of (4.88) with nonzero asymptotic behaviour in the limit $|x| \to \infty$. In fact, as the leading order behaviours are cube roots of unity, the three nonzero asymptotic solutions are related to each other by the symmetry (4.89).

The vanishing asymptotic solution of (4.88) is described by

$$w(x) = \sum_{r=1}^{\infty} \frac{b_r}{x^r}, \tag{4.94}$$

as $|x| \to \infty$ where

$$b_1 = 1, \tag{4.95}$$

$$b_2 = 0, \tag{4.96}$$

$$b_3 = 0, \tag{4.97}$$

$$b_r = \sum_{j=2}^{r-2} \sum_{k=1}^{j-1} \sum_{m=1}^{r-j-1} b_k b_{j-k} b_m b_{r-j-m} q^{j-2k}, \tag{4.98}$$

for $r \geq 4$. In particular, it was shown by Joshi that the coefficients, b_r, in (4.94) have the behaviour

$$b_{3r+1} = \mathcal{O}(|q|^{3r(r-1)/2} \, (-1; q^{-3})_r^2), \tag{4.99}$$

as $r \to \infty$ where $(a; q)_r$ is the q-Pochhammer symbol defined in (4.14).

Equation (4.99) shows that the late-order terms behaviour of vanishing type asymptotics grow as q^{r^2} as $r \to \infty$, and hence the series expansion (4.94) is divergent. Furthermore, Joshi showed there exist true solutions of (4.88), which are asymptotic to (4.94) by applying the contraction mapping theorem. In particular, under the change of variables $w_n = W_n + v_n$ where W_n is the formal power series solution defined by (4.94), equation (4.88) becomes

$$v_{n+1} + \left(2\frac{W_{n+1}}{W_n} - \frac{1}{W_n^2 W_{n-1}}\right) v_n + \frac{W_{n+1}}{W_{n-1}} v_{n-1} = \mathcal{R}_2(v_n, v_{n-1}, t), \tag{4.100}$$

where $t = 1/x$ and

$$\begin{aligned}\mathcal{R}_2(v_n, v_{n-1}, t) =& \frac{W_n + v_n - t}{(W_{n-1} + v_{n-1})(W_n + v_n)^2} - W_{n+1}, \\ & - \frac{W_{n+1}}{W_n}\left(\frac{1}{W_{n+1} W_n W_{n-1}} - 2\right) v_n + \frac{W_{n+1}}{W_{n-1}} v_{n-1}.\end{aligned} \tag{4.101}$$

It was also shown that the Taylor expansion of (4.101) starts with an arbitrarily small constant term and quadratic terms in v_n and v_{n-1} [**80**]. Joshi then studied the homogeneous solution of (4.100), P_n, which satisfies the equation

$$P_{n+1} + \left(2\frac{W_{n+1}}{W_n} - \frac{1}{W_n^2 W_{n-1}}\right) P_n + \frac{W_{n+1}}{W_{n-1}} P_{n-1} = 0, \tag{4.102}$$

and shows there exist two solutions of (4.102), denoted by $P_n^{\pm}$, with the following asymptotic behaviours as $n \to \infty$,

$$P_n^+ \sim c_+ q^{3n(n-5/3)/2}, \tag{4.103}$$

$$P_n^- \sim c_- q^{-3n(n+5/3)/2}, \tag{4.104}$$

where $c_\pm$ are constants. For fixed values of q, Joshi was able to compute the anti-Stokes curves by comparing the sizes of (4.103) and (4.104) in the limit $n \to \infty$. The anti-Stokes curves are given by

$$\left|\frac{P_n^+}{P_n^-}\right| = \mathcal{O}(1), \tag{4.105}$$

which is equivalent to the condition given by (2.66). Using (4.103) and (4.104) we find that

$$\left|\frac{P_n^+}{P_n^-}\right| = \left|\frac{c_+}{c_-} q^{3n^2}\right|. \tag{4.106}$$

Then by letting $x = x_0 q^n$, and writing $x/x_0 = re^{i\theta}$, we find that $n = \log(x/x_0)/\log(q)$. In particular,

$$n = \frac{\log(r) + i\theta}{\log(q)}, \tag{4.107}$$

and hence by substituting (4.107) in (4.106) the exponent of q in (4.106) can be rewritten as

$$\frac{3}{(\log(q))^2}\left((\log(r))^2 - \theta^2 + 2i\theta\log(r)\right). \tag{4.108}$$

Since both r and θ are real, the anti-Stokes curves are described by $(\log(r))^2 = \theta^2$ where $x = re^{i\theta}$. As a result, the anti-Stokes curves of (4.88) for fixed values of q, are described by q-spirals.

In our asymptotic analysis, we apply the continuum limit-like approach to study solutions of (4.88) in the limit $|q| \to 1$ rather than $|x| \to \infty$. Then, by using exponential asymptotic methods we find solutions of (4.88), which are described by asymptotic power series containing exponentially small behaviour. In particular, this approach will allow us to capture the Stokes behaviour present in these asymptotic solutions of q-$\mathrm{P_I}$ in the limit $|q| \to 1$.

4.4.2. Asymptotic analysis of the first q-Painlevé equation.

We first rewrite (4.88) as an additive difference equation by setting $x = q^n$, which gives

$$w_{n+1}w_{n-1} = \frac{1}{w_n} - \frac{1}{q^n w_n^2}, \tag{4.109}$$

where $w(n) = w(x)$. In our analysis, we will introduce a small parameter, ϵ, by rescaling the variables appearing in (4.109). However, recall that the term q^n is not expandable in powers of n in the limit $n \to \infty$. Following the strategy demonstrated in Section 4.3, we also rescale the parameter, q.

The rescalings we apply are given by

$$s = \epsilon n, \qquad q = 1 + \epsilon, \qquad w(x) = W(s). \tag{4.110}$$

Under these rescalings, q-$\mathrm{P_I}$, (4.88) becomes

$$W(s+\epsilon)W(s)^2W(s-\epsilon) = W(s) - \frac{1}{(1+\epsilon)^{s/\epsilon}}, \tag{4.111}$$

where we now consider the limit $\epsilon \to 0$. Due to the choice of rescalings, the limit $\epsilon \to 0$ no longer corresponds to a limit involving the independent variable as in Chapter 3, but is instead equivalent to the limit $|q| \to 1$. Hence, we investigate the asymptotic behaviour of solutions of (4.88) in the limit $|q| \to 1$.

Under the scalings (4.110), the corresponding symmetry of q-$\mathrm{P_I}$, (4.89), becomes

$$W \mapsto \lambda W, \quad \text{with} \quad s \mapsto s - \frac{\epsilon \log(\lambda)}{\log(1+\epsilon)} \sim s - \log(\lambda) + \mathcal{O}(\epsilon), \tag{4.112}$$

as $\epsilon \to 0$ and where $\lambda^3 = 1$.

Furthermore, under the rescalings (4.110), the term, $(1+\epsilon)^{-s/\epsilon}$, in (4.111) can now be expanded as

$$(1+\epsilon)^{-s/\epsilon} \sim 1 + e^{-s}\left(\epsilon\frac{s}{2} + \epsilon^2\frac{(3s-8)s}{24} + \mathcal{O}(\epsilon^3)\right), \tag{4.113}$$

as $\epsilon \to 0$. In general, the term $(1+\epsilon)^{s/\epsilon}$ can be expanded as a power series of the form

$$(1+\epsilon)^{s/\epsilon} = e^s \sum_{n=0}^{\infty} \epsilon^n P_n(s), \tag{4.114}$$

as $\epsilon \to 0$ where the coefficients, $P_n(s)$ are given by

$$P_n(s) = \sum_{r=0}^{n} s^r \sum_{k=0}^{r} \frac{(-1)^{r-k}}{(r-k)!} \frac{s_1(k+n,k)}{(k+n)!}, \tag{4.115}$$

where $s_1(n,k)$ are the Stirling numbers of the first kind [**2**]. The full details of this derivation are provided in Appendix D. By rescaling the parameter, q, we are able to describe solutions of (4.111) as an asymptotic power series in ϵ.

4.4.3. Asymptotic Series Expansion.

We expand the solution, $W(s)$, as an asymptotic power series in ϵ by writing

$$W(s) \sim \sum_{r=0}^{\infty} \epsilon^r W_r(s), \tag{4.116}$$

as $\epsilon \to 0$. Substituting (4.116) into (4.111) and matching terms of $\mathcal{O}(\epsilon^r)$ we obtain the recurrence relation

$$\sum_{q=0}^{r} \left(\sum_{m=0}^{q} \left(\sum_{k=0}^{m} \frac{(-1)^k W_{m-k}^{(k)}}{k!} \sum_{j=0}^{q-m} \frac{W_{q-m-j}^{(j)}}{j!} \sum_{b=0}^{r-q} W_{r-q-b} W_b \right) \right) = W_r - e^{-s} P_r(-s) \tag{4.117}$$

for $r \geq 0$ and where the polynomials $P_n(s)$ are given by (4.115). From (4.117) we find that the leading order behaviour satisfies

$$W_0^4 = W_0 - e^{-s}. \tag{4.118}$$

Equation (4.118) is invariant under $s \mapsto s + 2\pi i$ as the function e^s is $2\pi i$-periodic. As a result, the leading order behaviour, $W_0(s)$, is $2\pi i$-periodic. Consequently, the singularity structure of $W_0(s)$ is also $2i\pi$-periodic. Furthermore, we will show in Section 4.5 that the Stokes structure of the asymptotic solutions we study only depend on the leading order behaviour, W_0, and hence we may restrict ourselves to the domain $\mathcal{D}_0$ as we did in the analysis of the q-Airy equation. As W_0 satisfies a quartic we therefore have four possible leading order behaviours as $\epsilon \to 0$. We first define the following

$$A = 4\left(\frac{2}{3}\right)^{1/3} e^{-s}, \tag{4.119}$$

$$B = 9 + \sqrt{3}\sqrt{27 - 256e^{-3s}}, \tag{4.120}$$

$$C = 2^{1/3} 3^{2/3}, \tag{4.121}$$

$$D = \frac{A}{B^{1/3}} + \frac{B^{1/3}}{C}. \tag{4.122}$$

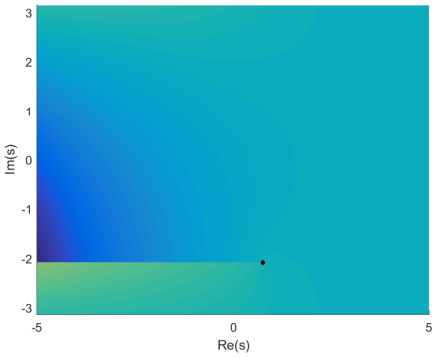

(A) Real part of $W_{0,1}$.

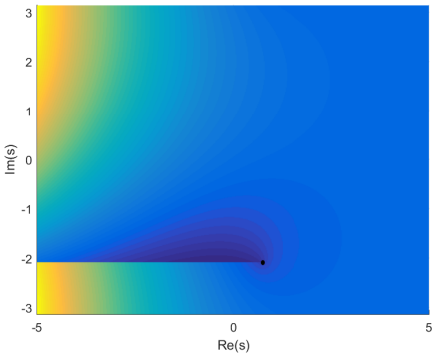

(B) Imaginary part of $W_{0,1}$.

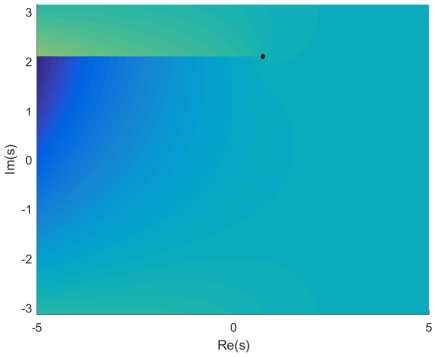

(C) Real part of $W_{0,2}$.

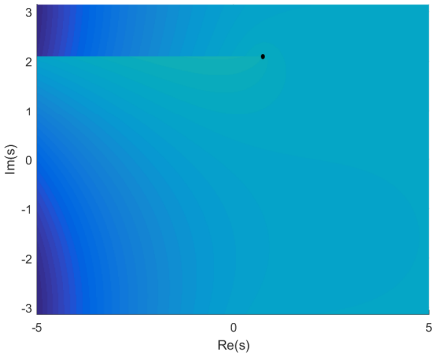

(D) Imaginary part of $W_{0,2}$.

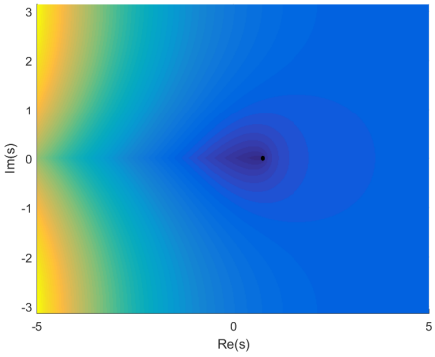

(E) Real part of $W_{0,3}$.

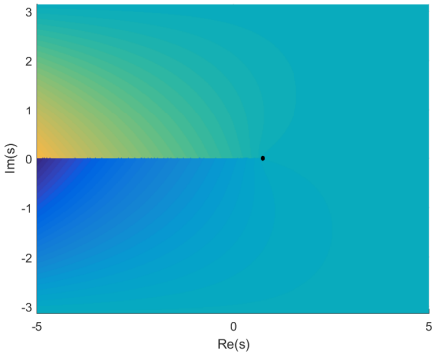

(F) Imaginary part of $W_{0,3}$.

FIGURE 4.7. This figure illustrates plots of the real and imaginary parts of $W_{0,1}$, $W_{0,2}$, and $W_{0,3}$ in $\mathcal{D}_0$. The leading order behaviour, $W_{0,j}$, is possibly singular at the points $s_{0,j}$ as described by equations (4.131)-(4.132). Figures 4.7a and 4.7b show that $W_{0,1}$ is only singular at $s_{0,1}$; Figures 4.7c and 4.7d show that $W_{0,2}$ is only singular at $s_{0,2}$; Figures 4.7e and 4.7f show that $W_{0,3}$ is only singular at $s_{0,3}$.

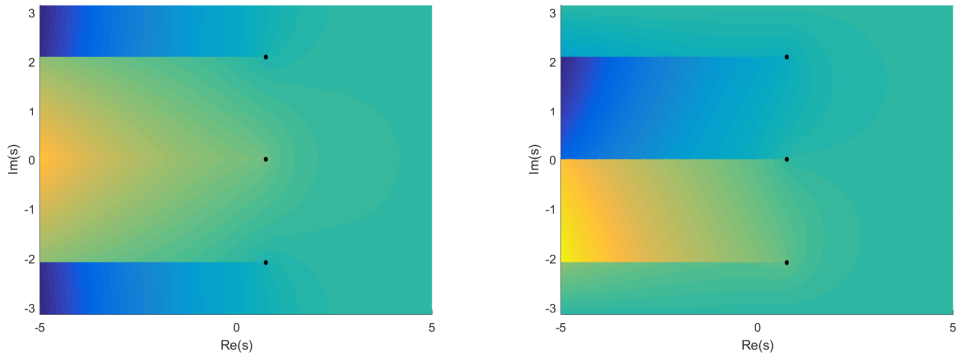

(A) Real part of $W_{0,4}$. (B) Imaginary part of $W_{0,4}$.

FIGURE 4.8. Plots of the real and imaginary parts of $W_{0,4}$ in $\mathcal{D}_0$. We see that $W_{0,4}$ is singular at the points $s_{0,1}$, $s_{0,2}$, and $s_{0,3}$ as given in equations (4.130)-(4.132).

Then the four solutions for W_0 are given by

$$W_{0,1} = -\frac{1}{2}\sqrt{D} + \frac{i}{2}\sqrt{D + \frac{2}{\sqrt{D}}}, \tag{4.123}$$

$$W_{0,2} = -\frac{1}{2}\sqrt{D} - \frac{i}{2}\sqrt{D + \frac{2}{\sqrt{D}}}, \tag{4.124}$$

$$W_{0,3} = \frac{1}{2}\sqrt{D} + \frac{1}{2}\sqrt{-D + \frac{2}{\sqrt{D}}}, \tag{4.125}$$

$$W_{0,4} = \frac{1}{2}\sqrt{D} - \frac{1}{2}\sqrt{-D + \frac{2}{\sqrt{D}}}. \tag{4.126}$$

As equation (4.118) does not have a cubic term, the sum of roots of (4.118) is equal to zero, and hence we find that

$$W_{0,4}(s) = -\sum_{j=1}^{3} W_{0,j}(s). \tag{4.127}$$

Figure 4.7 illustrates the plots of $W_{0,1}, W_{0,2}$ and $W_{0,3}$ in $\mathcal{D}_0$. In this figure we find that each $W_{0,j}$ is only singular at three distinct points. We will show that the singular points of $W_{0,j}$ are given by (4.130) - (4.132), which we denote by $s_{0,j}$, where $j = 1, 2, 3$. However, we see in Figure 4.8 that the leading order behaviour $W_{0,4}$ which is given by (4.126) is singular at each of these points.

The singularities of W_0 are located at the points for which the argument of the square root term in (4.120) is equal to zero. That is, when

$$27 - 256e^{-3s} = 0, \tag{4.128}$$

which occurs at the points

$$s_0 = \frac{1}{3}\left(\log\left(\frac{256}{27}\right) + 2ik\pi\right), \tag{4.129}$$

where $k \in \mathbb{Z}$. Let us denote the singularities

$$s_{0,1} = \frac{1}{3}\left(\log\left(\frac{256}{27}\right) - 2i\pi\right), \tag{4.130}$$

$$s_{0,2} = \frac{1}{3}\left(\log\left(\frac{256}{27}\right) + 2i\pi\right), \tag{4.131}$$

$$s_{0,3} = \frac{1}{3}\log\left(\frac{256}{27}\right). \tag{4.132}$$

From (4.129), we see that the singularities of $W_0(s)$ are vertical translations of the singularities in (4.130)-(4.132) by integer multiples of $2i\pi$. This is actually a consequence of the $W_0(s)$ being $2i\pi$-periodic. This was also the case when we considered the singularity structure of the asymptotic solutions of the q-Airy equation in Section 4.3. Consequently, the Stokes structure in the whole complex s-plane may be obtained by vertical translations of the Stokes structure found in the domain $\mathcal{D}_0$ by integer multiples of $2i\pi$. Following the analysis of the q-Airy equation, we restrict the analysis to the domain $\mathcal{D}_0$, in which the relevant singularities are precisely those given by (4.130)-(4.132).

The local behaviour of $W_{0,k}(s)$ near the singular points (4.129) is given by

$$W_{0,k} \sim \left(\frac{1}{4}\right)^{1/3} e^{2ik\pi/3} + \left(\frac{1}{8\sqrt{2}}\right)^{1/3} e^{2ik\pi/3}\sqrt{s - s_{0,k}} + \mathcal{O}(s - s_{0,k}), \tag{4.133}$$

as $s \to s_{0,k}$ for $k = 1, 2, 3$. In the subsequent analysis, we will find in Sections 4.5 and 4.6 that the Stokes and anti-Stokes curves emanate from these singularities.

The formula (4.127) shows that $W_{0,4}(s)$ is the sum of $W_{0,1}(s), W_{0,2}(s)$ and $W_{0,3}(s)$ and is therefore singular at the points $s_{0,1}, s_{0,2}$ and $s_{0,3}$ in $\mathcal{D}_0$. Therefore, $W_{0,4}$ has the most complicated behaviour in the sense that the associated Stokes structure for $W_{0,4}(s)$ will be comprised of Stokes and anti-Stokes curves emanating from more than one point.

These two types of leading order behaviours can then be distinguished by the number of points at which they are singular in $\mathcal{D}_0$. In the subsequent analysis, we will refer to solutions with leading order behaviour described by (4.123), (4.124) or (4.125) as type A, while those with leading order behaviour described by (4.126) as type B. Consequently, type A solutions are those which are singular at one point in $\mathcal{D}_0$ while type B solutions are singular at three points in $\mathcal{D}_0$.

In order to determine the form of the asymptotic series expansion (4.116) we investigate the behaviour of its coefficients. The first few coefficients are given by

$$W_1 = -\frac{e^{-s}s}{2(4W_0^3-1)}, \tag{4.134}$$

$$W_2 = -\frac{e^{-s}(3s^2-8s)}{24(4W_0^3-1)} - \frac{6W_0^2W_1^2 + W_0^2W_0'^2 + W_0^3W_0''}{(4W_0^3-1)}, \tag{4.135}$$

$$W_3 = -\frac{e^{-s}(s^3-8s^2+12s)}{48(4W_0^3-1)} - \frac{4W_0W_1^3 + 12W_0^2W_1W_2 - 2W_0W_1W_0'^2 - 2W_0^2W_0'W_1' + 3W_0^2W_1W_0'' + W_0^3W_1''}{(4W_0^3-1)}. \tag{4.136}$$

From the expressions of the first few terms of W_r, we find that calculation of successive coefficient terms of (4.116) involve repeated differentiation. Since the leading order term is singular at the points, s_0, successive coefficient terms will also be singular at s_0. As a result, the coefficients of (4.116) will have behaviour described by the factorial-over-power form (2.43) in the limit $r \to \infty$. Consequently, the asymptotic series expansion (4.116) are therefore factorially divergent.

In particular, equations (4.135) and (4.136) shows that the calculation of W_2 requires two derivatives of W_0 while W_3 requires two derivatives of W_1 yet no derivatives of W_2 are taken. As more terms are calculated, this pattern continues, and we deduce that the calculation of W_r involves two derivatives of W_{r-2}.

Before we proceed to determine the form for late-order order terms we first rewrite the recurrence relation described by (4.117) as

$$\begin{aligned} &2W_0^3W_r + W_0^3\sum_{k=0}^{r}\frac{\left((-1)^k+1\right)W_{r-k}^{(k)}}{k!} + 2W_0^2W_1\sum_{k=0}^{r-1}\frac{\left((-1)^k+1\right)W_{r-k-1}^{(k)}}{k!} \\ &\quad + 6W_0^2W_1W_{r-1} + W_0^2W_0'\sum_{k=0}^{r-1}\frac{\left((-1)^k-1\right)W_{r-k-1}^{(k)}}{k!} + W_0^2W_1\sum_{k=0}^{r-1}\frac{\left((-1)^k+1\right)W_{r-k-1}^{(k)}}{k!} \\ &\quad + W_0^2\sum_{b=2}^{r-2}W_{r-b}W_b + W_0(W_0'+W_1)\sum_{b=1}^{r-2}W_{r-b-1}W_b + \cdots = W_r - e^{-s}P_r(-s), \end{aligned} \tag{4.137}$$

for $r \geq 0$, where we have omitted the terms which are of size $\mathcal{O}(W_{r-2})$ as $r \to \infty$. This rearranged form of the recurrence relation will be useful when we apply the factorial-over-power ansatz for the behaviour of the late-order terms of (4.116).

4.5. Type A solutions of q-Painlevé I

In this section we investigate type A solutions of (4.111). Recall that these are solutions of (4.111) with leading order behaviour described by either (4.123), (4.124) or (4.125) in the limit

$\epsilon \to 0$. In particular, we will perform the analysis of type A solutions with leading order behaviour $W_{0,3}$ as $\epsilon \to 0$. In doing so, we will drop the subscript 3 for notational convenience. The results for the remaining type A asymptotic solutions described by $W_{0,1}$ or $W_{0,2}$ to leading order, may be obtained using the symmetry (4.112). As the symmetry (4.112) relates the three distinct type A solutions we will find that type A solutions correspond to the nonzero asymptotic solutions found by Joshi [**80**].

In the subsequent analysis, we will first calculate the late-order terms behaviour, $W_r(s)$. Once the form of the late-order terms are computed, we will optimally truncate the asymptotic series (4.116) and investigate the optimally-truncated error in order to describe Stokes behaviour present within these asymptotic solutions.

4.5.1. Late-Order Terms Behaviour.

In this section we determine the form of the late-order terms of (4.116) for the choice of $W_0 = W_{0,3}$. In general, the analysis applies for $W_0 = W_{0,j}$ for $j = 1, 2, 3$ however, the remaining two type A solutions can be obtained from the symmetry given by (4.112).

As the calculation of the coefficients of (4.116) involve repeated differentiation, the late-order terms will be described by the following factorial-over-power ansatz

$$W_r(s) \sim \frac{U(s)\Gamma(r+\gamma)}{\chi(s)^{r+\gamma}}, \tag{4.138}$$

as $r \to \infty$ where γ is a constant. We substitute (4.138) into (4.137) to obtain

$$\begin{aligned} &2W_0^3 W_r + W_0^3 \sum_{k=0}^{r} \frac{\left((-1)^k + 1\right)}{k!}(-\chi')^k W_r + 6W_0^2 W_1 W_{r-1} \\ &+ W_0^3 \sum_{k=0}^{r} \frac{\left((-1)^k + 1\right)}{k!} \left(\binom{k}{1}(-\chi')^{k-1}\frac{U'}{U} + \binom{k}{2}(-\chi')^{k-2}(-\chi'') \right) W_{r-1} \\ &+ \sum_{k=0}^{r-1} \frac{\left((-1)^k + 1\right)}{k!}(-\chi')^k \left(3W_0^2 W_1 + W_0^2 W_0'\right) W_{r-1} + \mathcal{O}(W_{r-2}) = W_r + \cdots, \end{aligned} \tag{4.139}$$

where the remaining terms are negligible for the purposes of this demonstration as $r \to \infty$. Then, by matching terms of $\mathcal{O}(W_r)$ as $r \to \infty$, we find from (4.139) that the leading order equation is given by

$$2W_0^3 + W_0^2 \sum_{k=0}^{r} \frac{\left((-1)^k + 1\right)}{k!}(-\chi')^k = 1. \tag{4.140}$$

as $r \to \infty$. Matching at the next subsequent order, that is, matching terms of $\mathcal{O}(W_{r-1})$ we find from (4.139) that

$$W_0^3 \sum_{k=0}^{r} \frac{\left((-1)^k+1\right)}{k!}\left(\binom{k}{1}(-\chi')^{k-1}\frac{U'}{U}+\binom{k}{2}(-\chi')^{k-2}(-\chi'')\right)+6W_0^2W_1$$
$$+3W_0^2W_1\sum_{k=0}^{r-1}\frac{\left((-1)^k+1\right)}{k!}(-\chi')^k+W_0^2W_0'\sum_{k=0}^{r-1}\frac{\left((-1)^k-1\right)}{k!}(-\chi')^k=0. \tag{4.141}$$

as $r \to \infty$.

4.5.1.1. *Calculating the singulant, χ.*

In this section we determine the form of the singulant, χ, and hence we consider equation (4.140). Following Chapter 3, we replace the upper limit of the sums in (4.140) by infinity, which only introduces error which is exponentially small as $r \to \infty$. Evaluating the infinite sum appearing in (4.140) gives

$$\cosh(-\chi') = \frac{1-2W_0^3}{2W_0^3}, \quad \chi(s_{0,3}) = 0. \tag{4.142}$$

We set

$$\sigma(s) = \frac{1-2W_0(s)^3}{2W_0(s)^3}, \tag{4.143}$$

for algebraic convenience. The solution of (4.142) is given by

$$\chi(s) = \pm\int_{s_{0,3}}^{s} \cosh^{-1}(\sigma(t)) + 2iM\pi\, dt, \tag{4.144}$$

where $M \in \mathbb{Z}$. However, as in Chapter 3, we take the case where $M = 0$ as this is the value for which $|\chi|$ is smallest. From (4.144) we find that there are two expressions for $\chi(s)$. Hence we set

$$\chi_1(s) = \int_{s_{0,3}}^{s} \cosh^{-1}(\sigma(t))dt, \tag{4.145}$$

$$\chi_2(s) = -\int_{s_{0,3}}^{s} \cosh^{-1}(\sigma(t))dt. \tag{4.146}$$

4.5.1.2. *Calculating the prefactor, U.*

In order to determine the prefactor, U, we replace the upper limit of the sum appearing in (4.141) by infinity following the previous section. This gives

$$-2W_0^3\sinh(\chi')\frac{U'}{U} - W_0^3\chi''\cosh(\chi') + 2W_0^2W_0'\sinh(\chi') + 3\frac{W_1}{W_0} = 0. \tag{4.147}$$

To find the solutions of (4.147) we first consider the differential equation

$$-2W_0^3\sinh(\chi')\frac{F'}{F} - W_0^3\chi''\cosh(\chi') + 2W_0^2W_0'\sinh(\chi') = 0, \tag{4.148}$$

which is simply equation (4.147) without the $3W_1/W_0$ term. Using standard integration methods, it is possible to show that the solution of (4.148) is given by

$$F(s) = \frac{\Upsilon W_0}{\sqrt{\sinh(\chi')}}, \tag{4.149}$$

where Υ is a constant of integration. Then, by making the substitution

$$U(s) = F(s)\phi(s), \tag{4.150}$$

into (4.147) we obtain

$$\frac{\phi'}{\phi} = \frac{3W_1}{2W_0^4 \sinh(\chi')}, \tag{4.151}$$

where we have used (4.148) to cancel terms. By taking the derivative of equation (4.142) we find that

$$\sinh(\chi') = -\frac{3W_0'}{2W_0^4\chi''},$$

and hence equation (4.151) can be simplified to give

$$\frac{\phi'}{\phi} = -\frac{W_1\chi''}{W_0'}. \tag{4.152}$$

Integrating (4.152) then gives

$$\phi(s) = \tilde{\Upsilon} \exp\left(\int^s -\frac{W_1(t)\chi''(t)}{W_0'(t)}dt\right), \tag{4.153}$$

where $\tilde{\Upsilon}$ is a constant. Therefore, the expression for the prefactor, U, is given by

$$U(s) = \frac{\Lambda W_0}{\sqrt{\sinh(\chi')}} \exp\left(\int^s -\frac{W_1(t)\chi''(t)}{W_0'(t)}dt\right), \tag{4.154}$$

where $\Lambda = \Upsilon\tilde{\Upsilon}$ is an constant. Since there are two singulant expressions, which differ by a change in sign, we obtain two prefactor expressions. If we let U_i denote the prefactor associated with the singulant χ_i, we find that

$$U_1(s) = \frac{\Lambda W_0 e^{-G}}{\sqrt{\sinh(\chi_1')}}, \quad U_2(s) = \frac{\tilde{\Lambda} W_0 e^{G}}{\sqrt{\sinh(\chi_1')}}, \tag{4.155}$$

where $\Lambda, \tilde{\Lambda}$ are constants and

$$G(s) = \int^s \frac{W_1(t)\chi_1''(t)}{W_0'(t)}dt. \tag{4.156}$$

By substituting (4.145)-(4.146) and (4.155) into (4.138) we find that the late-order terms are given by

$$W_r(s) \sim \frac{W_0\Gamma(r+\gamma_1)}{\sqrt{\sinh(\chi_1')}\chi_1^{r+\gamma_1}}\left(\Lambda e^{-G} + \frac{\tilde{\Lambda}e^G}{(-1)^{r+\gamma_1}}\right), \tag{4.157}$$

as $r \to \infty$, where $\gamma_1, \Lambda, \tilde{\Lambda}$ are constants and G is given by (4.156).

In order to completely determine the form of the late-order terms we must determine the values of γ_1 and Λ in (4.157). Following the analysis of the second discrete Painlevé II equation in Chapter 3, we determine the value for γ_1 by matching the strength of the singularity to the leading order behaviour in the neighbourhood of the singularity. We therefore determine the behaviour of χ and U in the neighbourhood of the singularity.

4.5.1.3. *Calculating the value of* γ_1.

In order to determine the value of γ_1 in (4.157) we calculate the local behaviour of χ and U. As both the singulant and prefactor depend on the leading order behaviour, $W_{0,3}$, we require the local behaviour of $W_{0,3}$, which is given by equation (4.133). Using (4.133) in equations (4.142) and (4.147) we can show that

$$\chi(s) \sim \frac{4i\sqrt{6\sqrt{2}}}{5}(s-s_{0,3})^{5/4}, \tag{4.158}$$

$$U(s) \sim \frac{\Lambda}{\sqrt{i\sqrt{6\sqrt{2}}}(s-s_{0,3})^{1/8}}, \tag{4.159}$$

as $s \to s_{0,3}$. Furthermore, using the local behaviour of W_0, which is given by (4.133), it is possible to show that

$$W_1(s) = \frac{A_1}{(s-s_{0,3})^{1/2}} + \mathcal{O}\left((s-s_{0,3})^{-1/2}\right), \tag{4.160}$$

as $s \to s_{0,3}$, where A_1 is some nonzero constant. Hence, from equations (4.160) and (4.156) we find that

$$e^{\pm G(s)} = 1 \pm A_2(s-s_{0,3})^{1/4} + \mathcal{O}\left((s-s_{0,3})^{1/2}\right), \tag{4.161}$$

as $s \to s_{0,3}$ for some nonzero constant A_2. The local behaviour of the late-order terms near the singularity is therefore given by

$$W_r(s) \sim \left(\frac{5}{4}\right)^{r+\gamma_1} \frac{\Gamma(r+\gamma_1)}{\left(i\sqrt{6\sqrt{2}}\right)^{r+\gamma_1+1/2}(s-s_{0,3})^{5(r+\gamma_1)/4+1/8}} \left(\Lambda e^{-G} + \frac{\tilde{\Lambda}e^{G}}{(-1)^{r+\gamma_1}}\right), \tag{4.162}$$

as $s \to s_{0,3}$. We note that the term $\Lambda + (-1)^{-\gamma_1}\tilde{\Lambda}$ in (4.162) is constant. Recall from (4.137) that the dominant behaviour of W_r is due to the term $W''_{r-2}/(4W_0^3-1)$. Hence, if W_{r-2} has a singularity at s_0 with strength ν, then W_r has a singularity at s_0 with strength $\nu+5/2$. In particular, since we know that W_0 is singular at $s_{0,3}$ with strength $-1/2$ then W_{2r} will also be singular at $s_{0,3}$ but with strength $5r/2-1/2$. Similarly, as W_1 is singular at $s_{0,3}$ with strength $1/2$, then W_{2r+1} is singular at $s_{0,3}$ with strength $5r/2+1/2$.

We first observe from (4.161) that

$$\left(\Lambda e^{-G}+\frac{\tilde{\Lambda}e^{G}}{(-1)^{r+\gamma_1}}\right)\sim\begin{cases}\Lambda+i\tilde{\Lambda}+A_2(-\Lambda+i\tilde{\Lambda})(s-s_{0,3})^{1/4}+\mathcal{O}((s-s_{0,3})^{1/2}), & \text{for even } r,\\ \Lambda-i\tilde{\Lambda}+A_2(-\Lambda-i\tilde{\Lambda})(s-s_{0,3})^{1/4}+\mathcal{O}((s-s_{0,3})^{1/2}), & \text{for odd } r,\end{cases} \tag{4.163}$$

as $s\to s_{0,3}$.

Thus, in order for the singularity behaviour of (4.162) to be consistent with the singularity behaviour of W_{2r}, we require $5r/2-1/2=5(2r+\gamma_1)/4+1/8$ under the condition $\Lambda+i\tilde{\Lambda}\neq 0$. Hence, we deduce that $\gamma_1=-1/2$ and the leading order behaviour of the late-order terms is given by

$$W_r(s)\sim\frac{W_0\Gamma(r-1/2)}{\sqrt{\sinh(\chi_1')}\chi_1^{r-1/2}}\left(\Lambda e^{-G}+\frac{\tilde{\Lambda}e^{G}}{(-1)^{r-1/2}}\right), \tag{4.164}$$

as $r\to\infty$. We must also check that the strength of the singularity of W_{2r+1} matches to $5r/2+1/2$. From (4.163) and (4.164) we find that first two terms of W_{2r+1} are proportional to

$$\frac{\Lambda-i\tilde{\Lambda}}{(s-s_{0,3})^{5r/2+3/4}},\quad\text{and}\quad\frac{-A_2(\Lambda+i\tilde{\Lambda})}{(s-s_{0,3})^{5r/2+1/2}},$$

as $s\to s_{0,3}$. Hence, in order for W_{2r+1} to have the correct singular behaviour in the limit $s\to s_{0,3}$ we impose the condition $\Lambda-i\tilde{\Lambda}=0$, which gives

$$\tilde{\Lambda}=-i\Lambda. \tag{4.165}$$

Hence, the leading order behaviour of the late-order terms, is given by

$$W_r(s)\sim\frac{\Lambda W_0\Gamma(r-1/2)}{\sqrt{\sinh(\chi_1')}\chi_1^{r-1/2}}\left(e^{-G}-\frac{ie^{G}}{(-1)^{r-1/2}}\right), \tag{4.166}$$

as $r\to\infty$. In particular, we find that the late-order terms may be separated into even and odd late-order terms. More specifically, we have

$$W_{2r}(s)\sim\frac{2W_0\Lambda\cosh(G)\Gamma(2r-1/2)}{\sqrt{\sinh(\chi_1')}\chi_1^{2r-1/2}}, \tag{4.167}$$

$$W_{2r+1}(s)\sim\frac{-2W_0\Lambda\sinh(G)\Gamma(2r+1/2)}{\sqrt{\sinh(\chi_1')}\chi_1^{2r+1/2}}, \tag{4.168}$$

as $r\to\infty$.

4.5.2. q-Painlevé I inner problem.

The expression for the late-order terms given by (4.166) contains a constant Λ, which is yet to be determined. In order to determine the value of Λ we perform an inner analysis of (4.111) near the singularity, $s_{0,3}$ and determine the inner expansion of the inner solution. We then use the method of matched asymptotics to match the outer expansion to the inner expansion following Van Dyke's matching principle [**69**].

In view of the leading order behaviour given by (4.133), we study the inner solution by applying the scalings

$$s = s_{0,3} + \epsilon^{4/5}\zeta, \qquad W(s) = a_3 + \epsilon^{2/5}\psi_1(\zeta) + \epsilon^{3/5}\psi_2(\zeta), \tag{4.169}$$

where ζ is the inner variable, ψ_1 and ψ_2 are the first two terms of the inner solution, ψ. In particular, we recall that

$$s_{0,3} = \frac{1}{3}\log\left(\frac{256}{27}\right), \quad a_3 = \left(\frac{1}{4}\right)^{1/3}, \quad b_3 = \left(\frac{1}{8\sqrt{2}}\right)^{1/3}. \tag{4.170}$$

Substituting (4.169) into (4.111) we obtain

$$\begin{aligned}(a_3^4 - a_3 + e^{-s_{0,3}}) &+ \epsilon^{2/5}(4a_3^3 - 1)\psi_1, \\ &+ \epsilon^{3/5}(4a_3^3 - 1)\psi_2 + \epsilon^{4/5}(6a_3^2\psi_1^2 - e^{-s_{0,3}}\zeta + a_3^3\psi_1''), \\ &+ \epsilon\left(\frac{s_{0,3}}{2}e^{-s_{0,3}} + 12a_3^2\psi_1\psi_2 + a_3^3\psi_2''\right) + \mathcal{O}(\epsilon^{6/5}) = 0,\end{aligned} \tag{4.171}$$

as $\epsilon \to 0$ and where the prime denotes derivatives with respect to ζ. Using the values of a_3, b_3 and $s_{0,3}$ given in (4.170) we find that the coefficients of $\epsilon^0, \epsilon^{2/5}$ and $\epsilon^{3/5}$ are identically zero. Therefore, the leading order equation of the inner solution is given by

$$\psi_1^2 - b_3^2\zeta + \frac{a_3}{6}\frac{d^2\psi_1}{d\zeta^2} = 0, \tag{4.172}$$

as $\epsilon \to 0$. From equation (4.171) we see that the term ψ_2 does not appear in the leading order equation in the limit $\epsilon \to \infty$. This therefore reinforces the fact that the odd terms are indeed negligible in the limit $\epsilon \to 0$ as the term ψ_2 corresponds to the first odd coefficient term in the outer problem (far field expansion), (4.116).

To study the inner solution, we analyze (4.172) in the limit $|\zeta| \to \infty$. Using the method of dominant balance, equation (4.172) has a solution described by $\psi_1 \sim b_3\sqrt{\zeta}$ as $|\zeta| \to \infty$. For algebraic convenience, we rescale the inner solution by setting $\psi = b_3\sqrt{\zeta}\Psi$, where

$$\Psi(\zeta) = \sum_{r=0}^{\infty} \frac{E_r}{\zeta^{5r/2}} \tag{4.173}$$

with $E_0 = 1$. We then substitute (4.173) into (4.172) and match terms of $\mathcal{O}(\zeta)$ in the limit $|\zeta| \to \infty$. Doing this, we obtain the following nonlinear recurrence relation

$$E_r = -\frac{1}{2b_3^2}\left(\frac{a_3 b_3}{24}(5r-4)(5r-6)E_{r-1} + b_3^2\sum_{k=1}^{r-1} E_{r-k}E_k\right), \tag{4.174}$$

for $r \geq 1$. The inner solution therefore has an expansion of the form

$$\psi_1(\zeta) \sim b_3\sqrt{\zeta}\sum_{r=0}^{\infty}\frac{E_r}{\zeta^{5r/2}}, \tag{4.175}$$

as $|\zeta| \to \infty$. We can express (4.175) in terms of the outer variables by reversing the scalings given in (4.169). Doing this, we find that the inner expansion of the outer solution is given by

$$W(s) \sim a_3 + b_3 \sum_{r=0}^{\infty} \frac{\epsilon^{2r} E_r}{(s - s_{0,3})^{(5r-1)/2}}, \tag{4.176}$$

as $\epsilon \to 0$. Recall that the outer expansion is given by the expression

$$W(s) \sim \sum_{r=0}^{\infty} \epsilon^{2r} W_{2r}(s) + \sum_{r=0}^{\infty} \epsilon^{2r+1} W_{2r+1}(s), \tag{4.177}$$

as $\epsilon \to 0$, and where the behaviour of $W_{2r}(s)$ and $W_{2r+1}(s)$ are given by (4.167) and (4.168), respectively. By matching the expansions (4.177) and (4.176) it follows that

$$\Lambda = \lim_{r\to\infty} b_3 E_r \frac{\sqrt{i\sqrt{6\sqrt{2}}}}{\Gamma(2r - 1/2)} \left(\frac{4i\sqrt{6\sqrt{2}}}{5} \right)^{2r-\frac{1}{2}}. \tag{4.178}$$

We then compute the first 1000 E_r terms using the recurrence relation (4.174). Then, by using the formula (4.178) we find numerically that the approximate value of Λ is

$$\Lambda \approx -0.04364. \tag{4.179}$$

The approximate value for Λ is shown in Figure 4.9.

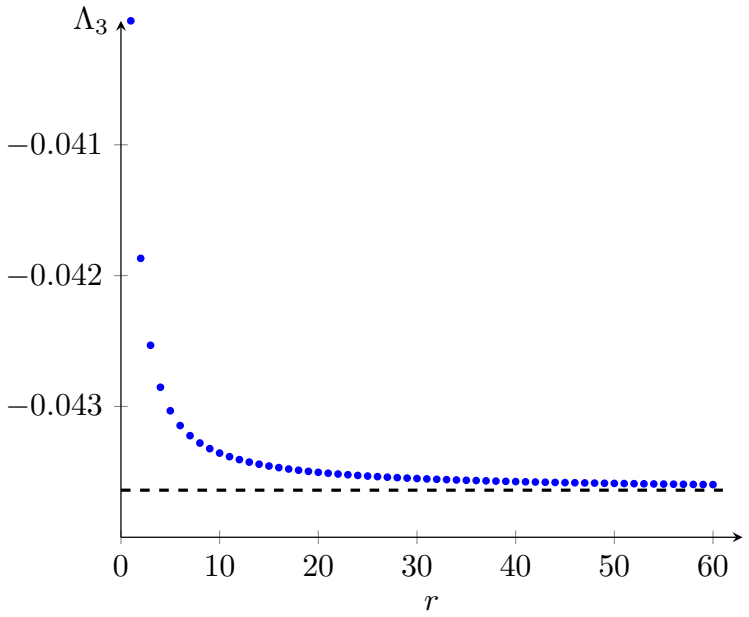

FIGURE 4.9. This figure illustrates the approximation for Λ appearing in the even late-order terms (4.162). As r increases, the approximation for Λ tends to the limiting value of -0.04364, which is denoted by the black dashed line.

4.5.3. Analysis of the remainder using exponential asymptotics.

As the form of the asymptotic power series (4.116) has been determined, we may optimally-truncate (4.116) in order to study the exponentially small terms present within type A solutions.

Recall from Section 4.5.1 that the leading order behaviour of the late-order terms may be separated into even and odd terms. Consequently, the asymptotic series (4.116) also separate into two asymptotic series; one with even powers of epsilon and the other with odd powers of epsilon. In the subsequent analysis we will proceed by truncating the asymptotic series with even powers of epsilon and find that the optimally-truncated error will be proportional to $U\exp(-\chi/\epsilon)$.

The asymptotic series with odd powers of epsilon may also be optimally-truncated. However, this will produce an error proportional to $\epsilon U\exp(-\chi/\epsilon)$, which is asymptotically smaller than the error produced by optimally truncating the even-powered asymptotic series. As such, we truncate (4.116) at the least even term by writing

$$W(s) = \sum_{r=0}^{2N_{\text{opt}}-1} \epsilon^r W_r(s) + R_N(s), \tag{4.180}$$

where N_{opt} is the optimal truncation point. For algebraic convenience, we adopt the following notation

$$T(s) = \sum_{r=0}^{2N_{\text{opt}}-1} \epsilon^r W_r(s), \tag{4.181}$$

and use the shift notation denoted by $F = F(s), \overline{F} = F(s+\epsilon), \underline{F} = F(s-\epsilon)$. Under this notation (4.180) can be expressed as $W = T + R$ and

$$T(s) = W(s) - R_N(s). \tag{4.182}$$

Using the late-order terms (4.138) to truncate, we find using the heuristic (2.25) that the optimal truncation point occurs at approximately $N_{\text{opt}} \sim |\chi|/(2\epsilon)$ as $\epsilon \to 0$. Hence, we let

$$N_{\text{opt}} = \frac{1}{2}\left(\frac{|\chi|}{\epsilon} + \kappa\right), \tag{4.183}$$

where $\kappa \in [0, 2)$ is chosen such that $N_{\text{opt}} \in \mathbb{Z}$. By substituting the truncated series, (4.180), into the governing equation (4.111) we obtain

$$\overline{T}T^2\underline{T} + T^2\underline{T}\overline{R} + 2\overline{T}T\underline{T}R + \overline{T}T^2\underline{R} + \cdots = T + R - \frac{1}{(1+\epsilon)^{s/\epsilon}}, \tag{4.184}$$

where the terms neglected are quadratic in R_N. We may use the recurrence relation (4.137) to cancel terms in (4.184), which leaves terms of size $\mathcal{O}(\epsilon^{2N})$. Hence, after rearrangement, we obtain

from (4.184) the equation

$$T^2\underline{T}\overline{R} + 2\overline{T}T\underline{T}R + \overline{T}T^2\underline{R} - R = -\overline{T}T^2\underline{T} + T - \frac{1}{(1+\epsilon)^{s/\epsilon}} + \cdots,$$
$$\sim \epsilon^{2N}(4W_0^3 W_{2N} - W_{2N}), \tag{4.185}$$

as $\epsilon \to 0$, where the terms neglected are of size $\mathcal{O}(\epsilon^{2N+1}W_{2N+1})$ and terms quadratic in R_N. Terms of these sizes are negligible compared to the terms kept in (4.185) as $\epsilon \to 0$.

4.5.3.1. *Analysis for the homogeneous remainder equation.*

As in Chapter 3, the behaviour of R_N away from the Stokes curve may be determined by considering the homogeneous form of (4.185). We therefore apply a WKB ansatz of the form

$$R_{N,\text{hom}}(s) = \alpha(s)e^{\beta(s)/\epsilon}. \tag{4.186}$$

Substituting (4.186) into the homogeneous version of (4.185) and matching terms of $\mathcal{O}(R_N)$ we find that the leading order equation is given by

$$W_0^3 \sum_{j=0}^{\infty} \frac{(-1)^j(\beta')^j}{j!} + 2W_0^3 + W_0^3 \sum_{j=0}^{\infty} \frac{(\beta')^j}{j!} = 1, \tag{4.187}$$

as $\epsilon \to 0$. Equation (4.187) can be simplified and rearranged to give

$$\cosh(\beta') = \frac{1 - 2W_0^3}{2W_0^3}. \tag{4.188}$$

Comparing (4.188) to (4.142) shows that (4.187) is satisfied if $\beta' = -\chi'$. We therefore set $\beta(s) = -\chi(s)$.

Continuing to the next order involves matching terms of $\mathcal{O}(\epsilon R_N)$. By collecting terms of this size in (4.185) we obtain the equation

$$2W_0^3 \sum_{j=0}^{\infty} \frac{1}{(2j)!}\left(\binom{2j}{1}(\beta')^{2j-1}\frac{\alpha'}{\alpha} + \binom{2j}{2}(\beta')^{j-2}\beta''\right),$$
$$+ 6W_0^2 W_1 \sum_{j=0}^{\infty} \frac{(\beta')^{2j}}{(2j)!} - 2W_0^2 W_0' \sum_{j=0}^{\infty} \frac{(\beta')^{2j+1}}{(2j+1)!} + 6W_0^2 W_1 = 0. \tag{4.189}$$

By substituting $\beta' = -\chi'$ in equation (4.189), and using equation (4.142) to simplify, equation (4.189) can be rewritten as

$$-2W_0^3 \sinh(\chi')\frac{\alpha'}{\alpha} - W_0^3\chi''\cosh(\chi') + 2W_0^2 W_0' \sinh(\chi') + 3\frac{W_1}{W_0} = 0. \tag{4.190}$$

By comparing equation (4.190) to (4.147) we find that α satisfies to same equation as the prefactor, U, and hence $\alpha(s) \propto U(s)$. Hence, away from the Stokes curves the solution of (4.185) is given by

$$R_{N,\text{hom}}(s) \sim C_1 U(s) e^{-\chi(s)/\epsilon}, \tag{4.191}$$

as $\epsilon \to 0$, where C_1 is a constant.

4.5.3.2. *Stokes Smoothing for q-P_I.*

In order to determine the Stokes switching behaviour, which occurs in the neighbourhood of Stokes curves, we set

$$R(s) = \mathcal{S}(s)U(s)e^{-\chi(s)/\epsilon}, \tag{4.192}$$

where $\mathcal{S}(s)$ is the Stokes multiplier. We substitute (4.192) into (4.185) and use equations (4.142) and (4.147) to cancel terms. Doing this we find that the Stokes multiplier satisfies

$$\begin{aligned}\frac{d\mathcal{S}}{ds} &\sim \frac{\epsilon^{2N-1}(1-4W_0^3)W_{2N}}{2W_0^3\sinh(\chi')U(s)}e^{\chi/\epsilon},\\ &\sim \epsilon^{2N-1}\sqrt{1-4W_0^3}\frac{\Gamma(2N+\gamma_1)}{\chi^{2N+\gamma_1}}e^{\chi/\epsilon},\end{aligned} \tag{4.193}$$

as $\epsilon \to 0$. We note that we have used equation (4.142) and conjunction with the hyperbolic identity

$$\cosh^2(x) - \sinh^2(x) = 1,$$

to replace the hyperbolic sine by

$$\sinh(\chi') = \frac{\sqrt{1-4W_0^3}}{2W_0^3}$$

in equation (4.193). We make the change of variables to write $\mathcal{S}$ as a function of χ rather than s. Under this change of variables, equation (4.193) becomes

$$\frac{d\mathcal{S}}{d\chi} \sim \frac{\epsilon^{2N-1}\sqrt{1-4W_0^3}}{\chi'}\frac{\Gamma(2N+\gamma_1)}{\chi^{2N+\gamma_1}}e^{\chi/\epsilon}, \tag{4.194}$$

as $\epsilon \to 0$. By noting the form of the optimal truncation point, (4.183), we follow [**32**, **92**, **121**] and change to polar coordinates by letting

$$\chi = \rho \mathrm{e}^{i\theta}, \tag{4.195}$$

where we rewrite the equations in terms of the fast variable, θ. We note that under this change of variables, $\rho = |\chi|$ and

$$\frac{d}{d\chi} = -\frac{i\mathrm{e}^{-i\theta}}{\rho}\frac{d}{d\theta}.$$

Applying the change of variables given by (4.195) and substituting (4.183) we have

$$\frac{d\mathcal{S}}{d\theta} \sim i\rho\epsilon^{\rho/\epsilon+\kappa-1}\frac{\sqrt{1-4W_0^3}}{\chi'}\frac{\Gamma(\rho/\epsilon+\kappa-1/2)}{\rho^{\rho/\epsilon+\kappa-1/2}}\exp\left(\frac{\rho}{\epsilon}e^{i\theta}+i\theta-i\theta\left(\frac{\rho}{\epsilon}+\kappa-\frac{1}{2}\right)\right), \tag{4.196}$$

as $\epsilon \to 0$. Using Stirling' formula [**2**], we replace the Gamma function by its asymptotic behaviour in (4.196) to obtain

$$\frac{d\mathcal{S}}{d\theta} \sim \frac{i\sqrt{2\pi\rho}\sqrt{1-4W_0^3}}{\chi'}\exp\left(\frac{\rho}{\epsilon}(e^{i\theta}-1-i\theta)-i\theta(\kappa-3/2)\right), \tag{4.197}$$

as $\epsilon \to 0$. For simplicity, we will let $H(s(\theta);\rho) = \sqrt{1-4W_0^3}/\chi'$. From (4.197) we find that the variation of the Stokes multiplier is exponentially small except when

$$e^{i\theta} - 1 - i\theta = 0,$$

which occurs when $\theta = 0$. This is exactly the location of the Stokes curve since χ is purely real and positive when $\theta = 0$. In order to capture the Stokes switching behaviour we analyze (4.197) near the Stokes curve. We therefore rescale to the neighbourhood of the Stokes curve by setting $\theta = \sqrt{\epsilon}\hat{\theta}$. Note that under this scaling, $H(s(\theta);\rho) \sim H(|\chi|)$ as $\epsilon \to 0$, which is therefore independent of θ. Applying the scaling $\theta = \sqrt{\epsilon}\hat{\theta}$ to (4.197) gives

$$\begin{aligned}\mathcal{S} &\sim i\sqrt{2\pi\epsilon}H(|\chi|)\int^{|\chi|\hat{\theta}} e^{-x^2/2}dx,\\ &= i\pi\sqrt{\epsilon}H(|\chi|)\left(\operatorname{erf}\left(\theta\sqrt{\frac{|\chi|}{2\epsilon}}\right)+C\right),\end{aligned} \tag{4.198}$$

where C is an arbitrary constant. From (4.198) we may determine the jump in $\mathcal{S}$ as the Stokes curves are crossed. The variation of the jump varies rapidly as $\hat{\theta}$ varies between $-\infty$ and ∞. Hence, we have

$$\begin{aligned}\Delta\mathcal{S} \sim& i\sqrt{2\pi\epsilon}H(|\chi|)\int_{-\infty}^{\infty} e^{-x^2/2}dx,\\ =& 2i\pi\sqrt{\epsilon}H(|\chi|),\end{aligned} \tag{4.199}$$

and therefore

$$\Delta R_N \sim 2i\pi\sqrt{\epsilon}H(|\chi|)U(s)e^{-\chi(s)/\epsilon}, \tag{4.200}$$

as $\epsilon \to 0$.

Hence, the asymptotic power series expansion of type A solutions to (4.111) up to exponentially small corrections is given by

$$\begin{aligned}W(s) \sim& W_{0,3}(s) + \sum_{r=1}^{N-1}\epsilon^{2r}W_{2r}(s),\\ &+i\pi\sqrt{\epsilon}H(|\chi|)\left(\operatorname{erf}\left(\theta\sqrt{\frac{|\chi_3|}{2\epsilon}}\right)+C\right)U_3(s)e^{-\chi_3(s)/\epsilon},\end{aligned} \tag{4.201}$$

as $\epsilon \to 0$, and where we have reintroduced the subscripts for the prefactor and singulant to explicitly denote they are associated with $W_{0,3}$. Furthermore, we recall that W_r is described by

$$W_r(s) \sim \frac{\Lambda_3 U_3(s)\Gamma(2r-1/2)}{\chi_3(s)^{2r-1/2}}, \tag{4.202}$$

as $r \to \infty$ where Λ_3 was numerically calculated to be approximately -0.0436 and U_3 and χ_3 are solutions to (4.147) and (4.142), respectively. Recall that the remaining type A solutions may be

obtained from the symmetry (4.112). By applying the symmetry

$$\lambda^3 = 1, \quad W \mapsto \lambda W, \quad \text{with,} \quad s \mapsto s - \frac{\epsilon \log(\lambda)}{\log(1+\epsilon)} \sim s - \log(\lambda),$$

as $\epsilon \to 0$ to (4.201) we find that the other type A solutions are given by

$$\begin{aligned} W(s) \sim & W_{0,1}(s) + \lambda_1 \sum_{r=1}^{N-1} \epsilon^{2r} W_{2r}(s), \\ & + i\lambda_1 \pi \sqrt{\epsilon} H(|\chi|) \left(\text{erf}\left(\theta \sqrt{\frac{|\chi_1|}{2\epsilon}} \right) + C \right) U_1(s) e^{-\chi_1(s)/\epsilon}, \end{aligned} \tag{4.203}$$

$$\begin{aligned} W(s) \sim & W_{0,2}(s) + \lambda_2 \sum_{r=1}^{N-1} \epsilon^{2r} W_{2r}(s), \\ & + i\lambda_2 \pi \sqrt{\epsilon} H(|\chi|) \left(\text{erf}\left(\theta \sqrt{\frac{|\chi_2|}{2\epsilon}} \right) + C \right) U_2(s) e^{-\chi_2(s)/\epsilon}, \end{aligned} \tag{4.204}$$

as $\epsilon \to 0$ where $\lambda_1 = e^{-2i\pi/3}$, $\lambda_2 = e^{2i\pi/3}$ and

$$\chi_1(s) = \chi_3(s + 2i\pi/3), \tag{4.205}$$

$$U_1(s) = U_3(s + 2i\pi/3), \tag{4.206}$$

$$\chi_2(s) = \chi_3(s - 2i\pi/3), \tag{4.207}$$

$$U_2(s) = U_3(s - 2i\pi/3). \tag{4.208}$$

In general, the late-order terms associated with the leading order behaviour $W_{0,j}$ is given by

$$W_{2r}(s) \sim \frac{\Lambda_j U_j(s) \Gamma(2r - 1/2)}{\chi_j(s)^{2r-1/2}}, \tag{4.209}$$

as $r \to \infty$ for $j = 1, 2, 3$. In particular, the values of Λ_j are

$$\Lambda_1 = \lambda_1 \Lambda_3 = e^{-2i\pi/3} \Lambda_3, \tag{4.210}$$

$$\Lambda_2 = \lambda_2 \Lambda_3 = e^{-2i\pi/3} \Lambda_3, \tag{4.211}$$

where Λ_3 is given by (4.179).

4.5.4. Stoke structure for type A solutions.

With the results for χ_j given by (4.145), we can now investigate the switching behaviour of the exponentially small contributions in both the complex s-plane and the complex x-plane. As demonstrated in Section 4.5.3.2, we found that the exponential contributions present in the series expansions (4.201), (4.203) and (4.204) are proportional to $\exp(-\chi_j/\epsilon)$. These terms are exponentially small when $\text{Re}(\chi_j) > 0$ and exponentially large when $\text{Re}(\chi_j) < 0$. In order to investigate the behaviour of these terms we consider the solution's Stokes structure as in Chapter 3. Once their

Stokes behaviour has been deduced in the complex s-plane we may reverse the rescalings (4.110) in order to determine the Stokes behaviour of type A solutions in the complex x-plane.

We recall that Stokes curves follow curves where $\mathrm{Im}(\chi_j) = 0$, while anti-Stokes curves follow curves where $\mathrm{Re}(\chi_j) = 0$. Additionally, we recall that Stokes switching occurs across Stokes curves where $\mathrm{Re}(\chi_j) > 0$.

We first illustrate and explain the Stokes structure and Stokes switching behaviour in the domain $\mathcal{D}_0$, described by (4.29). The upper and lower boundaries of $\mathcal{D}_0$ are described by the curves $\mathrm{Im}(s) = \pm\pi$ and are denoted by the dashed green curves in Figure 4.10a. In this figure we also see that there are two Stokes curves (red curves) and three anti-Stokes curves (blue curves) emanating from the singularity. The Stokes curves extending towards the upper boundary of $\mathcal{D}_0$ switches the exponential contribution associated with χ_3 as $\mathrm{Re}(\chi_3) > 0$. This Stokes curve is denoted by ③ in Figure 4.10b. While the Stokes curve extending towards the lower boundary of $\mathcal{D}_0$ does not switch any exponential contributions as $\mathrm{Re}(\chi_3) < 0$. Additionally, there is a branch cut (dashed curve) of χ_3 located along the negative real s axis emanating from the singularity, $s_{0,3}$. Using this knowledge, we can determine the switching behaviour as Stokes curves are crossed. Additionally, we observe in Figure 4.10a that the Stokes structure and the branch cut separate $\mathcal{D}_0$ into six regions.

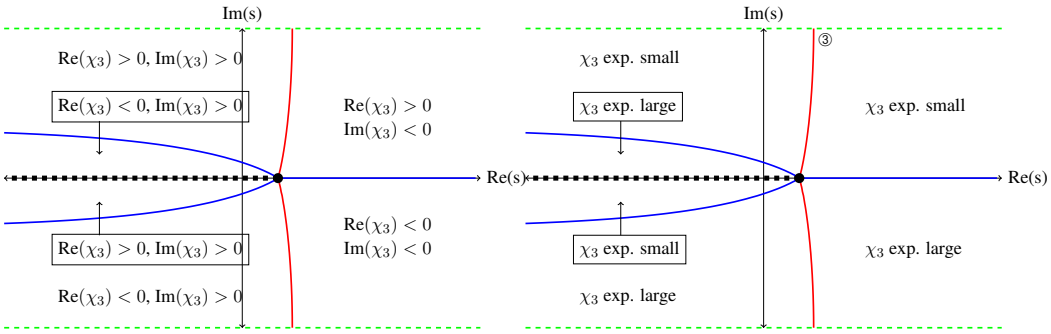

(A) Behaviour of χ_3.

(B) Exponential behaviour.

FIGURE 4.10. These figures illustrate the Stokes structure for type A solutions of q-$\mathrm{P_I}$ with leading order behaviour described by $W_{0,3}$, which is given by (4.125), in $\mathcal{D}_0$. Figure 4.10a illustrates the behaviour of χ_3 as Stokes and anti-Stokes curves (denoted by red and blue curves, respectively) are crossed. Figure 4.10b illustrates regions of $\mathcal{D}_0$ in which the exponential contribution associated with χ_3 is exponentially large or small.

We now determine regions in $\mathcal{D}_0$ in which the asymptotic behaviour of (4.111) is described by the power series expansion (4.201), referred to as regions of validity. From Figure (4.10a) we may deduce the regions in which the exponential contribution associated with χ_3 is exponentially large or small; this is illustrated in Figure 4.10b.

From Figure 4.10b we observe that the exponential contribution associated with χ_3 is exponentially small in the neighbourhood of the upper Stokes curves since $\text{Re}(\chi_3) > 0$, and therefore the presence of $\exp(-\chi_3/\epsilon)$ does not affect the dominance of the leading order behaviour in (4.201). Hence, the value of the Stokes multiplier, $\mathcal{S}_3$, in the neighbourhood of the upper Stokes curve may be freely specified, and will therefore contain a free parameter hidden beyond-all-orders. The values of $\mathcal{S}_3$ in the regions of $\mathcal{D}_0$ is illustrated in Figure 4.11a.

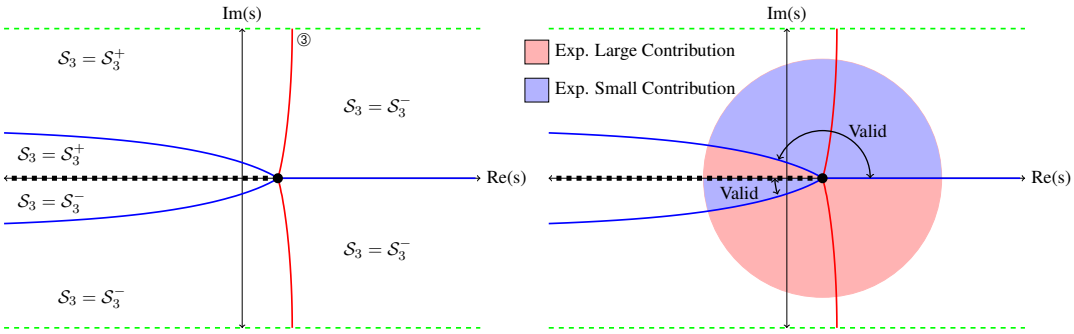

(A) General values of $\mathcal{S}_3$. (B) Regions of validity.

FIGURE 4.11. Figure 4.11a illustrates the value $\mathcal{S}_3$ as Stokes curves are crossed while Figure 4.11b illustrates the regions of validity for type A solutions of q-P$_{\text{I}}$ with leading order behaviour described by $W_{0,3}$. The regions of validity are those which are shaded in blue. The blue and red shaded regions denote regions in which the exponential contribution associated with χ_3 is small and large, respectively.

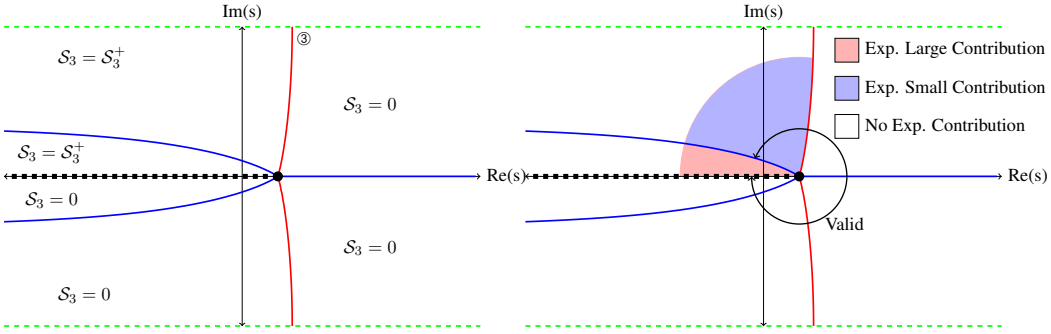

(A) Special values of $\mathcal{S}_3$. (B) Extended regions of validity.

FIGURE 4.12. Figure 4.12a illustrates the values $\mathcal{S}_3$ while Figure 4.12b illustrates the regions of validity for special type A solutions of q-P$_{\text{I}}$ with leading order behaviour described by $W_{0,3}$. The choice of $\mathcal{S}_3^- = 0$ gives an asymptotic solution of (4.111) with an extended region of validity. Non-shaded regions denote regions in which there are no exponential contributions present. The legend in this figure will be used throughout the remainder of this chapter, unless stated.

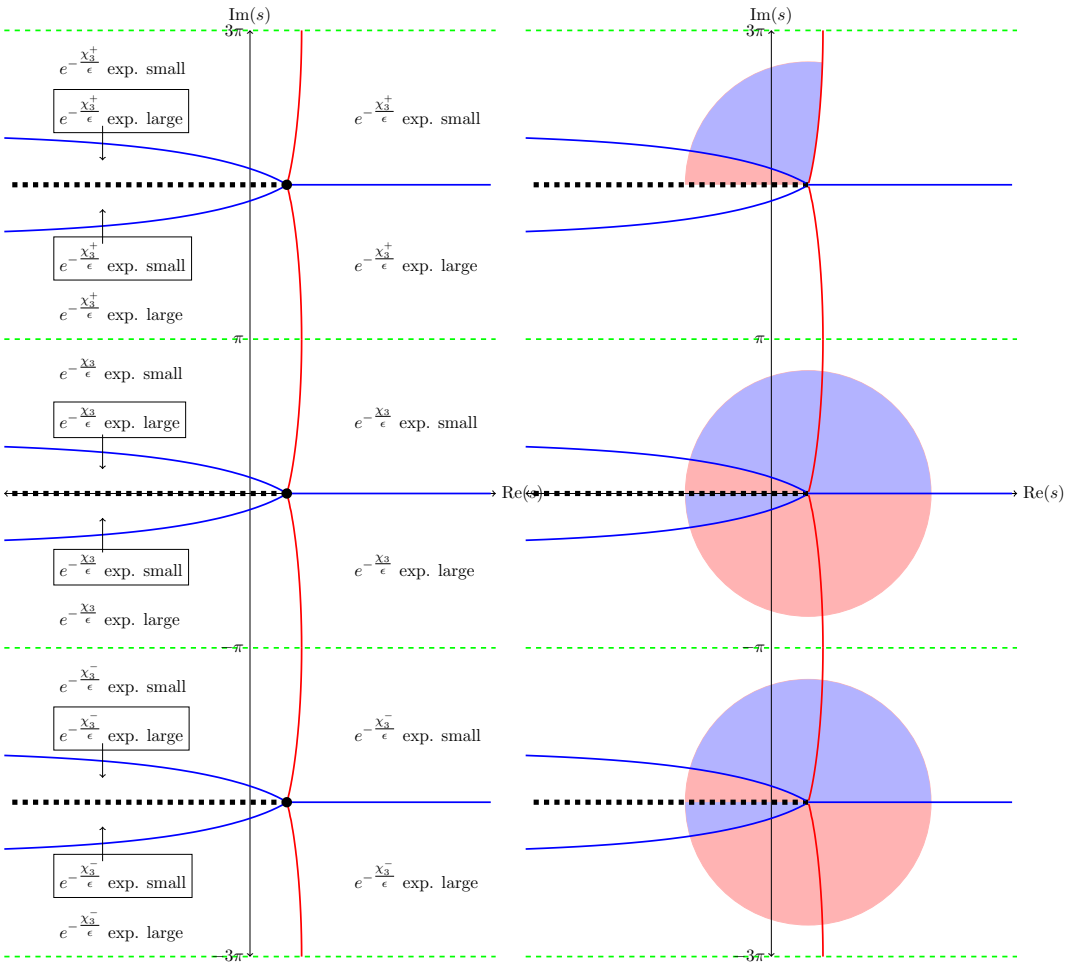

(A) Stokes structure of χ_3 in the domains $\mathcal{D}_0$, $\mathcal{D}_1$ and $\mathcal{D}_{-1}$.

(B) Exponential contributions originating from the domains $\mathcal{D}_0$, $\mathcal{D}_1$ and $\mathcal{D}_{-1}$.

FIGURE 4.13. This figure illustrates the Stokes structure depicted in Figure 4.10b extended to the adjacent domains $\mathcal{D}_1$ and $\mathcal{D}_{-1}$. In fact, the Stokes structure in the k^{th}-adjacent domains are identical to those in $\mathcal{D}_0$ since W_0 is $2\pi i$-periodic. Each adjacent domain provides an exponential contribution to the asymptotic solution described by (4.201). From figure 4.13a, we see that the presence of the exponential contribution from $\mathcal{D}_{-1}$ does not affect the dominance of (4.201) in $\mathcal{D}_0$ and hence its associated Stokes multiplier may be freely specified. However, the presence of the exponential contribution from $\mathcal{D}_1$ dominates the asymptotic solution, (4.201). In order for (4.201) to remain valid in $\mathcal{D}_0$, we require the value of the Stokes multiplier associated with exponential contribution in $\mathcal{D}_1$ must be chosen to be equal to zero. Figure 4.13b illustrates the regions where each exponential contribution are present.

The remainder term associated with χ_3 will exhibit Stokes switching and therefore varies as it crosses a Stokes curve; say, from state 1 to state 2 which we denote by $\mathcal{S}_3^-$ and $\mathcal{S}_3^+$, respectively. If we assume that the value of $\mathcal{S}_3$ is nonzero on either side of the upper Stokes curve, then we conclude that the exponentially small contribution associated with χ_3 is present in the regions bounded by the upper anti-Stokes curve and the anti-Stokes curve emanating from the singularity along the positive real s axis. Furthermore, the exponential contribution associated with χ_3 is also exponentially small in the region bounded by the branch cut and the lower anti-Stokes curve. The regions of validity of the asymptotic solution described by (4.201) is illustrated in Figure 4.11b.

However, for special choices of the free parameter hidden beyond-all-orders, we can obtain asymptotic solutions with an extended range of validity in $\mathcal{D}_0$. If we specify the value of $\mathcal{S}_3^-$ to be equal to zero, then the exponential contribution associated with χ_3 is no longer present in regions where it is normally exponentially large. In this case, the region of validity is extended by an additional two adjacent sectorial regions in $\mathcal{D}_0$ and is illustrated in Figure 4.12b. We note that the case where $\mathcal{S}_3^+ = 0$ is specified can also give type A solutions with an extended region of validity. However, this only extend the regions of validity of (4.203) by one additional sectorial region. In both cases the value of $\mathcal{S}_3$ is specified, and therefore the asymptotic solutions described by (4.201) are uniquely determined; we call these special type A asymptotic solutions.

Figure 4.13 illustrates the Stokes structure in the adjacent domains $\mathcal{D}_1$ and $\mathcal{D}_{-1}$ as described by (4.30). Due to the $2\pi i$-periodic nature of W_0, the Stokes structure is also $2\pi i$-periodic as shown in Figure 4.13. Hence, we obtain an exponential contribution in each adjacent domain $\mathcal{D}_k$. For integers $k \leq -1$, there are exponentially small contributions present in the adjacent domains $\mathcal{D}_k$. The presence of these exponentially small contributions do not affect the asymptotic behaviour in the principal domain, $\mathcal{D}_0$ and hence the corresponding Stokes multipliers may be freely specified. However, for integers $k \geq 1$ the exponential contributions originating from the adjacent domains $\mathcal{D}_k$ dominate those in $\mathcal{D}_0$ and hence affect the asymptotic behaviour in $\mathcal{D}_0$. In order for the asymptotic solution (4.201) to correctly describe the solution behaviour in $\mathcal{D}_0$, the value of the Stokes multipliers must be specified such that the are not present in $\mathcal{D}_0$. The presence of the exponential contributions in the domains $\mathcal{D}_{-1}, \mathcal{D}_0$ and $\mathcal{D}_1$ is illustrated in Figure 4.13b.

The corresponding analysis of the Stokes structure and switching behaviour of the exponential contributions present within the asymptotic solutions described by (4.203) and (4.204) can be determined using the same approach.

Figures 4.14a and 4.14b illustrate the Stokes structure associated with the singulants χ_1 and χ_2. Due to symmetry of the rescaled q-$\mathrm{P_I}$ equation which is given by (4.112), we observe that the Stokes structure associated with χ_1 and χ_2 are vertical translations of the Stokes structure associated with χ_3 by $\mp 2i\pi/3$, respectively.

The general values of the Stokes multipliers, $\mathcal{S}_1$ and $\mathcal{S}_2$, are shown in Figures (4.15a) and 4.15b, respectively. In the general case, the values of $\mathcal{S}_1$ and $\mathcal{S}_2$ may be freely specified and therefore contain a free parameter hidden beyond-all-orders. The ranges of validity for the asymptotic

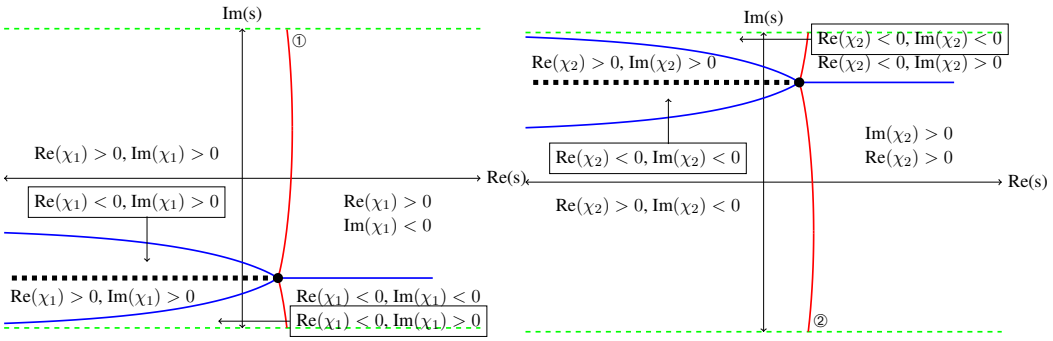

(A) Behaviour of χ_1. (B) Behaviour of χ_2.

FIGURE 4.14. Figures 4.14a and 4.14b illustrate the behaviours of the singulants, χ_1 and χ_2, as Stokes and anti-Stokes curves are crossed in the domain $\mathcal{D}_0$ in the complex s-plane, respectively. The subdominant exponential associated with χ_1 and χ_2 are switched across the Stokes curves labelled with ① and ②, respectively. We note that the Stokes structures in Figures 4.14a and 4.14b are vertical translations of Figure 4.10a by $\mp 2\pi/3$, respectively as a result of the symmetry (4.112). Furthermore, we note that the anti-Stokes curves of χ_1 and χ_2 asymptotically approach the lower and upper boundaries of $\mathcal{D}_0$.

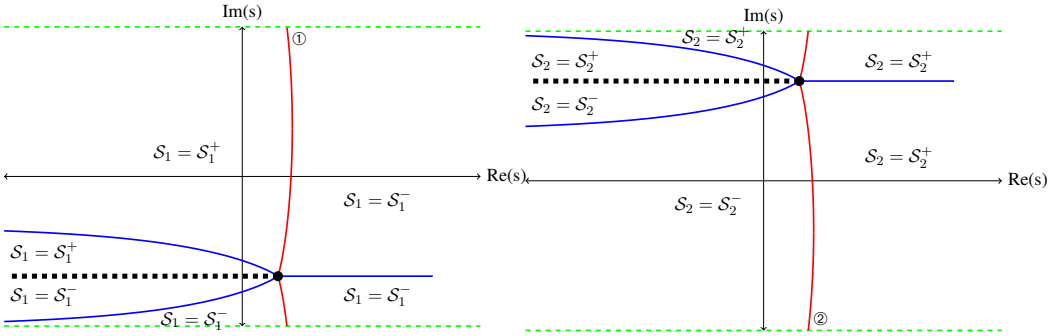

(A) General values of $\mathcal{S}_1$. (B) General values of $\mathcal{S}_2$.

FIGURE 4.15. Figures 4.15a and 4.15b illustrate the values of $\mathcal{S}_1$ and $\mathcal{S}_2$, as Stokes curves are crossed, respectively. $\mathcal{S}^-$ and $\mathcal{S}^+$, denotes the values of the Stokes multipliers in regions where $\mathrm{Im}(\chi) < 0$ and $\mathrm{Im}(\chi) > 0$ respectively. Furthermore, we see that the Stokes multipliers $\mathcal{S}_1$ and $\mathcal{S}_2$ change in value across the Stokes curves labelled by ① and ②, respectively.

solutions described by (4.203) and (4.204) are illustrated in Figures 4.16a and 4.17a. For special values of the free parameter hidden beyond orders, we also obtain special type A asymptotic solutions of (4.203) and (4.204) with an extended range of validity. These special solutions are therefore uniquely specified and their regions of validity are illustrated in Figures 4.16b and 4.17b.

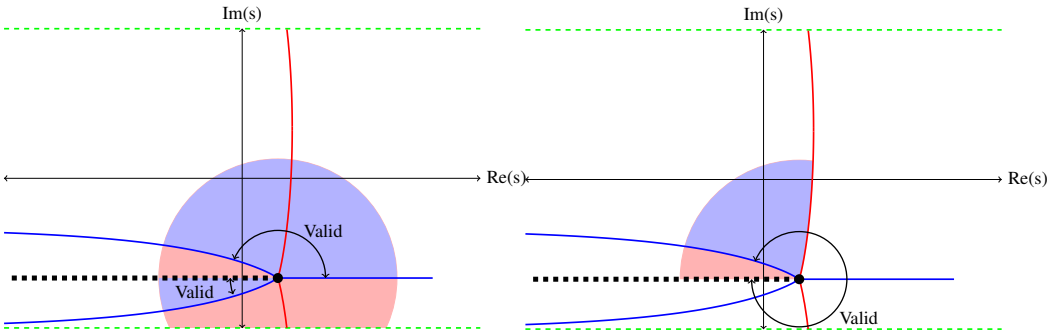

(A) Regions of validity. (B) Extended regions of validity.

FIGURE 4.16. Figure 4.16a illustrates the regions of validity for type A solutions of q-P$_{\text{I}}$ with leading order behaviour described by $W_{0,1}$, which is given by (4.123), and containing one free parameter. The blue and red shaded regions denote those in which the exponential contribution associated with χ_1 is small and large, respectively. Non-shaded regions denote those where there are no exponential contributions present in (4.203). Figure 4.16b illustrates the regions of validity for special type A solutions of q-P$_{\text{I}}$ with leading order behaviour described by $W_{0,1}$. This is possible by choosing $\mathcal{S}_1^- = 0$ and therefore the asymptotic solution described by (4.203) is uniquely specified.

As the Stokes structure and switching behaviour of the exponential contributions have been determined in the domain $\mathcal{D}_0$, we may finally determine the Stokes structure in the original complex x-plane. In order to determine the Stokes structure in the x-plane we reverse the scaling transformations (4.110). We recall that the choice of scalings were given by

$$x = q^n, \quad n = \frac{s}{\epsilon}, \quad q = 1 + \epsilon,$$

and therefore

$$s = \frac{\epsilon \log(x)}{\log(1+\epsilon)} \sim \log(x) + \mathcal{O}(\epsilon), \tag{4.212}$$

as $\epsilon \to 0$.

Without loss of generality, we demonstrate the Stokes structures of type A solutions for the choice of $q = 1 + 0.2i$. Using (4.212), the singulants, $\chi_j(s)$, can be written as a function of x. Then, we compute the Stokes structure in the complex x-plane using MATLAB. The corresponding Stokes structure of χ_3 in the complex x-plane is illustrated in Figure 4.18a while those for χ_1 and χ_2 are illustrated in Figures 4.19a and 4.20a, respectively. In these figures, Stokes curves and anti-Stokes curves are denoted by red and blue curves, respectively. The branch cuts of the singulants, χ_j, are denoted by the dashed curve which extend from the singularity to the origin of the x-plane. As in the case of the q-Airy, the asymptotic approximation described by (4.201) has a logarithmic branch cut (dashed green curves) the complex x-plane, which is due to the leading order term of the inverse transformation (4.212).

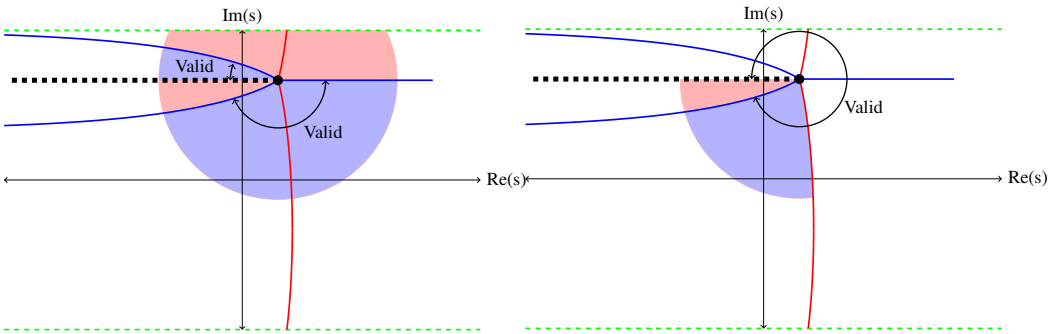

(A) Regions of validity. (B) Extended regions of validity.

FIGURE 4.17. Figure 4.17a illustrates the regions of validity for type A solutions of q-$\mathrm{P_I}$ with leading order behaviour described by $W_{0,2}$, which is given by (4.124), and containing one free parameter. The blue and red shaded regions denote those in which the exponential contribution associated with χ_2 is small and large, respectively. Non-shaded regions denote those where there are no exponential contributions present in (4.204). Figure 4.17b illustrates the regions of validity for special type A solutions with leading order behaviour described by $W_{0,2}$. This is possible by choosing $\mathcal{S}_2^- = 0$ and therefore the asymptotic solution described by (4.204) is uniquely specified.

The inverse transformation given by (4.212), maps the Stokes and anti-Stokes curves in the s-plane to q-spirals in the complex x-plane. Therefore, the Stokes and anti-Stokes curve separate the complex x-plane into sectorial regions bounded by arcs of spirals, as illustrated in Figures 4.18, 4.19 and 4.20.

We interpret the asymptotic results for the complex x-plane. Figure 4.18b illustrates the regions of validity of (4.201) which contain one free parameter in the complex x-plane. In this figure, the blue shaded regions are regions in which $\mathrm{Re}(\chi_3) > 0$ and hence the exponential contribution associated with χ_3 is exponentially small. In Figure 4.18a the subdominant exponential contribution associated with χ_3 exhibits Stokes switching as the Stokes curve labelled by ③ is crossed. In the red shaded regions, this exponential contribution is exponentially large. Consequently, the regions of validity of the asymptotic solution (4.201) containing one free parameter hidden beyond-all-orders are denoted by the regions shaded in the blue. The regions of validity of (4.201) for which the value of $\mathcal{S}_3^-$ is uniquely specified are illustrated in Figure 4.18c.

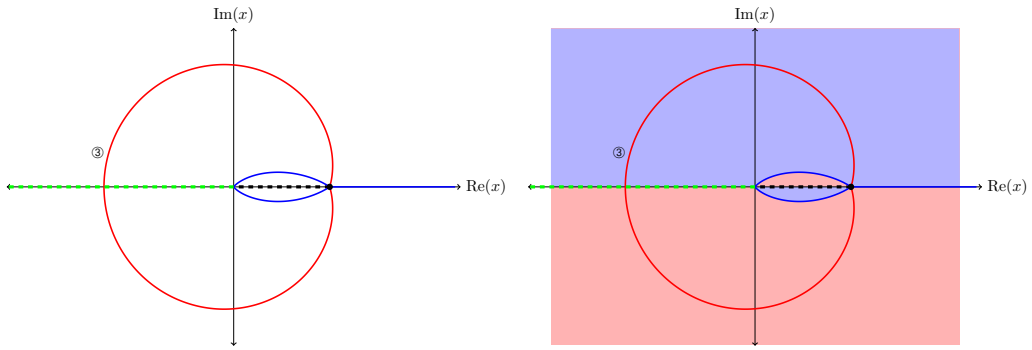

(A) Stokes structure of χ_3 in the x-plane. (B) Regions of validity of (4.201) in the x-plane.

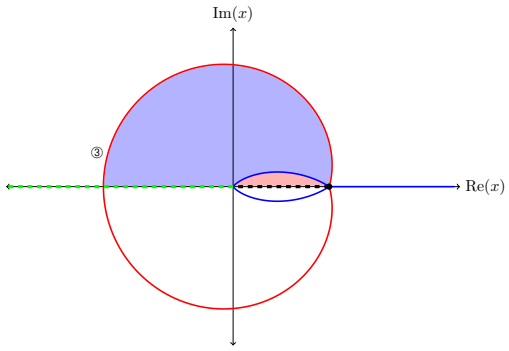

(C) Extended regions of validity of (4.201) in the x-plane.

FIGURE 4.18. This figure illustrates the Stokes structure of the series solution (4.201) of q-P$_{\text{I}}$ in the complex x-plane with $q = 1 + 0.2i$. Under the inverse transformation (4.212), the Stokes and anti-Stokes curves are now described by q-spirals in the x-plane. The branch cuts of χ_3 in the x-plane extends from the singularity and terminates at the origin. The dashed green curve denotes a logarithmic branch cut, which is due to the use of the leading order term of the inverse transformation. Figure 4.18b illustrates the region of validity (blue shaded regions) of (4.201) which contain a free parameter hidden beyond-all-orders. The regions of validity of (4.201) for which $\mathcal{S}_3^-$ is uniquely specified are illustrated in Figure 4.18c.

Due to the periodic nature of W_0, the Stokes curves which correspond to the different branches of (4.144) are identical to those in the principal sheet and therefore extend continuously across the logarithmic branch cut in both the complex s-plane as shown in Figure 4.13. Consequently, the Stokes curves in the complex x-planes extend continuously across the logarithmic branch cut (dashed green curve) onto the other Riemann sheets. In particular, the exponentially small contributions originating from the different Riemann sheets (from the domains $\mathcal{D}_k$ with $k \leq -1$) are sub-subdominant compared to optimally-truncated errors in (4.201), (4.203) and (4.204).

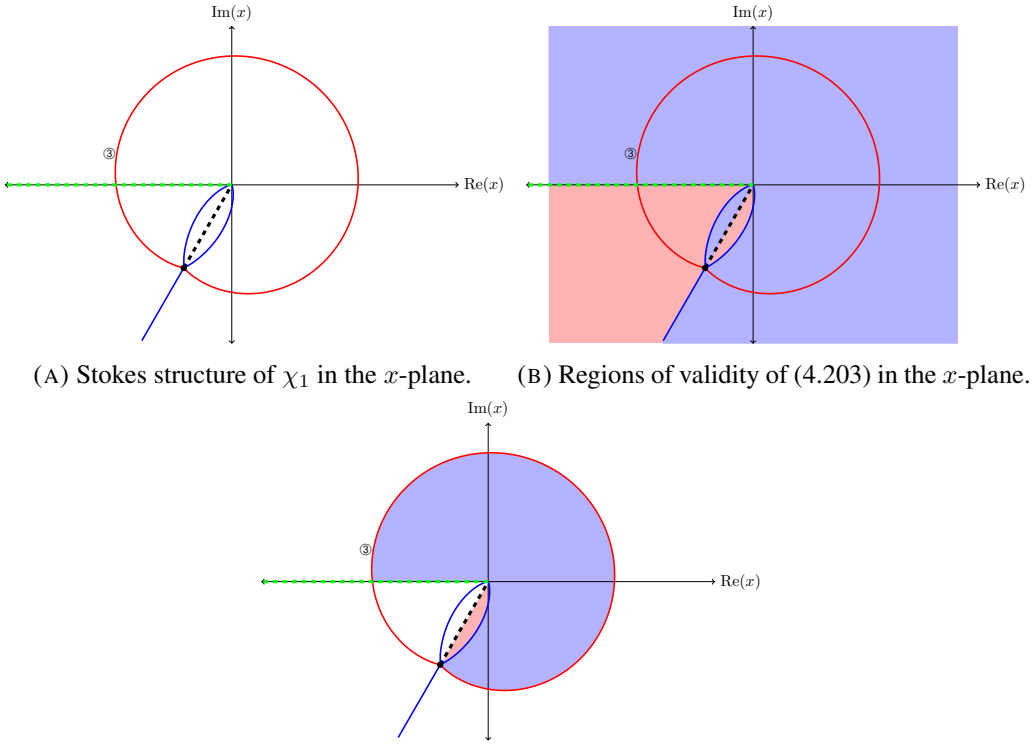

(A) Stokes structure of χ_1 in the x-plane. (B) Regions of validity of (4.203) in the x-plane.

(C) Extended regions of validity of (4.203) in the x-plane.

FIGURE 4.19. This figure illustrates the Stokes structure of the series solution (4.203) of q-$\mathrm{P_I}$ in the complex x-plane with $q = 1 + 0.2i$. Under the inverse transformation (4.212), the Stokes and anti-Stokes curves are now described by q-spirals in the x-plane. The branch cuts of χ_1 in the x-plane extends from the singularity and terminates at the origin. The dashed green curve denotes a logarithmic branch cut, which is due to the use of the leading order term of the inverse transformation. Figure 4.19b illustrates the region of validity (blue shaded regions) of (4.203) which contain a free parameter hidden beyond-all-orders. The regions of validity of (4.203) for which $\mathcal{S}_1^-$ is uniquely specified are illustrated in Figure 4.19c.

We note that the Stokes structures for each of the three type A asymptotic solutions illustrated in Figures 4.18, 4.19 and 4.20 are rotations of each other. This is a consequence of the symmetry of q-$\mathrm{P_I}$, which is given by (4.89). The regions of validity of the asymptotic solutions (4.203) and (4.204), which contain one free parameter hidden beyond-all-orders are depicted as the blue shaded regions in Figures 4.19b and 4.20b, respectively. While Figures 4.19c and 4.20c illustrate the regions of validity of the uniquely specified asymptotic solutions (4.203) and (4.204), respectively.

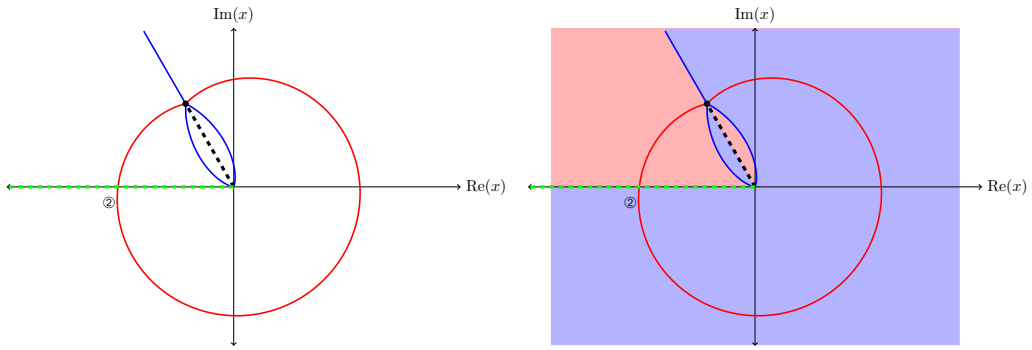

(A) Stokes structure of χ_2 in the x-plane. (B) Regions of validity of (4.204) in the x-plane.

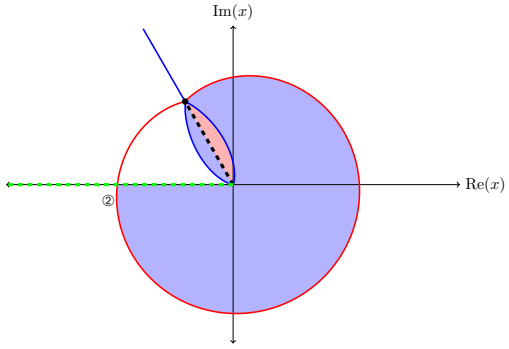

(C) Extended regions of validity of (4.204) in the x-plane.

FIGURE 4.20. This figure illustrates the Stokes structure of the series solution (4.204) of q-P$_{\rm I}$ in the complex x-plane with $q = 1 + 0.2i$. Under the inverse transformation (4.212), the Stokes and anti-Stokes curves are now described by q-spirals in the x-plane. The branch cuts of χ_2 in the x-plane extends from the singularity and terminates at the origin. The dashed green curve denotes a logarithmic branch cut, which is due to the use of the leading order term of the inverse transformation. Figure 4.20b illustrates the region of validity (blue shaded regions) of (4.204) which contain a free parameter hidden beyond-all-orders. The regions of validity of (4.204) for which $\mathcal{S}_2^+$ is uniquely specified are illustrated in Figure 4.20c.

4.6. Type B solutions

In this section we investigate type B solutions of (4.111). These are the asymptotic solutions of (4.111), which are described by (4.126) to leading order as $\epsilon \to 0$. Compared to type A solutions found in Section 4.5, which are singular at one point in $\mathcal{D}_0$, type B solutions are singular at three points in $\mathcal{D}_0$. Specifically, they are singular at the points $s_{0,1}$, $s_{0,2}$ and $s_{0,3}$ in $\mathcal{D}_0$, which are given by (4.130), (4.131) and (4.132), respectively. These solutions will therefore display more complicated behaviour than type A solutions as the Stokes curves emerge from three singular points rather than one.

The analysis for type B solutions can be similarly repeated as demonstrated for type A solutions in Section 4.5, although the complete analysis need not be repeated. As the analysis is near identical as the analysis for type A solutions, we state the main results. In fact, the analysis is exactly identical except for the calculation of the singulant. As type B solutions are singular at three points, the singulant for type B solutions will contain three contributions.

Type B solutions may be expanded as a power series in ϵ of the form

$$W(s) \sim W_{0,4}(s) + \sum_{r=1}^{\infty} \epsilon^r y_r(s), \tag{4.213}$$

as $\epsilon \to 0$. Following the analysis for type A solutions, it can be shown that the behaviour of y_r is also described by a factorial-over-power form. The behaviour of y_r is therefore described by

$$y_{2r}(s) \sim \frac{Y(s)\Gamma(2r+\gamma_2)}{\eta(s)^{2r+\gamma_2}}, \tag{4.214}$$

as $r \to \infty$. The analysis for type B solutions is near identical for the analysis of type A solutions. However, the main difference between type A and type B solutions is in the calculation of the singulant function, η. We recall that the singulant function, $\eta(s)$, is required to be singular at the singularities of the leading order behaviour, $W_{0,4}$. Since the leading order behaviour $W_{0,4}$ is singular at $s_{0,1}, s_{0,2}$ and $s_{0,3}$, we obtain three singulant contributions, which we denote by $\eta_j(s)$. This feature can be deduced from equation (4.127), which shows that $W_{0,4}$ is expressible as the sum of $W_{0,1}, W_{0,2}$ and $W_{0,3}$. Following the analysis in Section 4.5.1, $\eta_j(s)$ is given by

$$\eta_j(s) = \int_{s_{0,j}}^{s} \cosh^{-1}(\sigma(t))dt, \tag{4.215}$$

for $j = 1, 2, 3$ and where σ is given by (4.143) with u_0 replaced by $W_{0,4}$. Hence we obtain three contributions for η. Using the results for the late-order terms found in Section 4.5.1, we find that the late-order terms of (4.213) is given by

$$y_{2r}(s) \sim \sum_{j=1}^{3} \frac{Y_j(s)\Gamma(2r+\gamma_2)}{\eta_j(s)^{2r+\gamma_2}}, \tag{4.216}$$

as $r \to \infty$ and where $Y_j(s)$ are the prefactor terms corresponding to $\eta_j(s)$. Hence the asymptotic expansions of type B solutions of (4.111) is given by

$$W(s) \sim W_{0,4}(s) + \sum_{j=1}^{3}\sum_{r=1}^{\infty} \frac{\epsilon^{2r} Y_j(s)\Gamma(2r+\gamma_2)}{\eta_j(s)^{2r+\gamma_2}}, \tag{4.217}$$

as $\epsilon \to 0$. As there are three distinct singulant terms in (4.217) there will be three subdominant exponentials present and hence type B solutions will also display Stokes behaviour.

By applying the Stokes smoothing technique demonstrated in Section 4.5.3, the asymptotic series expansion of (4.217) which capture the Stokes behaviour of the subdominant exponential

correction terms is given by

$$W(s) \sim W_{0,4} + \sum_{j=1}^{3} \sum_{r=1}^{N_{\text{opt}}-1} \frac{\epsilon^{2r} Y_j(s) \Gamma(2r+\gamma_2)}{\eta_j(s)^{2r+\gamma_2}} + \sum_{j=1}^{3} \hat{\mathcal{S}}_j(s) \hat{\phi}(s) Y_j(s) e^{-\eta_j(s/\epsilon)}, \tag{4.218}$$

as $\epsilon \to 0$ and where N_{opt} is the optimal truncation point. In particular, the type B prefactor terms satisfy equation (4.154) with W_0 replaced by $W_{0,4}$. Similarly, the Stokes multipliers $\hat{\mathcal{S}}(s)$ satisfy (4.198) with u_0 and χ replaced by $W_{0,4}$ and η, respectively. In view of the formula (4.127), the leading order behaviour of the type B solution is a composition of the leading order behaviours of type A solutions. Consequently, the Stokes behaviour present in this solution will be more complicated as the Stokes curves emanate from more than one point. In particular, the Stokes structure for type B solutions may be obtained by investigating the singulant (4.215).

4.6.1. Stoke Geometry for type B solutions.

The Stokes and anti-Stokes curves of emanating from the singularities, $s_{0,j}$, may be determined by the conditions

$$\text{Im}(\eta_j(s)) = 0,$$

and

$$\text{Re}(\eta_j(s)) = 0,$$

respectively. The Stokes structure of type B asymptotic solutions in $\mathcal{D}_0$ is illustrated in Figure 4.21. In Figure 4.21 we see that there are three Stokes (red curves) and two anti-Stokes curves curves (blue curves) emanating from each of the singularities, $s_{0,j}$ for $j = 1, 2, 3$. The Stokes structure for type B solutions is more complicated as there are Stokes curves which cross into the branch cuts (dashed curves) of η_j as illustrated in Figure 4.21. These Stokes curves may have possible interaction effects with the exponentially small contributions from the different Riemann sheets of η_j.

However, we observe from Figure 4.21 that there are regions which do not contain the Stokes curves originating from the different Riemann sheets of η_j. This regions are labelled as regions I-IV in Figure 4.21. We first note that the Stokes curves emanating from the singularities $s_{0,1}$ and $s_{0,2}$ asymptote to $+\infty$ as $\text{Re}(s) \to \infty$ as illustrated in Figure 4.21a. In Figure 4.21a, we find that region I is the region bounded by the upper boundary of $\mathcal{D}_0$, the upper anti-Stokes curve emanating from $s_{0,1}$ and the Stokes curve emanating from $s_{0,2}$, which is labelled by ②; region II is the region bounded by the upper anti-Stokes curve emanating from $s_{0,1}$, and the Stokes curves labelled by ② and ③; region III is the region bounded by the lower anti-Stokes curve emanating from $s_{0,2}$, and the Stokes curves labelled by ① and ③; and finally region IV is the region bounded by the lower boundary of $\mathcal{D}_0$, the lower anti-Stokes curve emanating from $s_{0,2}$ and the Stokes curve emanating from $s_{0,1}$, which is labelled by ①.

Furthermore, $\text{Re}(\eta_j)$ is positive in each of these four regions and hence the exponential contributions associated with η_j are exponentially small there. This is illustrated by the blue shaded regions in 4.21b. We therefore restrict our analysis to regions I-IV as these are the regions in which

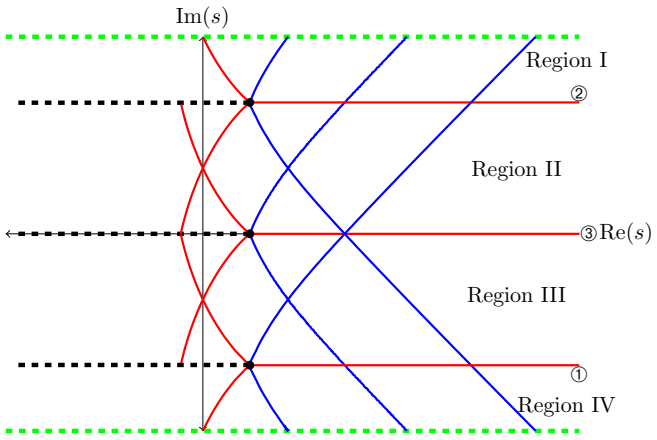

(A) Stokes structure of type B solutions in the complex s-plane

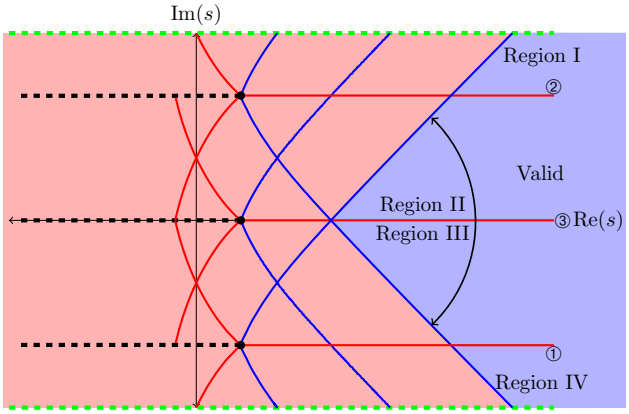

(B) Behaviour of the exponential contributions

FIGURE 4.21. Stokes structure of the series solution (4.217) of q-P$_{\rm I}$ in the domain $\mathcal{D}_0$. Regions I-IV denote regions in which the exponential contributions associated with η_j are exponentially small and therefore denote the regions of validity for (4.218).

the dominant asymptotic behaviour is described by (4.218). Consequently, the regions of validity of type B solutions is the region bounded by the anti-Stokes curves emanating from the singularity, $s_{0,3}$, the upper and lower boundaries of $\mathcal{D}_0$, containing the positive real s axis. This is the union of regions I-IV and is illustrated in Figure 4.21b.

In order to determine Stokes behaviour present in the asymptotic solution (4.218) we investigate the behaviour of η_j in regions I-IV. In Figure 4.21, regions I-IV denotes those of $\mathcal{D}_0$ in which $\mathrm{Re}(\eta_j) > 0$ and

- Region I : $\mathrm{Im}(\eta_j) > 0$,
- Region II : $\mathrm{Im}(\eta_1) > 0$, $\mathrm{Im}(\eta_2) < 0$, $\mathrm{Im}(\eta_3) > 0$,

- Region III : $\text{Im}(\eta_1) > 0$, $\text{Im}(\eta_2) < 0$, $\text{Im}(\eta_3) < 0$,
- Region IV : $\text{Im}(\eta_j) < 0$.

Hence, the Stokes curve separating regions I and II switches on the exponential contribution associated with η_2, the Stokes curve separating regions II and III switches on the exponential contribution associated with η_3 and the Stokes curve separating regions III and IV switches on the exponential contribution associated with η_1. To denote the Stokes switching behaviour of these subdominant exponentials, the Stokes curves are labelled by ①, ② and ③.

In regions I-IV, the presence of the exponential contributions associated with η_j are exponentially small since $\text{Re}(\eta_j) > 0$, and therefore do not affect the dominance of the leading order behaviour in (4.218). Hence, the values of $\hat{\mathcal{S}}_j$ may be freely specified in these regions and therefore the asymptotic solution described by (4.218) contains free parameters hidden beyond-all-orders.

In Section 4.5.4 we obtained special type A solutions, which are valid in an extended region of the complex plane. These special solutions were obtained by selecting values of the Stokes multipliers such that the exponential contributions are absence in regions where it is normally large. However, this is not possible for type B solutions. The reason this is not possible interaction effects of Stokes curves emerging from the different Riemann sheets of η_j.

Hence, in order to find special type B solutions, the exponential contributions on different Riemann sheets of η_j must be accounted for. As this is beyond the scope of this thesis, we restrict our attention to regions I-IV and therefore only obtain asymptotic solutions described by (4.218) which contain free parameters hidden beyond-all-orders.

Following the analysis in Section 4.5.4 we obtain the Stokes structure in the original x-plane by applying the inverse transformation given by (4.212). As in Section 4.5.4 we demonstrate the Stokes structure for the value of $q = 1 + 0.2i$. Using MATLAB, the Stokes structure of type B solutions is illustrated in Figure 4.22.

Figure 4.22 shows the corresponding regions I-IV in the complex x-plane. In this figure, the Stokes and anti-Stokes curves are denoted by red and blue curves, respectively. The branch cuts of η_j are depicted as the dashed curves, which connect the singularities to the origin in the complex x-plane. Furthermore, the green dashed curve denotes the logarithmic branch cut defined by the reverse transformation (4.212) for the choice of $q = 1 + 0.2i$.

Recall that the inverse transformation maps the Stokes and anti-Stokes curves in the complex s-plane to q-spirals in the complex x-plane. In particular, we find in Figure 4.22 that the Stokes curves of type B solutions extend to infinity in the complex x-plane. This is due to the fact that the Stokes curves in the complex s-plane extend to infinity as $\text{Re}(s) \to \infty$ as shown in Figure 4.21a. This was not case for the Stokes curves of type A solutions in Section 4.5.4. Instead the Stokes curves of type A solutions emanate from the singularities and approach the logarithmic branch cuts and enter a different Riemann sheet of the inverse transformation; this is illustrated in Figures 4.18a, 4.19a and 4.20a.

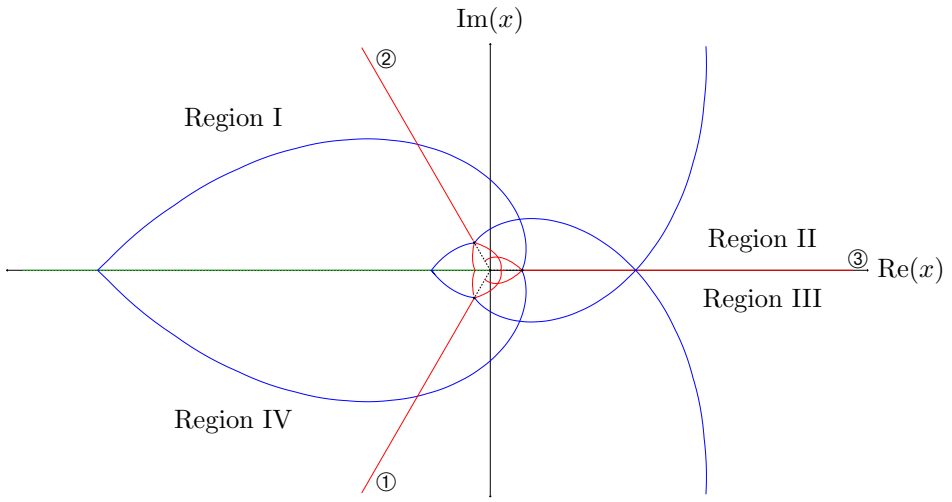

(A) Stokes structure associated with η_j in the complex x-plane

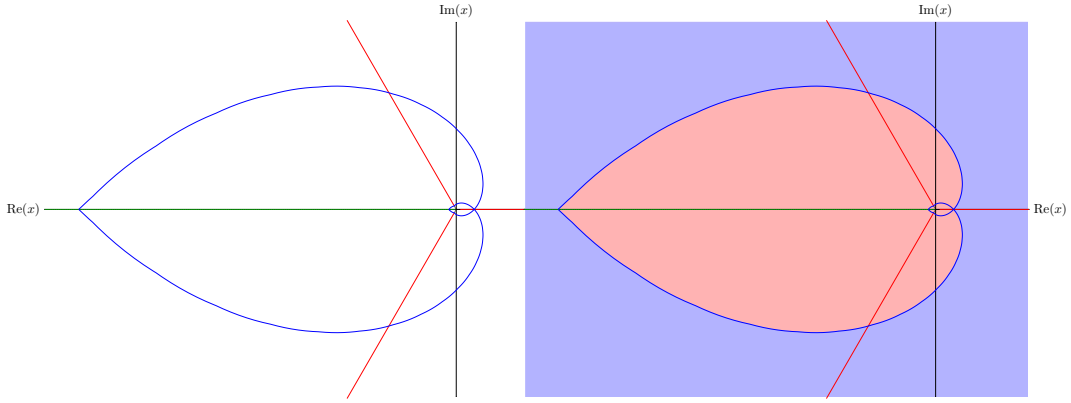

(B) Zoomed out version of Figure 4.22a (C) Regions of validity

FIGURE 4.22. This figure illustrates the Stokes structure of type B solutions of q-$\mathrm{P_I}$ in the original x-plane. Under the inverse transformation (4.212) the Stokes and anti-Stokes curves are described by q-spirals in the x-plane. The exponential contributions associated with η_1, η_2 and η_3 are switched across the Stokes curves labelled by ①, ② and ③, respectively as illustrated in Figure 4.22b. In Figure 4.22c the regions shaded in blue denote regions in which the asymptotic solution described by (4.218) is valid. These are the regions in which the exponential contributions present in (4.218) are exponentially small. The regions shaded in red are regions in which these exponential contributions are exponentially large and hence regions in which the asymptotic behaviour is not described by (4.218).

Furthermore, we recall that the dashed green curves denote the branch cuts of the inverse transformation, (4.212), and therefore the region of the x-plane bounded by these two branch cuts

is not covered by inverse transformation. Therefore, the Stokes and anti-Stokes curve separate the complex x-plane into sectorial regions bounded arcs of spirals.

We have therefore determined the regions of validity for type B asymptotic solutions of q-$\mathrm{P_I}$, (4.111), in the complex x-plane. Type B asymptotic solutions are described by the asymptotic power series expansion (4.218) as $\epsilon \to 0$ and contain a free parameter hidden beyond-all-orders. Furthermore, we have also calculated the Stokes behaviour present within these asymptotic solution, (4.218), which allowed us to determine regions in which this asymptotic description is valid.

4.7. Connection between type A and type B solutions and the nonzero and vanishing asymptotic solutions of q-Painlevé I

In this section we establish a connection between both type A and B solutions found in this study to the nonzero and vanishing asymptotic solutions of q-Painlevé I, respectively. We recall that the nonzero and vanishing asymptotic solutions were first found by Joshi in [**80**]. The nonzero asymptotic solutions of (4.88) are described by the series expansion given by (4.90) where the coefficients are given in (4.91). Whereas the vanishing asymptotic solutions are described by (4.94) where the coefficients are given in (4.95). In particular, the nonzero asymptotic solutions have the following behaviour

$$w(x) \sim \omega^3 + \mathcal{O}\left(\frac{1}{x}\right), \tag{4.219}$$

as $|x| \to \infty$, while the vanishing asymptotic solutions have the behaviour

$$w(x) \sim \frac{1}{x} + \mathcal{O}\left(\frac{1}{x^4}\right), \tag{4.220}$$

as $|x| \to \infty$.

Recall that the four possible solutions for $W_0(s)$ are denoted by $W_{0,j}(s)$, which are defined by (4.123)-(4.126), and the term D is defined by (4.122). In our investigation, we applied the scalings given in (4.110), in which the variable x has the behaviour

$$x \sim e^s + \mathcal{O}(\epsilon), \tag{4.221}$$

as $\epsilon \to 0$. The analysis for both type A and B solutions are valid in the limit $\epsilon \to 0$, which was shown to be equivalent to the limits $|q| \to 1$ and $n \to \infty$. However, under the additional limit, $s \to +\infty$, we see that the behaviour of x in (4.221) approaches infinity. Therefore, the limits $\epsilon \to 0$ and $s \to +\infty$ are equivalent to the limit $|x| \to \infty$.

We now study the behaviour of $W_{0,j}(s)$ under the additional limit $s \to +\infty$. In order to understand the behaviour of $W_{0,j}(s)$ as $s \to +\infty$ we must consider the limiting behaviour of the components A, B, C and D. As D is equal to

$$D = \frac{A}{B^{1/3}} + \frac{B^{1/3}}{C}, \tag{4.222}$$

where the terms A, B and C are defined by equations (4.119)-(4.121). From equations (4.119)-(4.121), we find that

$$\lim_{s\to+\infty} A = 0, \tag{4.223}$$

$$\lim_{s\to+\infty} B = 18, \tag{4.224}$$

$$\lim_{s\to+\infty} C = 2^{1/3}3^{2/3}, \tag{4.225}$$

and hence

$$\lim_{s\to+\infty} D = 1. \tag{4.226}$$

Applying the limit $s \to +\infty$ to the leading order behaviours of $W(s)$, which are given in (4.123)-(4.126) we find that

$$\lim_{s\to+\infty} W_{0,1} = -\frac{1}{2} + i\frac{\sqrt{3}}{2}, \tag{4.227}$$

$$\lim_{s\to+\infty} W_{0,2} = -\frac{1}{2} - i\frac{\sqrt{3}}{2}, \tag{4.228}$$

$$\lim_{s\to+\infty} W_{0,3} = 1, \tag{4.229}$$

$$\lim_{s\to+\infty} W_{0,4} = 0. \tag{4.230}$$

The limiting behaviour of type A solutions under the limit $s \to +\infty$ are therefore described by cube roots of unity. That is

$$W_{0,j} \sim \omega^3, \tag{4.231}$$

for $j = 1, 2, 3$ as $\epsilon \to 0$ and $s \to +\infty$ where $\omega^3 = 1$. However, we find from (4.230) that type B solutions vanish in the limit $s \to +\infty$. We therefore find that type A solutions of (4.111) tend to the nonzero asymptotic behaviour solutions found by Joshi [**80**] under the additional limit $s \to +\infty$.

In order to calculate the leading order behaviour of $W_{0,4}(s)$ as $s \to +\infty$, we need to keep terms up to order $\mathcal{O}(e^{-3s})$. From equation (4.120), we find that

$$B \sim 18 - \frac{128e^{-3s}}{3} + \mathcal{O}(e^{-6s}), \tag{4.232}$$

as $s \to +\infty$ and hence from (4.122) we obtain

$$D \sim 1 - \frac{4e^{-s}}{3} + \mathcal{O}(e^{-3s}), \tag{4.233}$$

as $s \to +\infty$. By substituting the behaviour of D by (4.233) in (4.126) we find that the behaviour of type B solutions are given by

$$\begin{aligned} W_{0,4} &\sim \frac{1}{2}\sqrt{1 - \frac{4e^{-s}}{3}} - \frac{1}{2}\sqrt{-\left(1 - \frac{4e^{-s}}{3}\right) + \frac{2}{1 - \frac{4e^{-s}}{3}}}, \\ &\sim e^{-s} + \mathcal{O}(e^{-3s}), \end{aligned} \tag{4.234}$$

as $s \to +\infty$. From (4.221) we find that (4.234) is equivalent to the behaviour $1/x$ as $|x| \to \infty$ and hence type B solutions correspond to the vanishing asymptotic behaviour of (4.88).

4.8. Numerical computation for q-Painlevé I

In this section we give a numerical example of (4.109) with the parameter choice of $q = 1 + 0.2i$. Given two initial conditions, w_0 and w_1, a sequence of solutions of (4.109) may be obtained by repeated iteration. In general, only a certain choice of initial conditions will give a solution of (4.109) which tends to the asymptotic behaviour of interest. As in Section 3.6 of Chapter 3 we follow the numerical method demonstrated by [**83**], originally based on the works of [**81**] to find appropriate initial conditions which tend to Type A solutions of (4.109).

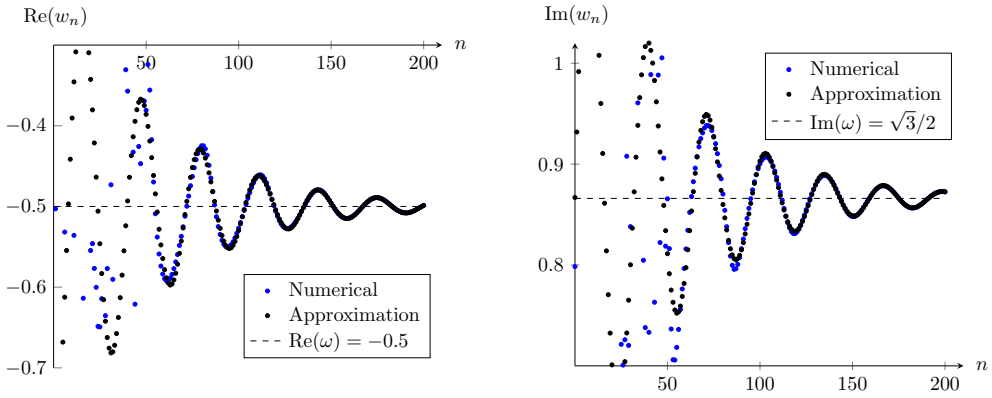

(A) Numerical values of Re(w_n).

(B) Numerical values of Im(w_n)

FIGURE 4.23. This figure illustrates the behaviour of the solutions to (4.109) with $q = 1+0.2i$. The boundary conditions are chosen such that $w_0 = 0.846885522+i0.798385416$ and $w_1 = -0.502881648 - i0.650433326$. The values of w_n are represented as blue circles, and the Type A asymptotic solution, $w_n \sim \omega$ as $n \to \infty$, where $\omega^3 = 1$, is represented by the black cross marks. From Figures 4.23a and 4.23b we see that the behaviour of the difference equation tends to the asymptotic expression for large n.

Figure 4.23 illustrates a comparison between the numerical solution of (4.109) with $q = 1 + 0.2i$ and the initial conditions $w_0 = 0.846885522 + i0.798385416$ and $w_1 = -0.502881648 - i0.650433326$ and the leading order term of (4.90) with $a_0 = (-1 + i\sqrt{3})/2$. Figure 4.23a and 4.23b show that real and imaginary part of w_n converges to $-1/2$ and $\sqrt{3}/2$ respectively for large n, which is precisely the leading order term of (4.90).

As in Section 3.6 of Chapter 3 we are unable to find appropriate initial conditions which give solutions of (4.109) that tend to Type B solutions using the numerical method of [**81**, **83**]. As for the vanishing type solutions of the second discrete Painlevé equation, more sophisticated numerical methods are required in order to capture the Type B solutions of the first q-Painlevé equation.

4.9. Conclusions

In this chapter, we extended the exponential asymptotic methods used in Chapter 3 to compute and investigate Stokes behaviour present in the asymptotic solutions of both the q-Airy equation and q-$\mathrm{P_I}$ in the limits $|q| \to 1$ and $n \to \infty$. In order to investigate the solution behaviour of q-difference equations we rescaled the variables and parameters in the problem such that the limits $|q| \to 1$ and $n \to \infty$ was equivalent to the limit $\epsilon \to 0$. As a result, we refer to this method as the continuum limit-like approach. The solutions of the q-Airy equation are described by the series expansion (4.77), while we found two types of solutions for q-$\mathrm{P_I}$; type A and type B solutions. Type A solutions of q-$\mathrm{P_I}$ are described asymptotically by either (4.201), (4.203) or (4.204), and type B solutions are described by (4.218). In particular, type A and type B are distinguished by the number of their singularities in the principal sheet of the complex plane. The asymptotic descriptions obtained in this analysis are given as a sum of a truncated asymptotic power series and an exponentially-subdominant correction term. We then determined the Stokes structure and used this information to deduce the regions of the complex plane in which these asymptotic solutions are valid.

In Section 4.3, we applied the WKB method for difference equations [**49**] to find that the asymptotic solution of the q-Airy equation is composed of two exponential contribution terms given by (4.74) and (4.75). From this behaviour, we determine the associated Stokes structure, illustrated in Figure 4.3 and qualitatively determine Stokes behaviour present in the asymptotic solution of the q-Airy equation in the limits $|q| \to 1$ and $n \to \infty$.

In Section 4.4 we then applied these methods to study the asymptotic solutions of the first q-Painlevé equation. By applying the continuum limit-like approach we found two classes of asymptotic solutions for (4.111); type A and type B solutions. In Section 4.5 we considered the asymptotic solutions of (4.111) described by type A solutions. Using exponential asymptotic methods, we determined the form of the subdominant exponential contribution present in the asymptotic solutions, which were found to be defined by one free Stokes-switching parameter. From this behaviour, we deduced the associated Stokes structure, illustrated in Figures 4.10a, 4.14a and 4.14b. By considering the Stokes switching behaviour of these subdominant exponentials, we found that the dominant asymptotic behaviour is described by either (4.201), (4.203) or (4.204) in a region in the complex s-plane containing the positive real axis. Furthermore, we found that it is possible to select the Stokes parameters so that the exponential contribution is absent in the regions where it would normally be large. Consequently, the regions of validity for the special type A solutions are larger than the regions of validity for generic type A solutions as illustrated in Figures 4.12b, 4.16b and 4.17b.

In Section 4.6, we considered the equivalent analysis for type B solutions of (4.111). Compared to type A solutions, type B solutions are those which are singular at three points rather than one. Although exponential asymptotic methods may be used again to determine the form of the exponential small contributions present in type B solutions, we noted that the analysis is near identical except for the determination of the singulant of this problem, η. The main difference is due

to the fact that type B solutions are singular at three points rather than one, and the remaining analysis was therefore identical as for type A solutions. Type B asymptotic solutions are given as a sum of a truncated asymptotic power series and three exponentially-subdominant correction terms as described in (4.218). The Stokes structure for type B solutions, illustrated in Figure 4.21, is significantly more complicated than the Stokes structure of type A solutions. In order to describe the Stokes switching behaviour in the domain $\mathcal{D}_0$ we must understand how the asymptotic solution (4.218) interacts with solutions on different Riemann sheets. However, we restrict ourselves to regions I-IV as these regions are free of the interaction effects originating from the different Riemann sheets. Furthermore, all three exponential contributions present in type B solutions are exponentially subdominant in regions I-IV and therefore represent the regions of validity of (4.218). Consequently, the asymptotic solutions described by (4.218) contain one free parameter defined by the Stokes multiplier.

By reversing the rescaling transformations we are then able to obtain the corresponding Stokes structure in the complex x-plane. In both investigations of the q-Airy and q-$\mathrm{P_I}$ equation, we found that the Stokes and anti-Stokes curves are described by q-spirals in the complex plane. As a result, the regions of validity are no longer described by traditional sectors bounded by rays but sectorial regions bounded by arcs of spirals.

In Section 4.7 we showed that type A and B solutions are related to the nonzero asymptotic and vanishing asymptotic solutions found by Joshi [**80**]. If the additional limit $s \to +\infty$ is also taken, then we find that type A solutions correspond to the nonzero asymptotic solutions of q-$\mathrm{P_I}$ while type B solutions correspond to the quicksilver solutions of q-$\mathrm{P_I}$ [**80**].

CHAPTER 5

Conclusions

In this thesis, we have shown how exponential asymptotic methods can be applied to both additive and multiplicative difference equations in order to investigate Stokes behaviour present in their solutions under some limit. The exponential methods we use are based on the works of Chapman, et al. [**32**] and King and Chapman [**92**] under the framework of matched asymptotic expansions developed by Olde Daalhuis [**121**]. The main equations of interest in this thesis were the discrete Painlevé equations. In particular, we studied the second discrete Painlevé equation and the first q-Painlevé equation. They were chosen as they are of potential use in mathematical physics problems and are regarded as defining new, nonlinear special functions.

In Chapter 3 we determined two types of solution behaviour for the second discrete Painlevé equation ($\mathrm{dP_{II}}$) which have vanishing and non-vanishing type behaviours in the limit as the independent variable approaches infinity. We achieve this by introducing a small parameter, ϵ, by rescaling the variables present in the problem. In doing so, the difference equation may then be transformed into another difference equation for which the step size is small in the limit $\epsilon \to 0$. The resulting difference equation can then be considered as a differential equation of infinite order. We call this the continuum limit-like approach. In both cases, we showed that solutions of $\mathrm{dP_{II}}$ with these limiting behaviours are asymptotic to two types of power series expansions which contain exponentially subdominant correction terms. We then studied Stokes behaviour present within these series expansions and used this information to deduce regions in the complex plane in which they are valid. We obtain a one-parameter family of asymptotic power series expansions of $\mathrm{dP_{II}}$. The free parameter contained within these asymptotic power series are hidden beyond-all-orders as they were shown to be encoded within the Stokes multipliers. Furthermore we showed it is possible to select particular values of the free parameter such the asymptotic power series expansions are valid in a wider domain, obtaining special asymptotic solutions for $\mathrm{dP_{II}}$.

In addition to obtaining one- and zero-parameter asymptotic series expansions for $\mathrm{dP_{II}}$, we found that these solutions share similar features to the tronquée and tri-tronquée solutions of the second Painlevé equation. When the scalings are undone, the asymptotic solutions we find are described by $x_n \sim -\gamma/\alpha n$ or $x_n \sim \pm i\sqrt{\alpha n/2}$ as $n \to \infty$. The (tri)-tronquée solutions of the second Painlevé equation are described to leading order by $y \sim -\mu/t$ or $y \sim \sqrt{-t/2}$ as $|t| \to \infty$. Furthermore, the tronquée solutions contain a free parameter hidden beyond-all-orders while the tri-tronquée solutions are uniquely specified, both of which are also described by asymptotic power series in certain sectors in the complex plane. The asymptotic solutions we find for $\mathrm{dP_{II}}$ may

therefore be regarded as the discrete analogues of the tronquée and tri-tronquée solutions of the second Painlevé equation.

In Chapter 4, we investigated Stokes behaviour in the asymptotic solutions of q-difference equations in the limits $|q| \to 1$ and $n \to \infty$. In order to demonstrate the applicability of the continuum limit-like approach to both linear and nonlinear q-difference equations, we studied a q-analogue of the Airy equation and the first q-Painlevé in the limits $|q| \to 1$ and $n \to \infty$. In particular, we chose to rescale q by setting $q = 1 + \epsilon$. We note that different choices of scalings may also be applied to the parameter q and the effects of these different choices of scalings may be considered as the subject of future work.

In the first part of Chapter 4 we use the WKB method to show that the asymptotic solution of the q-Airy equation is a linear combination of two exponential contribution terms where the constants are replaced q-periodic functions. In particular, these two asymptotic solutions describe two linearly independent solutions of the q-Airy equation. Although we did not determine the full asymptotic power series expansions of the q-Airy equation, we were still able to successfully deduce the Stokes structure and Stokes behaviour present within these asymptotic solution. We found that the Stokes and anti-Stokes curves are described by q-spirals in the original coordinate space and hence the regions of validity are no longer bounded by traditional rays but bounded by arcs of spirals. For further study, the complete asymptotic series expansion of the q-Airy should be computed. This would then allow the Stokes behaviour of the q-Airy function to be explicitly computed.

In the second part of Chapter 4, we then considered the first q-Painlevé equation in the limit as $|q| \to 1$. In particular, we were able to distinguish two types of solution behaviour which we called type A and type B solutions. Both type A and type B solutions were shown to be described by divergent asymptotic power series expansions which contain exponentially subdominant exponential terms. The distinguishing feature between type A and type B solutions is that type A solutions are singular at one point in the complex plane while type B solutions are singular at three points. As a result, type A solutions contain one exponentially subdominant correction term while type B solutions contain three exponentially subdominant correction terms in their asymptotic series expansions. As in the case of the q-Airy equation, we showed that the Stokes structure of the q-Painlevé equation is also described by q-spirals which separate the complex plane into sectorial regions bounded by arcs of these spirals.

Using exponential asymptotic methods, the asymptotic power series expansions of type A and type B solutions of q-$\mathrm{P_I}$ are given as a sum of a truncated asymptotic power series and exponentially subdominant correction terms which are valid in certain regions in the complex plane. Furthermore, these asymptotic descriptions contain a free parameter hidden beyond all order like those found in Chapter 3. Additionally, we also show that it is possible to select particular values of the free parameter such that the asymptotic descriptions of type A solutions are valid in a wider region of the complex plane. As the asymptotic power series expansion is uniquely specified, we call these the special type A asymptotic solutions of q-$\mathrm{P_I}$. However, this is not possible for type B solutions

due to its complicated Stokes structure. We found that there are Stokes curves emerging from the branch cuts which originate from the different Riemann sheets defined by type B solutions. Fortunately, we are able to identify regions in the complex plane which are free of such Stokes curves, and in which the exponential contributions present in the asymptotic series expansion of type B solutions are exponentially small. For future research, the interaction effects originating from the different Riemann sheets of type B solutions should be investigated. This introduces the possibility of higher-order Stokes phenomenon effects as the Stokes curves of the principle Riemann sheet may interact with the Stokes curves originating from other Riemann sheets. By understanding these interaction effects, it may be possible to determine special type B asymptotic solutions. This is currently beyond the scope of this thesis and will therefore be the subject of future research.

APPENDIX A

Singularity Confinement

In order to illustrate the idea of singularity confinement we consider the discrete Painlevé I, which is given by (1.14). Given any two initial conditions, say $x_n = \mu$ and $x_{n-1} = \nu$ we may iterate equation (1.14) forwards $(n \mapsto n+1)$ or backwards $(n \mapsto n-1)$ in order to obtain a sequence of solutions. We can do this indefinitely provided that $x_{n_0} \neq 0$ for some n_0, which is a singularity of (1.14).

In order to study how this singularity propagates upon successive iteration, we let $x_0 = \mu$ and $x_1 = \epsilon$ and iterate forward in time. By successive iteration we find that

$$x_2 \sim \frac{\alpha+\beta}{\epsilon}, \tag{A.1}$$

$$x_3 \sim -\frac{\alpha+\beta}{\epsilon}, \tag{A.2}$$

$$x_4 \sim -\frac{4\alpha+\beta}{\alpha+\beta}\epsilon, \tag{A.3}$$

$$x_5 \sim \frac{2\alpha\gamma+\mu\,(\alpha+\beta)}{4\alpha+\beta}, \tag{A.4}$$

as $\epsilon \to 0$. By starting arbitrarily close to the singularity, we find that the iterates x_2 and x_3 tend to $+\infty$ and $-\infty$, respectively. The singularity persists upon iteration, to leading order, and is therefore said to propagate upon iteration. The next iterate, x_4, is proportional to ϵ as $\epsilon \to 0$ as shown in (A.3). However, we find from (A.4) that x_5 is not dependent on ϵ. In particular, we also find that the initial condition, μ, appears in the leading order expression for x_5.

Therefore, we observe that the singularity disappears within four forward iterations and that the initial condition, $x_0 = \mu$, is recovered. In fact, it can be shown that further iterations are non-vanishing in the limit $\epsilon \to 0$ and thus the singularity is confined.

APPENDIX B

Error of the singulant and prefactor

Let us consider the sum

$$E(z;r) = \sum_{k=r}^{\infty} \frac{z^{2k}}{(2k)!}. \tag{B.1}$$

We will that the function $E(x;r)$ is exponentially small in z as $r \to \infty$. The sum in (B.1) can be rewritten as

$$\begin{aligned} E(z;r) &= \frac{z^{2r}}{(2r)!} \sum_{n=0}^{\infty} \frac{(1)_n}{(r+1/2)_n (r+1)_n} \frac{1}{n!} \left(\frac{z}{2}\right)^{2n}, \\ &= z^{2r} \sum_{n=0}^{\infty} \frac{z^{2n}}{\Gamma(2r+2n+1)}, \end{aligned} \tag{B.2}$$

where $(a)_k$ is the *falling factorial* [**2**]. For large values of r, we replace the Gamma function appearing in the denominator of the sum in (B.2) by Stirling's formula in order to obtain

$$E(z;r) \sim \frac{z^{2r}}{\sqrt{2\pi} e^{-2r} (2r)^{2r+1/2}} \sum_{n=0}^{\infty} \frac{z^{2n}}{(2r)^{2n}} = \frac{z^{2r} e^{2r}}{\sqrt{2\pi} (2r)^{2r+1/2}} \frac{4r^2}{2r^2 - z^2}, \tag{B.3}$$

which is exponentially small in z as $r \to \infty$.

APPENDIX C

Stokes smoothing via Borel summation

We consider a function $f(s)$, which is asymptotic to a factorially divergent power series in ϵ. In particular we consider

$$f(s) \sim \sum_{r=0}^{\infty} \epsilon^r \frac{F(s)\Gamma(r+\gamma)}{\chi(s)^{r+\gamma}}, \tag{C.1}$$

as $\epsilon \to 0$. We may optimally truncate (C.1) by writing

$$f(s) \sim \sum_{r=0}^{N-1} \epsilon^r \frac{F(s)\Gamma(r+\gamma)}{\chi(s)^{r+\gamma}} + \sum_{r=N}^{\infty} \epsilon^r \frac{F(s)\Gamma(r+\gamma)}{\chi(s)^{r+\gamma}}, \tag{C.2}$$

as $\epsilon \to 0$, where $N = |\chi|/\epsilon + \omega$. The error function smoothing of the asymptotic series (C.1) may be obtained by applying Borel summation methods to the divergent tail in (C.2) [**11**]. The Borel sum of the divergent tail is given by

$$\begin{aligned}\sum_{r=N}^{\infty} \epsilon^r \frac{F(s)\Gamma(r+\gamma)}{\chi(s)^{r+\gamma}} &= \int_0^{\infty} e^{-t} \frac{Ft^{\gamma-1}}{\chi^{\gamma}} \sum_{r=N}^{\infty} \left(\frac{\epsilon t}{\chi}\right)^n dt, \\ &= \frac{F}{\epsilon^{\gamma}} \int_0^{\infty} \exp\left(\frac{1}{\epsilon}(-\chi y + |\chi| \log(y))\right) \frac{y^{\omega}}{1-y} dy, \end{aligned} \tag{C.3}$$

as $\epsilon \to 0$. The integral (C.3) has a saddle point at $y = |\chi|/\chi$, which coincides with the pole of (C.3) for $\mathrm{Im}(\chi) = 0$ and $\mathrm{Re}(\chi) > 0$. This coincides with the characterization of Stokes curves in Section 2.4 of Chapter 2. Away from the Stokes curves, the leading order behaviour of the divergent tail may be obtained using the method of steepest descents [**8**]. To determine the behaviour of the divergent tail near the Stokes curves, we follow [**11, 24**] and let $T = y - 1$. Under this change of variable, (C.3) becomes

$$R_N \sim -\frac{F}{\epsilon^{\gamma}} \int_{-1}^{\infty} \exp\left(\frac{1}{\epsilon}(-\chi(1+T) + |\chi| \log(1+T))\right) \frac{(1+T)^{\omega}}{T} dT, \tag{C.4}$$

as $\epsilon \to 0$. Near the Stokes curve, the integrand of (C.4) is localized near $T = 0$. In particular, we have

$$-\chi(1+T) + |\chi| \log(1+T) \sim -\chi + (|\chi| - \chi)T - \frac{|\chi|}{2} T^2 + \mathcal{O}(T^3), \tag{C.5}$$

$$\frac{(1+T)^{\omega}}{T} \sim \frac{1}{T} + \mathcal{O}(1), \tag{C.6}$$

as $T \to 0$. If we let $\chi = |\chi|e^{i\theta}$, then we also have

$$|\chi| - \chi \sim -i|\chi|\theta, \tag{C.7}$$

as $\theta \to 0$. Using (C.5)-(C.6) and (C.7), we find that the behaviour of (C.4), after taking the Cauchy principal value integral, near the Stokes curve may be approximated by

$$R_N \sim -\frac{Fe^{-\chi/\epsilon}}{\epsilon^\gamma}\left(\int_{-\infty}^{\infty}\exp\left(-\frac{i|\chi|\theta T}{\epsilon} - \frac{|\chi|T^2}{2\epsilon}\right)\frac{1}{T}dT + \tilde{C}\right), \tag{C.8}$$

as $T \to 0$, where $\tilde{C}$ is a constant. To evaluate (C.8) we use the following Fourier transform identity [**24**]

$$\lim_{\delta\to 0}\left(-\frac{i}{2\pi}\int_{-\infty}^{\infty}\exp(-ikx)\exp(-a^2k^2)\frac{1}{k+i\delta}dk\right) = \frac{1}{2} + \frac{1}{2}\text{erf}\left(\frac{x}{2a}\right). \tag{C.9}$$

Using (C.9), we find that (C.8) may be evaluated to give

$$R_N \sim -\frac{Fe^{-\chi/\epsilon}}{\epsilon^\gamma}\left(i\pi\ \text{erf}\left(\theta\sqrt{\frac{|\chi|}{2\epsilon}}\right) + i\pi + \tilde{C}\right), \tag{C.10}$$

as $\epsilon \to 0$ near the Stokes curves. We denote the divergent tail as $R_N = \mathcal{S}Fe^{-\chi/\epsilon}$ where $\mathcal{S}$ is the Stokes multiplier. Then from (C.10) we find that the Stokes multiplier is given by

$$\mathcal{S} \sim -\frac{1}{\epsilon^\gamma}\left(i\pi\ \text{erf}\left(\theta\sqrt{\frac{|\chi|}{2\epsilon}}\right) + i\pi + \tilde{C}\right), \tag{C.11}$$

as $\epsilon \to 0$. Hence the asymptotic series (C.1) is given by

$$f(s) \sim \sum_{r=0}^{N-1}\epsilon^r\frac{F\Gamma(r+\gamma)}{\chi^{r+\gamma}} - \frac{Fe^{-\chi/\epsilon}}{\epsilon^\gamma}\left(i\pi\ \text{erf}\left(\theta\sqrt{\frac{|\chi|}{2\epsilon}}\right) + i\pi + \tilde{C}\right), \tag{C.12}$$

as $\epsilon \to 0$.

C1. Example from Chapman, King and Adams.

In the study by Chapman, King and Adams [**32**], they considered a problem with an asymptotic solution given by

$$\phi(s) \sim \sum_{r=0}^{\infty}\epsilon^{2r}\phi_r(s), \tag{C.13}$$

as $\epsilon \to 0$, where

$$\phi_r(s) \sim \frac{\Lambda\Gamma(2r+\gamma+1)(-1)^r}{\sqrt{\phi_0'}(s-\sigma)^{2r+\gamma+1}}, \tag{C.14}$$

as $r \to \infty$, where γ, Λ are constants and $\phi_0 = \phi_0(s)$. Using the Stokes smoothing method, the authors of [**32**] showed that

$$\phi(s) \sim \sum_{r=0}^{N-1}\epsilon^{2r}\phi_r(s) + \frac{\Lambda\pi e^{i\pi\gamma/2}e^{-i(s-\sigma)/\epsilon}}{2\epsilon^{\gamma+1}\sqrt{\phi_0'}}\left(\text{erf}\left((\theta+\pi/2)\sqrt{\frac{|s-\sigma|}{2\epsilon}}\right) + C\right), \tag{C.15}$$

as $\epsilon \to 0$, where C is a constant. We show that the form of the remainder term may also be obtained by Borel summation methods. We first rewrite (C.14) as

$$\phi_r(s) \sim \frac{\Lambda e^{i\pi(\gamma+1)/2}\Gamma(2r+\gamma+1)}{\sqrt{\phi_0'}((s-\sigma)e^{i\pi/2})^{2r+\gamma+1}}, \tag{C.16}$$

as $r \to \infty$. The Borel sum of the divergent tail of (C.13) is given by

$$\begin{aligned} R_N &\sim \frac{\Lambda e^{i\pi(\gamma+1)/2}}{\sqrt{\phi_0'}((s-\sigma)e^{i\pi/2})^{\gamma+1}} \int_0^\infty e^{-t}t^\gamma \sum_{r=N}^{\infty} \left(\frac{\epsilon t}{(s-\sigma)e^{i\pi/2}}\right)^{2r} dt, \\ &= \frac{\Lambda e^{i\pi(\gamma+1)/2}}{\sqrt{\phi_0'}((s-\sigma)e^{i\pi/2})^{\gamma+1}} \int_0^\infty e^{-t}t^\gamma \frac{\left(\frac{\epsilon t}{(s-\sigma)e^{i\pi/2}}\right)^{2N}}{1-\left(\frac{\epsilon t}{(s-\sigma)e^{i\pi/2}}\right)^2} dt, \end{aligned} \tag{C.17}$$

as $\epsilon \to 0$, and where $N = |s-\sigma|/(2\epsilon) + \alpha$. If we let $y = \epsilon t/((s-\sigma)e^{i\pi/2})$ then (C.17) becomes

$$R_N \sim \frac{\Lambda e^{i\pi(\gamma+1)/2}}{\epsilon^{\gamma+1}\sqrt{\phi_0'}} \int_0^\infty \exp\left(\frac{1}{\epsilon}\left(-(s-\sigma)e^{i\pi/2}y + |s-\sigma|\log(y)\right)\right) \frac{y^{2\alpha+\gamma}}{1-y^2} dy, \tag{C.18}$$

as $\epsilon \to 0$. The saddle point of (C.18) is located at $y = |s-\sigma|e^{-i\pi/2}/(s-\sigma)$, which coincides with the pole of (C.18) if $\mathrm{Re}(s-\sigma) > 0$ and $\mathrm{Arg}(s-\sigma) = -\pi/2$; which are the locations of the Stokes curves. To investigate the behaviour of (C.18) near the Stokes curves we apply the substitution $y = 1+T$ in (C.18) to give

$$R_N \sim \frac{\Lambda e^{i\pi(\gamma+1)/2}}{\epsilon^{\gamma+1}\sqrt{\phi_0'}} \int_{-1}^\infty \exp\left(\frac{1}{\epsilon}\left(-(s-\sigma)e^{i\pi/2}(1+T) + |s-\sigma|\log(1+T)\right)\right) \frac{(1+T)^{2\alpha+\gamma}}{1-(1+T)^2} dT, \tag{C.19}$$

as $\epsilon \to 0$. Near the Stokes curve, (C.19) is approximated by

$$R_N \sim -\frac{\Lambda e^{i\pi(\gamma+1)/2}e^{-i(s-\sigma)/\epsilon}}{2\epsilon^{\gamma+1}\sqrt{\phi_0'}} \left(\int_{-\infty}^\infty \exp\left(-\frac{i|s-\sigma|(\theta+\pi/2)T}{\epsilon} - \frac{|s-\sigma|T^2}{2\epsilon}\right)\frac{1}{T}dT + \hat{C}\right), \tag{C.20}$$

as $\epsilon \to 0$, where $\hat{C}$ is a constant. Using (C.9) we can evaluate (C.20) to obtain

$$R_N \sim \frac{\Lambda\pi e^{i\pi\gamma/2}e^{-i(s-\sigma)/\epsilon}}{2\epsilon^{\gamma+1}\sqrt{\phi_0'}} \left(\mathrm{erf}\left((\theta+\pi/2)\right)\sqrt{\frac{|s-\sigma|}{2\epsilon}} + \overline{C}\right), \tag{C.21}$$

as $\epsilon \to 0$, where $\overline{C}$ is a constant. Comparing the forms of the divergent tail in (C.21) and (C.13) show that they are identical. Hence, finding the form of the divergent tail may be obtained by either using the Stokes smoothing method demonstrated in [**32**, **92**, **121**] or by Borel summation.

APPENDIX D

Series expansion for $x = q^n$ as $\epsilon \to 0$

The choice of rescalings given by $n = \epsilon s$ and $q = 1+\epsilon$ allow us to expand the non autonomous term, $x = q^n$, as a power series in ϵ. In order to obtain the general series expansion of $x = q^n$ we follow the work of Brede [**27**]. We let

$$E(s) := (1+\epsilon)^{s/\epsilon}. \tag{D.1}$$

The goal is to determine the coefficients of the series expansion of (D.1) in powers of ϵ. The first step in determining the general form of the coefficients is to rewrite (D.1) as an exponential. We do this by writing

$$E(s) = \exp\left(\frac{s}{\epsilon}\log(1+\epsilon)\right) = e^s \sum_{k=0}^{\infty}\left(\frac{s}{\epsilon}\right)^k \left(\sum_{n=2}^{\infty}\frac{(-1)^{n+1}\epsilon^n}{n}\right)^k.$$

This function can then be rewritten as

$$E(s) = e^s\left(1 - \frac{s}{2}\epsilon + \left(\frac{s}{2}+\frac{s^2}{8}\right)\epsilon^2 - \left(\frac{s}{4}+\frac{s^2}{6}+\frac{s^3}{48}\right)\epsilon^3 + \cdots\right).$$

Hence, we infer that the function $E(s)$ has the form

$$E(s) = e^s \sum_{n=0}^{\infty} P_n(s)\epsilon^n, \tag{D.2}$$

where $P_n(s)$ is an n^{th} degree polynomial in s. The second part makes use of the Binomial theorem. Using the Binomial theorem, we may write (D.1) as

$$E(s) = \sum_{k=0}^{\infty}\binom{s/\epsilon}{k}\epsilon^k = \sum_{k=0}^{\infty}\frac{\epsilon^k}{k!}\left(\frac{s}{\epsilon}\right)_k,$$

where $(s/\epsilon)_k$ is the *falling factorial* [**2**]. By using the Stirling numbers of the first kind [**1**], $s_1(n,k)$, we can rewrite the above expression as

$$\begin{aligned} E(s) &= \sum_{n=0}^{\infty} \frac{\epsilon^n}{n!} \sum_{k=0}^{n} s_1(n,k) \left(\frac{s}{\epsilon}\right)^k, \\ &= \sum_{n=0}^{\infty} \frac{1}{n!} \sum_{k=0}^{n} \epsilon^k s^{n-k} s_1(n,n-k), \\ &= \sum_{k=0}^{\infty} \left(\frac{\epsilon}{s}\right)^k \sum_{n=k}^{\infty} \frac{s^n}{n!} s_1(n,n-k). \end{aligned} \tag{D.3}$$

The second equality can be obtained by explicitly writing out the second sum and by simple manipulation. While the third equality is a result of changing the order of summation. We have therefore obtained two different expressions for the series expansion of $E(s)$ in powers of ϵ. In particular, these two expansions must be equal to each other. By comparing the coefficients of ϵ in both (D.2) and (D.3) we find that

$$\begin{aligned} P_n(s) &= \sum_{m=0}^{\infty} \frac{(-1)^m s^m}{m! n} \sum_{k=0}^{\infty} \frac{s_1(k+n,k)}{(k+n)!} s^k, \\ &= \sum_{r=0}^{\infty} s^r \sum_{k=0}^{r} \frac{(-1)^{r-k}}{(r-k)!} \frac{s_1(k+n,k)}{(k+n)!}. \end{aligned}$$

However, we noted that $P_n(s)$ is an n^{th} degree polynomial in s. As a by product we obtain the result

$$\sum_{k=0}^{r} \frac{(-1)^{r-k}}{(r-k)!} \frac{s_1(k+n,k)}{(k+n)!} = 0,$$

for $r > n$ and

$$P_n(s) = \sum_{r=0}^{n} s^r \sum_{k=0}^{r} \frac{(-1)^{r-k}}{(r-k)!} \frac{s_1(k+n,k)}{(k+n)!}. \tag{D.4}$$

Thus, the function $E(s) = (1+\epsilon)^{s/\epsilon}$ may be written as (D.2) with $P_n(s)$ given by (D.4). Here are the first few expressions for $P_n(s)$:

$$\begin{aligned}
P_0(s) &= 1, \\
P_1(s) &= -\frac{s}{2}, \\
P_2(s) &= \frac{s(3s+8)}{24}, \\
P_3(s) &= \frac{-s(s^2+8s+12)}{48}, \\
P_4(s) &= \frac{s(15s^3+240s^2+1040s+1152)}{5760}.
\end{aligned}$$

References

[1] NIST Digital Library of Mathematical Functions. http://dlmf.nist.gov/, Release 1.0.17 of 2017-12-22. F. W. J. Olver, A. B. Olde Daalhuis, D. W. Lozier, B. I. Schneider, R. F. Boisvert, C. W. Clark, B. R. Miller and B. V. Saunders, eds.

[2] M. Abramowitz and I. A. Stegun. *Handbook of Mathematical Functions with Formulas, Graphs, and Mathematical Tables*. Dover Publications, Inc., New York, 1992.

[3] C. R. Adams. On the linear ordinary q-difference equation. *Ann. of Math. (2)*, 30:195–205, 1928/29.

[4] S. Ahmad and A. Ambroseti. *A Textbook on Ordinary Differential Equations*. Springer International Publishing, 2015.

[5] I. Aniceto, R. Schiappa, and M. Vonk. The resurgence of instantons in string theory. *Commun. Number Theory Phys.*, 6:339–496, 2012.

[6] T. Aoki, T. Koike, and Y. Takei. Vanishing of Stokes curves. In T. Kawai and K. Fujita, editors, *Microlocal Analysis and Complex Fourier Analysis*. World Sci. Publ., River Edge, NJ, 2002.

[7] P. Bachmann. *Analytische Zahlentheorie*, volume 2. Leipzig, 1894.

[8] C. M. Bender and S. A. Orszag. *Advanced Mathematical Methods for Scientists and Engineers.I*. Springer-Verlag, New York, 1999.

[9] H. L. Berk, W. M. Nevins, and K. V. Roberts. New Stokes' lines in WKB theory. *J. Math. Phys.*, 23:988–1002, 1982.

[10] M. V. Berry. Stokes' phenomenon; smoothing a Victorian discontinuity. *Publ. Math. Inst. Hautes Études Sci.*, 68:211–221, 1988.

[11] M. V. Berry. Uniform asymptotic smoothing of Stokes' discontinuities. *Proc. R. Soc. A*, 422:7–21, 1989.

[12] M. V. Berry. Asymptotics, superasymptotics, hyperasymptotics. . .. In H. Segur, S. Tanveer, and H. Levine, editors, *Asymptotics Beyond All Orders*. Plenum, New York, 1991.

[13] M. V. Berry and C. J. Howls. Hyperasymptotics. *Proc. R. Soc. A*, 430:653–668, 1990.

[14] M. V. Berry and C. J. Howls. Hyperasymptotics for integrals with saddles. *Proc. R. Soc. A*, 434:657–675, 1991.

[15] M. V. Berry and C. J. Howls. Unfolding the high orders of asymptotic expansions with coalescing saddles: singularity theory, crossover and duality. *Proc. R. Soc. A*, 443:107–126, 1993.

[16] M. Bertola and A. Tovbis. Asymptotics of orthogonal polynomials with complex varying quartic weight: Global structure, critical point behavior and the first Painlevé equation. *Constr. Approx.*, 41:529–587, 2015.

[17] G. D. Birkhoff. General theory of linear difference equations. *Trans. Amer. Math. Soc.*, 12:243–284, 1911.

[18] G. D. Birkhoff and P. E. Guenther. Note on a canonical form for the linear q-difference system. *Proc. Natl. Acad. Sci. USA*, 27:218–222, 1941.

[19] G. D. Birkhoff and W. J. Trjitzinsky. Analytic theory of singular difference equations. *Acta Math.*, 60:1–89, 1933.

[20] L. Boelen, G. Filipuk, and W. Van Assche. Recurrence coefficients of generalized Meixner polynomials and Painlevé equations. *J. Phys. A*, 44:035202, 19, 2011.

[21] E. Borel. *Leçons sur les Series Divergentes*. Gauthier-Villars, 1901.

[22] S. Boscolo, S. K. Turitsyn, V. Y. Novokshenov, and J. H. B. Nijhof. Self-similar parabolic optical solitary waves. *Theoret. and Math. Phys.*, 133:1647–1656, 2002.

[23] P. Boutroux. Recherches sur les transcendantes de m. Painlevé et l'étude asymptotique des équations différentielles du second ordre. *Ann. Sci. École Norm. Sup.*, 30:255–375, 1913.

[24] J. P. Boyd. The devil's invention: asymptotic, superasymptotic and hyperasymptotic series. *Acta Appl. Math.*, 56:1–98, 1999.

[25] J. P. Boyd. Hyperasymptotics and the linear boundary layer problem: why asymptotic series diverge. *SIAM Rev.*, 47:553–575, 2005.

[26] B. L. J. Braaksma, G. K. Immink, M. Van der Put, and J. Top, editors. *Differential equations and the Stokes phenomenon*. Proceedings of the workshop held at the University of Groningen, Groningen, May 28–30, 2001, World Scientific Publishing Co., Inc., River Edge, NJ, 2002.

[27] M. Brede. On the convergene of the sequence defining Euler's number. *Math. Intelligencer*, 27:6–7, 2005.

[28] É. Brézin and V. A. Kazakov. Exactly solvable field theories of closed strings. *Phys. Lett. B*, 236:144–150, 1990.

[29] L. Brillouin. La mécanique ondulatoire de schrödinger: une méthode générale de resolution par approximations successives. *Comptes Rendus de l'Academie des Sciences*, 183:24–26, 1926.

[30] R. D. Carmichael. The General Theory of Linear q-Difference Equations. *Amer. J. Math.*, 34:147–168, 1912.

[31] S. J. Chapman, C. J. Howls, J. R. King, and A. B. Olde Daalhuis. Why is a shock not a caustic? The higher-order Stokes phenomenon and smoothed shock formation. *Nonlinearity*, 20:2425–2452, 2007.

[32] S. J. Chapman, J. R. King, and K. L. Adams. Exponential asymptotics and Stokes lines in nonlinear ordinary differential equations. *Proc. R. Soc. A*, 454:2733–2755, 1998.

[33] S. J. Chapman and D. B. Mortimer. Exponential asymptotics and Stokes lines in a partial differential equation. *Proc. R. Soc. A*, 461:2385–2421, 2005.

[34] A. Cherman, D. Dorigoni, G. V. Dunne, and M. Ünsal. Resurgence in quantum field theory: Nonperturbative effects in the principle chiral model. *Phys. Rev. Lett.*, 112:5, 2014.

[35] T. Claeys and T. Grava. Painlevé II asymptotics near the leading edge of the oscillatory zone for the Korteweg-de Vries equation in the small-dispersion limit. *Comm. Pure Appl. Math.*, 63:203–232, 2010.

[36] P. A. Clarkson. Painlevé equations—nonlinear special functions. In *Proceedings of the Sixth International Symposium on Orthogonal Polynomials, Special Functions and their Applications (Rome, 2001)*, volume 153, pages 127–140, 2003.

[37] O. Costin. *Asymptotics and Borel Summability*. CRC Press, Boca Raton, FL, 2009.

[38] O. Costin and R. D. Costin. On the formation of singularities of solutions of nonlinear differential systems in antistokes directions. *Invent. Math.*, 145:425–485, 2001.

[39] O. Costin and R. D. Costin. Asymptotic properties of a family of solutions of the Painlevé equation $\mathrm{P_{VI}}$. *Int. Math. Res. Not. IMRN*, pages 1167–1182, 2002.

[40] O. Costin, R. D. Costin, and M. Huang. Tronquée solutions of the Painlevé equation PI. *Constr. Approx.*, 41:467–494, 2015.

[41] O. Costin and M. D. Kruskal. Optimal uniform estimates and rigorous asymptotics beyond all orders for a class of ordinary differential equations. *Proc. R. Soc. A*, 452:1057–1085, 1996.

[42] O. Costin and M. D. Kruskal. On optimal truncation of divergent series solutions of nonlinear differential systems. *Proc. R. Soc. A*, 455:1931–1956, 1999.

[43] G. Darboux. Mémoire sur l'approximation des fonctions de tresgrands nombres, et sur une classe étendue de développements en serie. *J. Math. Pures. Appl.*, 4:5–56, 1878.

[44] G. Darboux. Mémoire sur l'approximation des fonctions de tresgrands nombres, et sur une classe étendue de développements en serie. *J. Math. Pures. Appl.*, 4:377–416, 1878.

[45] P. A. Deift and X. Zhou. A steepest descent method for oscillatory Riemann-Hilbert problems. *Bull. Amer. Math. Soc. (N.S.)*, 26:119–123, 1992.

[46] E. Delabaere and C. J. Howls. Global asymptotics for multiple integrals with boundaries. *Duke Math. J.*, 112:199–264, 2002.

[47] L. Di Vizio and C. Zhang. On q-summation and confluence. *Ann. Inst. Fourier (Grenoble)*, 59:347–392, 2009.

[48] R. B. Dingle. *Asymptotic Expansions: their Derivation and Interpretation*. Academic Press, London-New York, 1973.

[49] R. B. Dingle and G. J. Morgan. WKB methods for difference equations. I, II. *Appl. Sci. Res.*, 18:221–237, 1967.

[50] M. Duits and A. B. J. Kuijlaars. Painlevé I asymptotics for orthogonal polynomials with respect to a varying quartic weight. *Nonlinearity*, 19:2211–2245, 2006.

[51] G. V. Dunne and M. Ünsal. Resurgence and trans-series in quantum field theory: the $\mathbb{CP}^{N-1}$ model. *J. High Energy Phys.*, 170, 2012.

[52] J. Écalle. *Les Fonctions Résurgentes. Tome I*. Université de Paris-Sud, Département de Mathématique, Orsay, 1981.

[53] S. Elaydi. *An Introduction to Difference Equations*. Springer, New York, 2005.

[54] G. Filipuk, W. Van Assche, and L. Zhang. The recurrence coefficients of semi-classical Laguerre polynomials and the fourth Painlevé equation. *J. Phys. A*, 45:205201, 13, 2012.

[55] A. S. Fokas and M. J. Ablowitz. Linearization of the Korteweg-de Vries and Painlevé II equations. *Phys. Rev. Lett.*, 47:1096–1100, 1981.

[56] A. S. Fokas, B. Grammaticos, and A. Ramani. From continuous to discrete Painlevé equations. *J. Math. Anal. Appl.*, 180:342–360, 1993.

[57] A. S. Fokas, A. R. Its, and A. V. Kitaev. Discrete Painlevé equations and their appearance in quantum gravity. *Comm. Math. Phys.*, 142:313–344, 1991.

[58] P. J. Forrester and N. S. Witte. Discrete Painlevé equations, orthogonal polynomials on the unit circle, and N-recurrences for averages over $U(N)$—$\mathrm{P}_{\mathrm{III}'}$ and P_{V} τ-functions. *Int. Math. Res. Not. IMRN*, pages 160–183, 2004.

[59] P. J. Forrester and N. S. Witte. Painlevé II in random matrix theory and related fields. *Constr. Approx.*, 41:589–613, 2015.

[60] R. Fuchs. Über lineare homogene Differentialgleichungen zweiter Ordnung mit drei im Endlichen gelegenen wesentlich singulären Stellen. *Math. Ann.*, 70:525–549, 1911.

[61] B. Gambier. Sur les équations différentielles du second ordre et du premier degré dont l'intégrale générale est a points critiques fixes. *Acta Math.*, 33:1–55, 1910.

[62] G. Gasper and M. Rahman. *Basic Hypergeometric Series*. Cambridge University Press, Cambridge, 2004.

[63] B. Grammaticos and A. Ramani. Discrete Painlevé equations: a review. In B. Grammaticos, T. Tamizhmani, and Y. Kosmann-Schwarzbach, editors, *Discrete Integrable Systems*. Springer, Berlin, 2004.

[64] B. Grammaticos, A. Ramani, and V. Papageorgiou. Do integrable mappings have the Painlevé property? *Phys. Rev. Lett.*, 67:1825–1828, 1991.

[65] C. C. Green, C. J. Lustri, and S. W. McCue. The effect of surface tension on steadily translating bubbles in an unbounded Hele-Shaw cell. *Proc. R. Soc. A*, 473:20170050, 20, 2017.

[66] V. I. Gromak, I. Laine, and S. Shimomura. *Painlevé Differential Equations in the Complex Plane*. Walter de Gruyter & Co., Berlin, 2002.

[67] T. Hamamoto, K. Kajiwara, and N. S. Witte. Hypergeometric solutions to the q-Painlevé equation of type $(A_1 + A_1')^{(1)}$. *Int. Math. Res. Not. IMRN*, page 84619, 2006.

[68] W. A. Harris Jr and Y. Sibuya. Asymptotic solutions of systems of nonlinear difference equations. *Arch. Ration. Mech. Anal.*, 15:377–365, 1964.

[69] E. J. Hinch. *Perturbation Methods*. Cambridge University Press, Cambridge, 1991.

[70] C. J. Howls. Hyperasymptotics for integrals with finite endpoints. *Proc. R. Soc. A*, 439:373–396, 1992.

[71] C. J. Howls. Hyperasymptotics for multidimensional integrals, exact remainder terms and the global connection problem. *Proc. R. Soc. A*, 453:2271–2294, 1996.

[72] C. J. Howls, P. J. Langman, and A. B. Olde Daalhuis. On the higher-order Stokes phenomenon. *Proc. R. Soc. A*, 460:2285–2303, 2004.

[73] C. J. Howls and A. B. Olde Daalhuis. Exponentially accurate solution tracking for nonlinear ODEs, the higher order Stokes phenomenon and double transseries resummation. *Nonlinearity*, 25:1559–1584, 2012.

[74] M. E. H. Ismail. Asymptotics of q-orthogonal polynomials and a q-Airy function. *Int. Math. Res. Not. IMRN*, 18:1063–1088, 2005.

[75] A. R. Its. The Painlevé transcendents as nonlinear special functions. In D. Levi and P. Winternitz, editors, *Painlevé Transcendents*. Plenum, New York, 1992.

[76] H. Jeffreys. On certain approximate solutions of linear differential equations of the second order. *Proc. Lond. Math. Soc.*, 23:428–436, 1925.

[77] M. Jimbo and T. Miwa. Monodromy preserving deformation of linear ordinary differential equations with rational coefficients. II. *Phys. D*, 2:407–448, 1981.

[78] D. S. Jones. Asymptotic behavior of integrals. *SIAM Rev.*, 14:286–317, 1972.

[79] N. Joshi. Irregular singular behaviour in the first discrete Painlevé equation. In *SIDE III-Symmetries and Integrability of Difference Equations (Sabaudia, 1998)*. Amer. Math. Soc., Providence, RI, 2000.

[80] N. Joshi. Quicksilver solutions of a q-difference first Painlevé equation. *Stud. Appl. Math.*, 134:233–251, 2015.

[81] N. Joshi and A. V. Kitaev. On Boutroux's tritronquée solutions of the first Painlevé equation. *Stud. Appl. Math.*, 107:253–291, 2001.

[82] N. Joshi and S. B. Lobb. Singular dynamics of a q-difference Painlevé equation in its initial value space. *J. Phys. A*, 49:1–24, 2016.

[83] N. Joshi and C. J. Lustri. Stokes phenomena in discrete Painlevé I. *Proc. R. Soc. A*, 471:1–22, 2015.

[84] N. Joshi, C. J. Lustri, and S. Luu. Stokes phenomena in discrete Painlevé II. *Proc. R. Soc. A*, 473:1–20, 2017.

[85] N. Joshi and P. Roffelson. Analytic solutions of q-$P(A_1)$ near its critical points. *Nonlinearity*, 29:3696–3742, 2016.

[86] N. Joshi and Y. Takei. On Stokes phenomena for the alternate discrete PI equation. In Galina Filipuk, Yoshishige Haraoka, and Sławomir Michalik, editors, *Analytic, Algebraic and Geometric Aspects of Differential Equations*, pages 369–381. Birkhäuser/Springer, Cham, 2017.

[87] K. Kajiwara. The discrete Painlevé II equation and the classical special functions. In *Symmetries and Integrability of Difference Equations*. Cambridge University Press, 1999.

[88] K. Kajiwara, T. Masuda, N. Noumi, Y. Ohta, and Y. Yamada. Hypergeometric solutions to the q-Painlevé equations. *Int. Math. Res. Not. IMRN*, 47:2497–2521, 2004.

[89] K. Kajiwara, N. Noumi, and Y. Yamada. Geometric aspects of Painlevé equations. *J. Phys. A*, 50:073001, 164, 2017.

[90] K. Kajiwara, Y. Ohta, J. Satsuma, B. Grammaticos, and A. Ramani. Casorati determinant solutions for the discrete Painlevé II equation. *J. Phys. A*, 27:915–922, 1994.

[91] K. Kajiwara, K. Yamamoto, and Y. Ohta. Rational solutions for the discrete Painlevé II equation. *Phys. Lett. A*, 232:189–199, 1997.

[92] J. R. King and S. J. Chapman. Asymptotics beyond all orders and Stokes lines in nonlinear differential-difference equations. *European J. Appl. Math.*, 4:433–463, 2001.

[93] A. Knizel. Moduli spaces of q-connections and gap probabilities. *Int. Math. Res. Not. IMRN*, pages 6921–6954, 2016.

[94] H. A. Kramers. Wellenmechanik und halbzahlige quantisierung. *Zeitschrift fur Physik*, 39:828–840, 1926.

[95] M. D. Kruskal. Asymptotology. In S. Drobot and P. A. Viebrock, editors, *Proceedings of Conference on Mathematical Models on Physical Sciences, Englewood Cliffs, NJ: Prentice Hall, 1963, 17-48*, 1962.

[96] M. D. Kruskal and H. Segur. Asymptotics beyond all orders in a model of crystal growth. *Stud. Appl. Math.*, 85:129–181, 1991.

[97] E. Laguerre. Sur la réduction en fractions continues d'une fraction qui satisfait à une équation différentielle linéaire du premier ordre dont les coefficients sont rationnels. *J. Math. Pures Appl.*, 1:135–165, 1885.

[98] E. Landau. *Handbuch der Lehre von der Verteilung der Primzahlen*. Leipzig, 1909.

[99] X. Lü and M. Peng. Painlevé-integrability and explicit solutions of the general two-coupled nonlinear Schrödinger system in the optical fiber communications. *Nonlinear Dynam.*, 73:405–410, 2013.

[100] C. J. Lustri and S. J. Chapman. Steady gravity waves due to a submerged source. *J. Fluid Mech.*, 732:660–686, 2013.

[101] C. J. Lustri and S. J. Chapman. Unsteady flow over a submerged source with low Froude number. *European J. Appl. Math.*, 25:655–680, 2014.

[102] C. J. Lustri, S. W. McCue, and B. J. Binder. Free surface flow past topography: a beyond-all-orders approach. *European J. Appl. Math.*, 23:441–467, 2012.

[103] C. J. Lustri, S. W. McCue, and S. J. Chapman. Exponential asymptotics of free surface flow due to a line source. *IMA J. Appl. Math.*, 78:697–713, 2013.

[104] A. P. Magnus. Painlevé-type differential equations for the recurrence coefficients of semi-classical orthogonal polynomials. *J. Comput. Appl. Math.*, 57:215–237, 1995.

[105] A. P. Magnus. Freud's equations for orthogonal polynomials as discrete Painlevé equations. In *Symmetries and Integrability of Difference Equations*. Cambridge Univ. Press, 1999.

[106] T. Mano. Asymptotic behaviour around a boundary point of the q-Painlevé VI equation and its connection problem. *Nonlinearity*, 23:1585–1608, 2010.

[107] T. Morita. A connection formula between the Ramanujan function and the q-Airy function. *arXiv preprint arXiv:1104.0755v2*, 2011.

[108] T. Morita. The Stokes phenomenon for the q-difference equation satisfied by the basic hypergeometric series ${}_3\varphi_1(a_1, a_2, a_3; b_1; q, x)$. In *Novel Development of Nonlinear Discrete Integrable Systems*. Res. Inst. Math. Sci. (RIMS), Kyoto, 2014.

[109] T. Morita. The Stokes phenomenon for the q-difference equation satisfied by the Ramanujan entire function. *Ramanujan J.*, 34:329–346, 2014.

[110] T. Morita. The Stokes phenomenon for the Ramanujan's q-difference equation and its higher order extension. *arXiv preprint arXiv:1404.2541v1*, 2014.

[111] F. W. Nijhoff. Discrete Painlevé equations and symmetry reduction on the lattice. In A. I. Bobenko and R. Seiler, editors, *Discrete Integrable Geometry and Physics*. Oxford Univ. Press, New York, 1999.

[112] F. W. Nijhoff and V. G. Papageorgiou. Similarity reductions of integrable lattices and discrete analogues of the Painlevé II equation. *Phys. Lett. A*, 153:337–344, 1991.

[113] Y. Ohyama. Expansions on special solutions of the first q-Painlevé equation around the infinity. *Proc. Japan Acad. Ser. A Math. Sci.*, 5:91–92, 2010.

[114] Y. Ohyama. Special solutions to the second q-Painlevé equation. *AIP Conference Proceedings*, 1281:1714–1717, 2010.

[115] Y. Ohyama. q-Stokes phenomenon of a basic hypergeometric series ${}_1\phi_1(0; a; q, x)$. *J. Math. Tokushima Univ.*, 50:49–60, 2016.

[116] K. Okamoto. Sur les feuilletages associés aux équations du second ordre à points critiques fixes de P. Painlevé. *Japan. J. Math. (N.S.)*, 5:1–79, 1979.

[117] A. B. Olde Daalhuis. Hyperasymptotic solutions of higher order linear differential equations with a singularity of rank one. *Proc. R. Soc. A*, 454:1–29, 1998.

[118] A. B. Olde Daalhuis. Inverse factorial-series solutions of difference equations. *Proc. Edinb. Math. Soc.*, 47:421–448, 2004.

[119] A. B. Olde Daalhuis. Hyperasymptotics for nonlinear ODEs I. a Riccati equation. *Proc. R. Soc. A*, 461:2503–2520, 2005.

[120] A. B. Olde Daalhuis. Hyperasymptotics for nonlinear ODEs II. The first Painlevé equation and a second-order Riccati equation. *Proc. R. Soc. A*, 462:3005–3021, 2005.

[121] A. B. Olde Daalhuis, S. J. Chapman, and J. R. King. Stokes phenomenon and matched asymptotic expansions. *SIAM J. Appl. Math.*, 55:1469–1483, 1995.

[122] F. W. J. Olver. Uniform, exponentially improved, asymptotic expansions for the generalized exponential integral. *SIAM J. Math. Anal.*, 22:1460–1474, 1991.

[123] F. W. J. Olver. *Asymptotics and Special Functions*. A K Peters, Ltd., Wellesley, MA, 1997.

[124] F. W. J. Olver. Resurgence in difference equations, with an application to Legendre functions. In C. Dunkl, M. Ismail, and R. Wong, editors, *Special Functions*. World Scientific, 2000.

[125] P. Painlevé. Mémoire sur les équations différentielles dont l'intégrale générale est uniforme. *Bull. Soc. Math. France*, 28:201–261, 1900.

[126] P. Painlevé. Sur les équations différentielles du second ordre et d'ordre supérieur dont l'intégrale générale est uniforme. *Acta Math.*, 25:1–85, 1902.

[127] R. B. Paris. Smoothing of the Stokes phenomenon for high-order differential equations. *Proc. R. Soc. A*, 436:165–186, 1992.

[128] R. B. Paris. Smoothing of the Stokes phenomenon using Mellin-Barnes integrals. *J. Comput. Appl. Math.*, 41:117–133, 1992.

[129] R. B. Paris and A. D. Wood. Exponentially-improved asymptotics for the gamma function. *J. Comput. Appl. Math.*, 41:135–143, 1992.

[130] V. Periwal and D. Shevitz. Exactly solvable unitary matrix models: Multicritical potentials and correlations. *Nuclear Phys. B*, 344:731–746, 1990.

[131] V. Periwal and D. Shevitz. Unitary-matrix models as exactly solvable string theories. *Phys. Rev. Lett.*, 64:1326, 1990.

[132] E. Picard. Mémoire sur la théorie des fonctions algébriquesde deux variables. *J: de Math*, 5:135–318, 1889.

[133] H. Poincaré. Sur les intégrales irréguliéres. *Acta Math.*, 8:295–344, 1886.

[134] G. R. W. Quispel, J. A. G. Roberts, and C. J. Thompson. Integrable mappings and soliton equations. *Phys. Lett. A*, 132:8–9, 1988.

[135] A. Ramani, B. Grammaticos, and J. Hiertarinta. Discrete versions of the Painlevé equations. *Phys. Rev. Lett.*, 67:1829–1832, 1991.

[136] A. Ramani, B. Grammaticos, and K. M. Tamizhmani. Painlevé analysis and singularity confinement: the ultimate conjecture. *J. Phys. A*, 26:L53–L58, 1993.

[137] A. Ramani, B. Grammaticos, T. Tamizhmani, and K. M. Tamizhmani. Special function solutions of the discrete Painlevé equations. *Comput. Math. Appl.*, 42:603–614, 2001.

[138] A. Ramani, B. Grammaticos, R. Willox, T. Mase, and M. Kanki. The redemption of singularity confinement. *J. Phys. A*, 48:11FT02, 2015.

[139] S. Ramanujan. *The Lost Notebook and other Unpublished Papers*. Springer-Verlag, Berlin; Narosa Publishing House, New Delhi, 1988.

[140] J. P. Ramis, J. Sauloy, and C. Zhang. Local analytic classification of q-difference equations. *Astérisque*, 355:vi+151, 2013.

[141] H. Sakai. Rational surfaces associated with affine root systems and geometry of the Painlevé equations. *Comm. Math. Phys.*, 220:165–229, 2001.

[142] J. Satsuma, K. Kajiwara, B. Grammaticos, J. Hiertarinta, and A. Ramani. Binlinear discrete Painlevé II and its particular solutions. *J. Phys. A*, 28:3541–3548, 1995.

[143] J. Sauloy. The Stokes phenomenon for linear q-difference equations. In *Symmetries and Related Topics in Differential and Difference Equations*. Amer. Math. Soc., Providence, RI, 2011.

[144] R. Schiappa and R. Vaz. The resurgence of instantons: multi-cut Stokes phases and the Painlevé II equation. *Comm. Math. Phys.*, 330:655–721, 2014.

[145] N. Seiberg and D. Shih. Flux vacua and branes of the minimal superstring. *J. High Energy Phys.*, 1:55–93, 2005.

[146] J. Shohat. A differential equation for orthogonal polynomials. *Duke Math. J.*, 5:401–417, 1939.

[147] G. G. Stokes. On the discontinuity of arbitrary constants which appear in divergent developments. In *Mathematical and Physical Papers*. Cambridge University Press, 1864.

[148] S. Tanveer. Analytic theory for the determination of velocity and stability of bubbles in a Hele-Shaw cell. *Theoret. Comput. Fluid Dynamics*, 1:135–163, 1989.

[149] T. Tokihiro, B. Grammaticos, and A. Ramani. From the continuous P_V to discrete Painlevé equations. *J. Phys. A*, 35:5943–5950, 2002.

[150] C. A. Tracy and H. Widom. Level-spacing distributions and the Airy kernel. *Phys. Lett. B*, 305:115–118, 1993.

[151] C. A. Tracy and H. Widom. Random unitary matrices, permutations and Painlevé. *Comm. Math. Phys.*, 207:665–685, 1999.

[152] W. Van Assche. Discrete Painlevé equations for recurrence coefficients of orthogonal polynomials. In *Difference equations, Special functions and Orthogonal polynomials*, pages 687–725. World Sci. Publ., Hackensack, NJ, 2007.

[153] W. Van Assche, G. Filipuk, and L. Zhang. Mutiple orthogonal polynomials associated with an exponential cubic weight. *J. Approx. Theory*, 190:1–25, 2015.

[154] G. Wentzel. Eine verallgemeinerung der quantenbedingungen für die zwecke der wellenmechanik. *Zeitschrift fur Physik*, 38:518–529, 1926.

[155] E. T. Whittaker and G. N. Watson. *A Course of Modern Analysis. An Introduction to the General Theory of Infinite Processes and of Analytic Functions: with an Account of the Principal Transcendental Functions*. Cambridge University Press, New York, 1962.

[156] R Wong. *Asymptotic Approximations of Integrals*. Society for Industrial and Applied Mathematics (SIAM), Philadelphia, PA, 2001.

[157] S. X. Xu and Y. Q. Zhao. Asymptotics of discrete Painlevé V transcendents via the Riemann-Hilbert approach. *Stud. Appl. Math.*, 130:201–231, 2013.

[158] C. Zhang. Sur la sommabilité des séries entières solutions formelles d'une équation aux q-différences. I. *Comptes Rendus de l'Académie des Sciences. Série I. Mathématique*,

327:349–352, 1998.

[159] C. Zhang. Développements asymptotiques q-Gevrey et séries Gq-sommables. *Ann. Inst. Fourier (Grenoble)*, 49:227–261, 1999.

[160] C. Zhang. Une sommation discrète pour des équations aux q-différences linéaires et à coefficients analytiques: théorie générale et exemples. In *Differential Equations and the Stokes Phenomenon*. World Sci. Publ., River Edge, NJ, 2002.

[161] C. Zhang. Sur les fonctions q-Bessel de Jackson. *J. Approx. Theory*, 122:208–223, 2003.

[162] C. Zhang. Solutions asymptotiques et méromorphes d'équations aux q-différences. *Sémin. Congr.*, 14:341–356, 2006.